2017

Development of New Routes for the Synthesis of Carbaporphyrins and Carbachlorins

Navneet Sahota
Illinois State University, nsahot1@ilstu.edu

DEVELOPMENT OF NEW ROUTES FOR THE SYNTHESIS OF CARBAPORPHYRINS AND CARBACHLORINS

Navneet Sahota

250 Pages

Carbaporphyrins and carbachlorins are porphyrin analogs in which one of the nitrogens is replaced with a carbon atom within a porphyrin-like cavity. These systems form stable organometallic derivatives and exhibit unusual chemical reactivity. Most of the studies in this area have been carried out with benzocarbaporphyrins, where one of the pyrrole rings is replaced by an indene unit. Although syntheses of monocarbaporphyrins with fused benzene rings have been widely investigated over the past 20 years, few examples of carbaporphyrins without fused rings have been reported in the literature.

In this thesis, two projects were conducted to further explore carbaporphyrin and carbachlorin chemistry. The first project utilized a '3+1' condensation of a tripyrrane dicarboxylic acid with dimethyl 3,5-diformylcyclopentane-1,2-dicarboxylate in the presence of trifluoroacetic acid, followed by oxidation with 2,3-dichloro-5,6-dicyano-1,4-benzoquinone (DDQ), to yield a novel carbaporphyrin system in 40% yield together with a 9% yield of a related carbachlorin. This new carbaporphyrinoid system retained macrocyclic aromaticity and afforded stable silver(III) and gold(III) complexes. In addition, alkylation with methyl iodide and potassium carbonate gave a C-methyl derivative, and this underwent metalation with palladium(II) acetate and nickel(II) acetate to afford related organometallic species. The second project dealt with the development of a new route for synthesizing carbachlorins. Chlorins are a group of dihydroporphyrins and are important biological pigments. The study of core-modified chlorins has been limited compared to

that of core modified porphyrins. Carbachlorins are chlorin analogues where carbon atom is inserted into the chlorin core. They have interesting properties and are also promising candidates in many practical applications. Based on a "3+1" methodology, a novel carbachlorin was synthesized and characterized through various spectroscopic techniques, including NMR, UV-Vis spectroscopy, and mass spectrometry. The coordination chemistry of this carbachlorin was also investigated.

KEYWORDS: Carbaporphyrins, Carbachlorins, Porphyrins, Chlorins, Spectroscopic techniques

DEVELOPMENT OF NEW ROUTES FOR THE SYNTHESIS OF CARBAPORPHYRINS AND CARBACHLORINS

NAVNEET SAHOTA

A Thesis Submitted in Partial
Fulfillment of the Requirements
for the Degree of

MASTER OF SCIENCE

Department of Chemistry

ILLINOIS STATE UNIVERSITY

2017

DEVELOPMENT OF NEW ROUTES FOR THE SYNTHESIS OF CARBAPORPHYRINS AND CARBACHLORINS

NAVNEET SAHOTA

COMMITTEE MEMBERS:

Timothy D. Lash, Chair

Shawn R. Hitchcock

Christopher C. Mulligan

ACKNOWLEDGMENTS

The author wishes to acknowledge all of the members of her research group for all of their support throughout the duration of her time at Illinois State University. The author would also like to acknowledge the faculty, staff, and fellow students in the Chemistry Department at Illinois State University. The writer acknowledges financial support from the National Science Foundation under grants no. CHE-1465049 and CHE-1212691 and the Petroleum Research Fund.

The author would like to thanks the members of her committee, Dr. Hitchcock and Dr. Mulligan for all the guidance given. In addition, the author acknowledges Dr. Ferrence for providing X-ray crystal structures for a carbaporphyrin and related metalloporphyrinoids. Great thanks are given to her research advisor Dr. Timothy D. Lash for his encouragement, endless support, and patience. The writer feels truly privileged and thankful to have had such an excellent mentor for the past two years.

N.S

CONTENTS

FIGURES

SCHEMES

CHAPTER I

INTRODUCTION TO PORPHYRINS

Introduction

Porphyrins and porphyrinoids are important heterocyclic macrocycles that are widespread in nature.[1] They are usually deeply colored green, red or purple fluorescent crystalline pigments whose origins can be either synthetic or natural.[2] The parent porphyrin system is called porphin **1**, while substituted porphins are called porphyrins. The word porphyrin was derived from the Greek word porphyra meaning purple. It was in 1873 that a German chemist named Hoppe-Seyler isolated a purple crystalline compound from heating hemoglobin with sulfuric acid, and he subsequently coined the name hematoporphyrin for this material from the Greek words for blood and purple.[2] Over the last 150 years, porphyrins have been widely investigated. The interesting properties of porphyrins, which include their coordination chemistry and aromatic character, have stimulated research into this class of organic compounds. Porphyrins and their derivatives greatly contribute to the beauty of nature and play important roles in biological systems. For these reasons, they have been commonly referred to as the pigments or colors of life.[2]

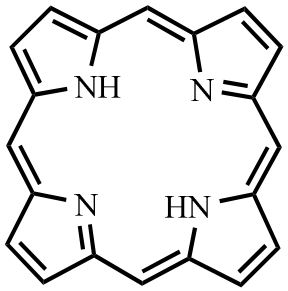

1

As mentioned above, many porphyrins and porphyrin-like compounds play significant roles in both animals and plants. In mammals, heme (**2**), an iron complex of porphyrin, is a component of hemoglobin and myoglobin. The former is involved in oxygen transportation around the body in the blood, while the latter stores oxygen in muscle tissue. Heme is also involved in redox reactions and electron transfer processes.[2] For instance, if the external environment of the heme is changed, it can facilitate completely different iron chemistry. Thus, in cytochrome c, it performs the function of electron transfer in cell respiration, as the iron atom cycles through +2 and +3 oxidation states.

In vitamin $B_{12,}$ nature makes use of a coordinated cobalt ion within a corrin core **3**. The complex is used to transfer hydrogen atoms and to reduce organic species. Vitamin B_{12} is a water-soluble vitamin and plays essential roles in the formation of red blood cells and in maintaining healthy nerve cells. Lack of vitamin B_{12} leads to a disease called pernicious anemia where the shortage of red cells and hemoglobin leads to impairment of the central nervous system. This disease usually results from the imperfect absorption of the vitamin by the intestines.[2]

In plants, chlorophylls (**4**), magnesium complexes of porphyrin-like structures, capture photons of light in the near-ultraviolet and red regions of the visible spectrum which therefore make them important for photosynthesis. The magnesium ion in the reduced porphyrin macrocycle of chlorophyll serves to modulate the energy transfer and light absorbing characteristics of chlorophyll, while acting as a center for binding water. A number of chlorophyll molecules are arranged into tiny molecular antennae that harvest large quantities of photons.[1] The energy of the photons is trapped as excited electrons, which are led away by a chain of electron-transporting proteins to generate high energy molecules necessary for turning carbon dioxide into carbohydrates during photosynthesis.[2]

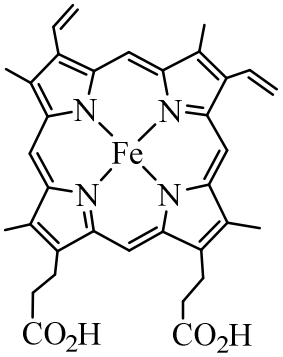

Heme

2

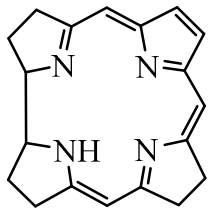

Corrin

3

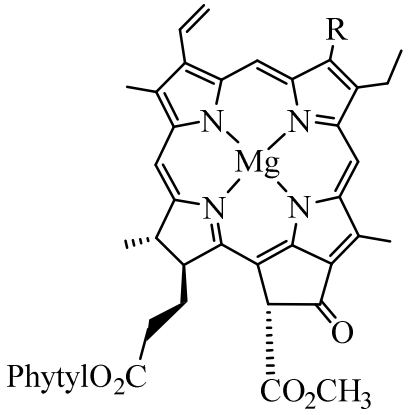

R = Me (Chlorophyll a)
R = CHO (Chlorophyll b)

4

Structure of Porphyrins

The macrocyclic structure of porphyrin was first proposed by Küster in 1912.[1] The macrocycle is composed of four pyrrole units connected by methine bridges at the α-carbons.[1,2] The methine carbons are also referred as *meso*-carbons and the hydrogens attached to these carbons are known as *meso*-protons. The pyrrole unit is a five-membered aromatic ring consisting of four carbon atoms and one nitrogen atom and possesses two formal double bonds. Pyrrole is an electron-rich aromatic system and has four dipolar resonance contributors (Figure 1) due to the presence of an electron-donating nitrogen atom.[3]

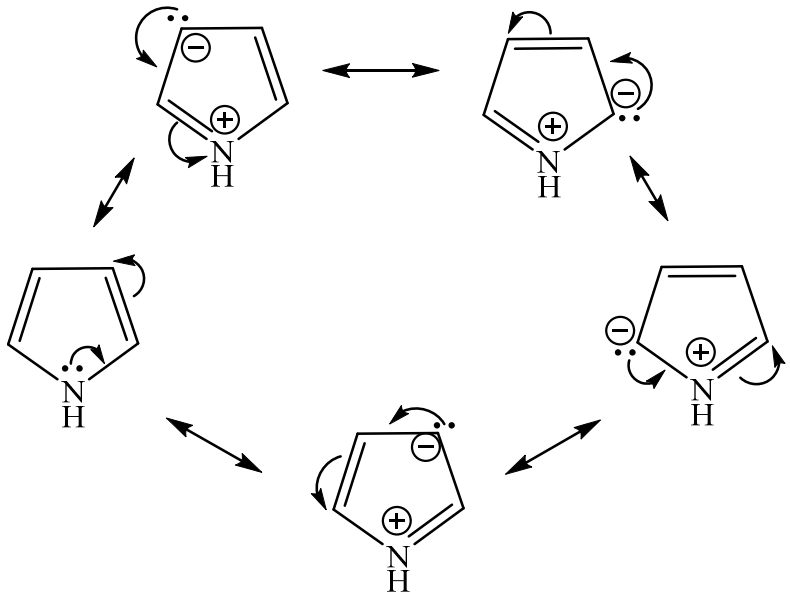

Figure 1 Resonance Structures of Pyrrole

Pyrrole is essentially non-basic since the lone pair of electrons on the nitrogen is delocalized into the ring in order to make the structure aromatic. Due to the resonance structures of this molecule, pyrrole is relatively electron-rich and therefore is likely to undergo electrophilic aromatic substitution.[3] The chemical and physical properties of porphyrins are very different from the properties of the pyrrole. For instance, porphyrins are usually very deeply colored compounds whereas pyrroles are off-white solids or colorless liquids. In addition, two of the nitrogens within the porphyrin core are basic and the π-electrons are delocalized over the entire macrocycle.[2]

A large number of synthetic routes have been developed for preparing pyrroles. Among these, the two of the most common methods used to synthesize substituted pyrroles are the Knorr pyrrole synthesis and the Hantzsch pyrrole synthesis.[2] In the Knorr pyrrole synthesis (Scheme 1), a substituted pyrrole **5** is formed by the condensation of an α-amino ketone **6** with a β-dicarbonyl compound **7**. In order to form the reactive α-amino ketone, an oxime **8** is reduced using zinc dust in acetic acid.[2]

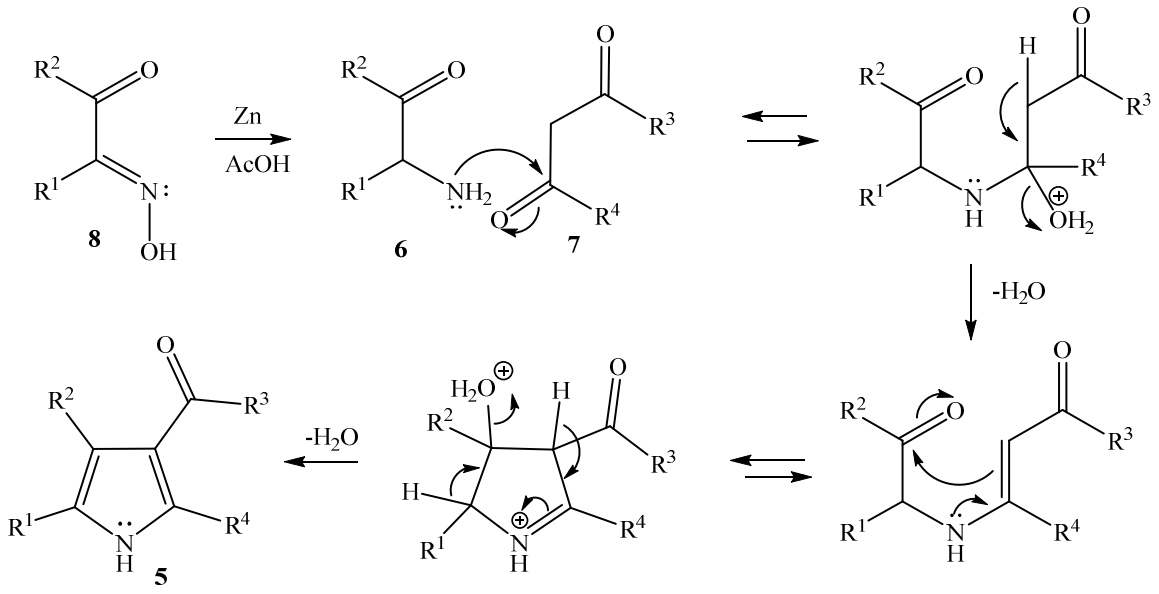

Scheme 1 Mechanism of the Knorr Pyrrole Synthesis

The second most common method is the Hantzsch pyrrole synthesis. In this approach, an α-haloketone is reacted with a β-ketoester and a primary amine or ammonia.[2] Nucleophilic attack by the amine or ammonia occurs on the carbonyl carbon of a β-ketoester **9**, and subsequent elimination of water results in the formation of an enamine **10**. Condensation of enamine **10** with the α-haloketone **11**, followed by ring closure, yields the substituted pyrrole **12** (Scheme 2).[2]

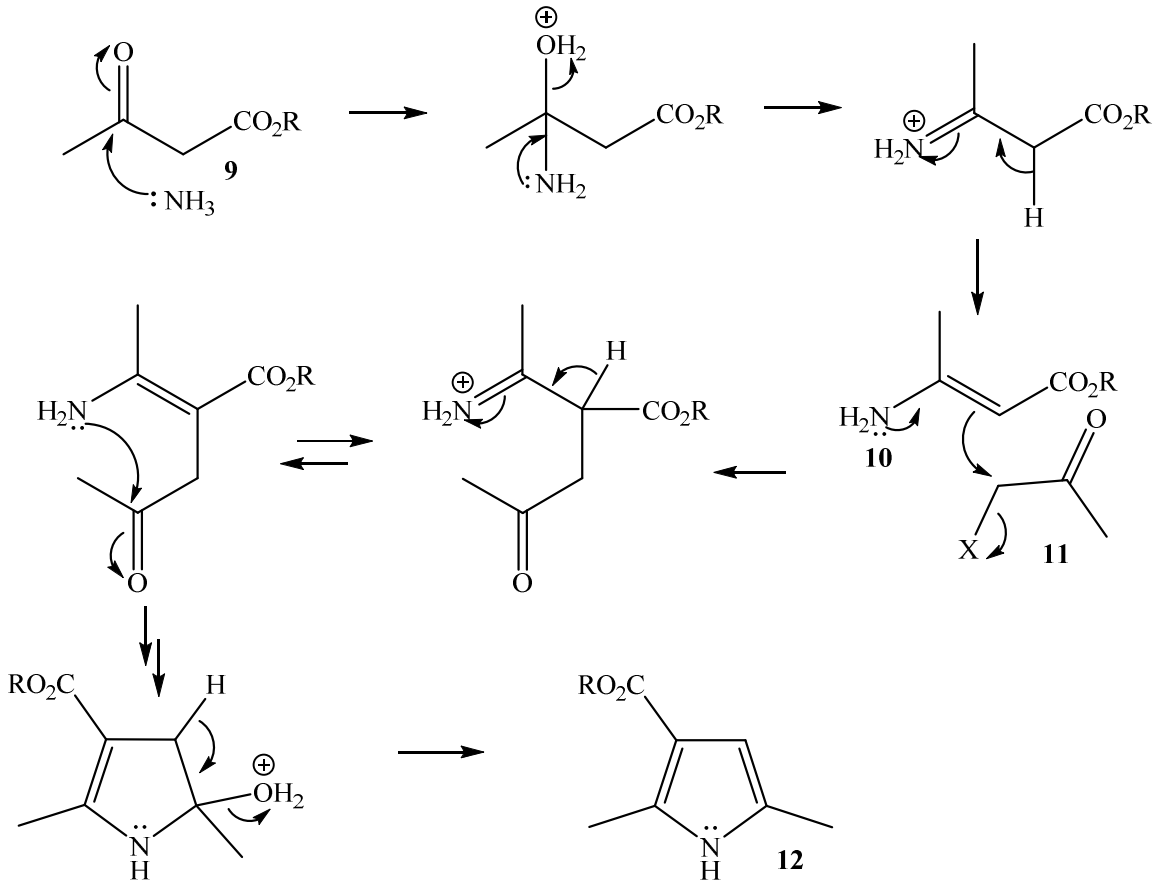

Scheme 2 Mechanism for the Hantzsch Synthesis of Substituted Pyrroles

Porphyrins can exist in several tautomeric forms, three of which are shown below (structures **1a**, **1b** and **1c)**. Although structures **1a** and **1b** are equivalent and are interconverting tautomers, tautomer **1c** is less favored due to the close proximity of two adjacent internal hydrogens that results in steric crowding effects.[2] In the porphyrin core, there are two pyrrolenine nitrogens, which can undergo protonation in the presence of acid to form mono- (**1**H^+) or dications (**1**H_2^{2+}) (Scheme 3).

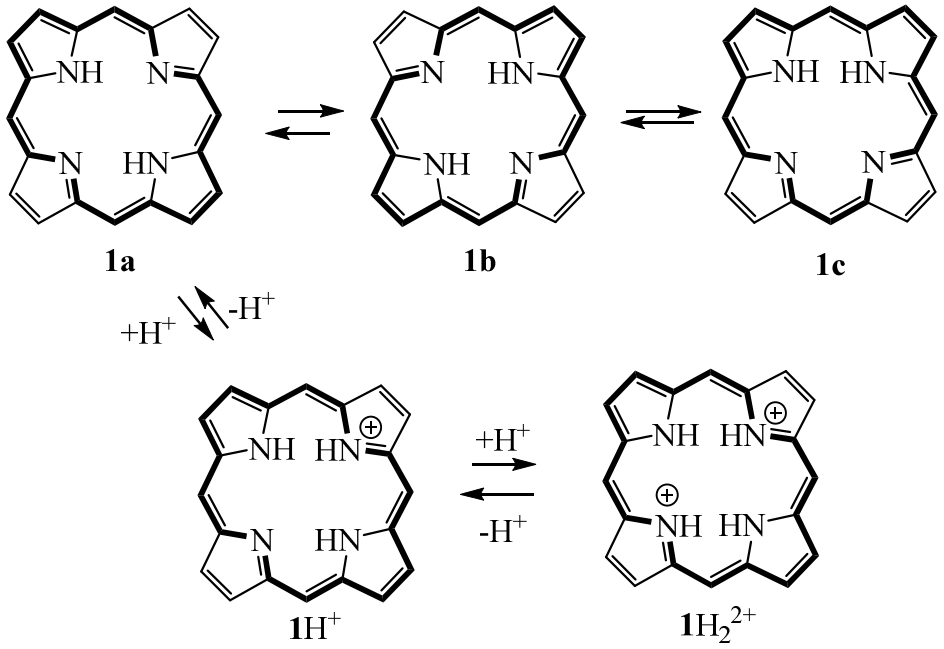

Scheme 3 Tautomerization and Protonation of Porphyrin

Aromatic Properties

Porphyrins are highly conjugated compounds, and it is the conjugated nature of these macrocycles that is, in part, responsible for their aromatic characteristics.[1,2] The concept of aromaticity was first introduced by Kekulé in 1865.[4] The term aromatic was proposed by Hoffmann because many benzene derivatives have a sweet odor.[5] As studies of aromatic compounds progressed, it was seen that a common property for these compounds was not their aroma but their relatively high stability. In 1931, Hückel was able to mathematically predict the aromaticity of unsaturated cyclic systems.[2] This led to the well-known Hückel's rule for aromaticity, according to which there needs to be $[4n+2]\pi$ electrons for a molecule to be aromatic, where n is zero or any positive integer.

Aromatic compounds are found to be more stable when compared to unsaturated compounds that are not aromatic, and the stability is due to the delocalized electron cloud also

known as resonance energy. Along with having sufficient π electrons, it is also required that the molecule is sufficiently planar, cyclic and continuously conjugated. The more planar the molecule, the easier it is for the π electrons to interact with one another to create a delocalized system.[2]

Benzene is the classic system which illustrates aromaticity. It is cyclic, has 6π electrons and is continuously conjugated, so it follows Hückel's rule for aromaticity and is very stable. Like benzene, porphyrin also follows Hückel's rule for aromaticity. Although porphyrins contain 22 conjugated π electrons (26π electrons counting the lone pairs of electrons on the nitrogen atoms), only 18 of them participate in a continuous delocalization pathway and therefore follow Hückel's rule where n = 4.[2] Unsaturated systems can also be classified as anti-aromatic or non-aromatic (Figure 2). Hückel described anti-aromatic species as cyclic and having a fully conjugated [4n]π electron pathway. Anti-aromatic compounds are still planar, but are considerably less stable than aromatic compounds (e.g. cyclobutadiene). On the other hand, non-aromatic structures are unsaturated systems that are not fully conjugated and may be non-planar. For instance, cyclooctatetraene is non-aromatic and adopts a tub-like shape making the structure non-planar. Non-aromatic polyenes are quite reactive as they are relatively unstable.[3]

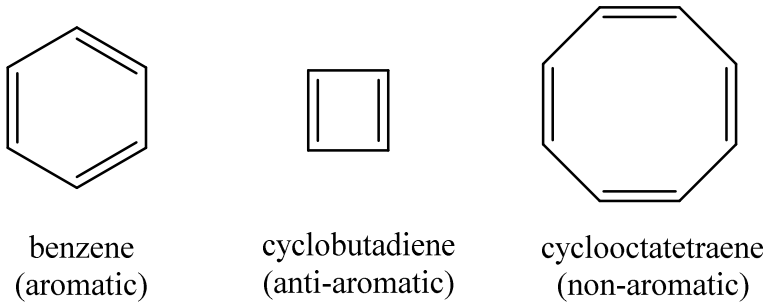

Figure 2 Examples of Cyclic Structures Depicting Differences in Aromaticity

Benzene and related compounds are unusually unreactive and do not have the typical reactivity that is associated with olefins. For example, in the case of cyclooctatetraene, which is an unusually reactive non-aromatic species, Br_2 can readily add across the double bonds giving addition products. However, benzene is quiet stable and unreactive, and no addition reactions are observed.[3] In benzene or other aromatic compounds, due to the interaction of the π electrons to create a delocalized π electron cloud, the bond lengths are found to be in between those of single bonds and double bonds.

Porphyrins can be considered to be the [18]annulenes of nature.[6] Annulenes are completely conjugated hydrocarbon macrocycles with the general formula of C_nH_n (where n is an even number) or C_nH_{n+1} (where n is an odd number), n here stands for the number of carbon atoms in the ring. Annulenes, like other cyclic systems, can be aromatic, non-aromatic or anti-aromatic. [18]Annulene (**13**) is an aromatic compound with nine double bonds. The macrocycle is reasonably planar and has 18π electrons that are fully delocalized over 18 carbon atoms. Therefore it follows Hückel's [4n+2]π electron rule for aromaticity, where n = 4. [18]Annulene was first synthesized by Sondheimer et al. in 1962[6] (Figure 3), and its conjugation pathway closely resembles the aromatic circuit present in porphyrins.

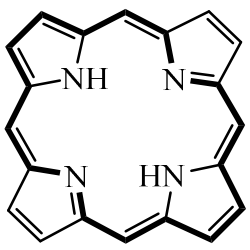

1

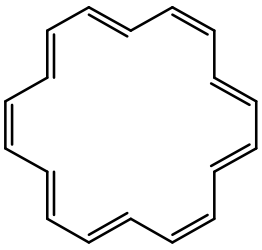

13

Figure 3 Structures of Porphyrin and [18]Annulene

Reduced porphyrin systems may also retain aromatic properties. Chlorins **14** bacteriochlorins **15** and isobacteriochlorins **16** all possess 18 π electron delocalization pathways and are aromatic compounds. Porphyrins can be reduced under a variety of conditions to generate hydroporphyrins such as chlorins, in which two or more hydrogens have been added across the β-β double bonds of one or more pyrrole moieties to produce pyrroline rings **14** (Figure 4). Chlorins are relatively stable compounds that can be oxidized back up to the porphyrin by high potential quinones such as 2,3-dichloro-5,6-dicyano-1,4-benzoquinone (DDQ) and chloranil. In chlorins, reduction at the β-pyrrole carbons does not interrupt the continuously conjugated delocalisation pathway. In fact, two more hydrogens may be added across another β-β double bond to give tetra-hydroporphyrins while retaining the 18 π electron pathway. If the double bonds are reduced on opposite pyrrole units bacterochlorins are formed, but reduction of the adjacent pyrrole units affords isobacterochlorin.[2]

However, other reduced forms of porphyrin, such as phlorins **17**, may not be aromatic like chlorins. This is due to phlorin containing a reduced double bond at one of the bridges linking two pyrrole units together.[2] Without the methine bridge, continuous conjugation throughout the macrocycle is not possible, therefore breaking one of Hückel's rules for aromaticity.

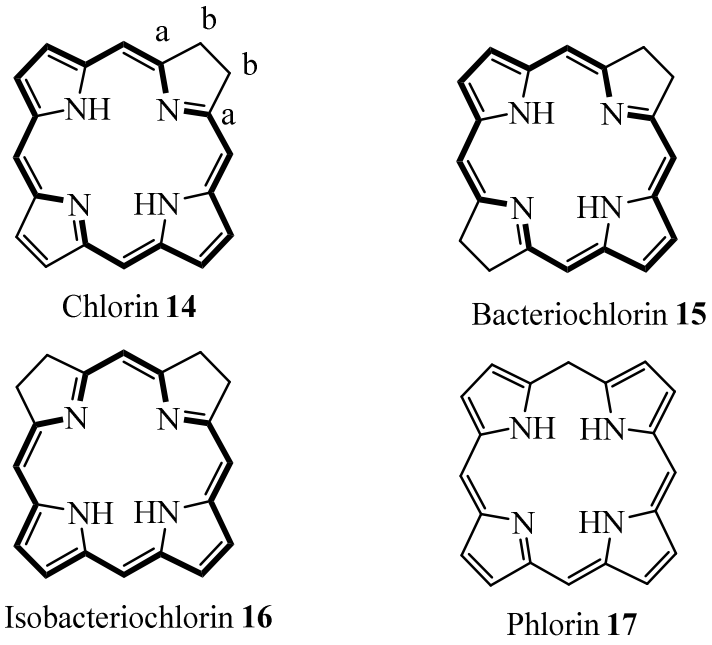

Figure 4 Reduced Forms of Porphyrin

A number of factors can lead to distortions from planarity in the porphyrin macrocycle. For instance, the presence of bulky substituents on the macrocyclic system can inhibit the planarity due to steric interactions. In addition, distortions can arise from the binding of a metal ion within the cavity of the macrocyclic system. When an appropriate sized metal cation binds in the cavity of the porphyrin, it may increase the planarity of the molecule. However, if the binding metal cation is too small or too big for the cavity, the porphyrin ring will distort itself in order to bind to the metal and hence the planarity will decrease making the ring system potentially less aromatic. For example, 2,3,7,8,12,13,17,18-octaethylporphyin (OEP) in its free base form is quite planar. However, when OEP binds to nickel(II), which is a relatively small cation for the cavity of the porphyrin, the macrocycle twists out of a planar conformation in order to coordinate with the metal. Porphyrins can tolerate considerable distortion while retaining aromatic properties.[2]

The aromatic character of porphyrins can be readily assessed using proton nuclear

magnetic resonance (NMR) spectroscopy and UV-vis spectroscopy. In particular, the diatropic character of these systems can easily be analyzed using proton NMR spectroscopy. When these macrocycles are introduced into a magnetic field, their π electrons circulate to create an aromatic ring current. The concept of aromatic ring currents was first introduced by Pauling in relation to the anisotropic diamagnetic susceptibilities of benzenoid hydrocarbons.[7] These susceptibilities were explained in terms of an induced circulation of the delocalized π-electrons in the presence of an applied magnetic field that produces an induced magnetic field. The strength of the induced magnetic field generated by the ring current is dependent on the orientation of the aromatic system with respect to the applied magnetic field. Typically, for porphyrins, the diamagnetic ring current deshields the β-pyrrole protons and the *meso*-protons. Because the *meso*-protons are attached to electron-deficient carbons, they are shifted even further downfield than the β-pyrrole protons and appear near +10 ppm. However, the inner N-H protons are shifted far upfield, beyond tetramethylsilane (TMS, the arbitrary standard for NMR measurements), showing up around -4 ppm. This is because the induced ring current, which deshields protons from the external magnetic field outside the macrocycle, shields them if they are inside the macrocycle (Figure 5). This shielding effect is not observed in the case of benzene as there are no internal protons. However, in some larger aromatic molecules (e.g. [18]annulene), the internal protons may be observed diamagnetically shielded and hence shifted upfield.

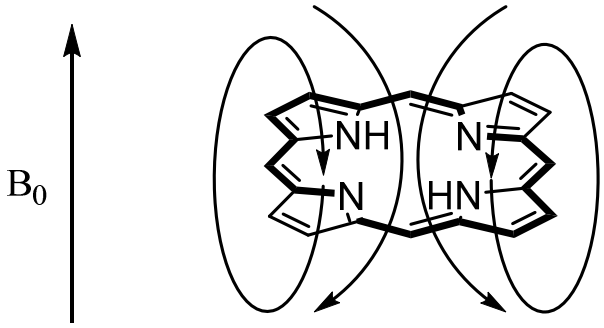

Figure 5 Induced Ring Current Effects on Porphyrin
as Observed in Nuclear Magnetic Spectroscopy

The diamagnetic ring currents observed in the case of porphyrins are valuable indicators of variations in aromatic character. Upon the addition of acid, porphyrins are mono-protonated or diprotonated, and the resulting cationic species show even stronger diamagnetic ring currents. For example, in the proton NMR spectrum of porphyrin dications, the *meso*-protons are shifted slightly further downfield, while the internal NH protons move upfield.[7]

Porphyrins have their own characteristic UV-visible spectra. Like benzene, and its homologues, there are mainly two distinct regions in the porphyrin absorption spectra. However, unlike benzene, porphyrins are deeply colored compounds due to the absorptions appearing in the near-ultraviolet and visible regions of the electromagnetic spectrum.[1] Highly conjugated systems tend to absorb light in the near UV and visible regions of their electronic spectra because conjugated π bonds are able to absorb light at higher wavelengths when compared to isolated π bonds. Thus, increasing the π bond conjugation of a system increases the wavelengths for absorption in the UV-Vis spectrum, and this leads to them being colored compounds.

Porphyrins characteristically exhibit intense peaks around 400 nm in the near ultraviolet region.[2] In 1883, Soret,[8] while studying hemoglobin, noticed these intense peaks and they were

later named as “Soret bands” or B bands. At higher wavelengths, other less intense peaks known as Q bands are also observed. The intensity of the Soret bands has been correlated to the aromaticity of the system. The more aromatic the macrocycle is, the more intense the Soret band.[2] In the case of tetraphenylporphyrin, an intense Soret band is observed at 417 nm and four Q bands can be seen at 514 nm, 549 nm, 589 nm, and 646 nm (Figure 6).[7]

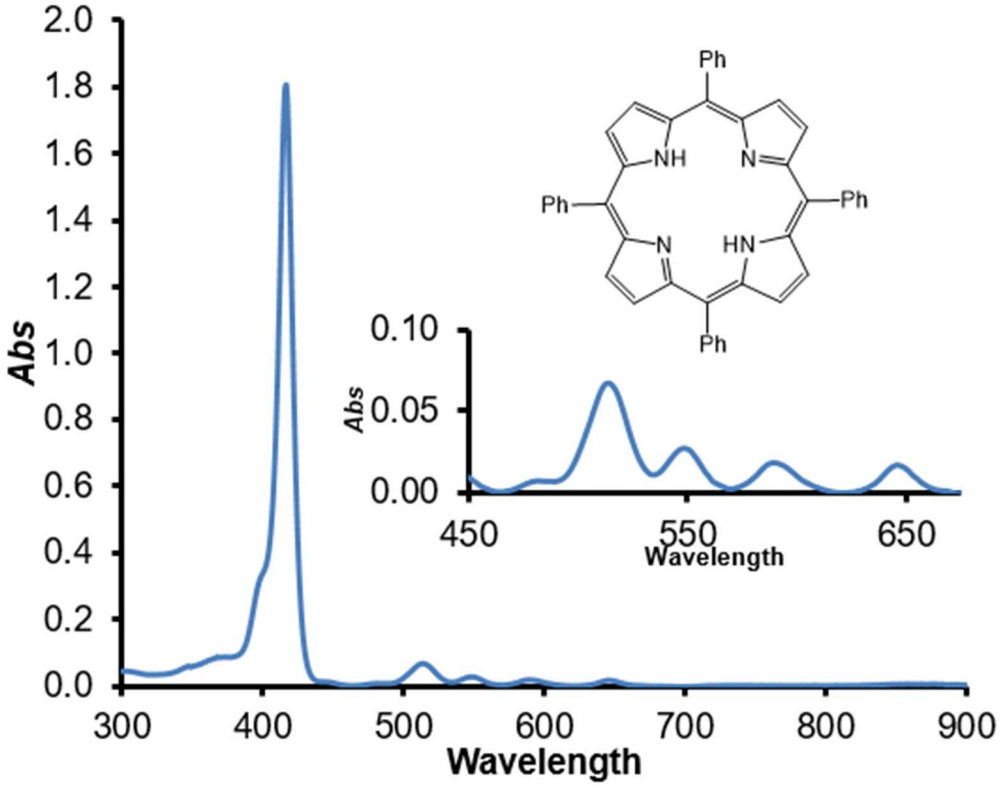

Figure 6 UV-Vis Spectrum of Tetraphenylporphyrin

Chlorins **14**, although they have less π electron density, still exhibit a Soret band in their UV-Vis spectra because these structures retain an 18π electron pathway. However, phlorins **17** do not exhibit Soret bands as there is an interruption of the 18π electron conjugated system due to reduction at one of the methine bridges. Similarly, porphyrinogens, the reduced intermediates in the biosynthesis of porphyrins, are also not conjugated structures and in this case are colorless compounds.[2]

The differences in the colors of porphyrinoid macrocycles are due to variations in their absorptions in the visible spectrum. For example, unlike porphyrins, chlorins tend to have a characteristic absorption near 650 nm, and this results in their characteristic green coloration. This explains why chlorophyll, a magnesium chlorin, is excellent at absorbing red light.[2]

The number and intensity of the Q and B bands can give powerful clues about the substitution pattern of porphyrins and whether they are metalated or not. Protonation of the porphyrin also alters the UV-vis spectrum. Diprotonation of the macrocycle leads to increased symmetry compared to the free base form, and this produces a simplification of the Q band region. Essentially, the four Q bands collapse to two and this can lead to profound color changes.

Substitution at the β-pyrrole positions can also affect the UV-visible absorption spectra which in turn leads to color changes. Metalloporphyrins tend to be more symmetrical macrocycles than free-base porphyrins and for this reason they generally only have two Q bands.[1] The relative intensities of these two bands can be used as a qualitative check to see how well the metal cation fits into the macrocyclic cavity.

Biosynthesis of Heme

As mentioned above, in 1912 Küster was the first to propose the structure of porphyrin.[9] However, the existence of such a large macrocyclic structure was only fully accepted in 1929, when Fischer synthesized protoheme.[10] The biosynthesis of porphyrins takes place through several enzyme-catalyzed steps, starting with 5-aminolevulinic acid (ALA). The biosynthesis of hemoglobin, chlorophyll and vitamin B_{12} all begin with this precursor. The two substrates required for the biosynthesis of ALA are succinyl coenzyme A (CoA) and the amino acid glycine. Succinyl CoA is produced during the Krebs cycle (also known as the citric acid cycle).

In the first step of the pathway, succinyl CoA is condensed with glycine, catalyzed by ALA synthase, to generate ALA. The condensation of two molecules of ALA, with the aid of ALA dehydratase, forms the pyrrole intermediate porphobilinogen (PBG). Four pyrrole units then condense together, in the third step mediated by PBG deaminase, to form the open chain tetrapyrrolic structure hydroxymethylbilane. Then, uroporphyrinogen III cosynthetase facilitates the cyclization of the tetrapyrrolic intermediate to form uroporphyrinogen III (Scheme 4). The cyclization here is associated with an inversion of ring D to afford the type III arrangement of substituents that can be observed in nearly all naturally occurring porphyrin derivatives. The biosynthesis of vitamin B_{12} also branches from the uroporphyrinogen III precursor.[2]

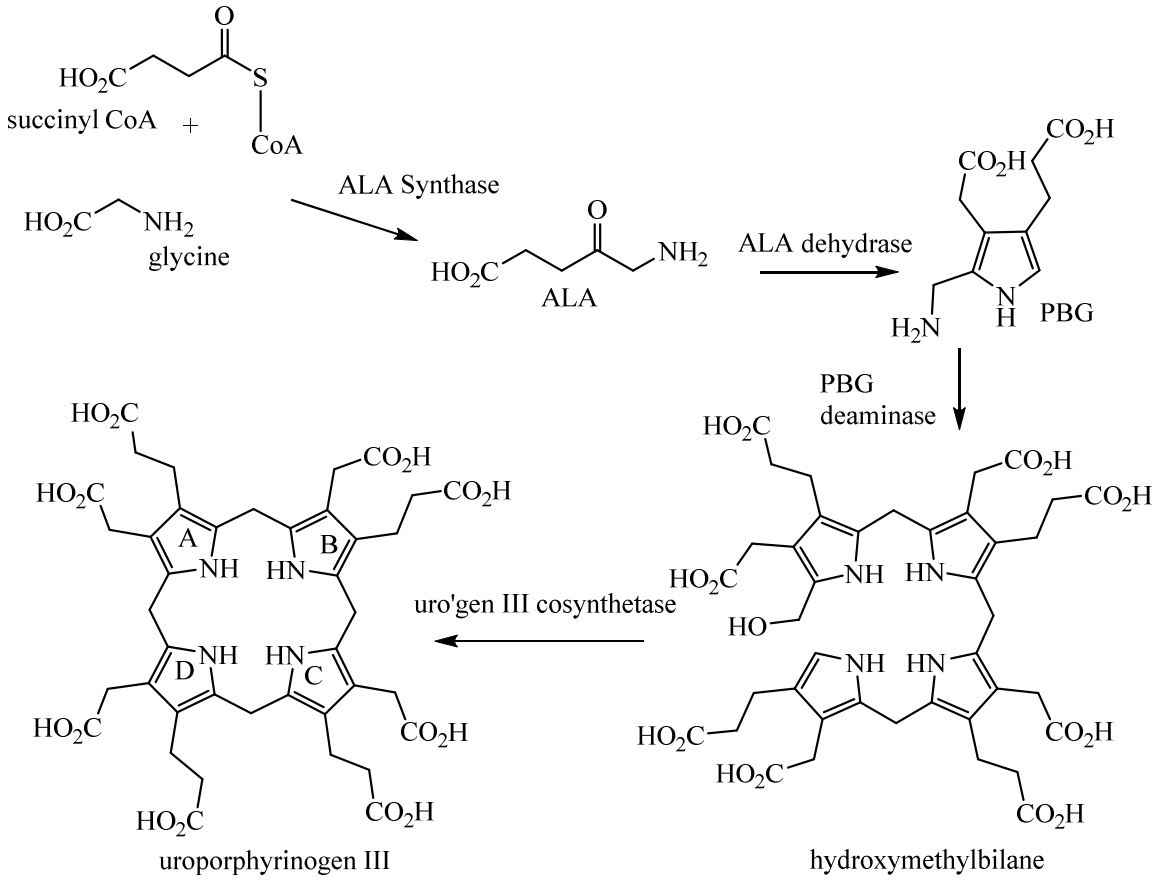

Scheme 4 Synthesis of Uroporphyrinogen III

The enzyme uroporphyrinogen decarboxylase mediates the decarboxylation of all four acetic acid side chains, while coproporphyrinogen oxidase subsequently oxidatively decarboxylates only two of the propionic acid side chains. Oxidation of protoporphyrinogen IX by the enzyme protoporphyrinogen IX oxidase then yields protoporphyrin IX. Insertion of iron(II) into protoporphyrin IX gives the metalloporphyrin heme (Scheme 5). Heme is then inserted into the appropriate protein to give hemoglobin or myoglobin, which are both vital moieties in many biological processes. Protoporphyrin IX is also the biosynthetic precursor to the chlorophylls.[2]

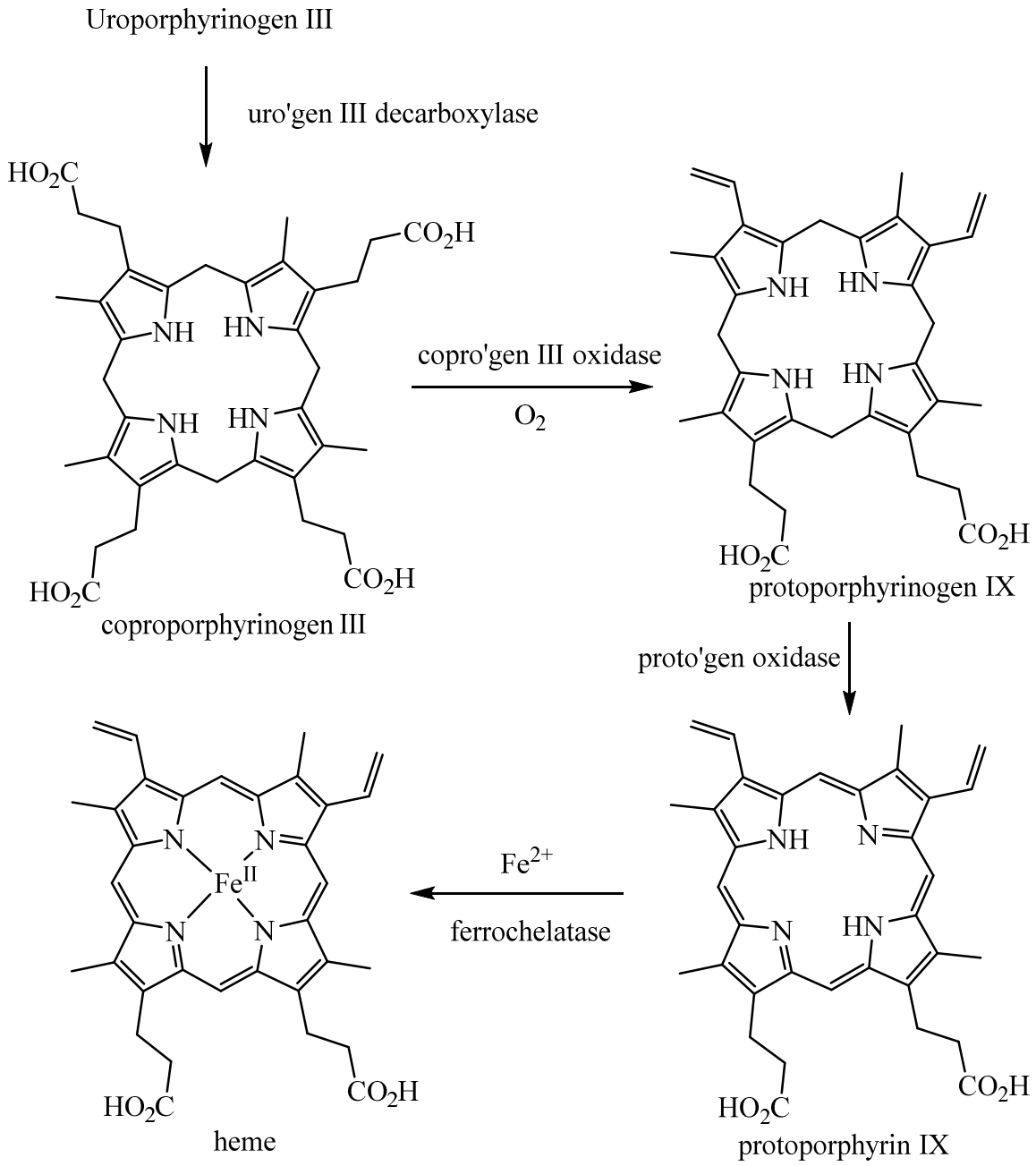

Scheme 5 Biosynthesis of Heme from Uroporphyrinogen III

Synthesis of Porphyrins

Over the years, a number of routes have been developed for porphyrin synthesis. Some of the earliest methods for porphyrin synthesis involved the degradation of naturally occurring pigments such as heme and chlorophyll. Metalloporphyrins are abundant in nature. For example, heme derived from blood or chlorophyll from plants, are convenient starting materials that can be used to prepare a wide variety of porphyrins.[2] Although, porphyrins can be synthesized from different natural sources, this approach can only be used to prepare structures with similar substitution patterns. For this reason, multistep syntheses have also been developed. The synthetic methods for the preparation of porphyrins and analogous systems can involve the intermediacy of monopyrrolic, dipyrrolic, tripyrrolic or tetrapyrrolic structures.[2,11]

Porphyrins can easily be formed by the tetramerization of monopyrroles. This technique is mainly used for the synthesis of highly symmetrical porphyrins such as tetraphenylporphyrin or octaethylporphyrin, and more sophisticated methods are usually required to prepare unsymmetrical structures.[11]

In the 1930s, tetraphenylporphyrin was first synthesized by Rothemund, albeit in low yields.[12] He initially investigated the synthesis of porphyrins by reacting acetaldehyde with pyrrole in methanol at different temperatures in sealed vessels. Based on the same strategy, he extended the scope of this methodology by reacting pyrrole **18** with several other aldehydes, including formaldehyde and propionaldehyde. When this reaction was conducted using benzaldehyde **19**, *meso*-tetraphenylporphyrin (TPP) **20** was isolated (Scheme 6).[12] In this reaction, pyrrole undergoes electrophilic substitution at the α positions with an aldehyde to form the macrocyclic ring. However, this reaction has many disadvantages. For instance, the reaction time was quite long and the setup required to do the experiment was inconvenient as it required that the reaction be carried

out under anaerobic conditions in a sealed tube. In addition, purification of the products was very difficult and poor yields were commonly obtained.[12]

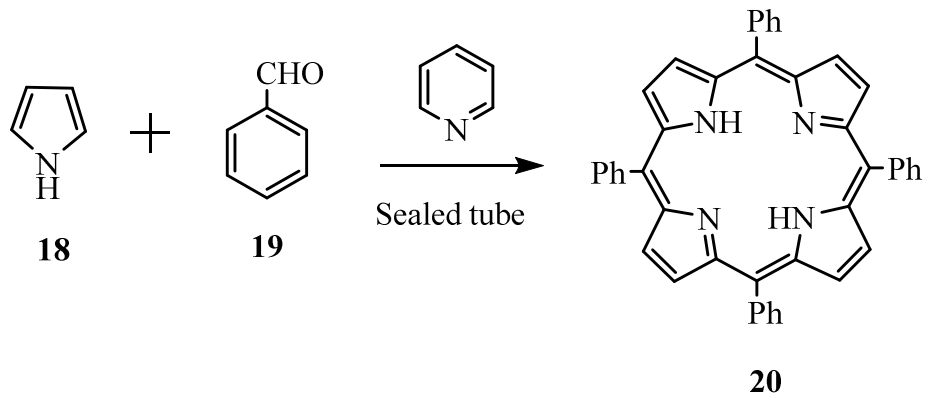

18 **19** **20**

Scheme 6 Rothemund Synthesis of TPP

Improvements on this approach were not reported until the 1960s. It was in 1967, that Adler and Longo reported an improved method for the synthesis of *meso*-substituted porphyrins **20**.[13] This was accomplished by heating benzaldehyde and pyrrole in the presence of refluxing propionic acid for 30 minutes (Scheme 7).[13] The porphyrin product precipitated from the reaction mixture in moderate yields of approximately 20%, which was a substantial improvement over Rothemund's method.[12] The Adler and Longo's method also required much shorter reaction times and could be done under aerobic conditions. However, this approach still had a few drawbacks. Firstly, many aldehydes could not tolerate the use of acidic conditions at elevated temperatures. Secondly, in cases where the porphyrin products did not precipitate, difficulties were encountered in removing side products that were also formed in these reactions.[2]

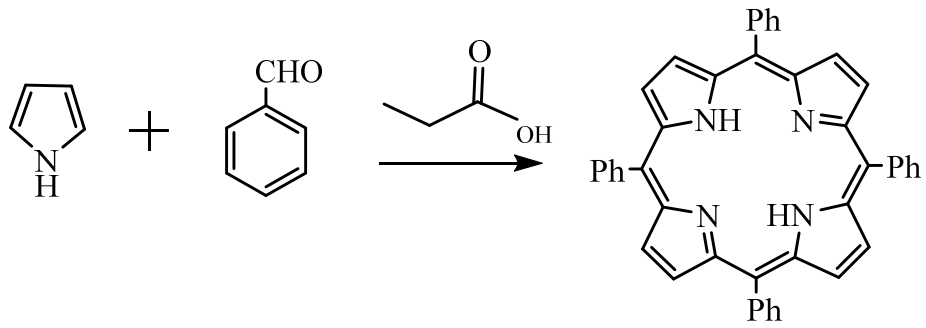

20

Scheme 7 Adler-Longo synthesis of TPP

In 1987, Lindsey et al. introduced a new methodology that greatly improved these syntheses.[14] In Lindsey's method, the porphyrin synthesis was done in two steps instead of one. The first step involves reaction of equimolar quantities of pyrrole and aldehyde in the presence of an acid catalyst such as boron trifluoride etherate or trifluoroacetic acid (TFA) in dichloromethane at room temperature. This results in the formation of a hexahydroporphyrin or porphyrinogen **21** (Scheme 8). Subsequently, in the second step oxidation of **21** with an electron deficient quinone, *p*-chloranil or 2,3-dichloro-5,6-dicyano-1,4-benzoquinone (DDQ), yields *meso*-substituted porphyrin **22** in approximately 40% yield (Scheme 8).[14] Due to the mild conditions of this procedure, the Lindsey method allowed for the use of aldehydes with sensitive functionality that could otherwise not be used under the relatively harsh conditions involved in previous routes to *meso*-substituted porphyrins.

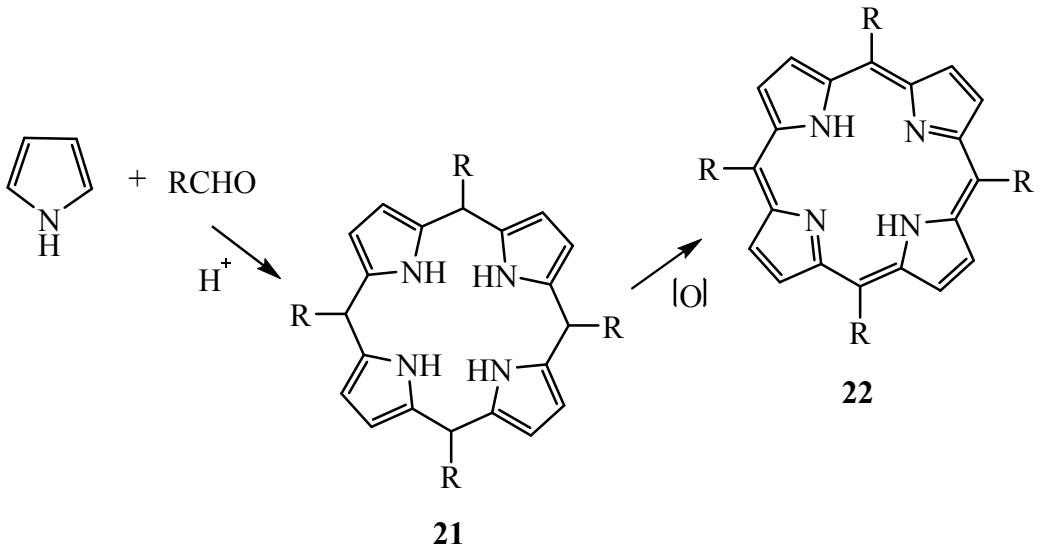

Scheme 8 Synthesis of *meso*-substituted porphyrins by Lindsey's method

The methods developed by Rothemund, Adler, Lindsey and others are only suitable for preparing symmetrical porphyrins and fall into the category of "One Pot Syntheses". Since 1960, many alternative routes to asymmetrical porphyrins have been developed including the '2+2' MacDonald condensation, '3+1' condensations, and the cyclization of open-chain tetrapyrroles.[11]

The '2+2' condensations rely on dipyrromethane or dipyrromethene intermediates such as **23** and **24** (Figure 7). These precursors both have two linked pyrrole units and are differentiated by the type of carbon linkage. Dipyrromethanes **23** have a saturated bridge, while dipyrromethenes **24** have an unsaturated bridge and are usually isolated as halide salts. Fischer made extensive use of '2+2' condensations of dipyrromethenes (Scheme 9) to synthesize asymmetrical porphyrins.[10]

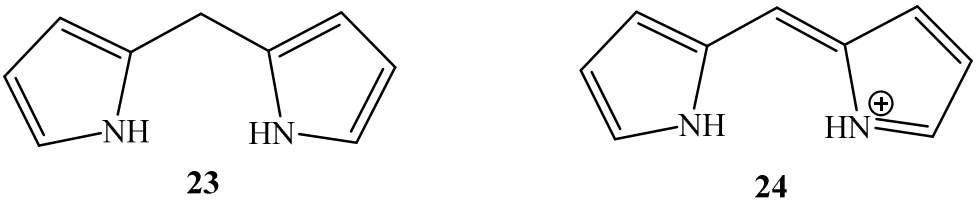

Figure 7 Structures of Dipyrrolic Intermediates

For example, dipyrromethenes **25** and **26** condensed together in a succinic acid melt to form deuteroporphyrin IX **27.** Deuteroporphyrin **27** was a key intermediate in the total synthesis of heme.[11]

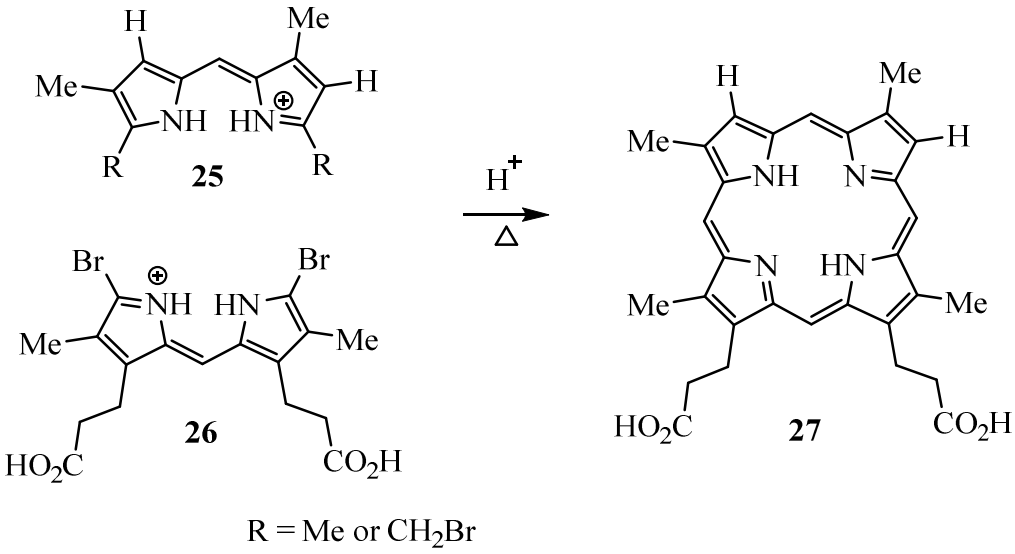

Scheme 9 Fischer Porphyrin Synthesis

The use of dipyrromethanes was initially overlooked, in part because they were considered to be too unstable to survive condensation reactions. However, in the 1960s, MacDonald was able to demonstrate that dipyrromethanes are reasonably stable and excellent porphyrin precursors. In

MacDonald's "2+2" condensation method, a 5,5'-dipyrrylmethane dialdehyde **28** was condensed with an α-unsubstituted dipyrrylmethane dicarboxylic acid **29** in the presence of an acid catalyst to generate a porphodimethene intermediate **30**, and subsequent air oxidation afforded the final porphyrin product **31** (Scheme 10).[15] Since the original report, the MacDonald reaction has been one of the most commonly used methods for preparing *meso*-unsubstituted porphyrins. In addition, a variation on MacDonald's condensation was a crucial step in the total synthesis of chlorophyll a.[15]

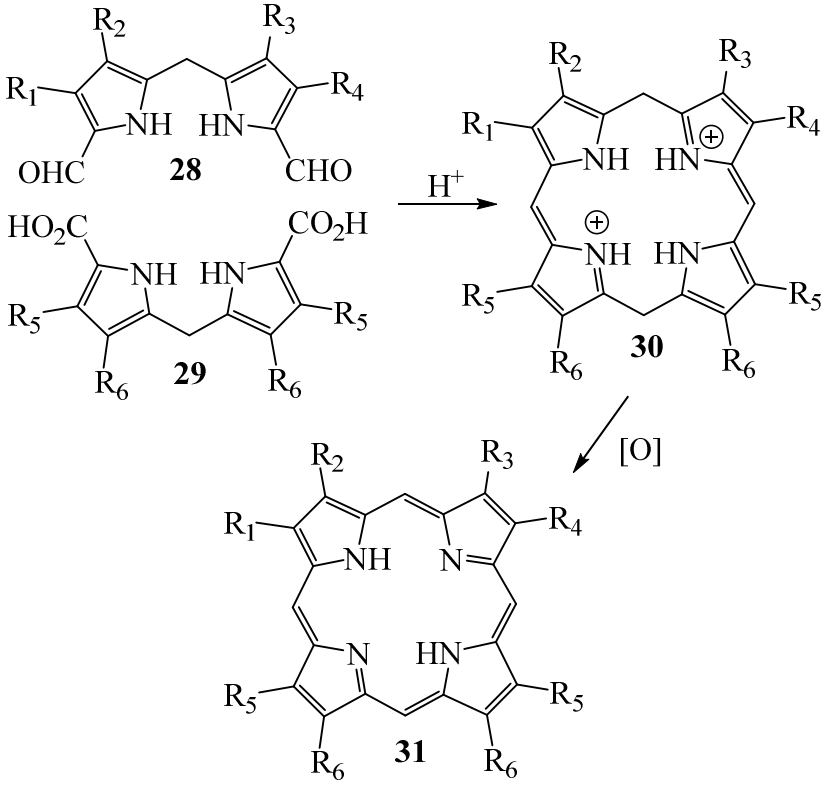

Scheme 10 MacDonald's "2+2" condensation reaction

Porphyrins can also be synthesized from oxophlorins **32**, which are cross-conjugated nonaromatic compounds that are the keto tautomers of *meso*-hydroxyporphyrins. Oxophlorin **32**

can be synthesized using MacDonald '2+2' conditions by reacting dipyrroketone dialdehydes **33** with dipyrromethanes **34** (Scheme 11).[11] Although oxophlorins favor the keto tautomer over the aromatic hydroxy tautomer, reaction of oxophlorins with acetic anhydride and pyridine traps the hydroxy tautomer as the corresponding acetoxyporphyrin **35**. Hydrogenation of **35** over palladium yields porphyrinogen **36**, and subsequent oxidation with DDQ affords the *meso*-unsubstituted porphyrin **37** in reasonable yields (Scheme 11).[11]

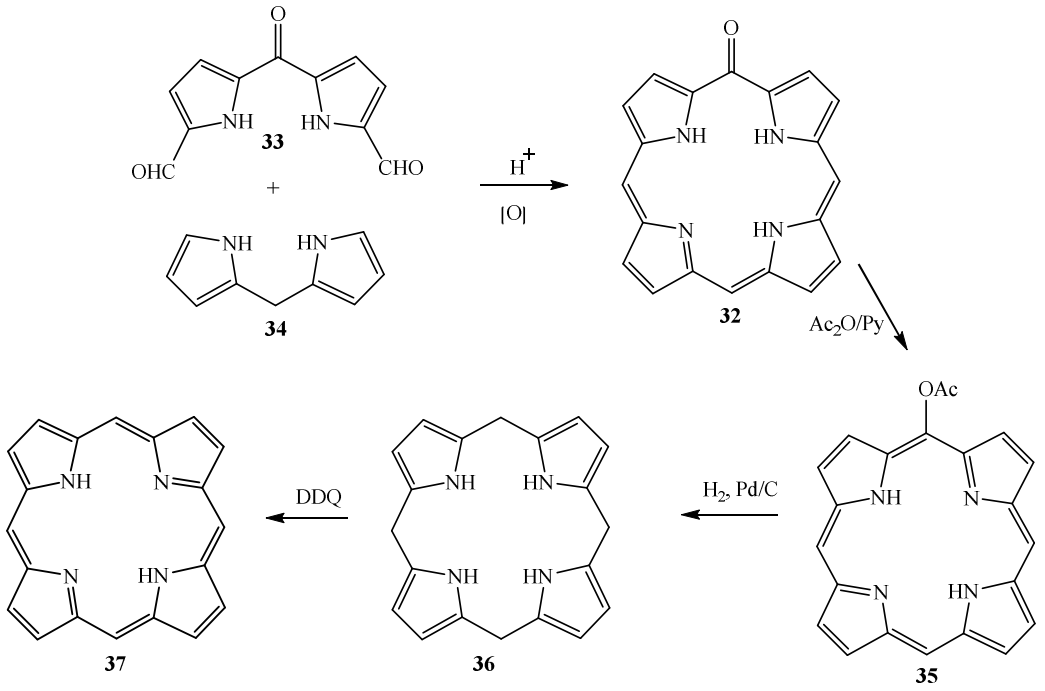

Scheme 11 Synthesis of Porphyrin from an Oxophlorin

In the synthesis of porphyrins using previously mentioned methods, the introduction and control of symmetry remains challenging. For instance, in the '2+2' approach one of the precursors must be symmetrical or mixture of isomers will be produced. In some cases, these isomeric mixtures can be separated by careful column chromatography but the yields of individual porphyrins will be low. An alternative '3+1' version of the MacDonald condensation has been

developed that enables the synthesis of structures that cannot be prepared by the "2+2" approach, although one of the intermediates must again be symmetrical. Johnson first reported a MacDonald type "3+1" method for porphyrin synthesis in 1971.[16] In this condensation reaction (Scheme 12), tripyrrane dicarboxylic acids were reacted with dialdehydes to afford phlorins, which on subsequent oxidation using DDQ or chloranil generated porphyrinoid structures. Johnson initially used this approach to prepare oxa- and thiaporphyrins, but this methodology was later extended to the synthesis of porphyrins and porphyrin analogues. This approach makes other types of substitution patterns accessible, thus considerably expanding the library of porphyrin structures.[16] In the synthesis of heteroporphyrins **38**, a furan or thiophene dialdehyde **39** was condensed with a tripyrrane **40** under acidic conditions and following oxidation yielded monoheteroporphyrins (Scheme 12).[16]

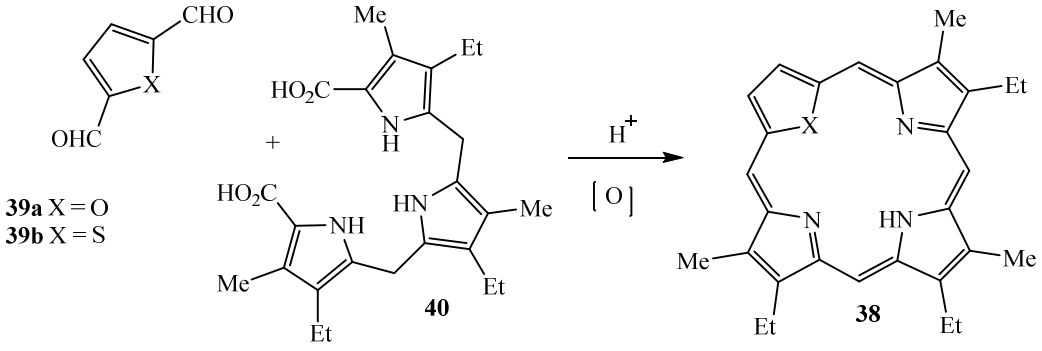

Scheme 12 Synthesis of Oxaporphyrins and Thiaporphyrins

The key precursors in the '3+1' MacDonald condensation are tripyrrolic intermediates commonly known as tripyrranes. The first example of a tripyrrane **41** was synthesized by Kenner and coworkers using 2-acetoxymethylpyrrole **42** and dipyrromethane **43**.[17] (Scheme 13). Sessler et al. later reported a more convenient method for preparing tripyrranes in which an α-unsubstituted

pyrrole **44** reacted with two equivalents of an acetoxymethylpyrrole **45** in the presence of an acid catalyst to generate **46**. Hydrogenation of **46** yields tripyrrane dicarboxylic acids **47** (Scheme 14).[18]

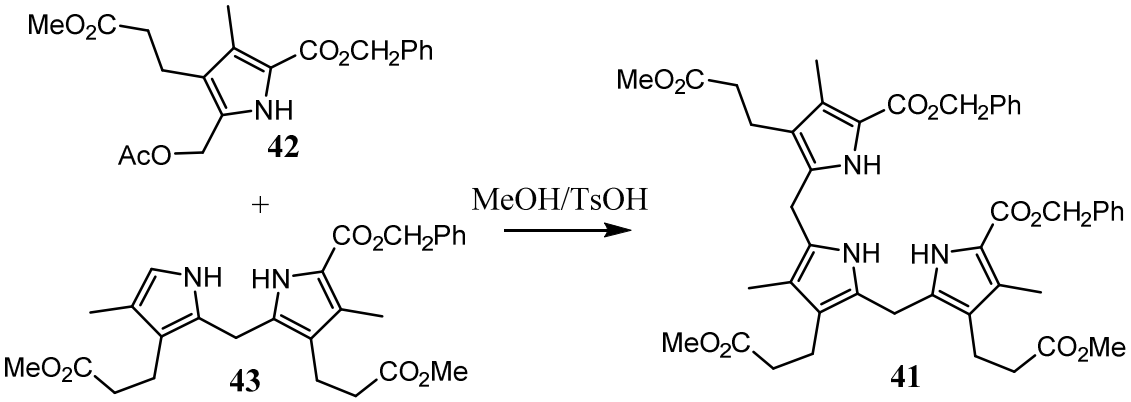

Scheme 13 Synthesis of the First Tripyrrane

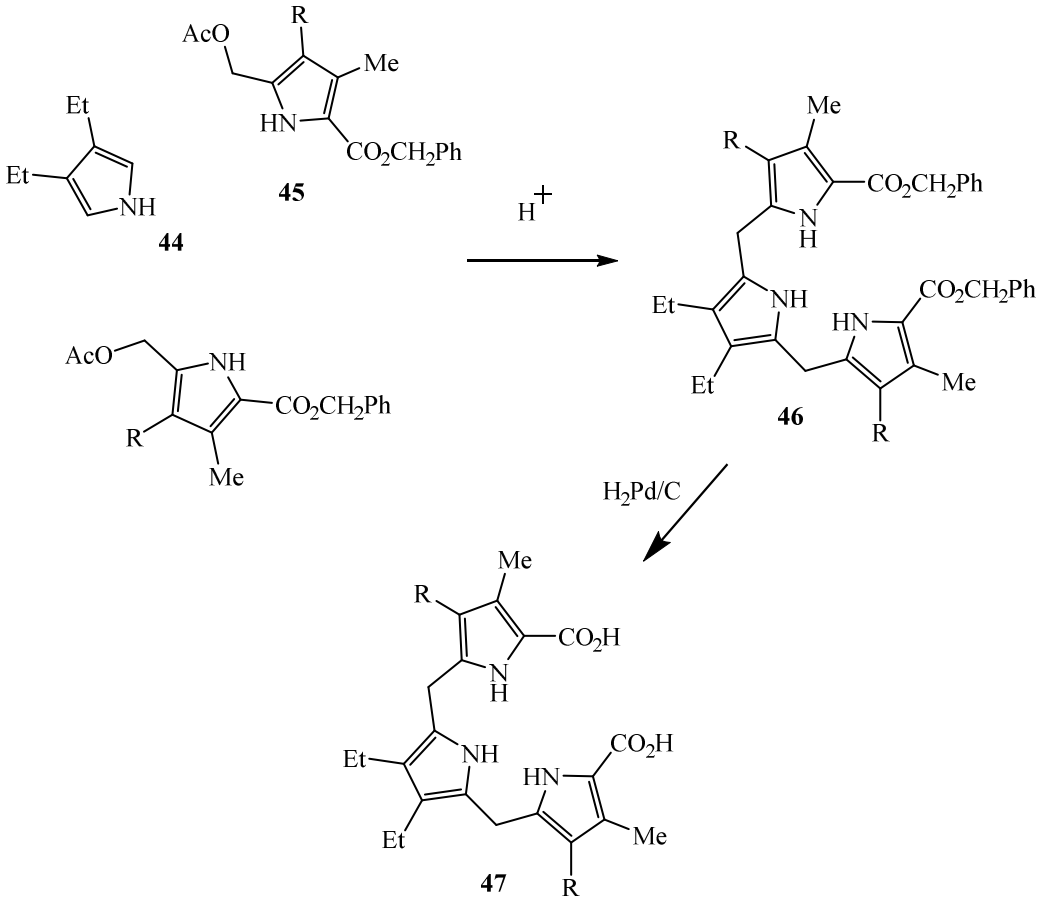

Scheme 14 Synthesis of Tripyrranes Reported by Sessler and Coworkers

Tripyrranes, in general, consist of three pyrrole rings linked by two methylene units. However, analogous structures have been prepared where the central pyrrole has been replaced with a heterocyclic or carbocyclic ring (Figure 8). Analogs of tripyrranes with benzene[19] or azulene[20] units in place of the central pyrrole ring have been prepared and have been utilized in the synthesis of highly modified porphyrinoid systems.[19,21,22] The '3+1' condensation has been used to prepare a variety of porphyrin analogs including carbaporphyrins. This method is very powerful and many different dialdehydes can be used to introduce exotic rings into the porphyrinoid framework.[23]

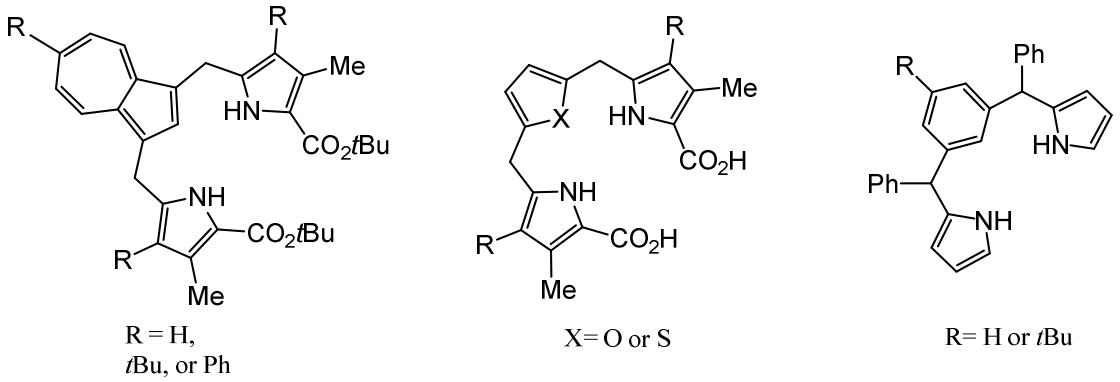

Figure 8 Structures of Tripyrrane Analogues Used in '3+1' Condensations

Porphyrins can also be synthesized by making use of tetrapyrrolic systems, such as bilanes, bilenes and biladienes. However, tetrapyrrole cyclizations are heavily conditions dependent. The tetrapyrrolic precursors are very reactive towards acid and can easily fragment or rearrange, hence limiting the scope of these reactions. However, when appropriate conditions are used, tetrapyrroles can remain intact and cyclize to generate isomerically pure porphyrins. For example, dipyrromethanes **48** and **49** condense under mild acidic conditions to generate b-bilene **50**. Following cleavage of the *tert*-butyl esters, the b-bilene cyclizes in the presence of a mixture of trifluoroacetic acid and trimethyl orthoformate, and following air oxidation generates isomerically pure porphyrin **51** in good yields (Scheme 15).[11]

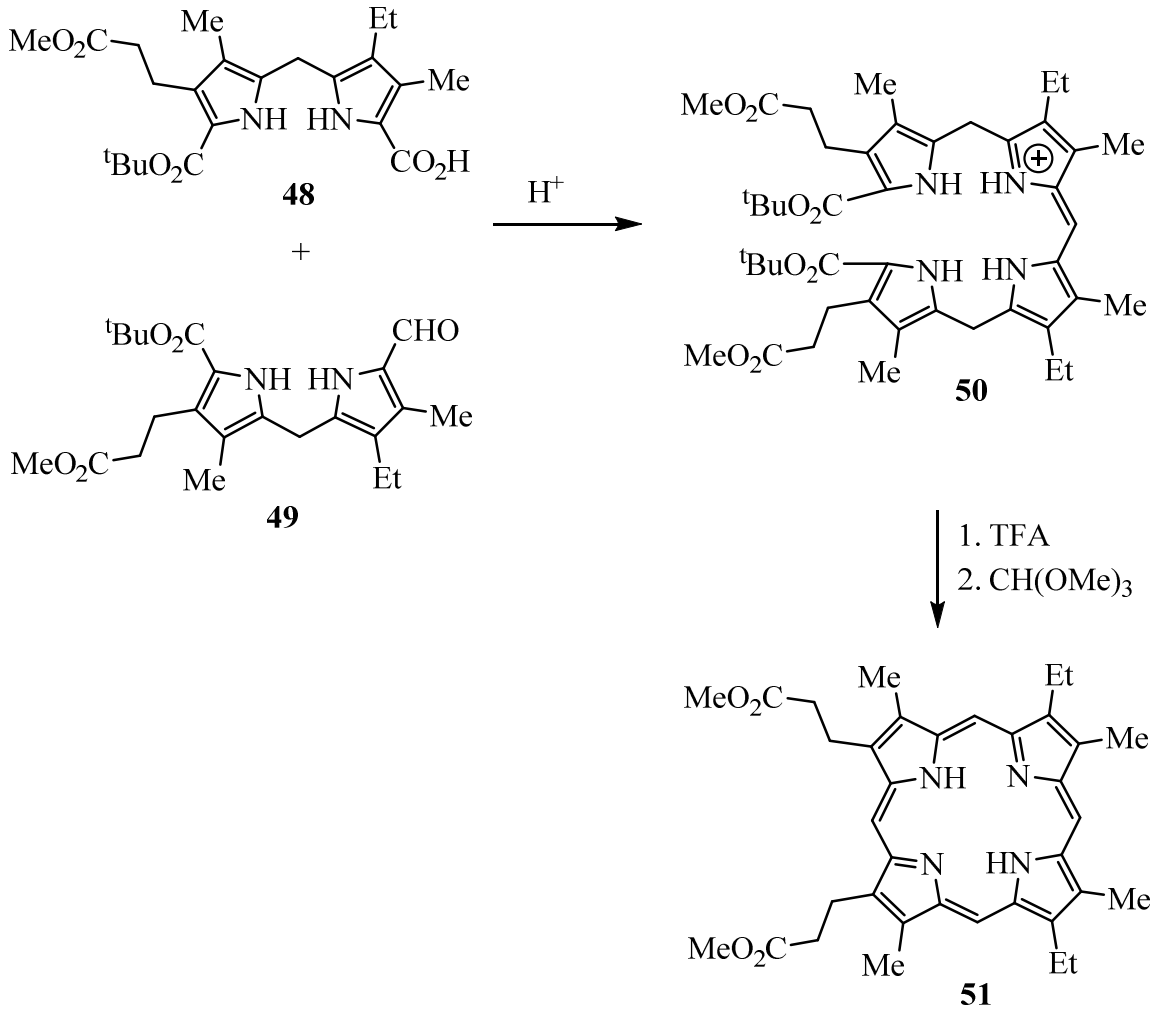

Scheme 15 Porphyrin Synthesis through a Tetrapyrrolic Intermediate

Reactivity of Porphyrins

Porphyrins are very reactive towards the formation of stable metal complexes. In fact, most of the porphyrins found in nature are present as metalated derivatives. Porphyrins have been found to form metal complexes with almost every metal and metalloid present in the periodic table; however, the first row transition metals, such as iron, cobalt etc. tend to form metalloporphyrins more readily compared to others.[2] Porphyrin analogs such as carbaporphyrins also coordinate with transition metal cations and in some cases stabilize unusual oxidation states. For instance,

benzocarbaporphyrins were shown to react with silver(I) acetate to form stable silver(III) complexes, and related gold(III) derivatives (Figure 9) have also been prepared from gold(III) acetate.[24] Other carbaporphyrin-like macrocycles have also been shown to give similar organometallic derivatives, e.g. tropiporphyrin (Figure 9).[37]

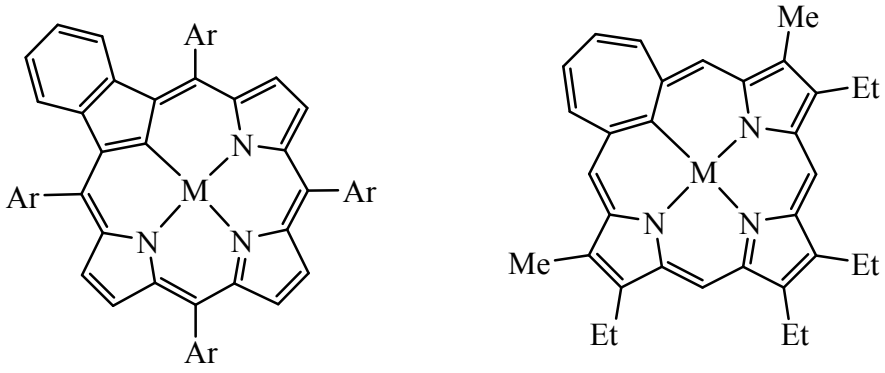

Figure 9 Carbaporphyrins Stabilizing Metals in Rare Oxidation States

Porphyrins and metalloporphyrins can readily undergo electrophilic substitution reactions. Metalloporphyrins are commonly substituted on their *meso*-carbons. However, if the coordinating metals used are in electrophilic oxidation states (e.g. Sn^{IV}), or the free-base porphyrin is used, the *meso*-carbons are deactivated towards electrophilic attack. This leads to electrophilic substitution being favored at the β-positions of the pyrrolic subunits. These differences are illustrated in Scheme 16 for the bromination of porphin.[2]

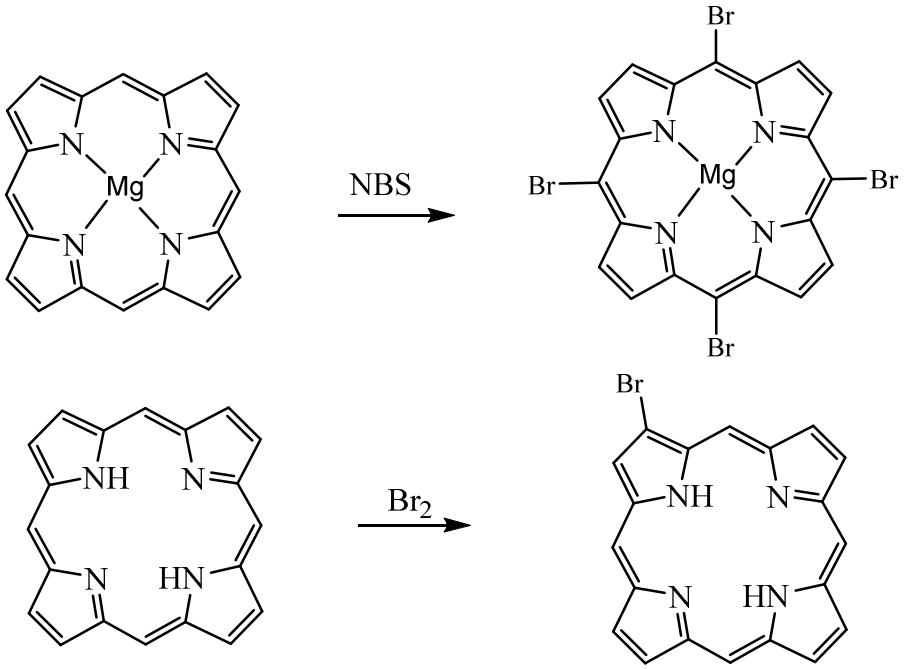

Scheme 16 Bromination of Porphyrins

Macrocycles Related to Porphyrins

Through the application of previously mentioned synthetic methods, such as 'one pot syntheses' and '3+1' condensations, many porphyrin-type macrocycles have been synthesized. These porphyrinoids include contracted porphyrins such as triphyrin **52**[25] and corrole,[2] and expanded porphyrins such as sapphyrin **53**[26] and texaphyrin[27] (Figure 10).

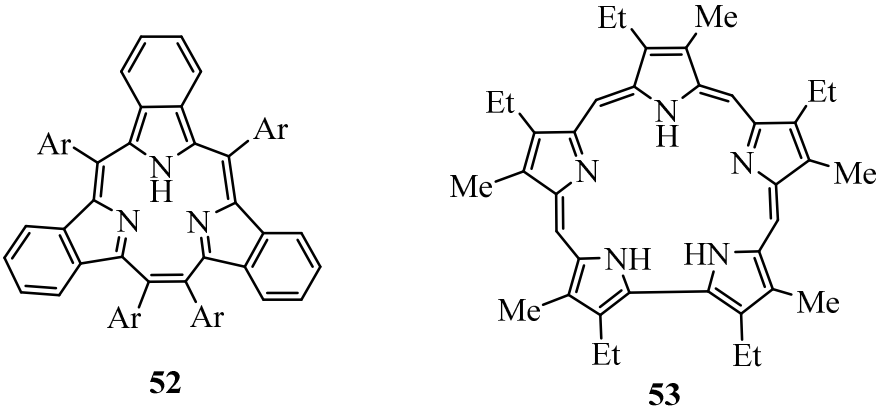

Figure 10 Structures of Contracted and Expanded Porphyrins

Phthalocyanines **54** are also structurally related to the porphyrins. These compounds are important synthetic pigments that are typically blue or green in color. They were first investigated by Sir Patrick Linstead, and like many other porphyrin-type structures, were found to be aromatic. In phthalocyanine **54**, each pyrrole ring is fused to a benzene ring and the pyrrole units are no longer connected by methine bridges but are instead linked by nitrogen atoms (Figure 11). Analogs of phthalocyanines have also been successfully synthesized. For instance, substitution of opposite isoindole units with benzene rings gave dicarbahemiporphyrazine **55,** although this structure no longer retains aromatic properties.[28]

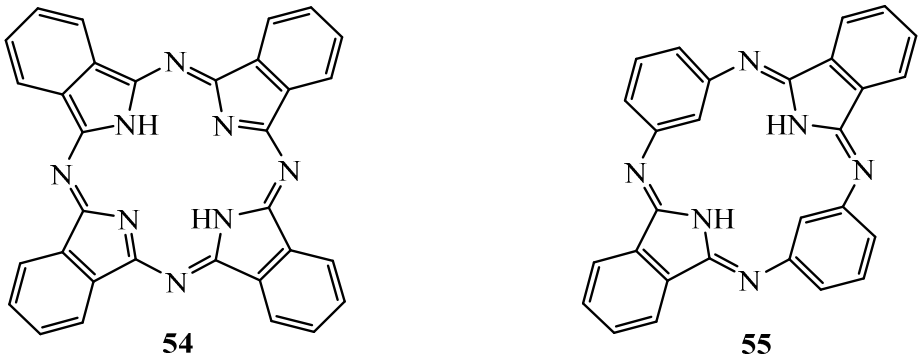

Figure 11 Structures of Phthalocyanine and Dicarbahemiporphyrazine

Applications

Synthetic porphyrins have a variety of applications, including as ligands in metal catalyzed reactions and as photosensitizers in photodynamic therapy (PDT). By changing the chromophores in porphyrin or its analogs, the macrocycle can be tuned for use in specific applications. For instance, in PDT (a treatment for cancer), the specific properties of the photosensitizer has great significance. PDT is a multistage process. Photosensitizer administration to the patient is carried out, either systemically or topically, in the absence of light. When a sufficient amount of photosensitizer appears in the diseased tissue, it is activated by exposure to light. The light dose supplies sufficient energy to stimulate the photosensitizer and transfer the energy to molecular oxygen. This results in the generation of reactive oxygen species such as singlet oxygen. The singlet oxygen thus formed is destructive, and damages the malignant tumor cells.[2] Porphyrins can be used as photosensitizers in PDT because they are good at absorbing light and transferring the absorbed energy to oxygen. They are excellent candidates as photosensitizers for PDT, as they tend to accumulate in malignant cells and not healthy cells.[29] In PDT, porphyrins or analogues that show strong absorptions in the 650-800 nm range are preferred as photosensitizers. N-confused porphyrins, carbachlorins and oxidized carbaporphyrins, for example, tend to have strong absorptions in the far red and thus can be used for this type of application.[23]

Metalloporphyrins have been widely used in asymmetric catalysis, including epoxidation,[30] cyclopropanation,[31] and Suzuki-Miyaura cross coupling.[32] Development of metalloporphyrins as catalysts was inspired by biological studies, such as the study of the cytochrome P450 family of monooxygenases. These enzymes contain hemes (iron porphyrins) that act as cofactors, and have been found to exhibit a broad range of functions. One of the most significant functions of this class of enzymes is the elimination of foreign molecules in the body

through biotransformation. This family of enzymes is responsible for partial metabolism of the majority of medicines consumed by humans.[33] Another example of metalloporphyrin catalysts are manganese porphyrins absorbed on a gold surface that can react with molecular oxygen from air to carry out epoxidation of cis-stilbene to cis-stilbenoxide.

Aside from catalyzing organic reactions or being used as medicinal agents, porphyrins in the modern world can also be utilized as chemosensors for nuclear waste. Expanded porphyrin analogues have been found to bind with actinides and other heavy elements better than traditional porphyrins. These expanded macrocyclic systems can also be used for the detection of hazardous metals such as uranium or plutonium that are often used as a source for nuclear energy.[34]

Phthalocyanines, which are closely related to porphyrin macrocycles, have also been shown to have numerous applications. They are also very stable compounds. For example, one of the first phthalocyanines characterized by Linstead was stable up to 500 °C and in the presence of concentrated sulfuric acid. Thus, these macrocycles and their analogues can be used as dyes for inks, paper, and paint and have applications as lubricants and semiconductors.[2]

Porphyrins and phthalocyanines have also been shown to exhibit phosphorescence and fluorescence properties.[28] The phosphorescence and fluorescence properties of porphyrins can be quenched by molecular oxygen. Thus, another application of porphyrins and phthalocyanines is monitoring of oxygen levels used in various arenas from ecological, industrial, and medicinal standpoints. These macrocycles can therefore serve the purpose of optical sensors for molecular oxygen.[28] The concentration of molecular oxygen in the gas or liquid phase is proportional to the decay of phosphorescence in the porphyrin and phthalocyanine.[28] The most common porphyrin optical sensors are palladium(II) and platinum(II) metalloporphyrins. In addition, ruthenium(III) and iridium(III) metalloporphyrins have also exhibited high phosphorescence at room temperature

and could possibly be used as alternative oxygen sensors in the near future.[2]

Carbaporphyrins

In order to gain a better understanding of the reactivity and characteristics of porphyrins, chemists began to investigate core modified porphyrins. The study of core modified porphyrins helps to reveal the effect that modification of a conjugated system has on its properties and its characteristics. Systems with a carbon atom inserted into the core of the porphyrin, the so-called carbaporphyrinoid systems, have been of particular interest. These systems have been widely investigated and have shown unique properties, such as formation of organometallic derivatives under mild conditions.[35] Related systems include N-confused porphyrin **56**,[36] benzocarbaporphyrins **57**,[35] tropiporphyrins **58,**[37] azuliporphyrins **59**[38] and benziporphyrin **60**[39] (Figure 12).[35]

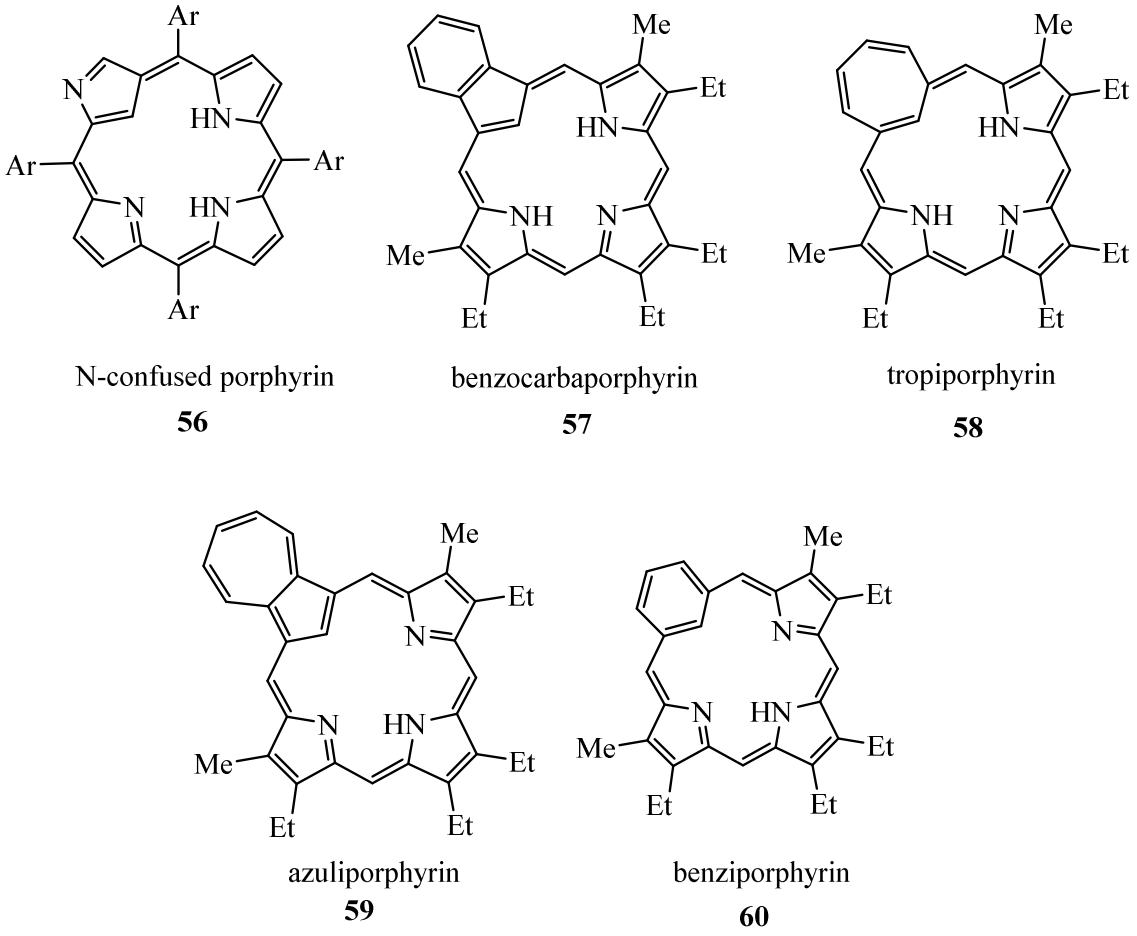

Figure 12 Monocarbaporphyrin Analogues

These porphyrin analogues can be subdivided into "true" carbaporphyrins and "modified" carbaporphyrins. In true carbaporphyrins, at least one of the pyrrolic units is replaced with a cyclopentadiene or indene unit. In modified carbaporphyrins, a carbocyclic ring system other than a cyclopentadiene unit is used to replace a pyrrole moiety.[35] For instance, by replacing a pyrrolic unit within the porphyrin framework with azulene, cycloheptatriene, or benzene, new families of porphyrin-like macrocycles were produced. True carbaporphyrins such as benzocarbaporphyrin **57** are fully aromatic structures, while benziporphyrins **60** do not have aromatic character, and azuliporphyrins **59** fall midway between the two extremes.[35]

In benzocarbaporphyrins **57**, porphyrin-like UV−vis spectra are retained and these compounds are highly diatropic, as judged by proton NMR spectroscopy. However, azuliporphyrins **59** are cross-conjugated and have considerably reduced diatropic character, while tropiporphyrins **58** have intermediary properties due to the nonplanar nature of the seven-membered ring.[35] In principle, if more than one nitrogen atom in the cavity is replaced with carbon atoms, this results in the formation of dicarbaporphyrins, tricarbaporphyrins and tetracarbaporphyrins (Figure 13).[41]

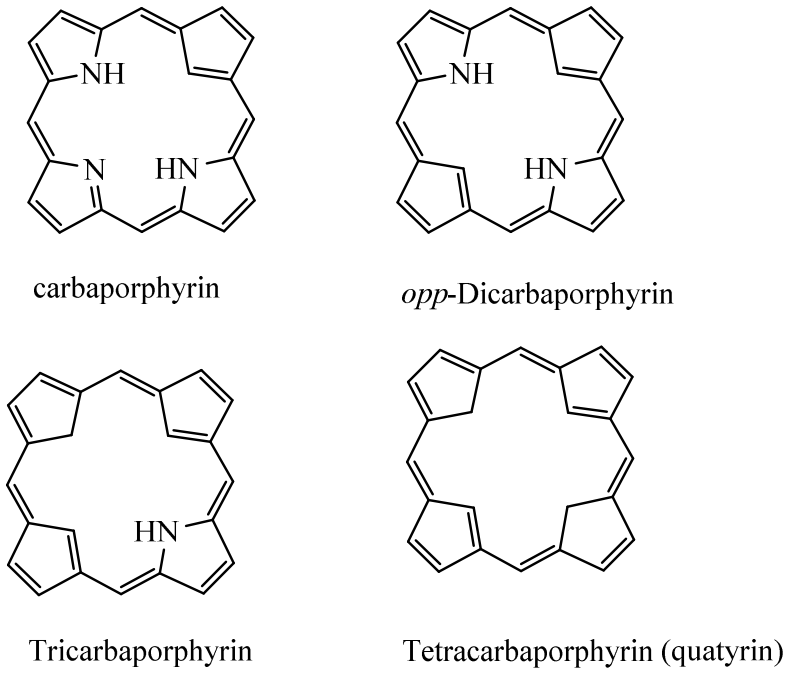

Figure 13 Mono-, Di-, Tri- and Tetracarbaporphyrins

Carbaporphyrins can easily be synthesized by the "3+1" condensation approach.[16] One of the best studied classes of carbaporphyrins are the benzocarbaporphyrins. In benzocarbaporphyrins **57**, one of the pyrrole units is replaced with an indene unit. These compounds are prepared by the acid catalyzed condensation of indene dialdehyde **61** with tripyrrane **62** (Scheme 17)[40]. Following

oxidation with 2,3-dichloro-5,6-dicyano-1,4-benzoquinone (DDQ), carbaporphyrin **57** was isolated in > 40% yield.

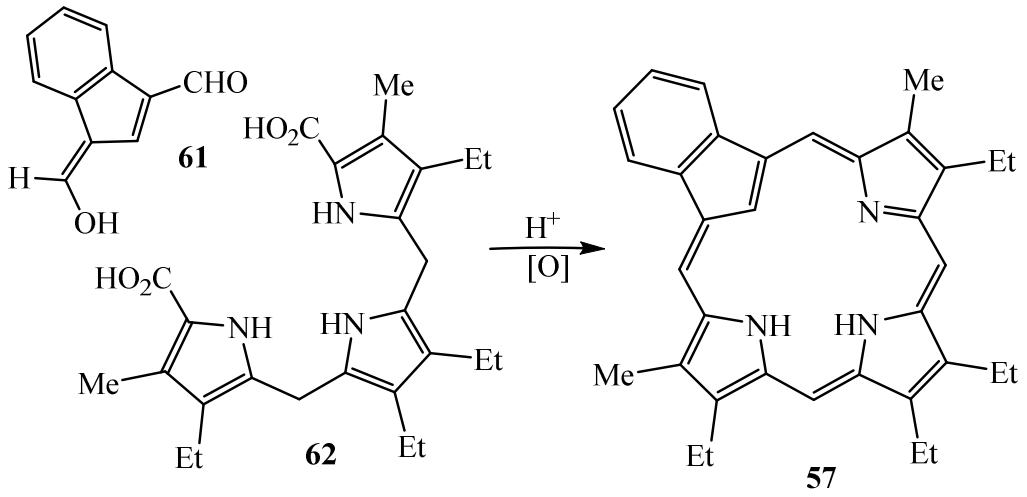

Scheme 17 Synthesis of Benzocarbaporphyrin

Benzocarbaporphyrins can also be prepared from azuliporphyrin **63**. In this method, azuliporphyrins **63** undergo an oxidative ring contraction when exposed to *tert*-butyl hydroperoxide under basic conditions to generate the fused benzene ring. This approach provides an indirect route to tetraaryl benzocarbaporphyrins **64** (Scheme 18).[42,43]

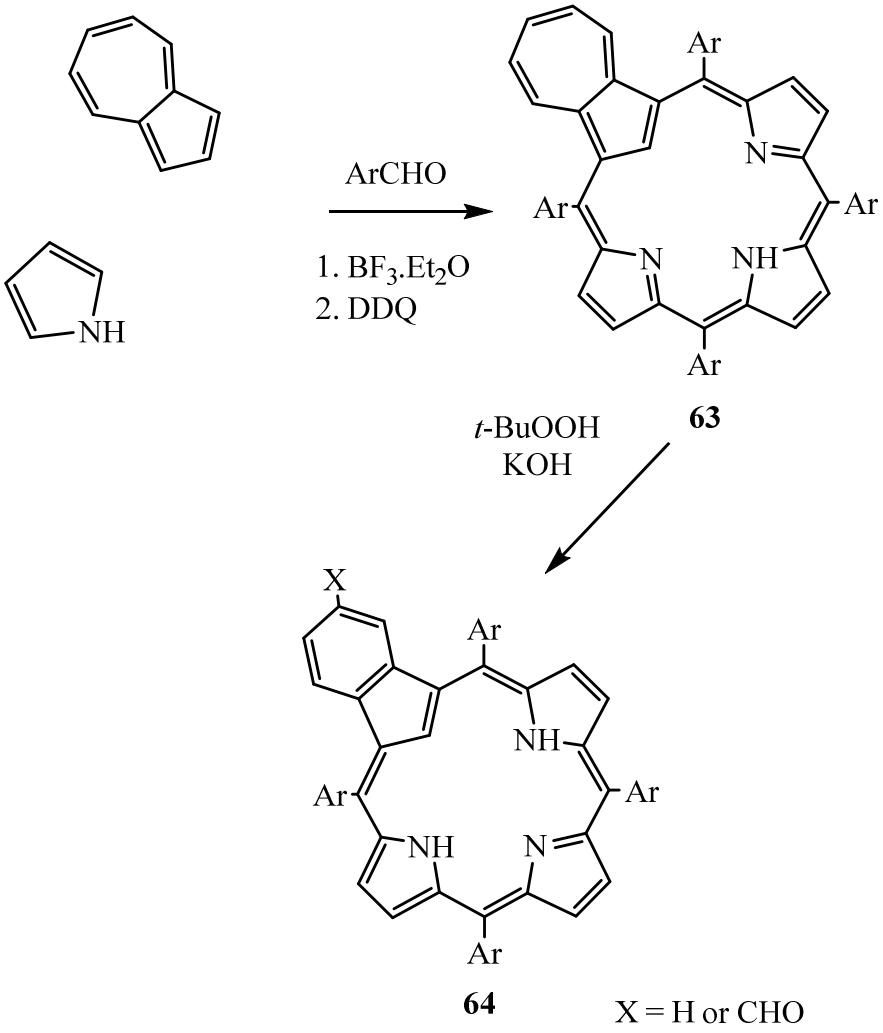

Scheme 18 Synthesis of Tetraaryl Benzocarbaporphyrins

from Tetraarylazuliporphyrins

Tetraarylazuliporphyrin **63** can be easily prepared by reacting pyrrole, azulene and an aromatic aldehyde together in the presence of boron trifluoride etherate. This route to benzocarbaporphyrins is less effective than the '3+1' methodology as two or more porphyrinoid products result from the oxidative ring contractions. Nevertheless, this approach is currently the only method available for synthesizing tetraaryl carbaporphyrins.[42,43]

Protonation of benzocarbaporphyrin **65** can lead to the formation of both mono and dicationic species.[44,45] Upon addition of acid, protonation initially occurs on the pyrrolenine nitrogen to give the monocation **65**H^+. At higher acid concentrations, further protonation takes place on the internal carbon to give dication **65**H_2^{2+} (Scheme 19).[45] The second protonation goes to completion in 50% TFA-chloroform solution, and results in the generation of a new chromophore. Proton NMR spectroscopy in 50% TFA-$CDCl_3$ strongly suggests that the dicationic species retains its aromatic characteristics. In azuliporphyrins, protonation of the internal carbon atom has not been observed.[35]

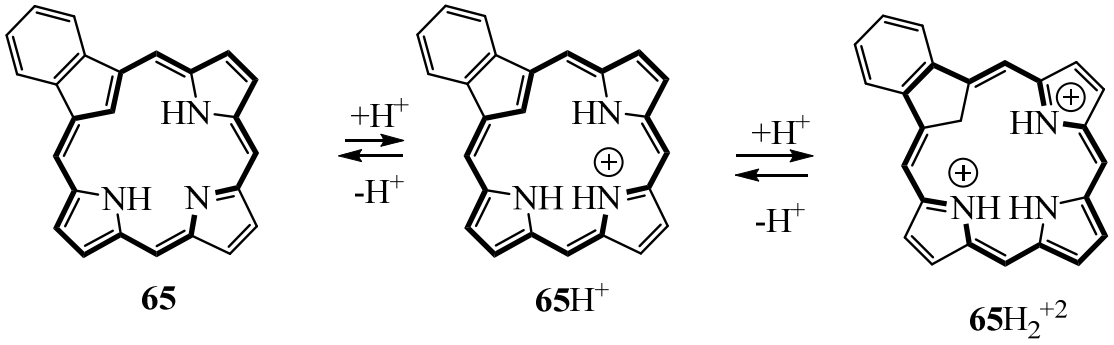

65 **65**H^+ **65**H_2^{+2}

Scheme 19 Protonation of Benzocarbaporphyrin

Benzocarbaporphyrins **66** were found to react with silver(I) acetate to give stable silver(III) organometallic complexes **67** (Scheme 20).[46,47] The silver complex retains porphyrin-like UV-vis spectra, showing strong a Soret band at 437 nm, along with characteristic Q bands at 482, 518, 555 and 593 nm. The *meso*-protons show up at 9.89 and 10.06 ppm, thereby confirming that the silver complex has strong diatropic character. Unlike the carbaporphyrin free base, the silver complex of benzocarbaporphyrin **67** was near planar and indene unit was only tilted by 5.08°.[46]

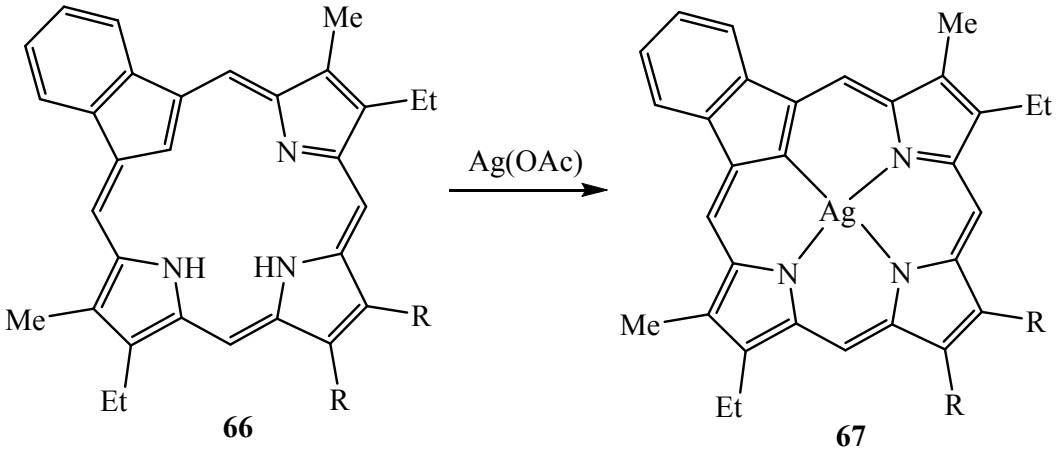

Scheme 20 Synthesis of Silver(III) Benzocarbaporphyrin

Reaction of *meso*-unsubstituted benzocarbaporphyrins **66** with gold(III) acetate gave low yields of the related gold(III) complexes **68** (Scheme 21).[47] However, much better yields were obtained in the metalation of *meso*-tetraaryl benzocarbaporphyrins **64**.[35] Gold complexes of benzocarbaporphyrins also have strongly aromatic characteristics and gave similar UV-visible spectra to silver complexes **67**.[35]

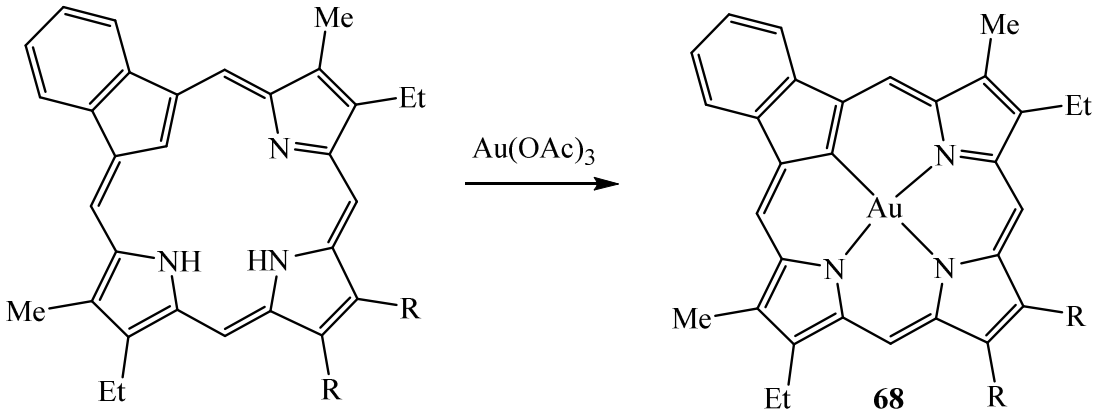

Scheme 21 Synthesis of Gold(III) Benzocarbaporphyrin

Recently, rhodium and iridium complexes of benzocarbaporphyrin **57** have also been obtained in good yields (Scheme 22). Reaction of **57** with 1 equiv of di-μ-chlorotetracarbonyldirhodium(I) in refluxing dichloromethane gave the rhodium(I) dicarbonyl complex **69** in 90% yield. The proton NMR spectrum for **69** showed the presence of strong diamagnetic ring currents. Upon refluxing **69** in pyridine, a hexacoordinate rhodium(III) complex **70** was generated in 55% yield. In addition, when **57** was reacted with $[Ir(COD)Cl]_2$ in refluxing pyridine, iridium(III) derivative **71** was generated in 22% yield. The X-ray structures for these derivatives showed that the macrocycle was near planar and the bond lengths were consistent with the aromatic structures.[48]

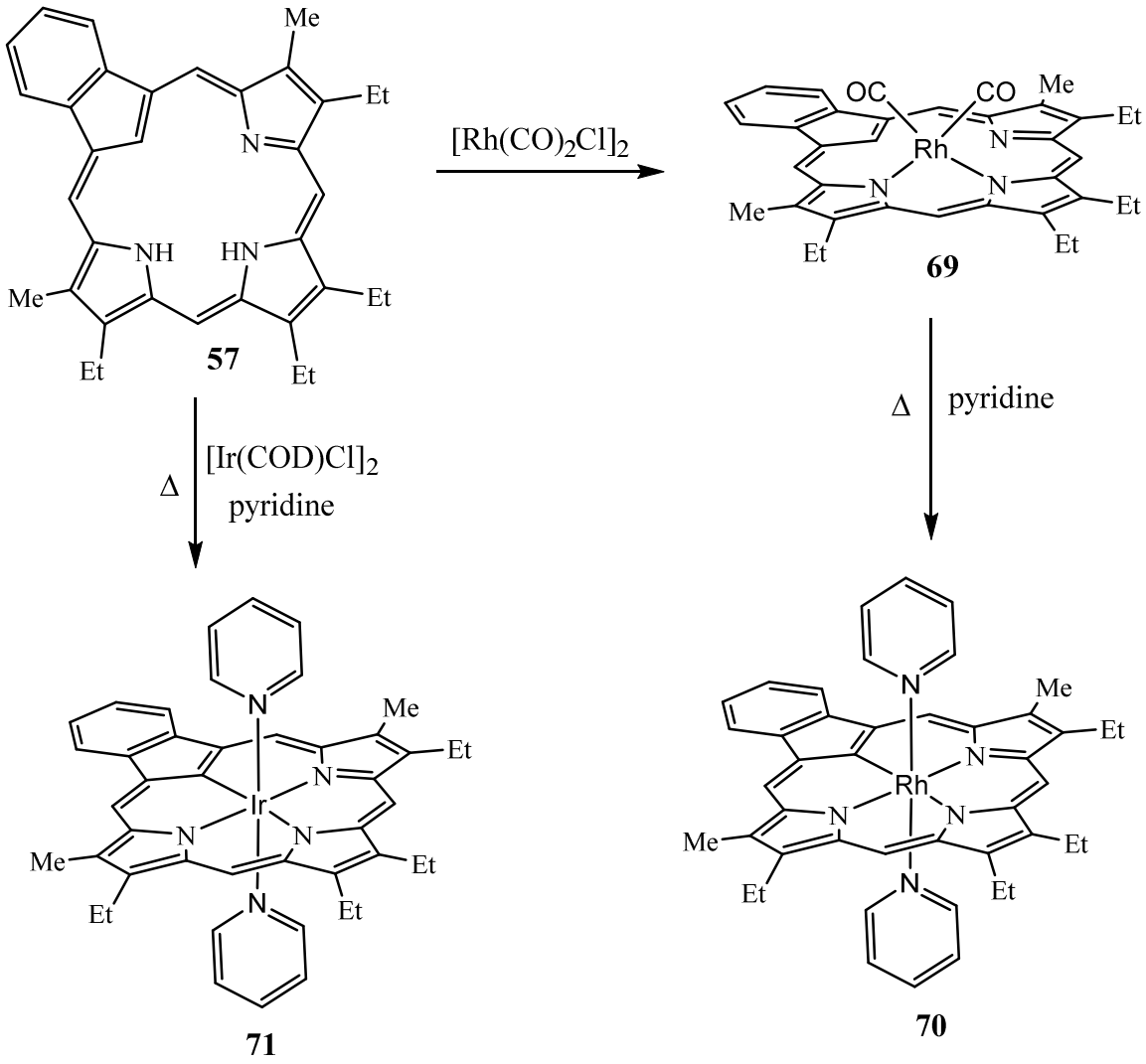

Scheme 22 Formation of Ir and Rh complexes of Benzocarbaporphyrin

Benzocarbaporphyrins also readily react with methyl iodide in the presence of potassium carbonate in refluxing acetone to give alkylated products. In this reaction, it was observed that N-methyl carbaporphyrin **72** was the major product along with some C-alkylated by-product **73** (Scheme 23). The major product of this reaction is a chiral system, whereas the minor C-methyl product possesses a plane of symmetry. Although the presence of internal substituents may reduce the planarity of these structures, these derivatives retain strongly diatropic characteristics.[49]

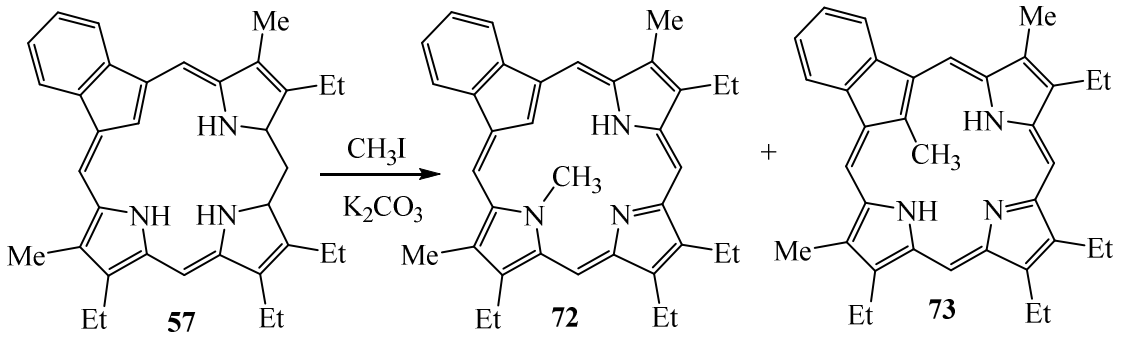

Scheme 23 Alkylation of Benzocarbaporphyrin

Unexpectedly, reaction of N-methyl carbaporphyrin **72** with palladium(II) acetate led to the formation of a palladium(II) complex **74** where the methyl group has migrated from the nitrogen atom to the carbon atom (Scheme 24).[49] The NMR spectrum of **74** showed that the complex is highly aromatic and the internal methyl resonance shifted upfield to -3.21 ppm.

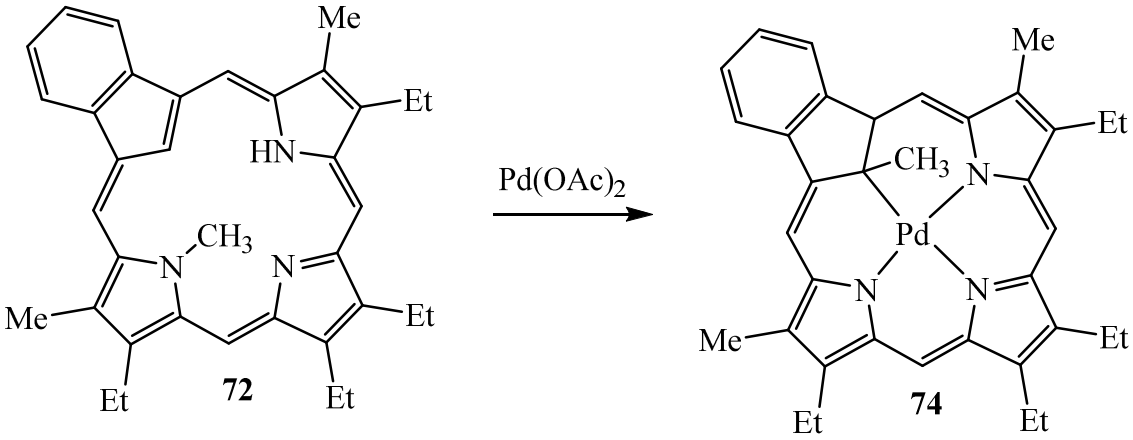

Scheme 24 Unexpected Alkyl Group Migration

Reaction of benzocarbaporphyrin **57** with ferric chloride did not generate metal complexes but instead gave various regioselective oxidation products.[50, 51] When the reaction was carried out using 500 equivalents of ferric chloride in a refluxing alcohol solvent, ketal derivatives **75** were generated in high yields. These ketal derivatives were isolated in the monoprotonated form, generally as the hydrochloride salt, and exhibited strong absorptions in the far red. Further protonation of **75** using trifluoroacetic acid generated the related dicationic species. The proton NMR spectra for **75** showed that these ketals retain strong diatropic characteristics and have a plane of symmetry. For this system, the *meso*-protons in the proton NMR spectra showed up at 9.68 and 10.93 ppm. The far-red absorptions exhibited by these derivatives indicate that carbaporphyrin ketals could have potential applications, for instance as photosensitizers in the photodynamic therapy (PDT). In fact, **75**·HCl has been shown to be an effective agent in the treatment of leishmaniasis.

When the oxidation reaction was attempted using an aqueous solvent system for one hour, a chloro derivative **76** was isolated in good yields. The chloro carbaporphyrin again retains strongly aromatic characteristics, and the proton NMR spectrum of **76** showed that the *meso*-protons were shifted to below 9.5 ppm. This is interesting as the X-ray crystal structure of the chloro derivative shows that the indene subunit is significantly tilted away from the macrocyclic plane due to the presence of a large internal Cl atom, hence substantially disturbing the planarity of the molecule. In addition, the UV−vis spectrum of **76** shows a split Soret band at 421 and 434 nm, and Q bands at 521, 560, 608, and 665 nm, again signifying its porphyrin-like characteristics.[51]

When the reaction was carried out with ferric bromide instead of ferric chloride, under the same reaction conditions, the corresponding bromo derivative of **76** was isolated in 7% yield. Even though the larger bromine atom will undoubtedly further distort the macrocycle, the proton NMR

spectrum for **76b** showed that the macrocycle surprisingly retained nearly all of its diatropic characteristics. As reactions carried out in the presence of refluxing alcohols led to the formation of ketals, it was anticipated that reactions using aqueous ferric chloride would afford the corresponding dihydroxy products **77** or the related ketone. When the reactions with aqueous ferric chloride were carried out for 16 h, a polar green byproduct **77** was isolated in 22% yield (Scheme 25).[51] The proton NMR spectrum for this diketone showed that this species was nonaromatic. The two carbonyl units gave rise to resonances at 173.6 and 197.6 ppm in the carbon-13 NMR spectrum, but the IR spectrum showed the C=O stretching peaks at unusually low wave numbers. The low frequencies can be attributed to the vinylogous amide nature of these bonds, which greatly reduce the bond strengths.[51]

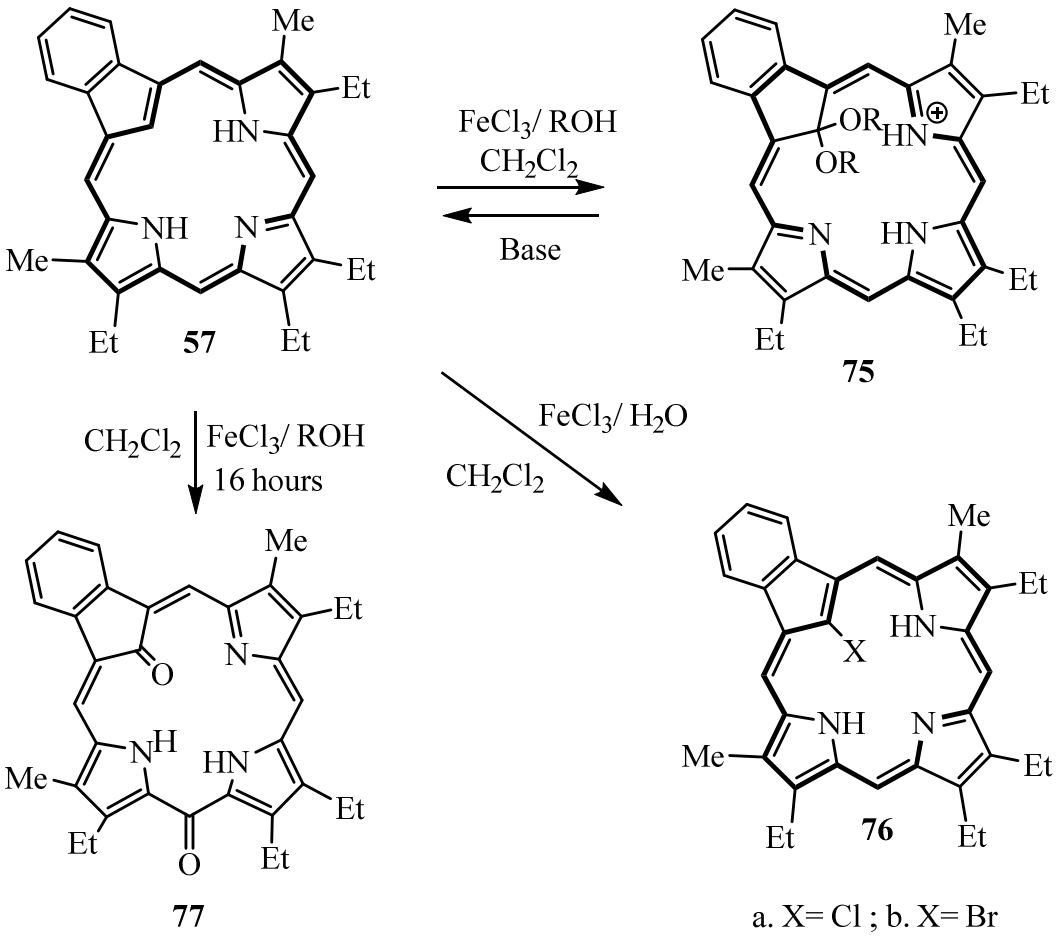

Scheme 25 Oxidation of Benzocarbaporphyrin with $FeCl_3$

As carbaporphyrins exhibit new and interesting chemistry, steps toward the synthesis of doubly modified systems were also undertaken. In the first successful synthesis of this type, indane dialdehyde **78** was reacted with one molar equivalent of diethylpyrrole **44** in the presence of a strong acid, and subsequent oxidation with $FeCl_3$ generated the dibenzo *opp*-dicarbaporphyrin **79** in moderate yields (Scheme 26).[52] Dibenzo *opp*-dicarbaporphyrin **79** proved to be somewhat unstable in solution. Also, the low solubility of **79** in halogenated solvents made characterization and in-depth reactivity studies very difficult. However, spectroscopic studies did show that the

system has strongly diatropic character as the proton NMR spectrum showed an upfield singlet for the internal CH proton near -6 ppm, while the NH protons appeared near -5 ppm. The *meso*-protons for this compound were strongly shifted downfield to around 9.8 ppm. The dicarbaporphyrin also gave a UV-Vis spectrum that closely resembled true porphyrins with a strong Soret band near 450 nm and a series of weak Q bands in the visible region.[52]

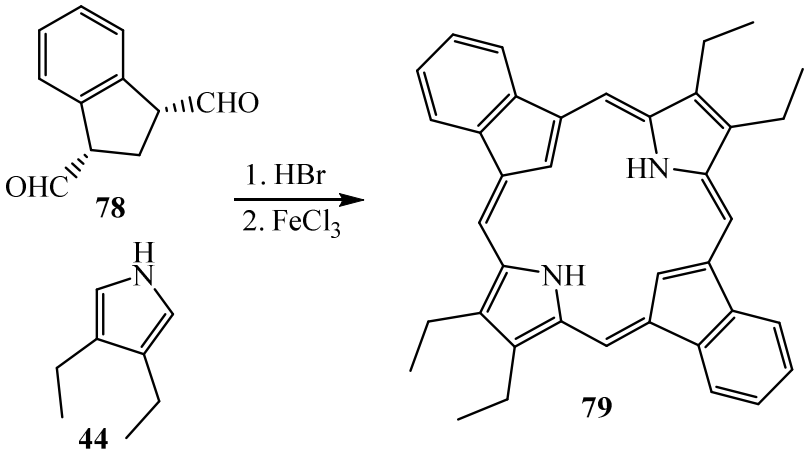

Scheme 26 Synthesis of Dibenzo *opp*-Dicarbaporphyrin

When **79** was protonated using a minimal amount of acid, it was observed that C-protonation readily occurred to give monocation **79**H^+ (Scheme 27),[52] and this caused a significant change in the UV-Vis spectrum of **79**. The Soret band was greatly diminished. In addition, a band developed near 500 nm, and a strong absorption emerged near 750 nm. Proton NMR spectroscopy showed that protonation had taken place at an internal carbon position, and this addition caused little change in the diatropic nature of the system. The internal sp^3 CH_2 protons of the protonated species were observed just above -4 ppm, while the CH proton was detected above -3 ppm. This slight reduction in the upfield shift was balanced by a slight downfield shift of the *meso* protons to

+10 ppm. Diprotonation of dibenzo *opp*-dicarbaporphyrin was never observed even with TFA concentrations in excess of 50%. This may be due in part to the increased steric hindrance that would result from placing six hydrogens within the porphyrin core.[52]

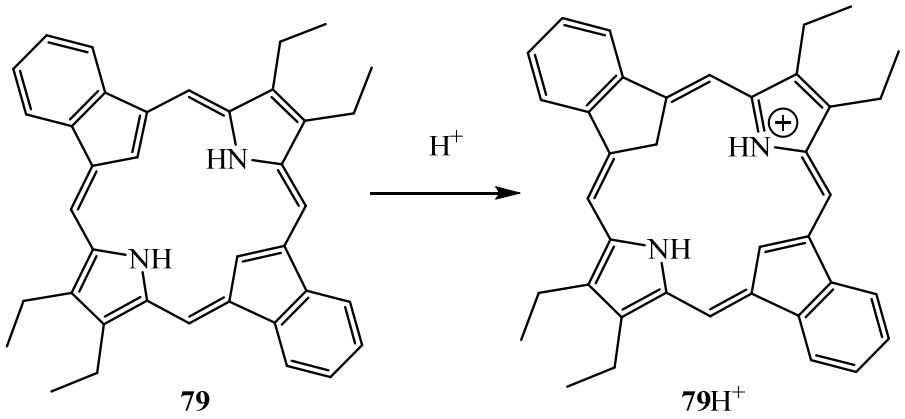

79 **79**H^+

Scheme 27 Protonation of Dibenzo *opp*-Dicarbaporphyrin

Carbachlorins

Chlorophylls are the central constituents in the engine of photosynthesis by which plants harvest their energy. The structural nucleus of the chlorophylls is a dihydroporphyrin or chlorin **14** where one of the β,β-pyrrolic double bonds has been reduced.[2] Studies of chlorin chemistry are very important due to several reasons. These include the structure elucidation and total synthesis of naturally occurring chlorophylls. In addition, chlorins show strong absorptions in the red region of their UV-Vis spectra and synthetic chlorins have potential applications as photosensitizers in PDT.

Even though one of the double bonds found in porphyrins has been reduced in chlorins, the system still possesses an 18 π electron delocalization pathway. For this reason, chlorins are aromatic compounds (Figure 14).[53]

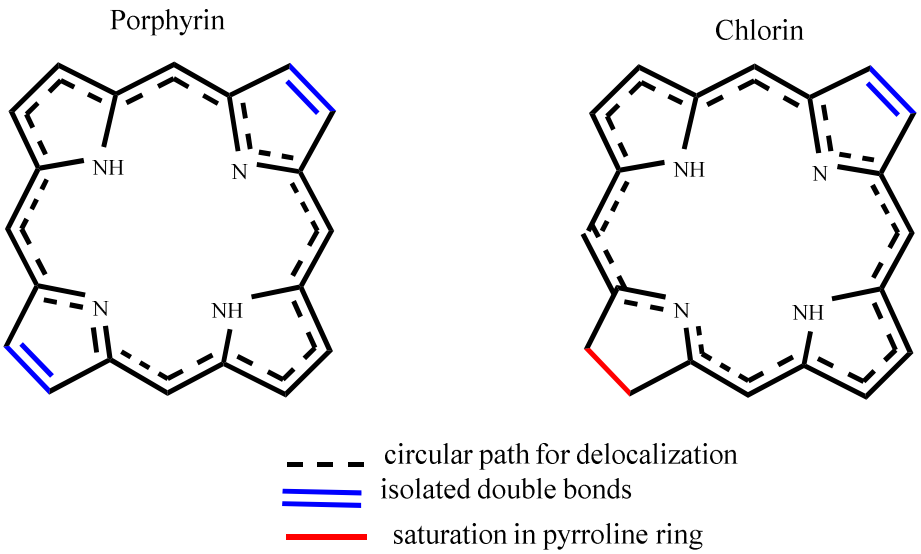

Figure 14 Aromatic Delocalization Pathways in Porphyrin and Chlorin

Chlorins are isomers of nonaromatic phlorins and can potentially interconvert by prototropic tautomerization (Scheme 28). In reactions that involve the intermediacy of *meso*-hydrogenated tetrapyrroles such as porphyrinogens, tautomerization followed by $4e^{-}/4H^{+}$ oxidation leads to the formation of chlorin. This type of tautomerization may be a source of chlorin contamination in one-flask syntheses of porphyrins.[53]

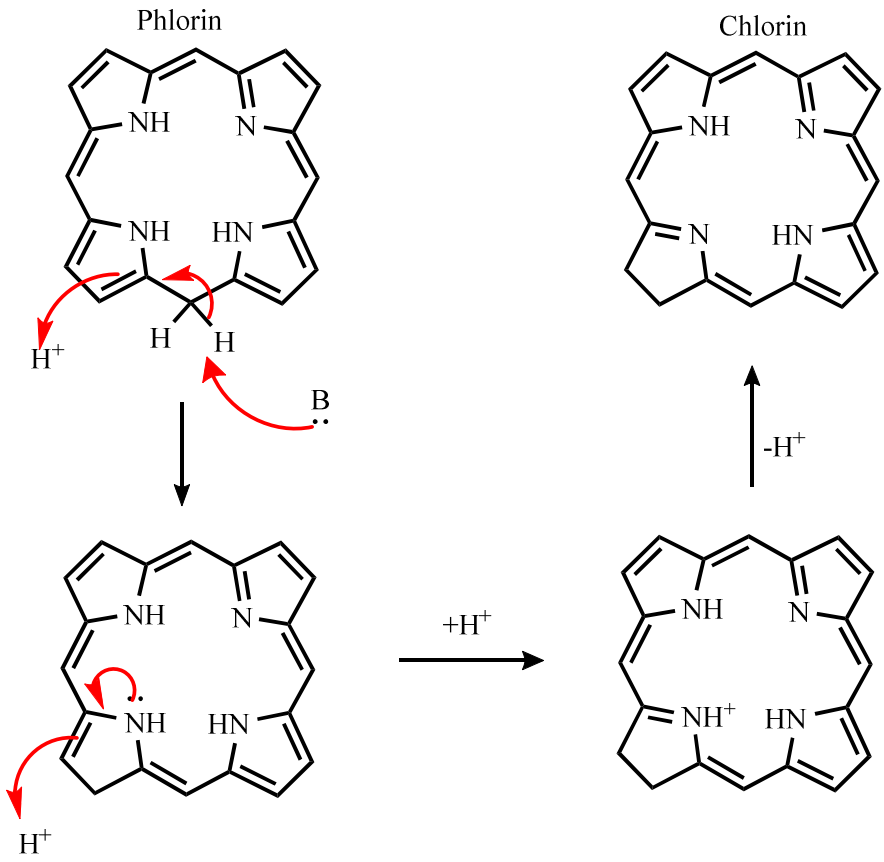

Scheme 28 Phlorin-Chlorin Conversion

Although a great deal of work has been carried out in the field of synthetic chlorin chemistry by various groups, few studies have explored the preparation of analogous systems such as carbachlorins that may have equally useful properties. Carbachlorins are chlorin analogues in which one of the core nitrogen atoms are replaced with a carbon atom (Figure 15).

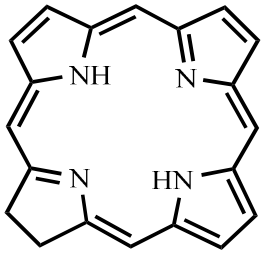

Chlorin

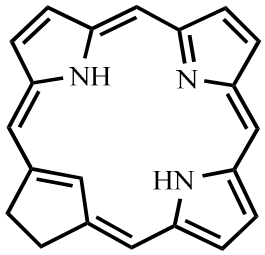

Carbachlorin

Figure 15 Structures of Chlorin and Carbachlorin

In 1998, Lash and Hayes reported the synthesis of carbachlorins **80** using a "3 + 1" variant on the MacDonald condensation (Scheme 29).[54] In this synthesis, bicyclic dialdehydes **81** were condensed with tripyrrane **62** in the presence of TFA and subsequent oxidation with DDQ led to the formation of propanocarbachlorin **80a** and propenocarbachlorin **80b** in moderate yields. It was interesting to note that these chlorin analogues retained aromatic characteristics, and in the proton NMR spectra the inner CH protons showed up around -7 ppm. The UV-vis spectra of these analogues were also very porphyrin-like, showing a strong Soret band at 404 nm and a series of small absorptions that culminated in a medium sized Q band at around 650 nm. However, although true chlorins are easily oxidized to give porphyrins, attempts to further oxidize chlorin analogues **80a** or **80b** to the corresponding carbaporphyrins **82** were unsuccessful.[54]

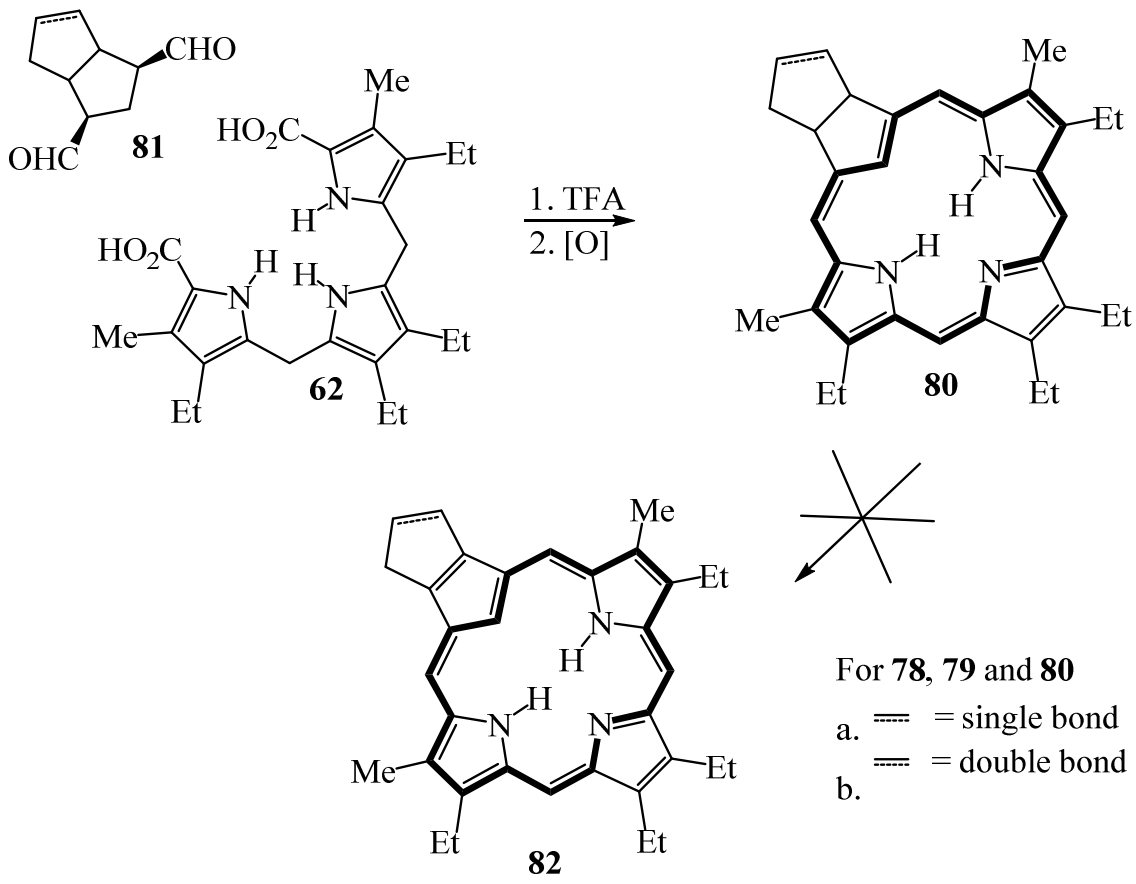

Scheme 29 Synthesis of Carbachlorins with Fused Five-membered Rings

In order to further explore the chemistry of carbachlorins, Lash and Hayes attempted to synthesize porphyrinoid **83** by condensing 1,3-cyclopentanedicarbaldehyde **84** with a tripyrrane **62** (Scheme 30).[55] However, no chlorinoid product was formed in these experiments. It was speculated that the presence of β-pyrrolic substituents or the additional five-membered rings in structure **82** aids in the generation of porphyrinoid products by altering the conformation of the intermediates and facilitating the cyclization. For instance, indene dialdehyde **85** on treatment with tripyrrane yields benzocarbaporphyrins **86** and cyclopentadiene trialdehyde **87** similarly reacted with tripyrrane to give carbaporphyrin aldehyde **88**, albeit in low yields (Scheme 30).[55]

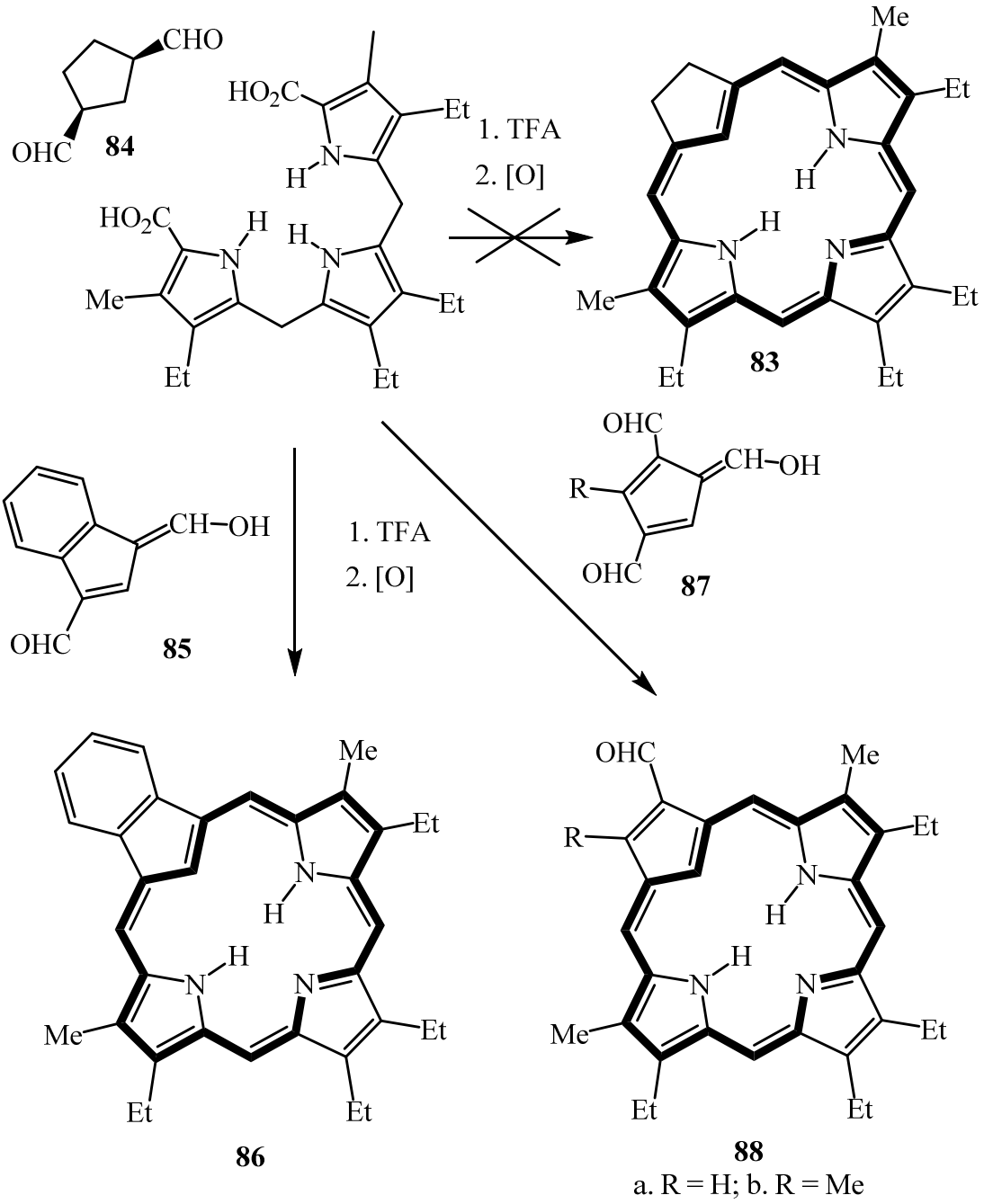

Scheme 30 Synthesis of Carbaporphyrins and an Attempted Synthesis of a Carbachlorin

These results indicate that conjugated dialdehydes or aromatic dialdehydes such as **85** and **87** are more effective precursors in the "3 + 1" condensation reactions than aliphatic dialdehydes

such as **84**. Therefore, in later studies, conjugated cyclopentene dialdehydes such as **89** were targeted as precursors for carbachlorin formation (Scheme 31). Attempts to prepare **89** from a related acetal were unsuccessful but a similar enol ether **90** could be obtained instead (Scheme 32). This species was very unstable and was immediately used to prepare carbachlorin **83**.

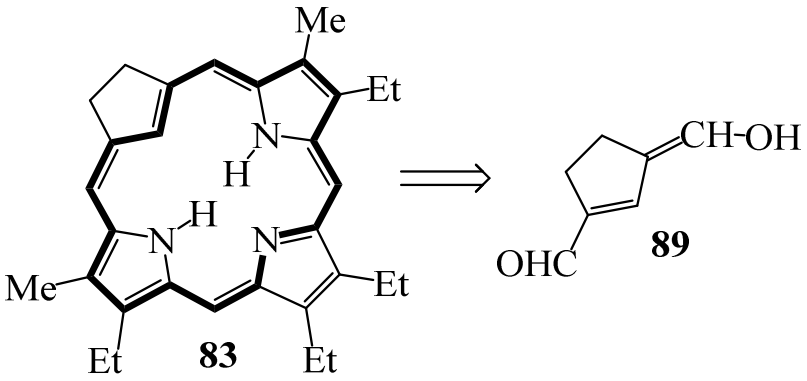

Scheme 31 Retrosynthesis of Desired Dialdehyde

In the reaction, **90** was directly condensed with tripyrrane dicarboxylic acid to generate carbachlorin **83** in 11 – 16% yield (Scheme 32).[55]

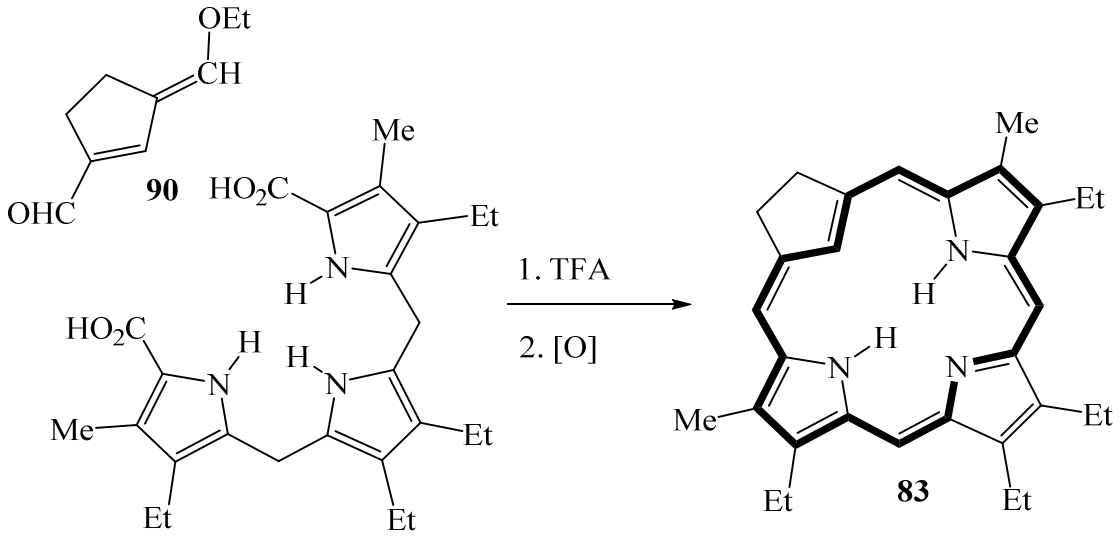

Scheme 32 Synthesis of Carbachlorin

Carbachlorin **83** was aromatic in the free base form, displaying strong diatropic character with the internal CH proton showing up at -6.93 ppm, while the *meso*-protons were downfield appearing at 9.01 and 9.68 ppm. Since there were only two signals for the four *meso*-protons, the carbachlorin system must possess a plane of symmetry. When carbachlorin **83** was treated with trifluoroacetic acid, the corresponding monocation **83**H^+ was generated (Scheme 33).[55] The proton NMR spectrum for **83**H^+ indicated that the aromatic character was increased as the internal CH now showed up at -7.00 ppm. Protonation also split the Soret band in the UV-visible spectrum of carbachlorin **83** to give two different peaks showing up at 409 and 426 nm. Both the proton and carbon-13 NMR spectra of **83**H^+ confirmed that the cation retained a plane of symmetry.[55]

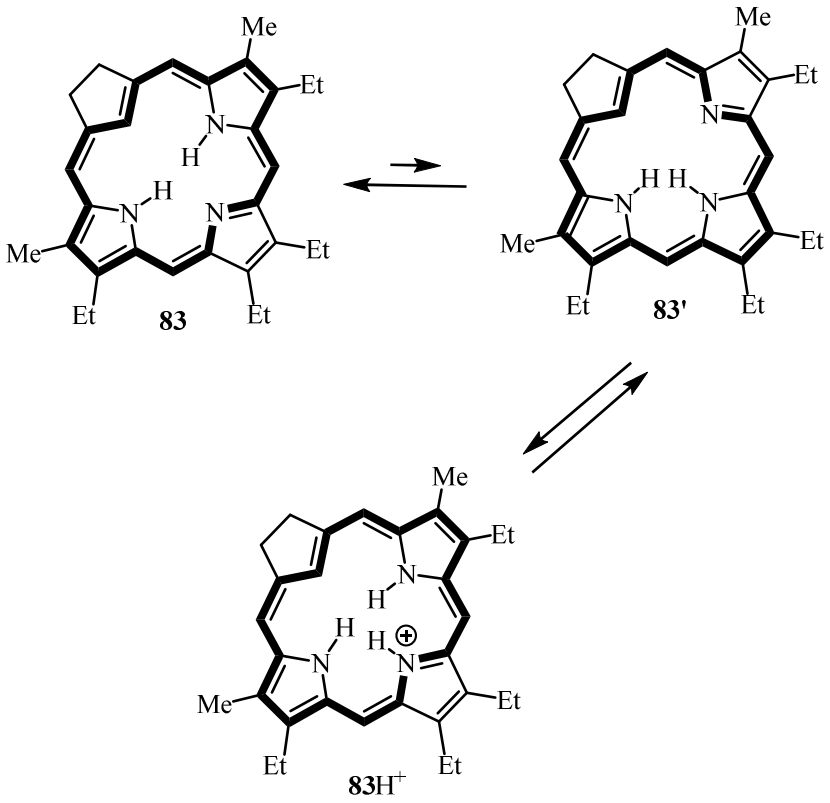

Scheme 33 Protonation of Carbachlorin

Attempts to oxidize carbachlorins **80** (Scheme 29, page 54) to the corresponding carbaporphyrins had been unsuccessful, but this may have been due in part to the presence of a fused five-membered ring on carbachlorin **80.** This unit would not favor the presence of the sp^2 hybridized carbons generated upon oxidation due to the associated angle strain.[15] In contrast, when **83** was heated with DDQ in toluene, oxidation readily occurred to give the corresponding carbaporphyrin **91** (Scheme 34).[55] Carbaporphyrin **91** is also highly aromatic and the proton NMR spectrum gave a resonance for the internal CH at -6.91 ppm, while the NHs produce a broad peak at -3.92 ppm. The *meso*-protons of **91** appeared downfield as two 2H singlets at 9.77 and 9.83

ppm. The proton and carbon-13 NMR spectra for **91** also confirmed that the macrocycle has a plane of symmetry, and this result is consistent with tautomer **83** (Scheme 33).[55]

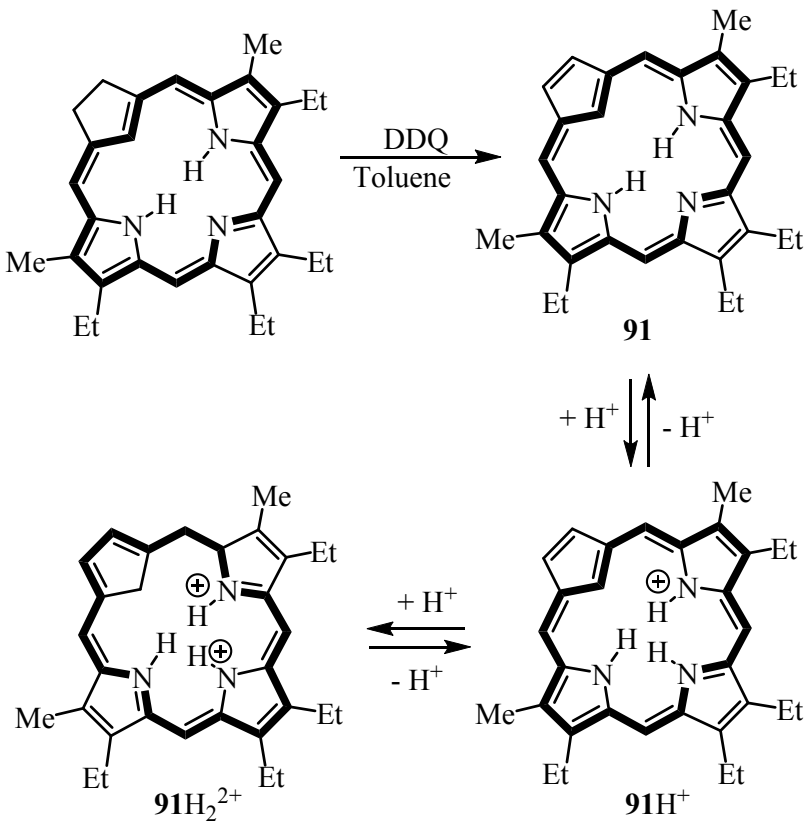

Scheme 34 Oxidation of Carbachlorin

The UV-vis spectrum of carbaporphyrin **91** was less porphyrin-like, showing two broad absorptions in the Soret region at 377 and 421 nm, and broad Q bands at higher wavelengths. This contrasts to previously mentioned benzocarbaporphyrins and formylcarbaporphyrins, which show strong Soret bands and better-defined Q bands in their UV-vis spectra. The corresponding monocation **91**H^+, generated by the addition of trace amounts of TFA, showed a strong Soret band at 385 nm together with a broad absorption at 409 nm and Q bands at 563, 574 and 614 nm. Further

addition of TFA gave rise to a third species corresponding to the *C*-protonated dication **91**H_2^{2+} (Scheme 34).[55]

It is interesting to note that the formation of benzocarbaporphyrin *C*-protonated dications is only complete in approximately 50% TFA solutions, whereas diprotonation of **91** was essentially complete in 5% TFA solutions. The proton NMR spectrum of **91**H_2^{2+} showed the presence of a very strong diatropic ring current in which the internal CH_2 gave a resonance at -8.27 ppm while the external cyclopentadiene protons showed up at 11.11 ppm and the *meso*-protons appeared nearby as two 2H singlets at 11.00 and 11.45 ppm. These data clearly demonstrated that the dication has enhanced aromaticity when compared to the free base form. However, the downfield shift of the outer cyclopentadiene protons in **91**H_2^{2+} is due to the relocation of the 18π electron delocalization pathway through the five-membered carbon ring as shown in bold (Scheme 34).[55]

Carbaporphyrinoids such as **56, 57** and **58** readily react with silver(I) acetate to give silver(III) organometallic derivatives.[32,33] The formation of silver complexes of carbaporphyrins **57** occurs rapidly in mixtures of dichloromethane and methanol at room temperature in the presence of 3 equiv. of silver(I) acetate. However, in the case of carbachlorin **83** the formation of the silver(I) complex is rather slow under these conditions. With carbachlorin **83**, the silver(III) derivative **92** was isolated in 11% yield after almost 16 hr (Scheme 35). It was interesting to observe that when the reaction was continued for several days, under same set of conditions, the yield was raised to 31%. However, when 7 equivalents of silver(I) acetate was used, only low yields (6%) of impure silver(III) carbaporphyrin **93** could be isolated.[55]

Further attempts to react carbaporphyrin **91** with silver(I) acetate led to decomposition without forming any metalated product. These results clearly indicate that the exposed carbocyclic ring is prone to oxidative degradation, and the data suggest that the presence of a fused benzene

ring in **57** is beneficial in stabilizing these structures and hence promotes metalation. The UV-vis spectrum for **92** was porphyrin-like, showing a strong Soret band at 411 nm and a relatively strong Q band at 599 nm. The proton NMR spectrum for **92** indicated that the complex retained strongly aromatic properties as the *meso*-protons showed up downfield at 9.23 and 9.90 ppm and the carbachlorin CH_2CH_2 unit gave a 4H singlet at 5.02 ppm.[55] The presence of a plane of symmetry was evident in the proton and carbon-13 NMR spectra, and the molecular formula was confirmed by high resolution electron impact mass spectrometry.

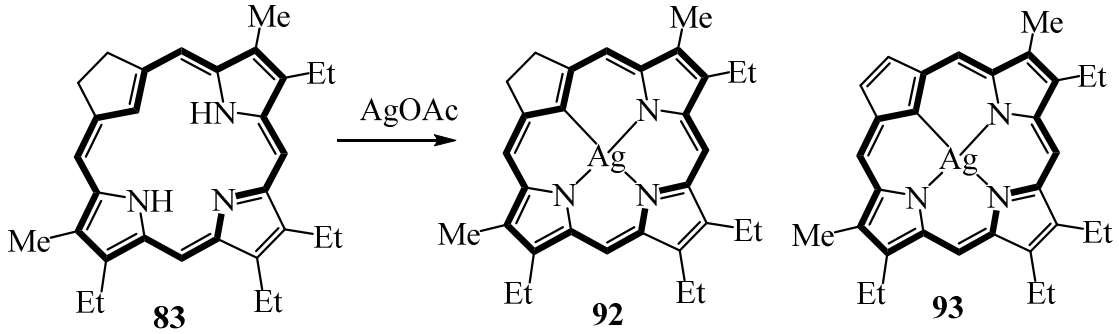

Scheme 35 Formation of Silver(I) Complex of Carbachlorin

Benzocarbaporphyrin **57** as such does not give any isolatable products in reactions with palladium(II) salts. However, as mentioned previously, the *N*-alkyl derivatives of benzocarbaporphyrins were found to give palladium(II) complexes when reacted with palladium(II) acetate in refluxing acetonitrile. This chemistry is interesting because the metalation is associated with an alkyl group migration from the nitrogen to the internal carbon atom.[35] A similar alkylation-metalation sequence was conducted on carbachlorin **83**.[35]

Reaction of **83** with methyl iodide and potassium carbonate in refluxing acetone for 16 h gave the *N*-methyl derivative **94** in 34% yield (Scheme 36). Prolonged reaction times did not

improve the yield as unidentified side products were formed. The site of alkylation was deduced from the proton and carbon-13 NMR spectra as the product shows a complete loss of symmetry. For instance, the *meso*-protons for **94** showed up as four 1H singlets at 8.89, 9.04, 9.37 and 9.58 ppm.[35]

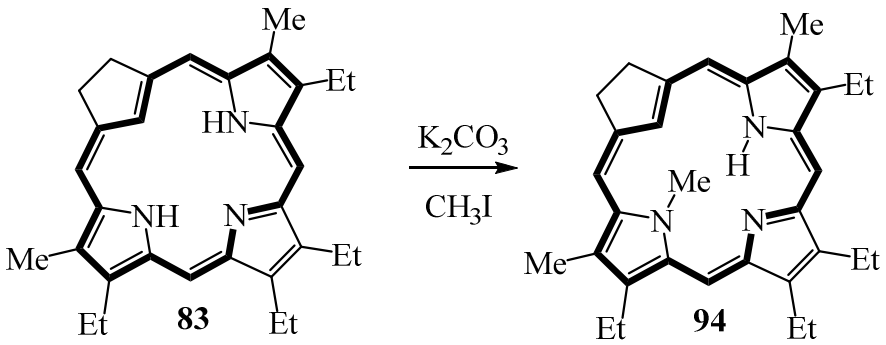

Scheme 36 Formation of N-methylated Carbachlorin

The alkylation does introduce steric crowding within the macrocyclic cavity but the NMR data showed that the chlorin retained most of its diatropic character. In the proton NMR spectrum of **94**, the internal methyl group gave a 3H singlet at -4.27 ppm, while the inner CH produced a resonance at -6.31 ppm. As the methyl group is too large to pass through the cavity, carbachlorin **94** is chiral and this leads to some complexity in the proton NMR spectrum. The chirality, makes the six methylene units present in the structure all nonequivalent and the individual protons diastereotopic, so in principle this could lead to twelve different resonances. However, due to a significant amount of overlap in this structure, far fewer peaks resolve and the carbachlorin CH_2CH_2 unit gave rise to only three multiplets appearing at 4.40 (1H), 4.54 (1H) and 4.79 ppm (2H).[55]

The UV-vis spectrum for **94** in CH_2Cl_2 is somewhat broadened compared to the spectrum for **83**. The alkylated carbachlorin has a Soret band at 407 nm and less well-defined Q bands

showing up between 500 and 664 nm. These differences in the UV-visible spectrum presumably result from distortion of the carbachlorin chromophore due to the presence of the internal methyl group. Addition of TFA resulted in the formation of a cation **94**H^+ with a split Soret band at 415 and 428 nm, and again the spectrum was somewhat broadened compared to **94**.[55]

Methylated chlorin **94** reacted with palladium(II) acetate in refluxing acetonitrile to give a palladium complex. Column chromatography on silica gel gave two fractions with similar polarities corresponding to metalated products from the N-methyl carbachlorin. It was anticipated that the product of this chemistry would be *N*-methyl palladium(II) complex **95**. Methyl group migration would not be expected in this case because that would interrupt the macrocyclic conjugation pathway. Unexpectedly, the main product was identified as palladium(II) carbaporphyrin **96** where an oxidation had occurred in addition to the methyl group migration. Palladium complex **96** was isolated in 17% yield (Scheme 37).[55]

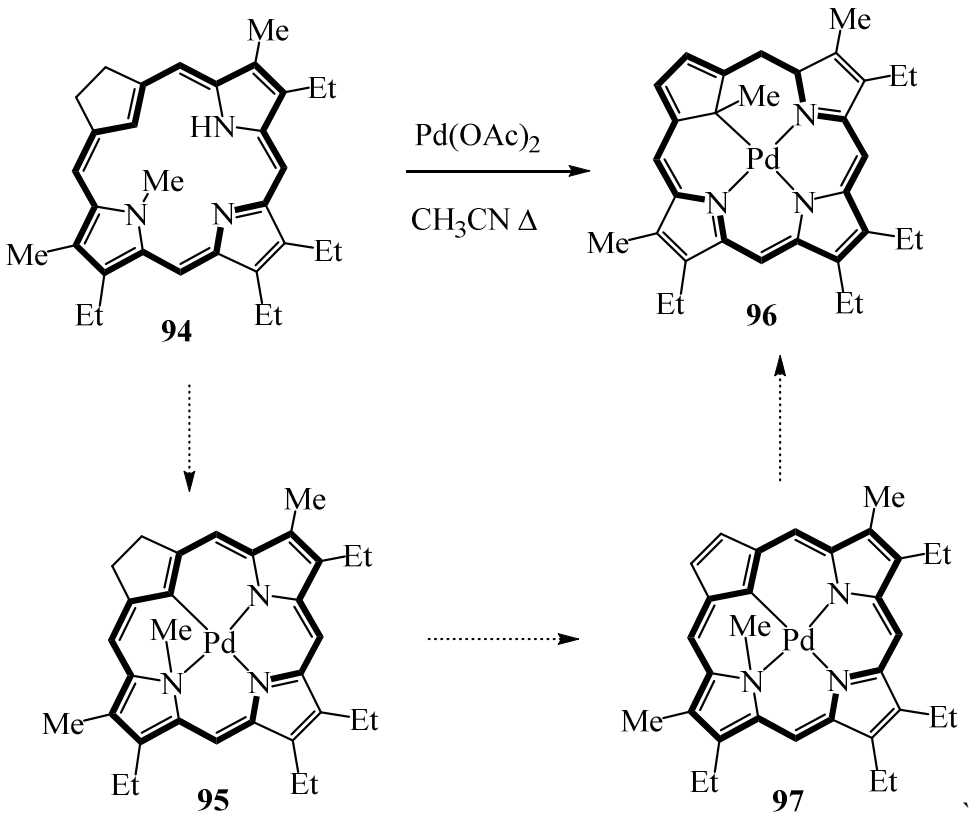

Scheme 37 Unexpected Formation of Pd Complex

The remaining fraction appeared to consist primarily of the expected palladium(II) chlorin **95**, but this could not be isolated in pure form. The samples were always contaminated with **96**, and it soon became apparent that **95** was slowly converting into **96**. In order to speed up the oxidation and improve the yield of **96**, the crude reaction solution was diluted with dichloromethane and stirred vigorously with an aqueous ferric chloride solution for 24 h. Following work up, the yield of palladium(II) complex **96** was raised to 34%. It is likely that initial oxidation affords the *N*-methyl palladium(II) carbaporphyrin **97** (Scheme 37)[55] and this subsequently undergoes a rearrangement to give **96**. The mechanism of the rearrangement is not

known, but it could be a stepwise process involving the transient formation of a Pd-methyl bond. Palladium complex **96** has regained a plane of symmetry and retains strongly diatropic characteristics. The proton NMR spectrum showed the internal methyl group at -4.46 ppm, while the *meso*-protons appeared downfield as two 2H singlets at 10.00 and 10.42 ppm. The cyclopentadiene protons are directly connected to the 18π electron delocalization pathway and as a result are deshelded to give a 2H singlet at 9.60 ppm. The UV-vis spectrum is less distinctive, giving broad bands in the Soret region at 394 and 440 nm.[55] The molecular formula for **96** was confirmed by high resolution electron impact mass spectrometry.

Although some intriguing results have been obtained for carbachlorins, these studies have been limited due to the difficulties encountered in preparing this system. Furthermore, an effective methodology for synthesizing carbaporphyrins without fused aromatic rings has not been reported previously. In this thesis, a new synthetic route for preparing carbaporphyrins and carbachlorins has been developed. The new porphyrinoids, which are stabilized by electron-withdrawing ester functionalities, were prepared in excellent yields from cyclopentanedialdehydes. The carbaporphyrin system proved to be an excellent organometallic ligand, forming complexes with nickel(II), palladium(II), silver(III) and gold(III).

CHAPTER II

SYNTHESIS OF CARBAPORPHYRINS

Introduction to Carbaporphyrin

The synthesis of macrocyclic structures related to porphyrins has attracted considerable attention, in part because modified structures may enhance valuable properties that are exhibited by regular porphyrins.[12] Carbaporphyrinoid systems, where one or more of the core nitrogens have been replaced by carbon atoms, have been widely investigated over the past 20 years. Although detailed studies on benzocarbaporphyrins have been reported, carbaporphyrins without a fused benzene unit have only been prepared in low yields, and an improved route to carbaporphyrins of this type is needed. Specifically, porphyrinoid **98** with two ester functionalities attached to the carbocyclic ring is an appealing target for synthesis. This represent a new type of carbaporphyrinoid structure. The proposed methodology for preparing this system is modeled after the synthesis of porphyrin analogues containing bicyclooctane units previously developed in Dr. Lash's lab.[22]

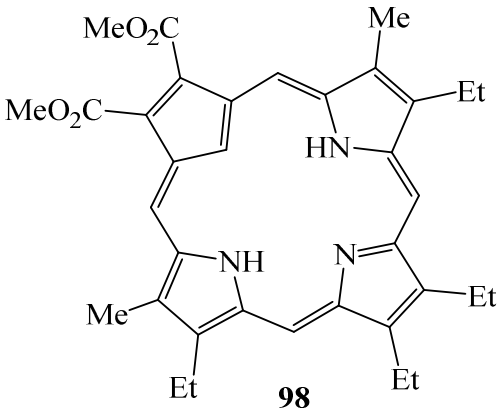

98

Results and Discussion

A retrosynthetic analysis suggested that carbaporphyrin **98** and a related chlorin could be obtained from cyclopentane dialdehyde **99** and the known tripyrrane **62**. It was speculated that acid catalyzed "3+1" condensation of dialdehyde **99** with tripyrrane **62** in presence of trifluoroacetic acid, following oxidation with DDQ, would afford the targeted carbaporphyrin **(**Scheme 38).[54] In order to utilize the "3+1" methodology, it was initially necessary to synthesize tripyrrane **62**. The preparation of this tripyrrane can be carried out in 12 synthetic steps, where two key pyrrolic intermediates **100** and **44** needed to be generated (Scheme 39). The tripyrrane was initially formed with benzyl ester protective groups but these can be removed by hydrogenolysis over Pd/C to afford the required dicarboxylic acid **62** (Scheme 38).

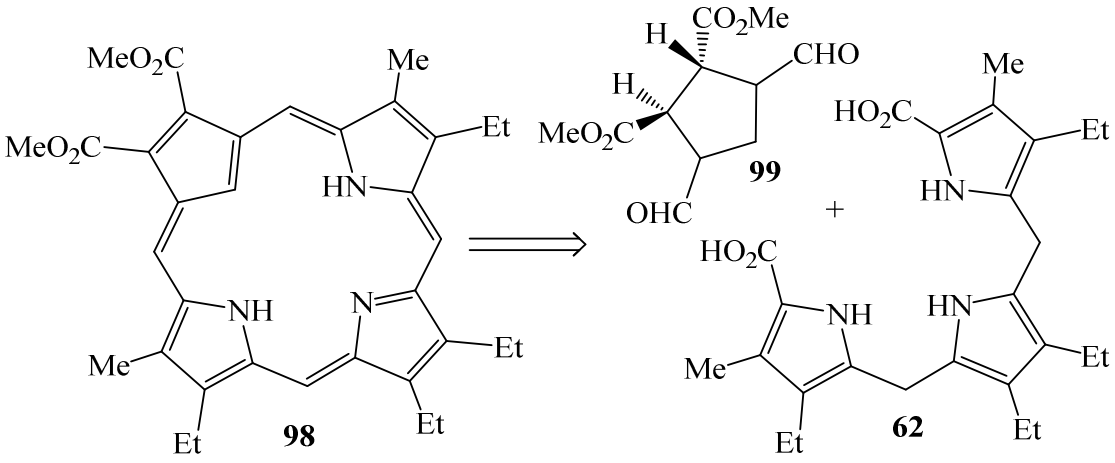

Scheme 38 Retrosynthetic Analysis of Carbaporphyrin **98**

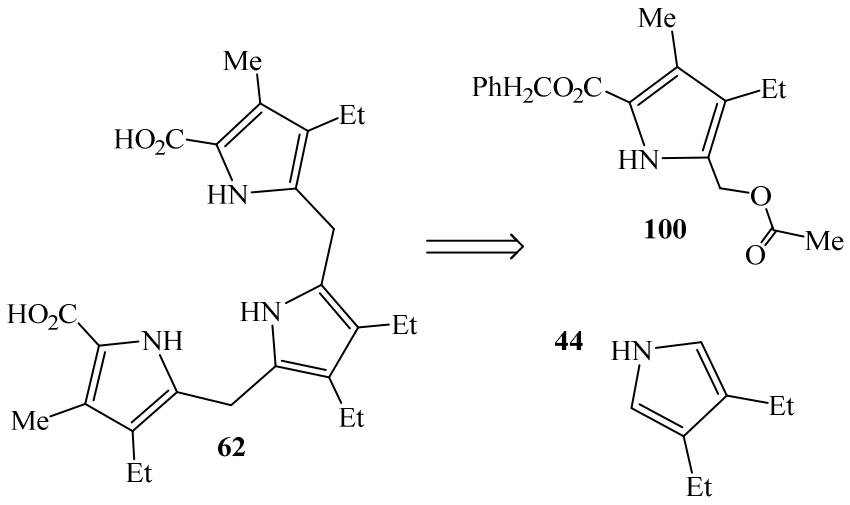

Scheme 39 Retrosynthetic Analysis of the Tripyrrane Intermediate

In order to synthesize pyrrole **100**, it was first necessary to prepare pyrrole ester **101**. Reaction of diethyl malonate with sodium nitrite and acetic acid afforded oxime **102** and this was reduced under hydrogen over 10% Pd/C to give diethyl aminomalonate **103**. Alkylation of 2,4-pentanedione with ethyl iodide and potassium carbonate in refluxing acetone gave the ethyl substituted diketone **104**, and this was condensed with **103** in refluxing acetic acid to produce pyrrole ethyl ester **101** (Scheme 40).

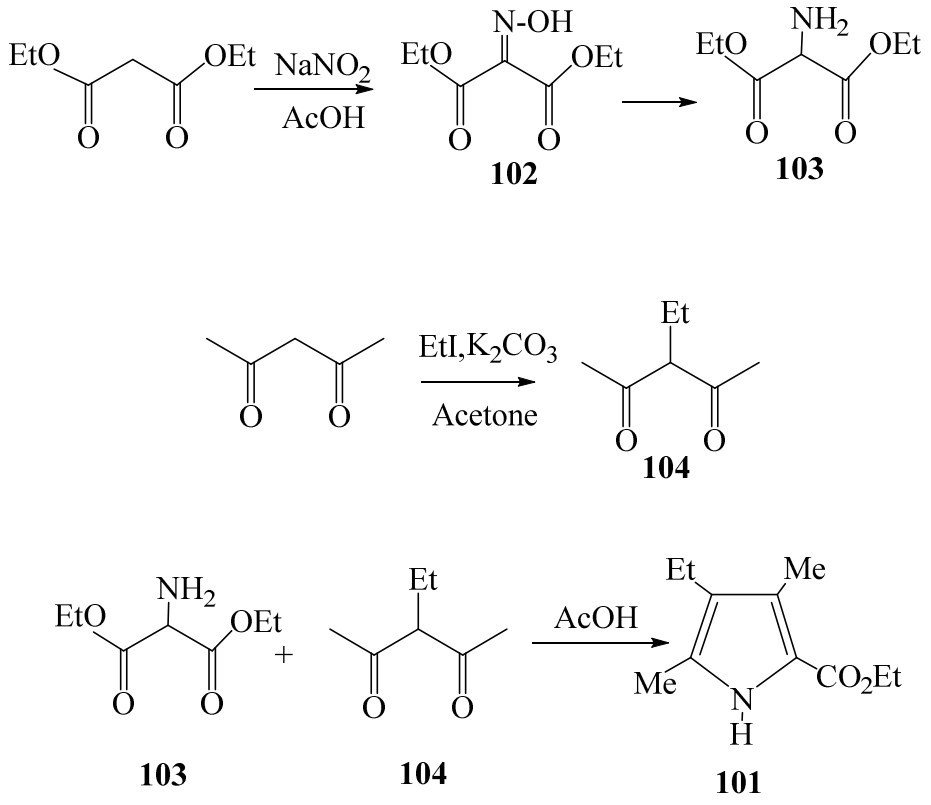

Scheme 40 Preparation of Pyrrole Ester **101** using a Knorr-Type Synthesis

Pyrrole ethyl ester **101** was transesterified using benzyl alcohol in the presence of sodium benzyloxide to give the corresponding benzyl ester **105** (Scheme 41).

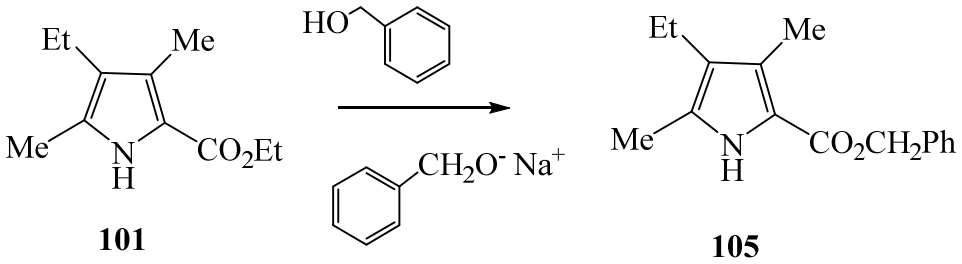

Scheme 41 Formation of a Pyrrole Benzyl Ester

Pyrrole **105** was then selectively oxidized with lead tetraacetate in acetic acid to afford the required acetoxymethyl pyrrole precursor **100** in good yields (Scheme 42)**.**

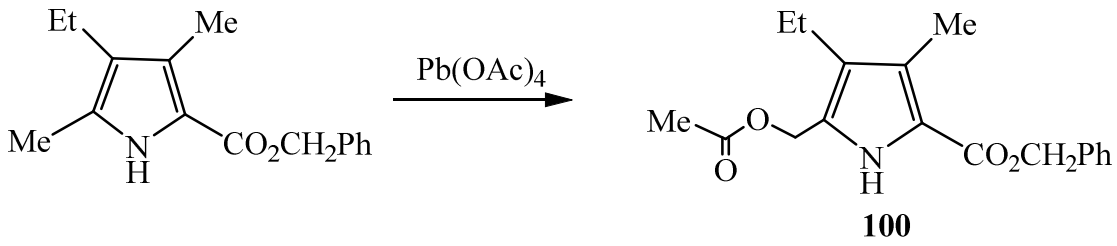

Scheme 42 Formation of an Acetoxymethylpyrrole

The second pyrrolic precursor 3,4-diethylpyrrole **44**, was synthesized via the Barton-Zard methodology. Initially, glycine ethyl ester hydrochloride and triethylamine were heated to reflux in methyl formate to afford N-formylglycinate (Scheme 43). Subsequent dehydration with phosphorus oxychloride and triethylamine at 0 ℃ then gave ethyl isocyanoacetate **106**.

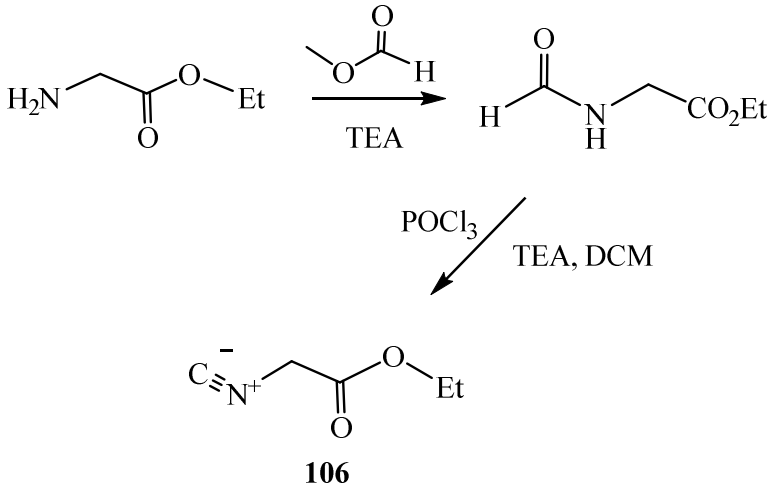

Scheme 43 Formation of Ethyl Isocyanoacetate **105**

Besides ethyl isocyanoacetate, acetoxy nitrohexane **107** was also required as a precursor to pyrrole **44**. Initially, a related nitro alcohol was prepared by reacting propionaldehyde with 1-nitropropane in the presence of potassium fluoride (Scheme 44). Subsequent treatment with acetic anhydride under acidic conditions then afforded the required acetoxy nitro hexane **107** in 96% yield. Barton-Zard condensation of acetoxy nitrohexane **107** with ethyl isocyanoacetate **106** in the presence of two equivalents of the base 1,8-diazabicyclo[5.4.0]undec-7-ene (DBU) resulted in the formation of pyrrole ethyl ester **108**. The crude pyrrole ester was then refluxed in a solution of sodium hydroxide in ethylene glycol at 190 ^{o}C and this resulted in saponification and decarboxylation to give diethyl pyrrole **44** in 48% yield (Scheme 44). However, the dialkyl pyrrole was found to be moderately unstable at room temperature and was stored in the freezer for future use.

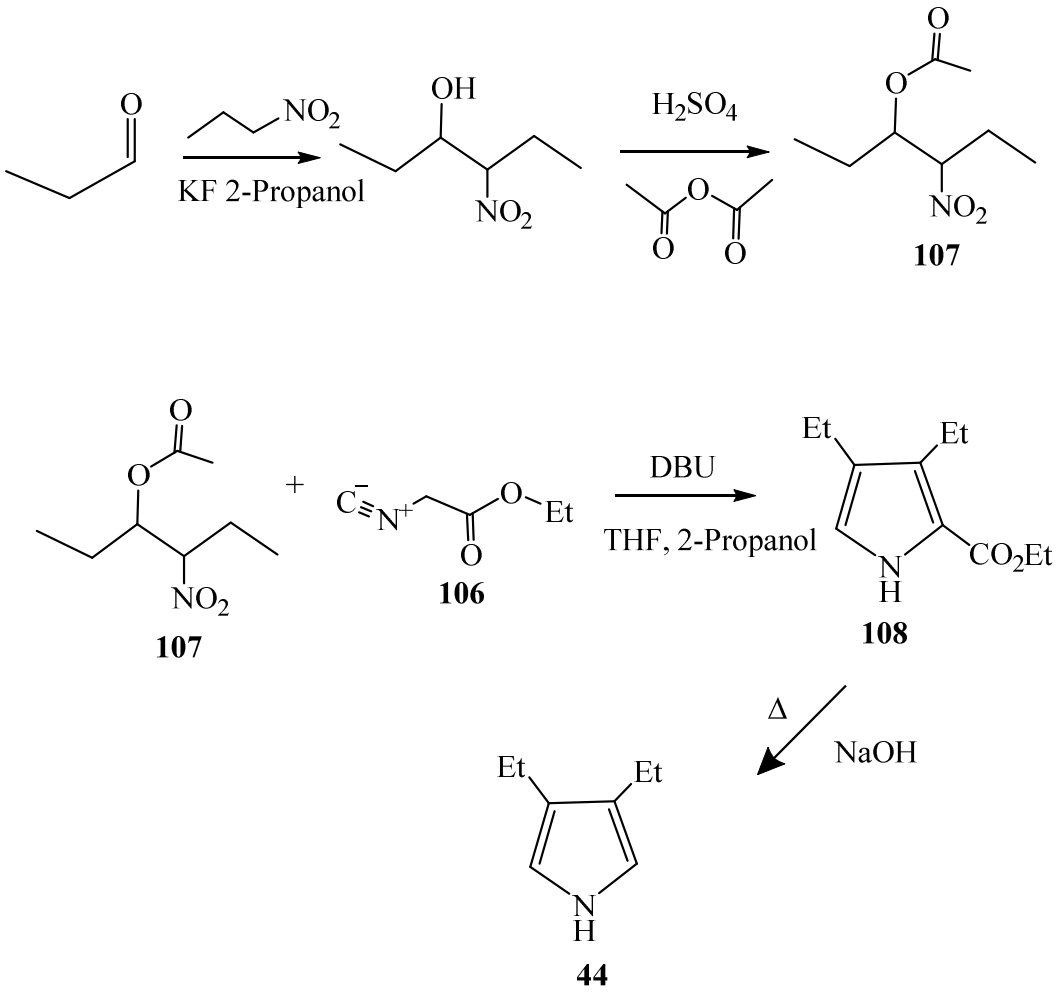

Scheme 44 Preparation of 3,4-Diethylpyrrole via a Barton-Zard Synthesis

Treatment of two equivalent of **100** with 3,4-diethylpyrrole **44** and acetic acid in refluxing ethanol gave tripyrrane dibenzyl ester in 92% yield. The benzyl ester protective groups were cleaved by hydrogenolysis over 10% Pd/C to give the corresponding dicarboxylic acid **62** (Scheme 45).[54] This product was relatively unstable and therefore had to be used within one week even when it was stored in the freezer.

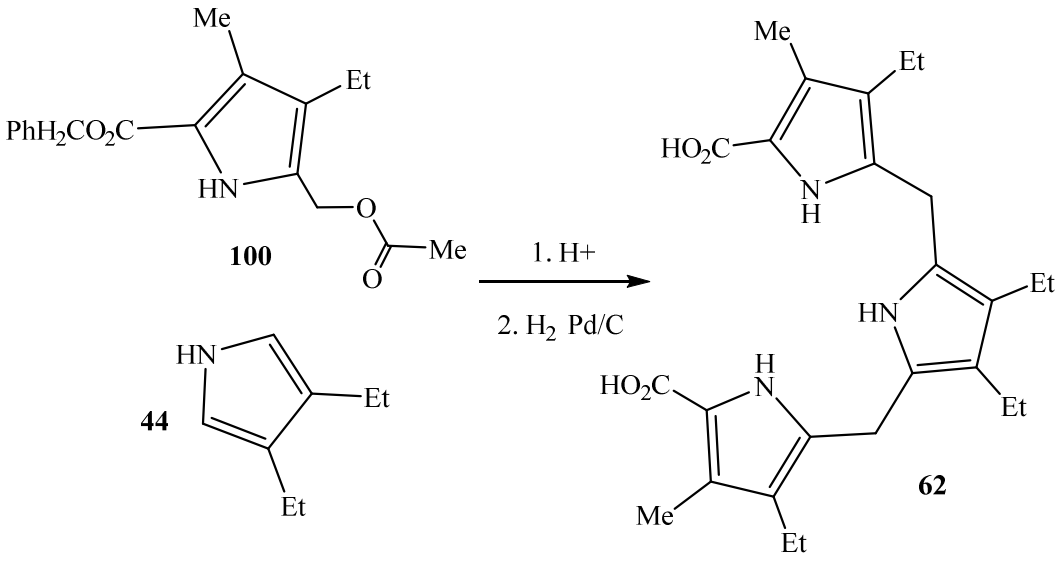

Scheme 45 Preparation of Tripyrrane **62**

In addition to preparing the tripyrrane, it was necessary to develop a synthetic route to cyclopentane dialdehydes such as **99**. In an initial attempt, dimethyl acetylenedicarboxylate (DMAD) **109** was reacted with cyclopentadiene **110** at room temperature to give the Diels-Alder adduct **111** (Scheme 46).[57]

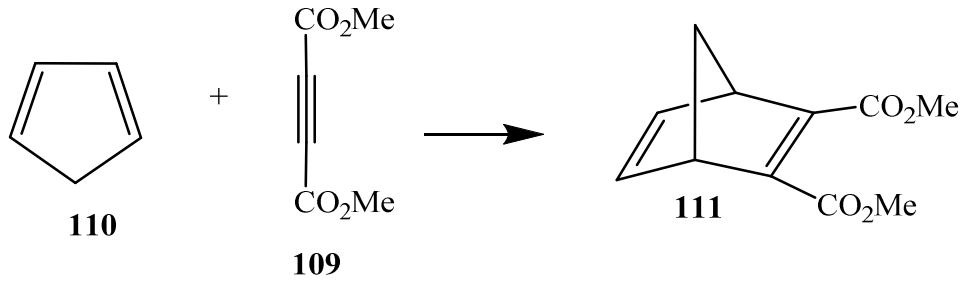

Scheme 46 Preparation of Bicyclic Adduct **111**

Göksu and coworkers reported that seven bicyclo[2.2.1]heptenes, including **111**, were cleaved to cyclic dialdehydes in good yields by oxidation with $KMnO_4$-$CuSO_4{\cdot}5H_2O$.[58] However, all attempts to reproduce this procedure with norbornadiene derivative **111** failed to generate any dialdehyde. Hence, an alternative synthetic method or a different precursor was needed. Donohoe and coworkers reported an alternative two steps route to dialdehydes.[59] In this synthetic route, a solution of norbornadiene **111** in *tert*-butyl alcohol was oxidized to give **112** using $KMnO_4$ and NaOH in *tert*-butyl alcohol and water at 0 ^oC (Scheme 47).[59] However, when we attempted to prepare **112** using this methodology, the yields were low.

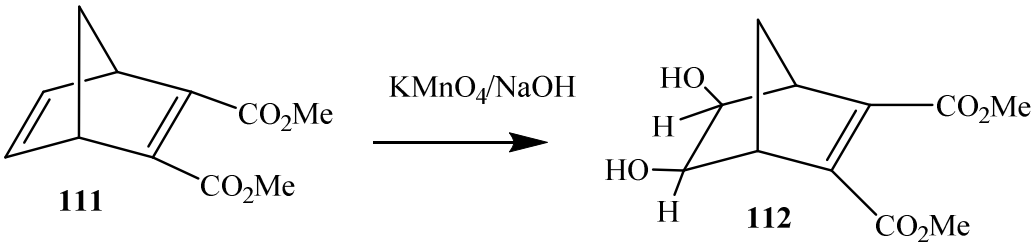

Scheme 47 Formation of Diol **112**

Alternative synthetic routes for diol formation were investigated. However, all of the conditions gave poor results. Some of the failed attempts to form diol **112** are shown in Scheme 48.[58,60,61] In order to circumvent this problem, the use of an alternative norbornene intermediate was considered.

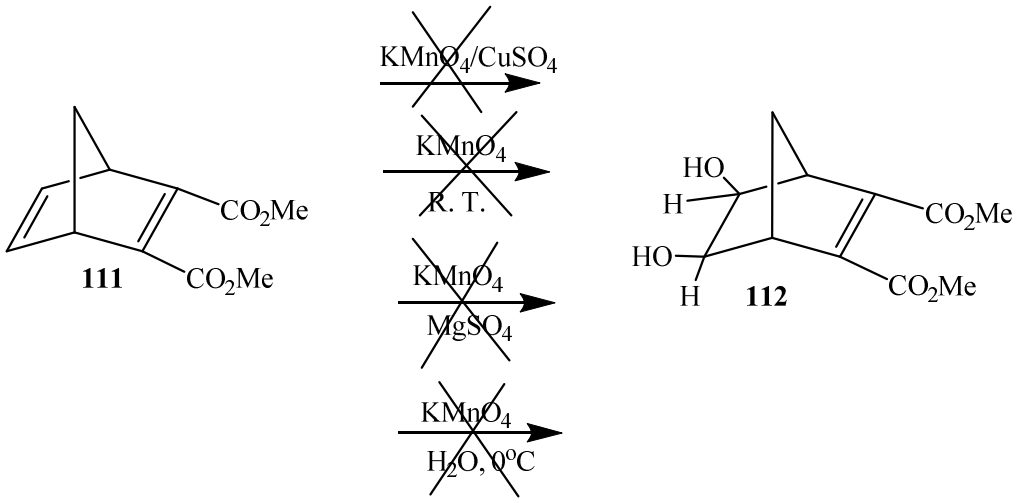

Scheme 48 Unsuccessful Attempts to Synthesize Diol **112**

Dimethyl fumarate (**113**), a readily available starting material, underwent a Diels-Alder cycloaddition with cyclopentadiene to form the bicyclic adduct **114** (Scheme 49). Several different procedures were attempted to carry out this transformation. Superior results were achieved using a literature procedure by Beare and coworkers.[62] In this procedure, freshly cracked cyclopentadiene was gradually added to an aqueous suspension of dimethyl fumarate (Scheme 49).[62] The mixture was stirred at room temperature for 150 minutes and then extracted with ethyl acetate to give an excellent yield of **114**. This norbornene derivative was then reacted with $KMnO_4$ and NaOH in *tert*-butyl alcohol and water at 0 °C to give the related dialcohol **115** (Scheme 50).[59]

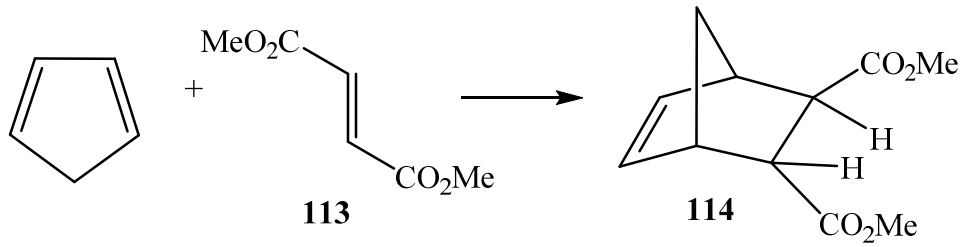

Scheme 49 Formation of Bicyclic Adduct **114**

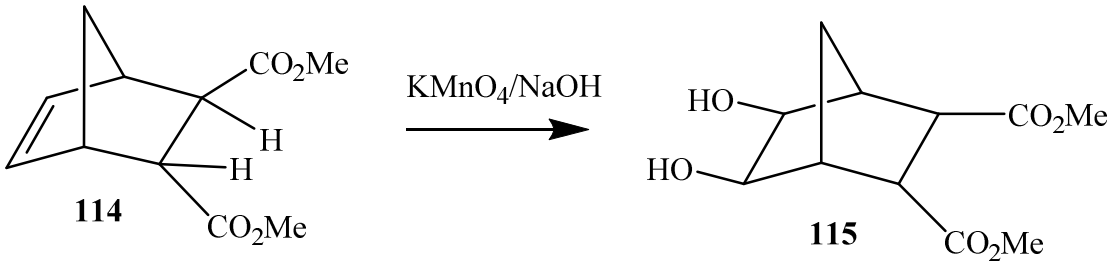

Scheme 50 Formation of Diol **115**

The diol product **115** was isolated as a white crystalline solid in 73% yield. In the ^{1}H NMR spectrum of resulting product, two broad resonances for the OH protons could be identified (Figure 16).

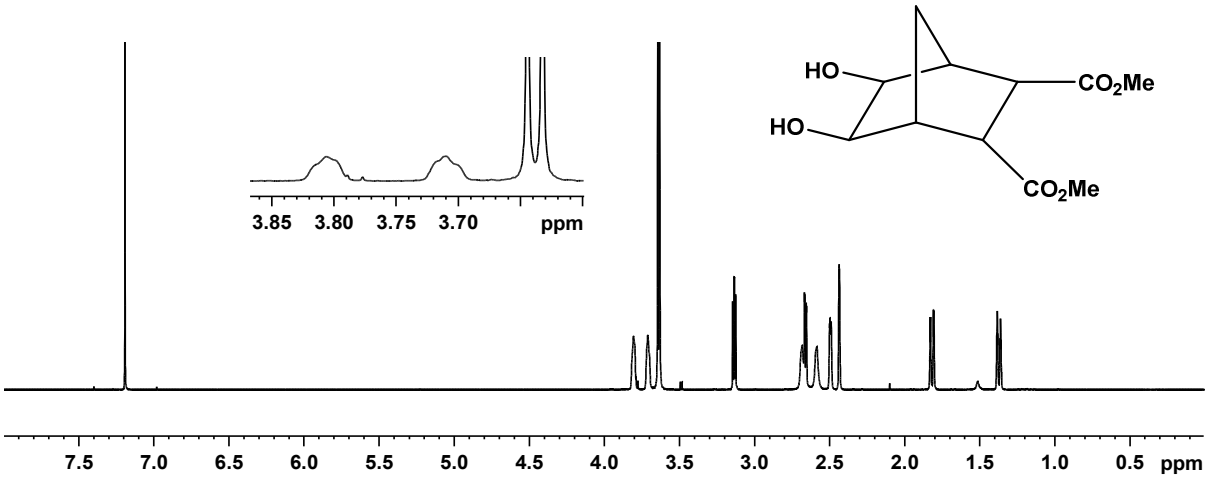

Figure 16 500 MHz ^{1}H NMR Spectrum of Fumarate Diol in $CDCl_3$

Diol **115** could be oxidatively ring opened using potassium periodate as an oxidizing agent to give dialdehyde **99** in 55% yield (Scheme 51).[54] The mechanism for ring opening of the bicyclic adduct to give a five-membered ring dialdehyde involved the formation of a transient cyclic periodate derivative. Elimination of an iodate ion affords the dialdehyde (Scheme 52). Dialdehyde **99** thus generated was very unstable and decomposed rapidly even at low temperatures. For this reason, it was immediately utilized in the preparation of carbaporphyrin.

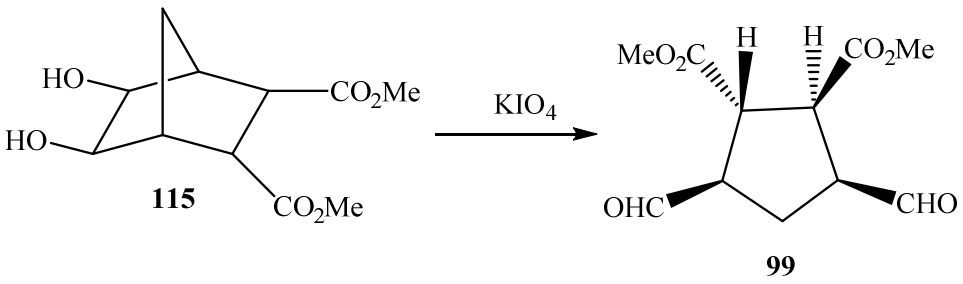

Scheme 51 Formation of Dialdehyde **99**

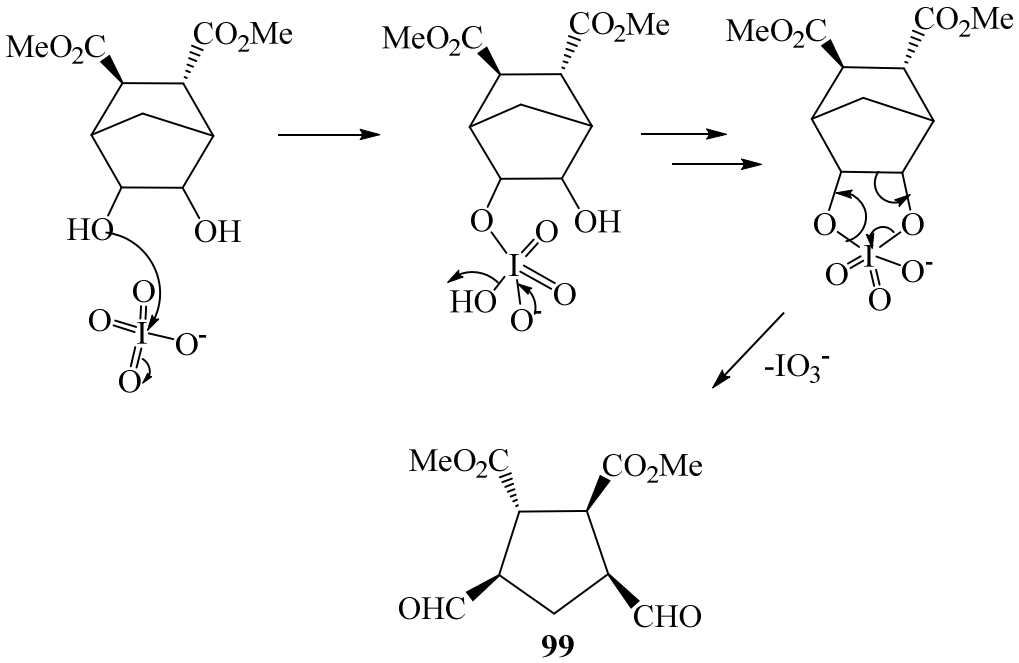

Scheme 52 Mechanism for Ring Opening

Dialdehyde **99** was condensed with tripyrrane dicarboxylic acid **62** in the presence of TFA/CH_2Cl_2**.** Initial condensation would be expected to produce a hexahydrocarbaporphyrin such as **116**. Following oxidation with DDQ in refluxing toluene, carbaporphyrin **98** was isolated as the major product along with some carbachlorin **117** as the minor product (Scheme 53).[54]

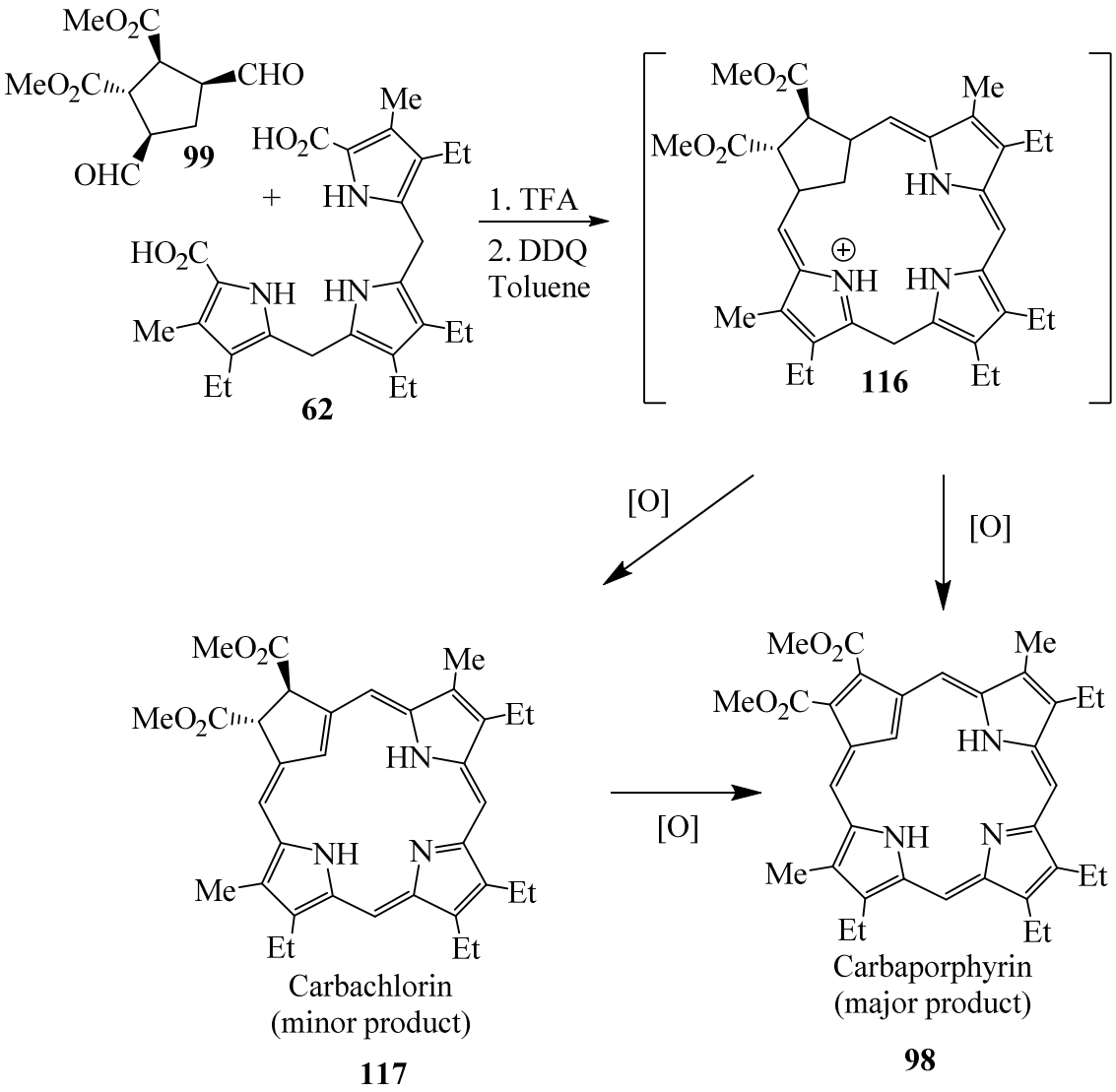

Scheme 53 Preparation of Carbaporphyrin **98**

During purification using column chromatography, three bands were collected. The first band to elute off the column was bright red, and corresponded to a small amount of porphyrin byproduct. The second major band corresponded to carbaporphyrin **98** and following recrystallization using chloroform and methanol, this product was isolated as purple crystals in 40% yield. A third green band was collected that corresponded to carbachlorin **117**, and following

recrystallization from chloroform and methanol the dihydroporphyrinoid was obtained as a green powder in 9% yield.

As expected, carbaporphyrin **98** proved to be a fully aromatic compound. The proton NMR spectrum for **98** (Figure 17) in $CDCl_3$ showed the presence of a strong diamagnetic ring current. The internal CH proton was found at -6.27 ppm, while the *meso*-protons were shifted downfield to give two 2H singlets at 10.24 and 9.51 ppm. As there were only two signals for the four *meso*-protons, the results indicate that the molecule is symmetrical.

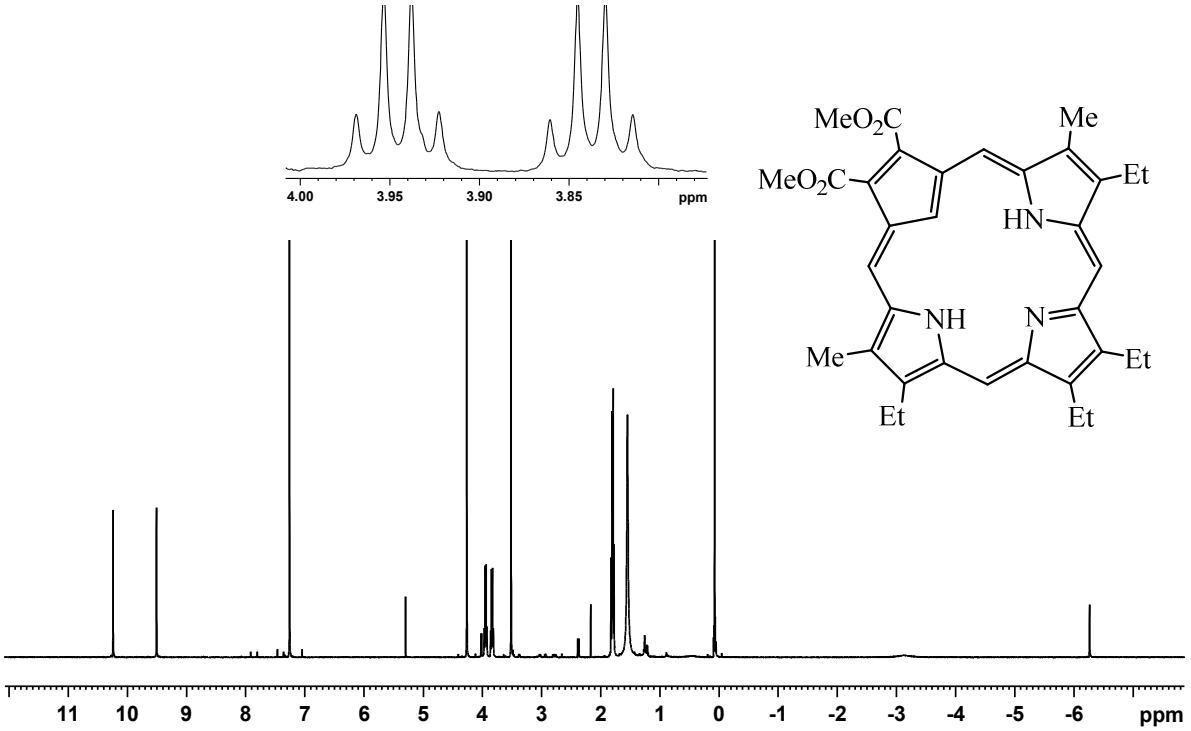

Figure 17 500 MHz proton NMR Spectrum of Carbaporphyrin **98** in $CDCl_3$

For the carbachlorin byproduct **117**, the proton NMR spectrum in $CDCl_3$ again showed the presence of a strong diamagnetic ring current. The internal CH proton was found further upfield at -7.14 ppm, while the *meso*-protons were still deshielded to between 9.85 and 9.48 ppm (Figure

18). The symmetry was maintained in the carbachlorin byproduct as can be seen in the figure below.

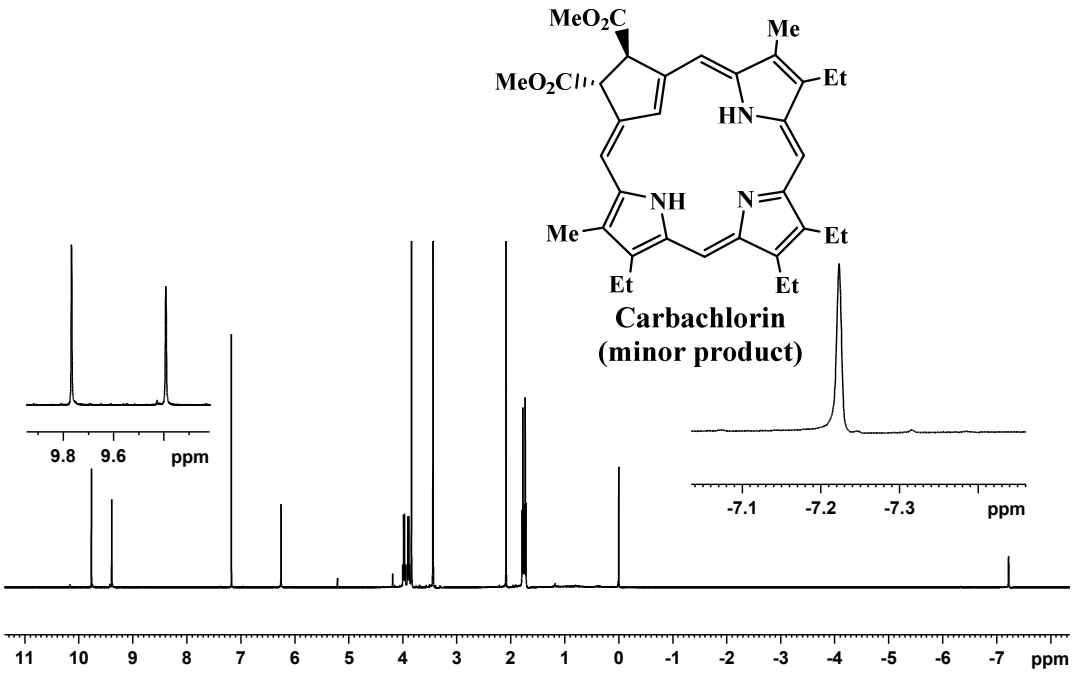

Figure 18 500 MHz proton NMR spectrum of the Carbachlorin byproduct in $CDCl_3$

The UV-Vis spectrum for the free base carbaporphyrin had a strong absorption in the Soret region at 436 nm, followed by a series of four weaker absorptions between 520 and 720 nm, which is characteristic aromatic porphyrinoids (Figure 19). In addition, the structure of carbaporphyrin **98** was also confirmed using X-ray crystallography (Figure 20).

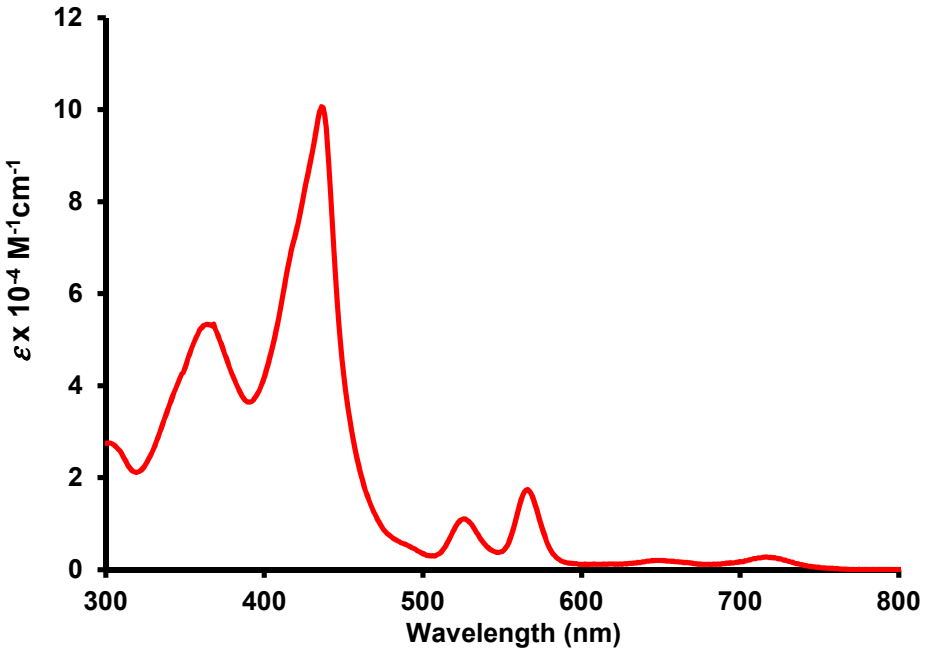

Figure 19 UV-Vis spectrum of Carbaporphyrin **98** in Dichloromethane

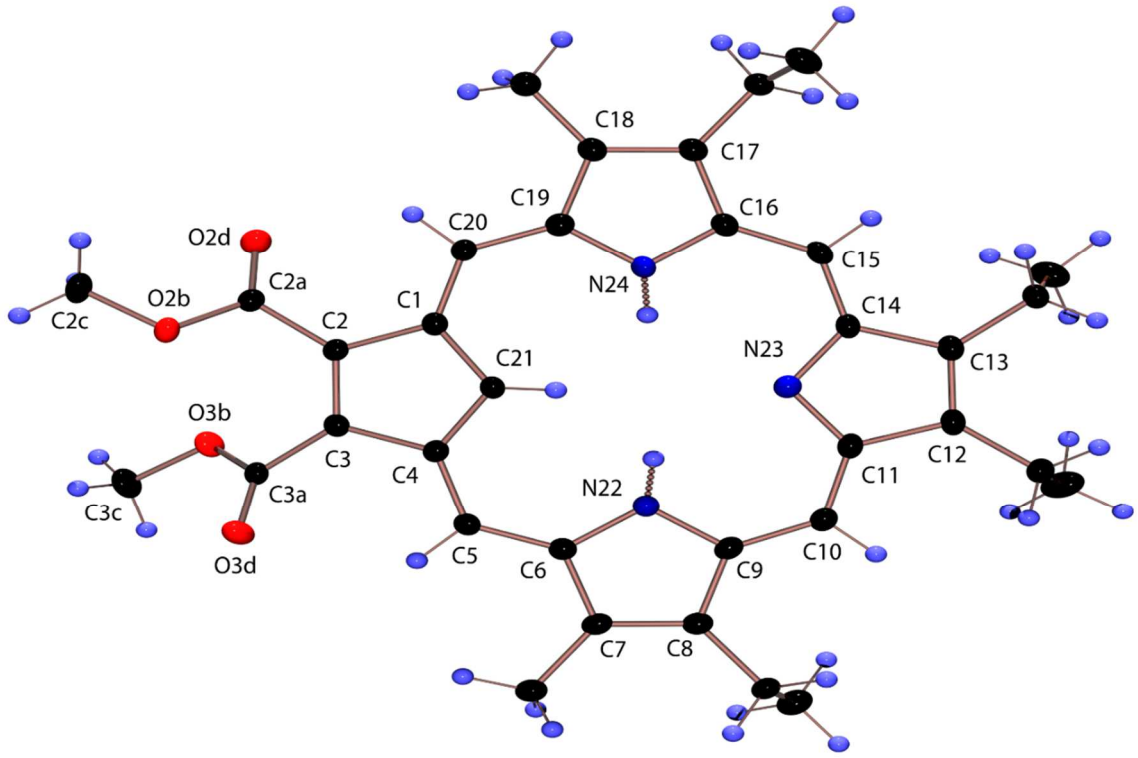

Figure 20 POV-Ray generated ORTEP III Drawing of **98**

The UV-vis spectrum for the free base carbachlorin byproduct **117**, has a strong absorption in the Soret region at 398 nm, followed by weaker absorptions at 490 nm and 588 nm. In addition, a strong red shifted peak was displayed at 648 nm (Figure 21), a feature that is also seen for tetrapyrrolic chlorins.

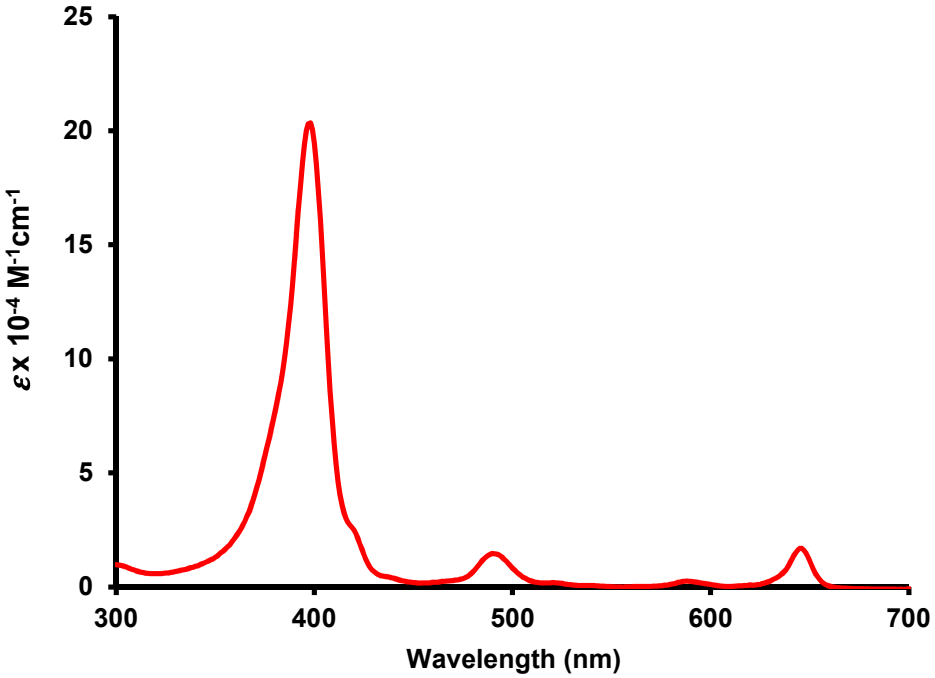

Figure 21 UV-Vis spectrum of Carbachlorin **117** in Dichloromethane

In principle, the monocation of **98** can be obtained when a trace amount of TFA is added. However, when one drop of TFA was added to an NMR tube containing a solution of **98** in $CDCl_3$, the resulting NMR spectrum appeared to correspond to mixture of mono **98**H^+ and dicationic species **98**H^{2+} (Figure 22).

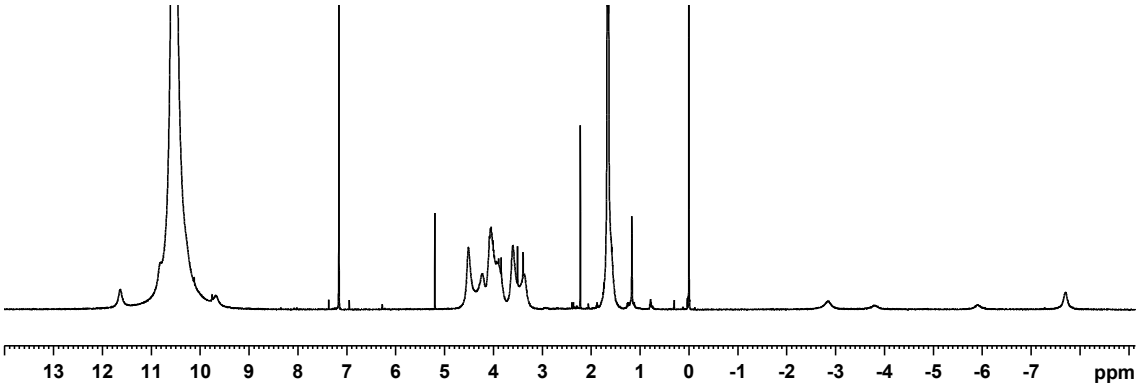

Figure 22 500 MHz proton NMR Spectrum of a Mixture of **98**H^+ and **98**H_2^{2+} in $CDCl_3$

When only 4 μL of TFA was added to the solution, the proposed monocation **98**H^+ (Scheme 54) could be observed by proton NMR and UV-Vis spectroscopy (Figure 23). The proton NMR spectrum of **98**H^+ showed that the addition of TFA to the carbaporphyrin had slightly increased the aromatic character of carbaporphyrin, as the *meso*-protons were shifted slightly further downfield to 10.40 and 9.74 ppm (Figure 24). The appearance of a broad peak at -3 ppm corresponds to the presence of an additional NH due to protonation. In addition, there was a significant change in the UV-Vis spectrum with the addition of the trace amounts of acid (Figure 23).

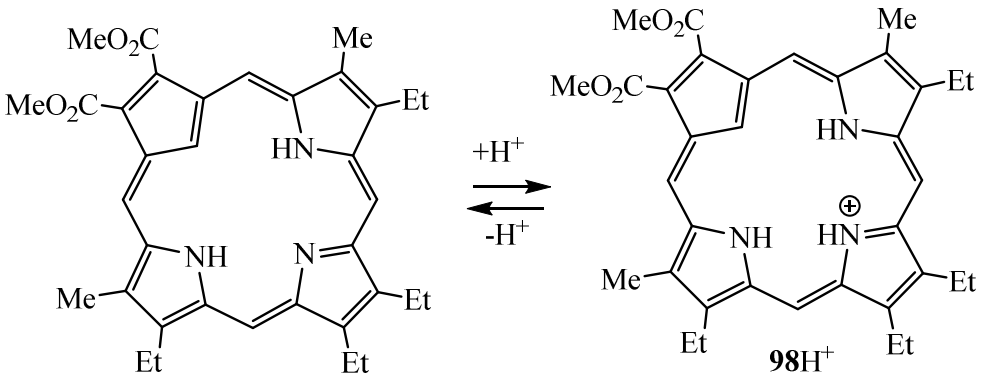

Scheme 54 Protonation of Carbaporphyrin **98**

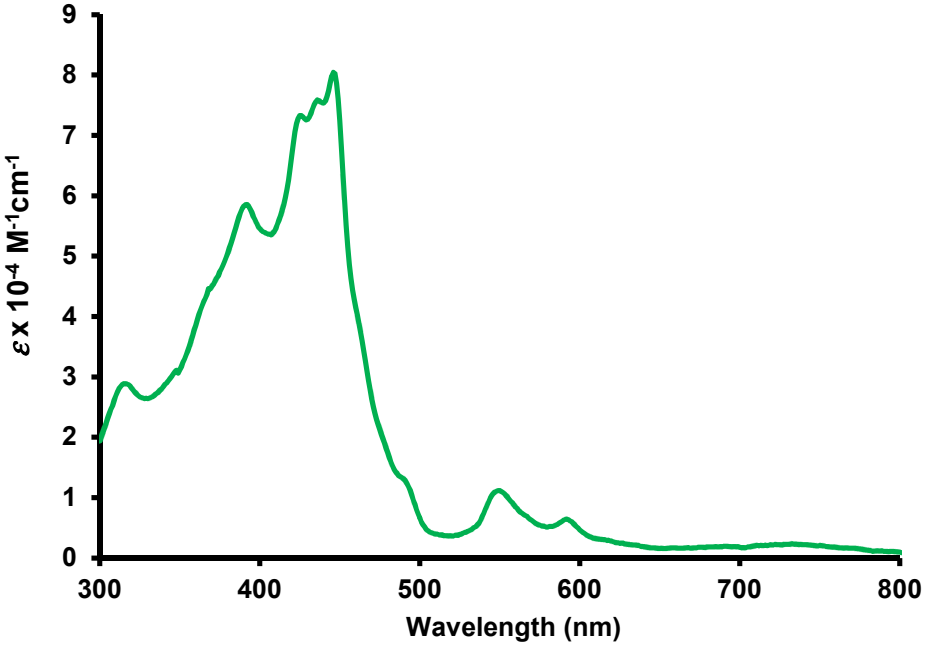

Figure 23 UV-Vis spectrum of Carbaporphyrin **98**H^+ in CH_2Cl_2

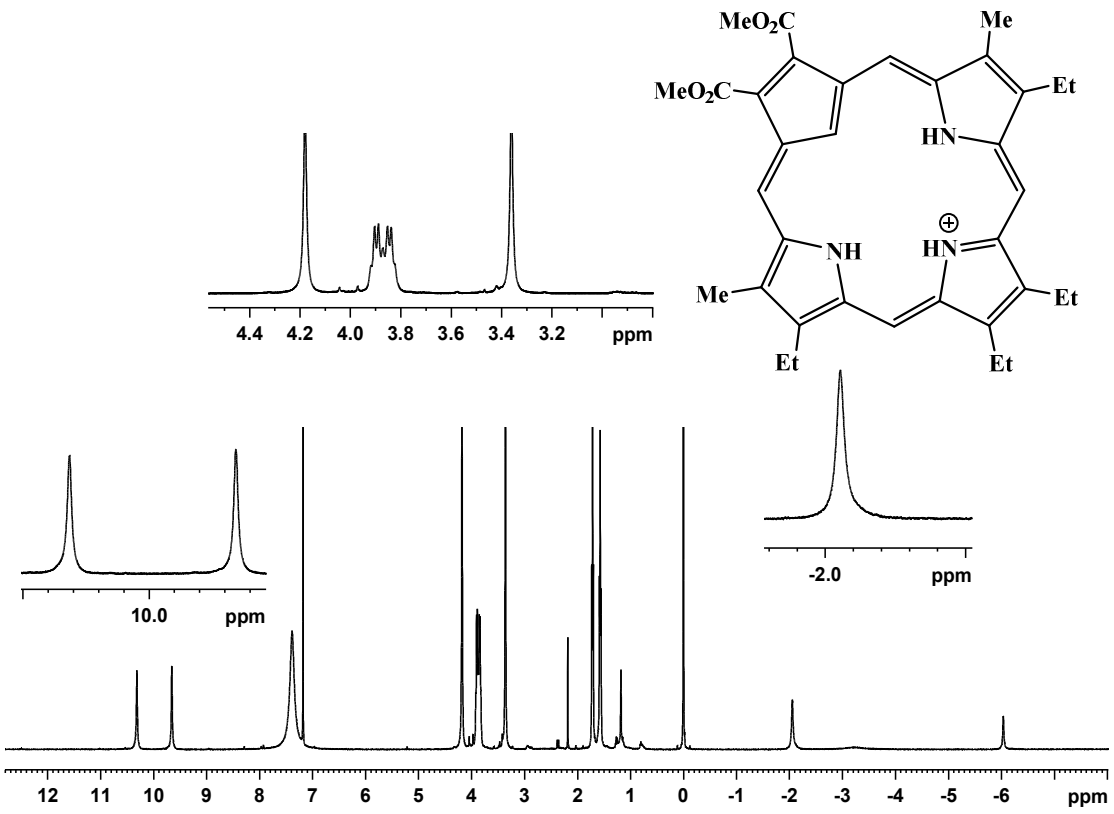

Figure 24 500 MHz proton NMR Spectrum of **98**H^+ in $CDCl_3$

Further addition of TFA led to the formation of dication **98**H_2^{2+} (Scheme 55). The proton NMR spectrum of **98**H_2^{2+} (Figure 25) showed a 2H singlet at -7.67 ppm due to the internal CH_2, and two 2H singlets at 11.80 and 11.00 ppm corresponding to the *meso*-protons. This not only confirmed that diprotonation had taken place but also indicated that the aromatic character of the conjugated system was further improved. In addition, the proton NMR spectrum for dication **98**H_2^{2+} confirmed that the compound retained a plane of symmetry.

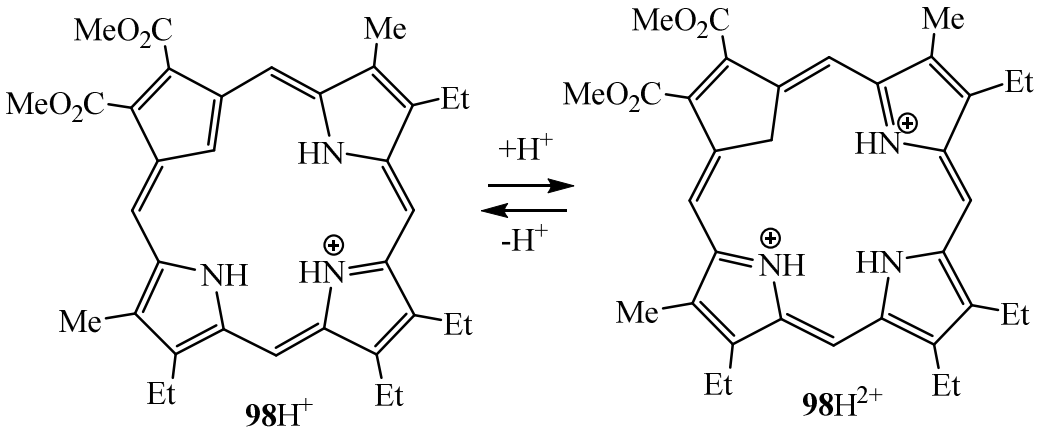

Scheme 55 Further Protonation of Carbaporphyrin **98**H^+

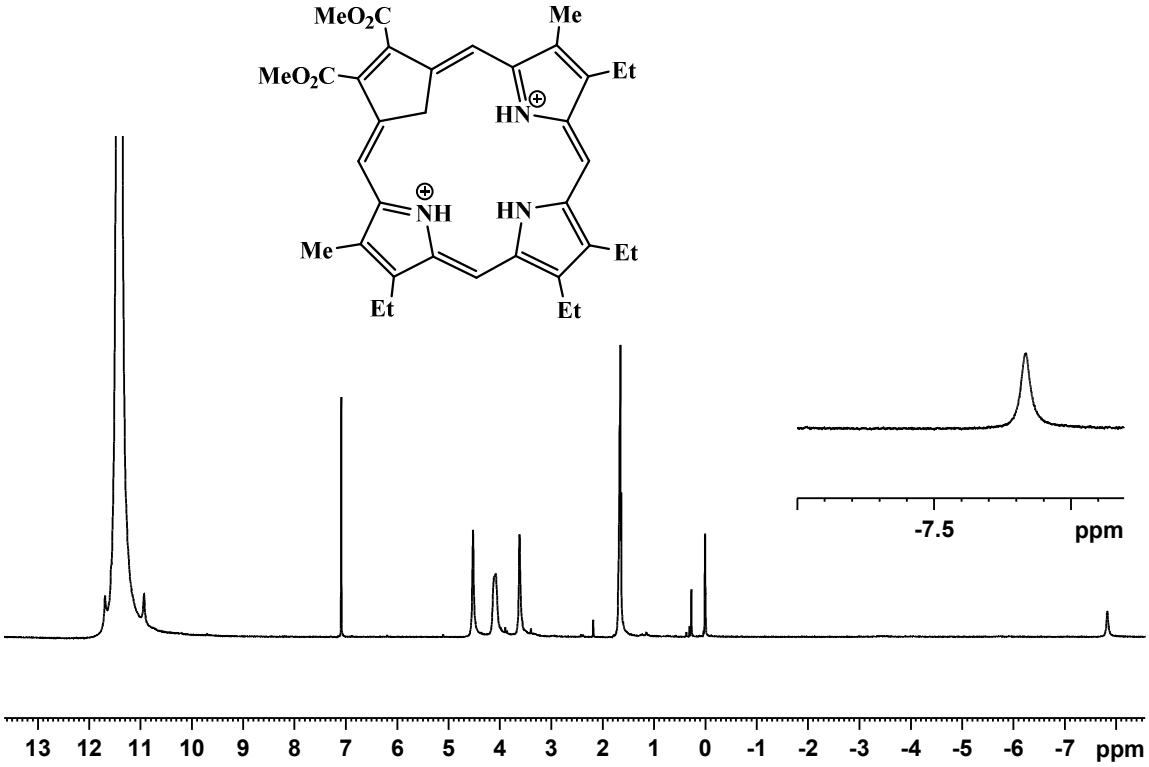

Figure 25 500 MHz ^{1}H NMR Spectrum of **98**H_2^{2+} in $CDCl_3$.

In order to further understand the reactivity of carbaporphyrin **98**, a few more experiments were performed to observe how the exchange of protons takes place with the addition of acid. It was interesting to note that addition of d-TFA to an NMR solution of **98** in $CDCl_3$ showed rapid exchange of the 21-H resonance and slow exchange of the *meso*-protons. As the solutions consisted of a mixture of protonated species, it was necessary to extract the sample before NMR analysis could be conducted. Two drops of d-TFA were added to the NMR tube and after 10 min the solution was neutralized by addition of NaOD in D_2O. The mixture was diluted with water, extracted with dichloromethane and the organic solutions dried over sodium sulfate. Following removal of the solvent, the residue was analyzed by proton NMR spectroscopy. The results showed that the internal CH had undergone exchange but no other resonances were affected (Figure 26). When the solution was exposed to d-TFA for 24 h, and the solution neutralized and extracted as before, significant reduction in the intensities of the *meso*-proton resonances were observed. The peak corresponding to the 5,20-protons was reduced by approximately 15%, while the 10,15-proton resonance was diminished by >40% (Figure 27) The results indicate that *meso*-protonated species such as monocations **98a**H^+ and **98b**$H^+$are energetically accessible and in equilibrium with **98**, **98**H^+ and **98**H_2^{2+} (Scheme 56). Similar results have previously been noted for benzocarbaporphyrins.

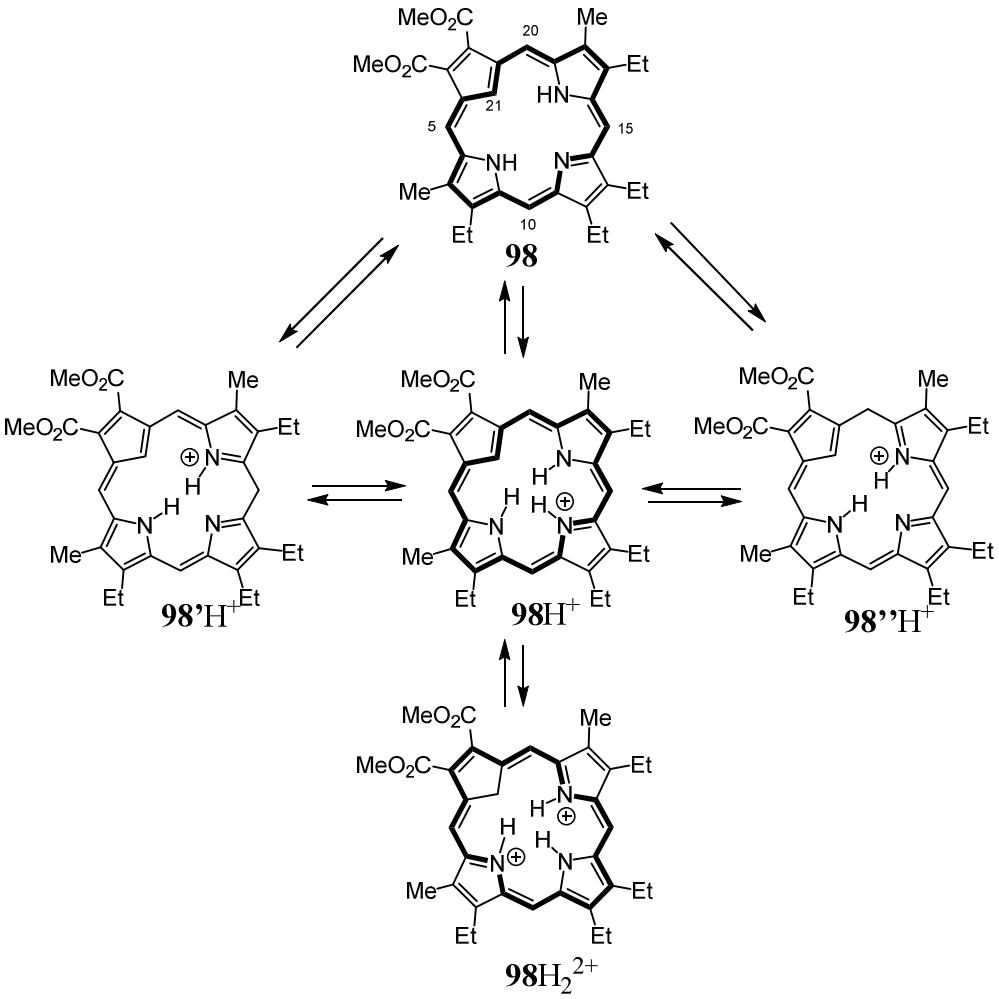

Scheme 56 Proposed Equilibria of Different Cationic Species for Carbaporphyrin **98**

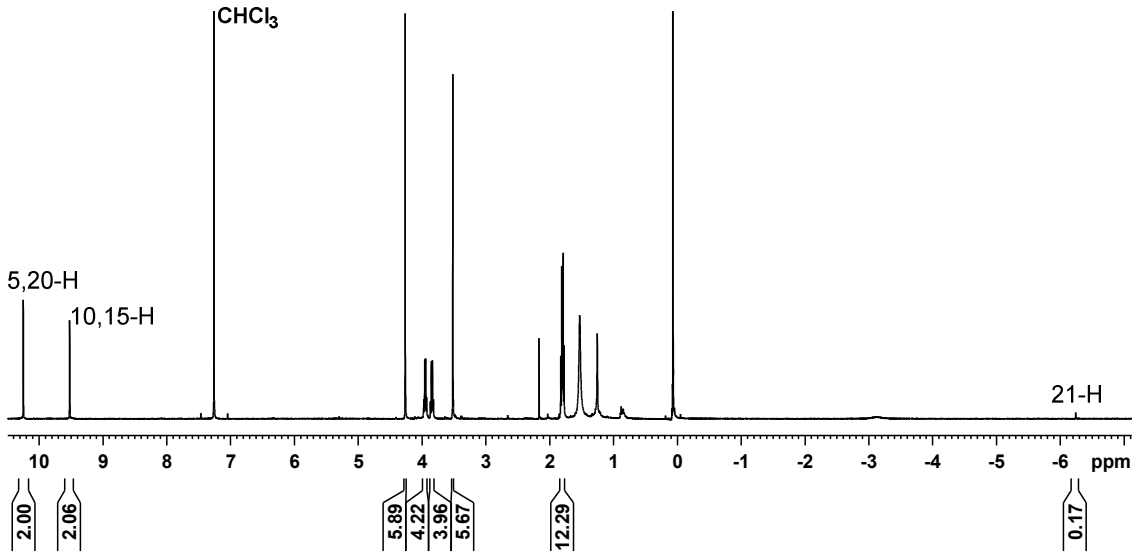

Figure 26 500 MHz proton NMR Spectrum of **98** Showing Exchange of the 21-H after 10 min Exposure to d-TFA

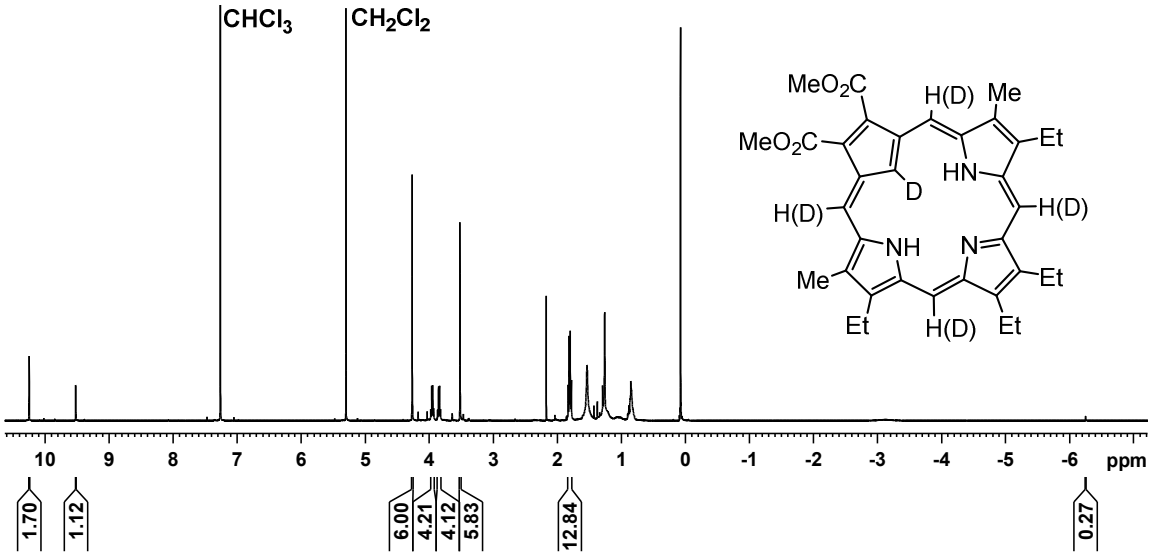

Figure 27 500 MHz proton NMR Spectrum of **98** Showing Partial Exchange of the *meso*-Protons after 24 hr Exposure to d-TFA

When carbachlorin **117** was exposed to a trace amount of TFA, a deep purple solution of the corresponding monocation **117**H^+ (Scheme 57) could be observed by proton NMR (Figure 28) and UV-Vis spectroscopy (Figure 29). The proton NMR spectrum for **117**H^+ showed that the addition of acid to the carbachlorin system had slightly increased its aromatic nature, and although the internal CH was still observed around -7 ppm, the *meso*-protons were shifted further downfield to 10.30 and 9.84 ppm (Figure 28). The appearance of an additional broad peak at -6.0 ppm confirmed the presence of an additional NH due to protonation. Unlike the related carbaporphyrins, further addition of TFA to **117**H^+ did not give a diprotonated species as protonation at the inner carbon would result in a disruption of macrocyclic aromatic character.

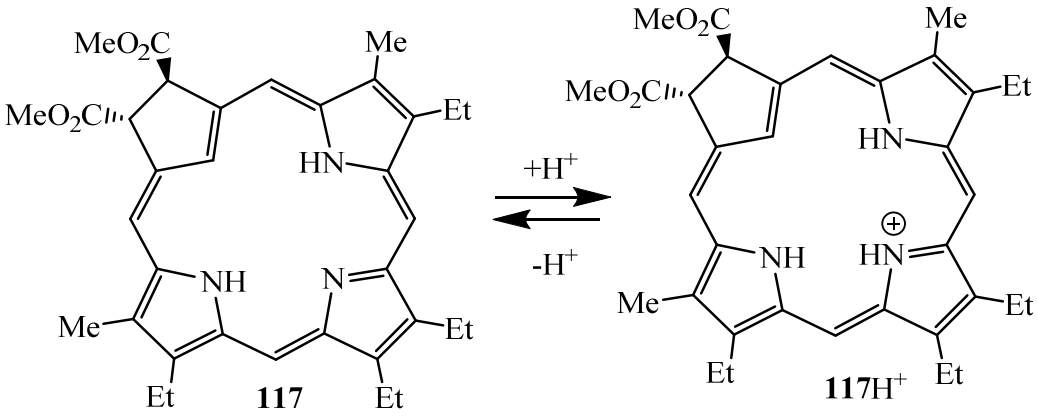

Scheme 57 Protonation of Carbachlorin byproduct **117**H^+

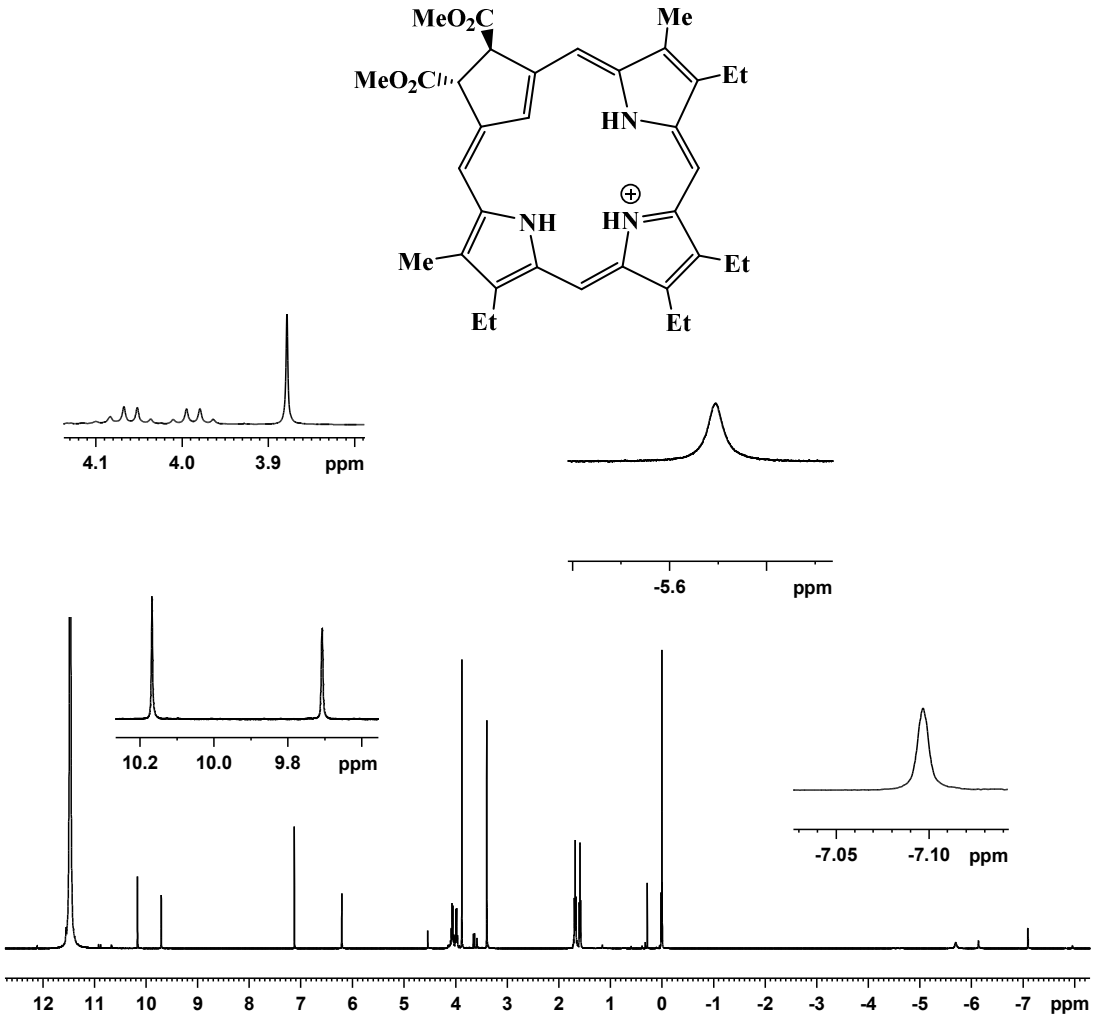

Figure 28 500 MHz ^{1}H NMR Spectrum of **117**H^{+} in $CDCl_3$

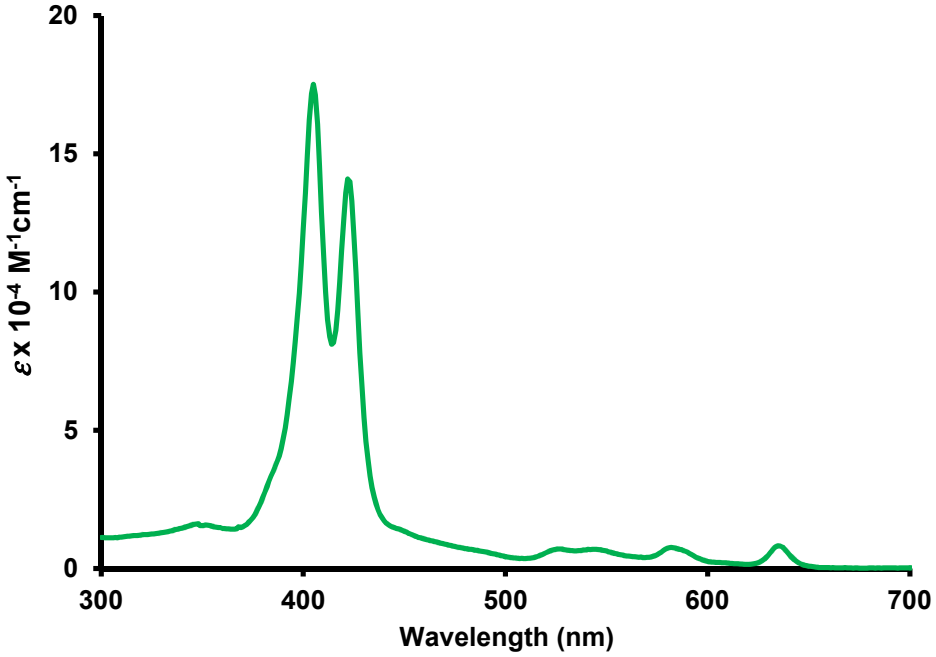

Figure 29 UV-vis spectrum of **117**H^+ in 5% TFA-Dichloromethane.

Metalation of carbaporphyrin **98** was also investigated. As several carbaporphyrinoid systems have been shown to form silver(III) derivatives, the synthesis of a silver(III) complex of carbaporphyrin **98** was attempted. A solution of carbaporphyrin **98** in CH_2Cl_2 was added to a suspension of silver(I) acetate in methanol, and the resulting mixture was stirred overnight at room temperature. After column chromatography, a red fraction was collected and recrystallized using chloroform and methanol to yield the organometallic complex **118** as a dark red powder in 60% yield (Scheme 58).[63] Silver complex **118** retains aromatic characteristics as indicated by proton NMR spectroscopy (Figure 30). The *meso*-protons were deshielded showing up as two 2H singlets at 9.91 and 8.79 ppm. However, due to metal complexation, there were no upfield resonances beyond the TMS reference as the core CH and NH protons of the carbaporphyrin are no longer present.

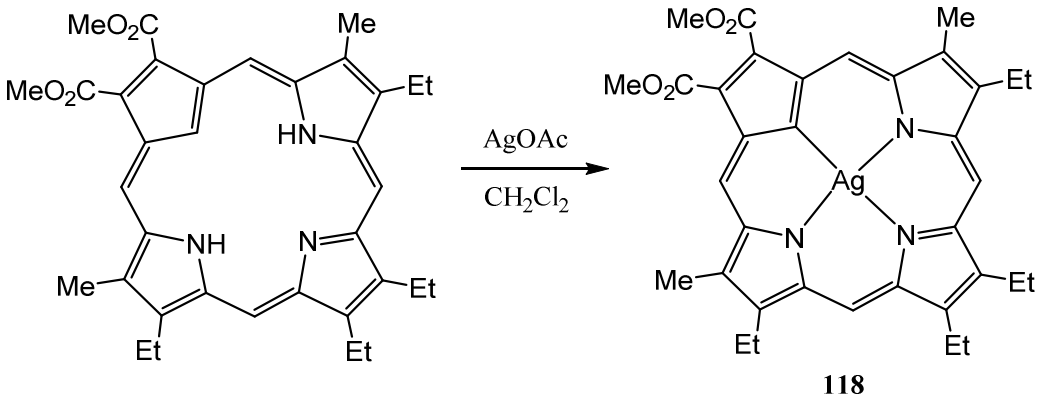

118

Scheme 58 Synthesis of Silver(III) Carbaporphyrin **118**

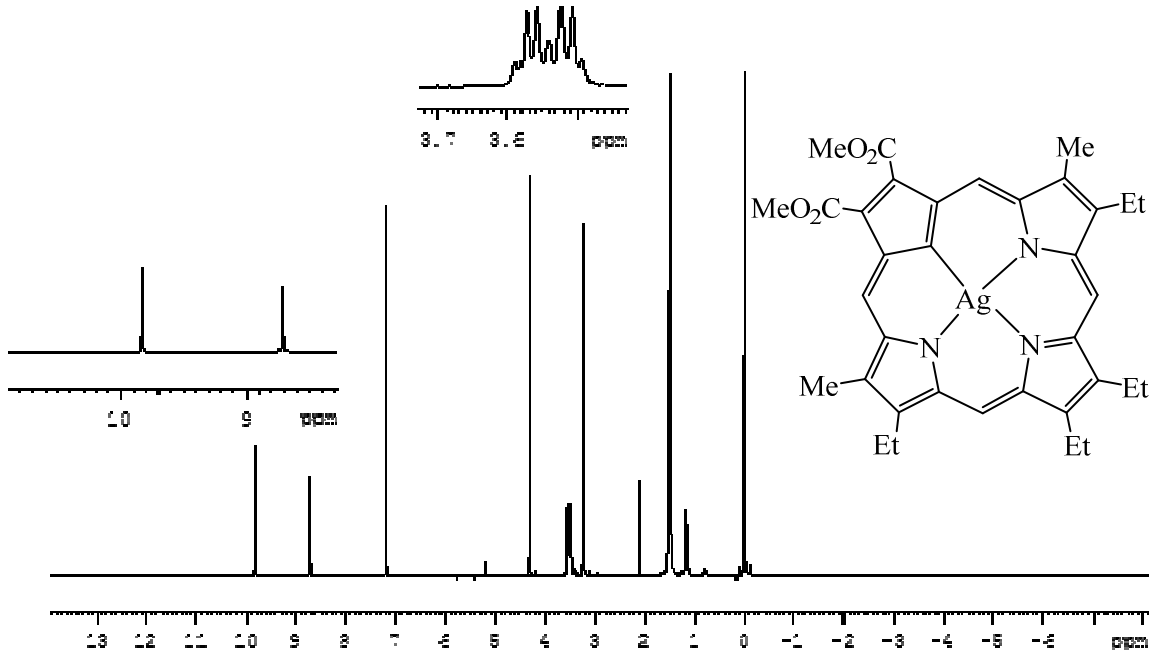

Figure 30 500 MHz ^{1}H NMR Spectrum of **118** in $CDCl_3$.

In addition to the silver complex, the formation of a related gold(III) complex using gold(III) acetate was attempted. Similar reaction conditions to those used for silver complex formation were implemented. However, this reaction did not yield the gold complex. Different

reaction conditions were tried using the same solvent system but no metalated product could be isolated. However, when **98** was refluxed with gold(III) acetate in pyridine, the solution rapidly changed color from brown to dark red once it started to reflux. After 5 minutes of refluxing, it was determined by TLC analysis that not all of the starting free base porphyrin **98** had reacted with the gold(III) acetate. After 30 minutes of reaction time it was observed that most of the conversion has taken place, and the reaction was stopped. Purification using column chromatography gave the gold(III) complex **119** in 11% yield (Scheme 59). The derivative also retained aromatic characteristics and gave a quite similar UV-vis spectrum to the silver complex.

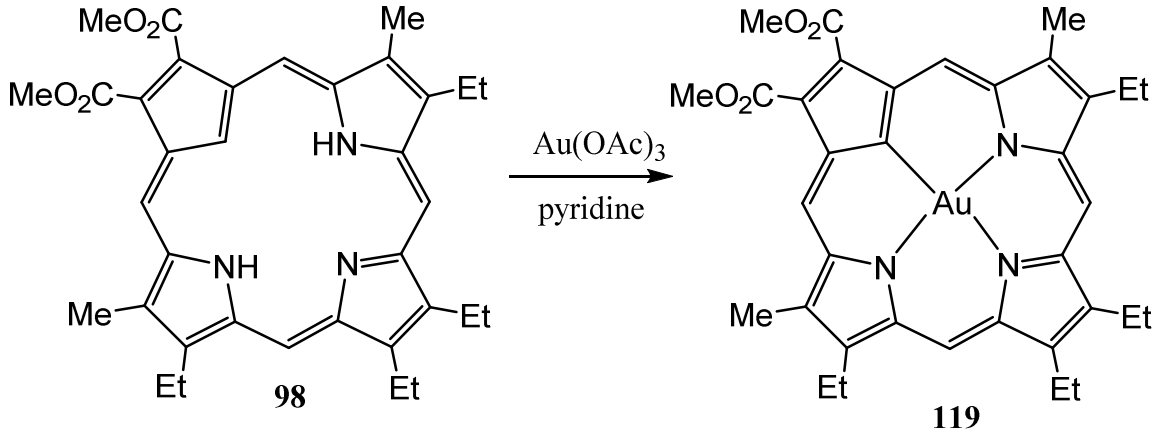

Scheme 59 Formation of Gold(III) Complex of Carbaporphyrin

Previously, a benzocarbaporphyrin had been shown to react with methyl or ethyl iodide and potassium carbonate in refluxing acetone to afford N- and C- alkylation products.[49] Therefore, it was of interest to see whether the new carbaporphyrin system, with two electron withdrawing ester groups on adjacent carbons, could also be alkylated under similar conditions. It was interesting to observe that when carbaporphyrin **98** was stirred with potassium carbonate and methyl iodide in refluxing acetone solution for 30 minutes, an alkylation product was obtained in

up to 55% yield after purification (Scheme 60).[64] However, unlike the alkylation of benzocarbaporphyrin **57**, only one monoalkylation product **120** was observed for this reaction.

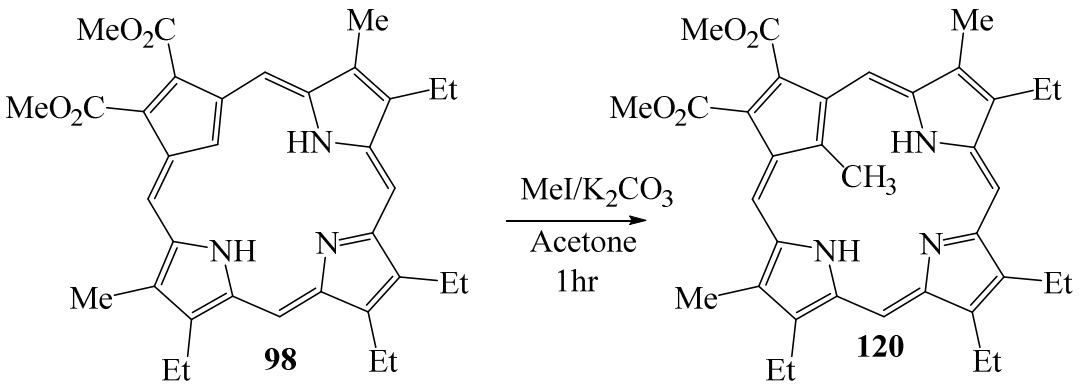

Scheme 60 Formation of C-methylated Carbaporphyrin **120**

In the proton NMR spectrum of **120** (Figure 31), the presence of singlet at -4.68 ppm (3H) indicated that a methyl group had been introduced within the macrocyclic cavity. The symmetry of the system was still maintained as there were only two signals for the *meso*-protons showing up at 9.90 and 9.28 ppm. The spectroscopic data were consistent with a C-methyl derivative rather than the alternative N-alkylation product.

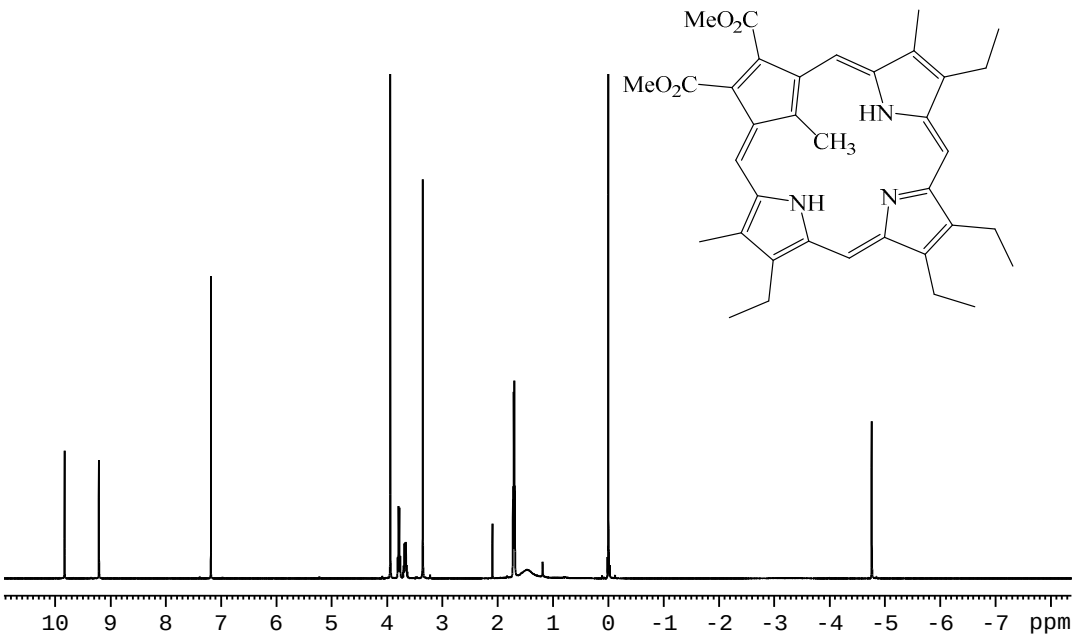

Figure 31 500 MHz ^{1}H NMR Spectrum of **120** in $CDCl_3$

When carbaporphyrin **98** was stirred with potassium carbonate using an excess of iodomethane in acetone and the reaction was refluxed overnight, further reaction took place. Following column chromatography, a major dialkylation product was isolated with methyl groups on both the inner carbon and an adjacent nitrogen atom (Scheme 61).[49] After recrystallization from chloroform-methanol, the dimethylated carbaporphyrin **121** was isolated as shiny purple crystals in 69% yield.

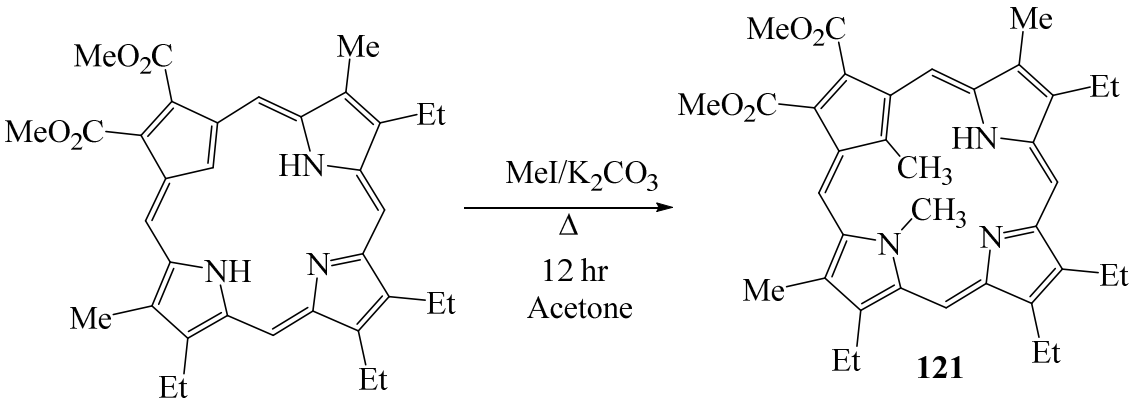

Scheme 61 Formation of Dimethylated Carbaporphyrin **121**

In the proton NMR spectrum for the dimethylated carbaporphyrin, the internal methyl groups showed up as two 3H singlets at -5.27 and -3.91 ppm. The four *meso*-protons appeared as four separate singlets indicating a loss of symmetry in the structure. This loss of symmetry could be explained if one of the methyl groups is attached to a pyrrole nitrogen that is flanking the carbocyclic ring. In addition, as the methyl groups are too large to fit within the cavity, they could both be placed to one side of the structure. It is also likely that the two methyl groups are placed on opposite sides of the macrocycle. The resulting structure is chiral and would exist as a pair of enantiomers. Although the presence of internal methyl groups may distort the structure, **121** is still a strongly aromatic compound. As noted above, the internal methyl resonances are highly shielded, while the *meso*-protons are relatively deshielded and show up at 8.90, 9.05, 9.52 and 9.54 ppm (Figure 32).

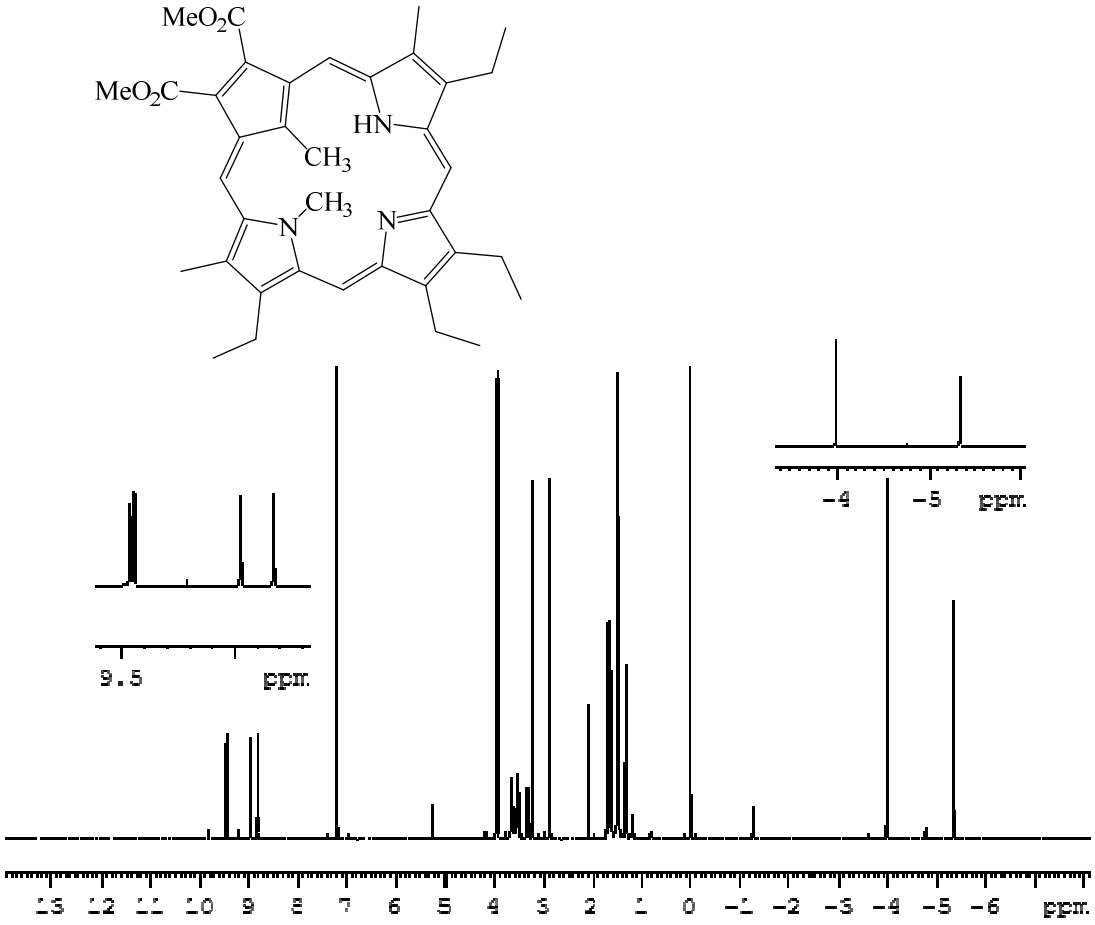

Figure 32 500 MHz ^{1}H NMR Spectrum of **121** in $CDCl_3$

Addition of TFA to a solution of C-methylcarbaporphyrin **120** led to the formation of monocation **120**H^+. The proton NMR spectrum for this species indicated a slight increase in aromatic character is developed on protonation, as the internal methyl resonance is shifted upfield to -5.41 ppm while the *meso*-protons are shifted downfield to 9.49 and 10.03 ppm (Figure 33).

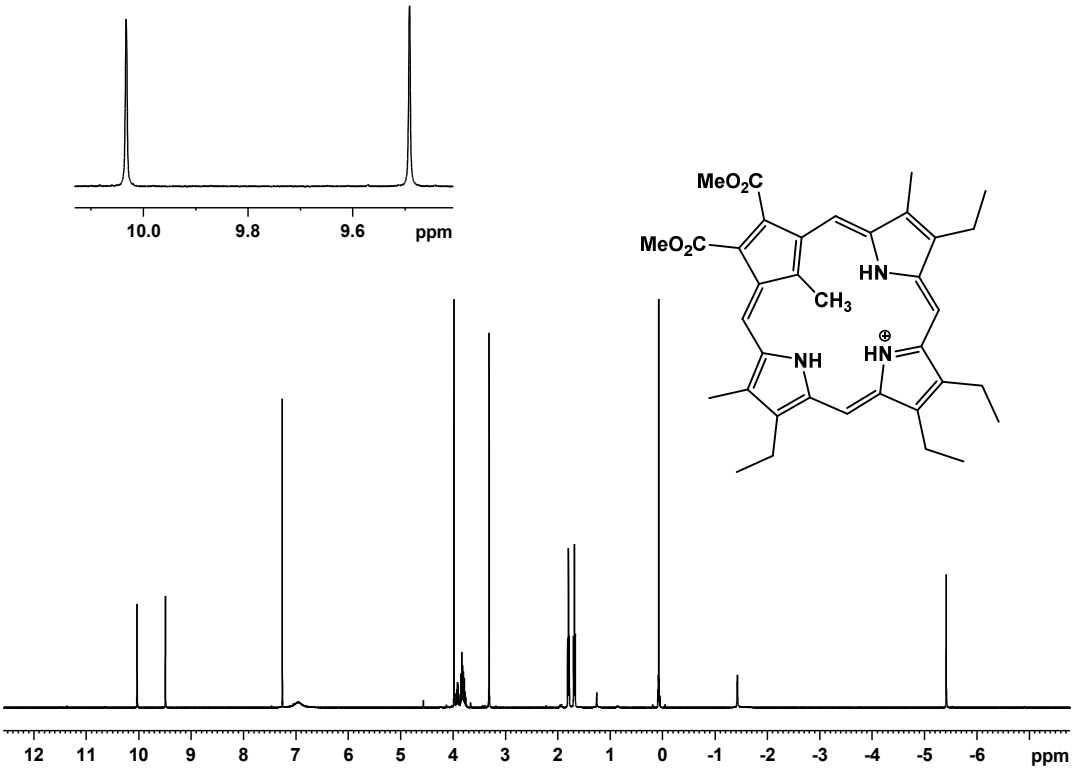

Figure 33 500 MHz ^{1}H NMR Spectrum of **120**H^{+} in $CDCl_3$

Further addition of TFA led to the formation of a diprotonated dication **120**H_2^{2+} showing a doublet at -6.55 ppm due to protonation at the internal methyl carbon (Figure 34). The *meso*-protons lie close to the TFA peak, showing up 11.08 and 11.7 ppm, indicating increased diamagnetic character. It is worth noting that both the mono and dications maintained the plane of symmetry.

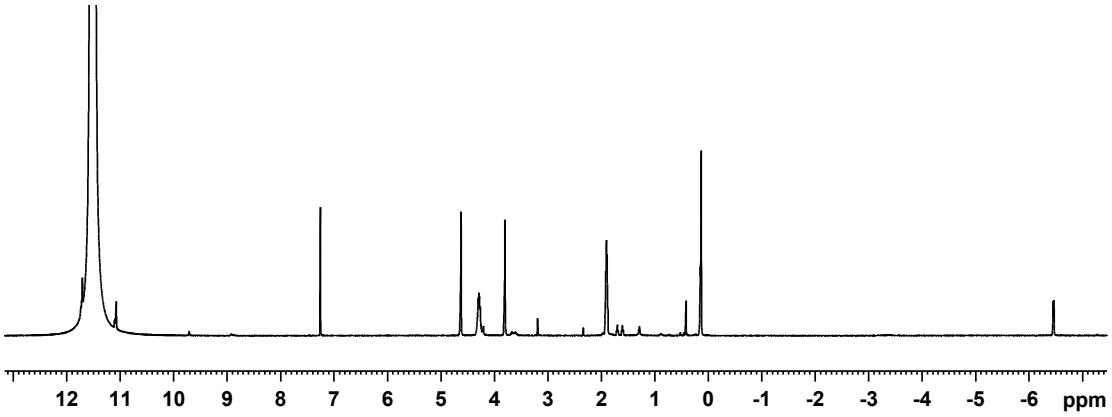

Figure 34 500 MHz ^{1}H NMR Spectrum of **120**H_2^{2+} in $CDCl_3$

Addition of TFA to a solution of dimethylcarbaporphyrin **121** led to the formation of monocation **121**H^+(Figure 35). However, further addition of acid did not generate the related dication. The proton NMR spectrum of **121**H^+ showed four singlets for the *meso*-protons at 9.92, 9.86, 9.46 and 9.45 ppm. The internal methyl resonances appeared at -3.54 and -4.91 ppm. The results indicate that the protonated species has a slightly stronger diatropic ring current than the free base form **121**.

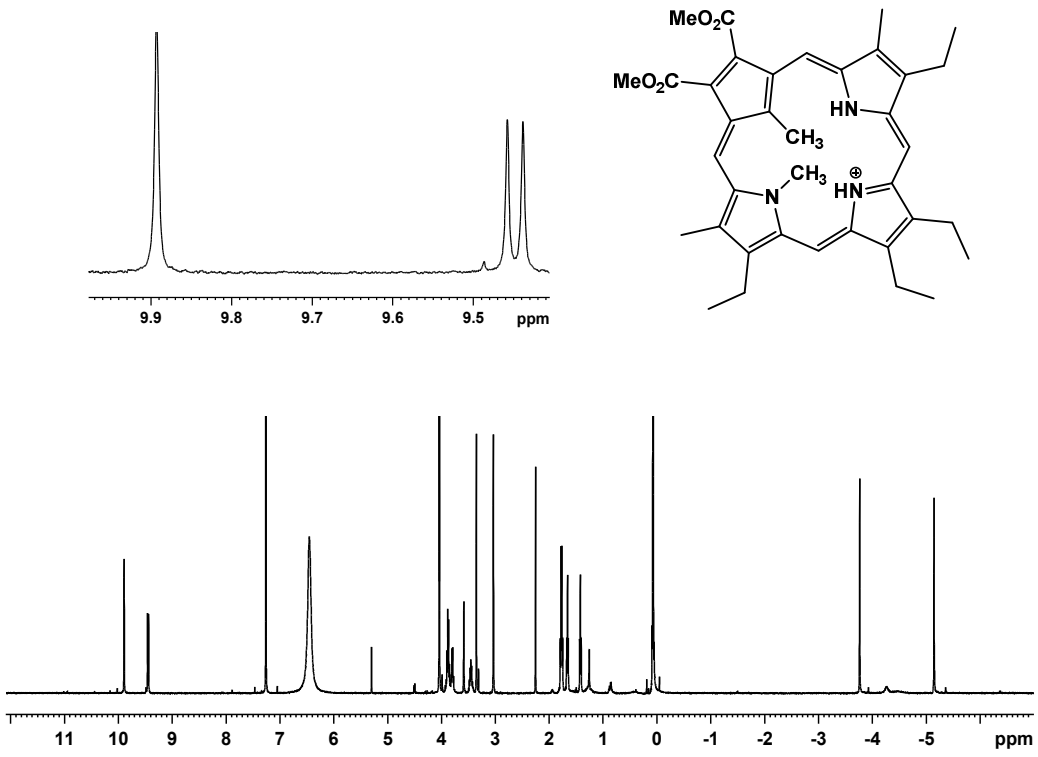

Figure 35 500 MHz ^{1}H NMR Spectrum of **121**H^{+} in $CDCl_3$

Metalation of N-methylated benzocarbaporphyrin with palladium(II) acetate in refluxing acetonitrile has previously been shown to give a palladium(II) organometallic derivative.[64] The metalation reaction in benzocarbaporphyrins is associated with an alkyl group migration from the nitrogen to the inner carbon atom. However, in **120** the methyl group is already attached to the internal carbon and no rearrangement would be necessary to form an analogous palladium complex. In fact, reaction of **120** with palladium(II) acetate is reflexing acetonitrile gave the organometallic derivative **122** in 63% yield (Scheme 62).[49] Although, the conjugation pathway in the metal complex has been altered, the macrocycle still remains fully aromatic.

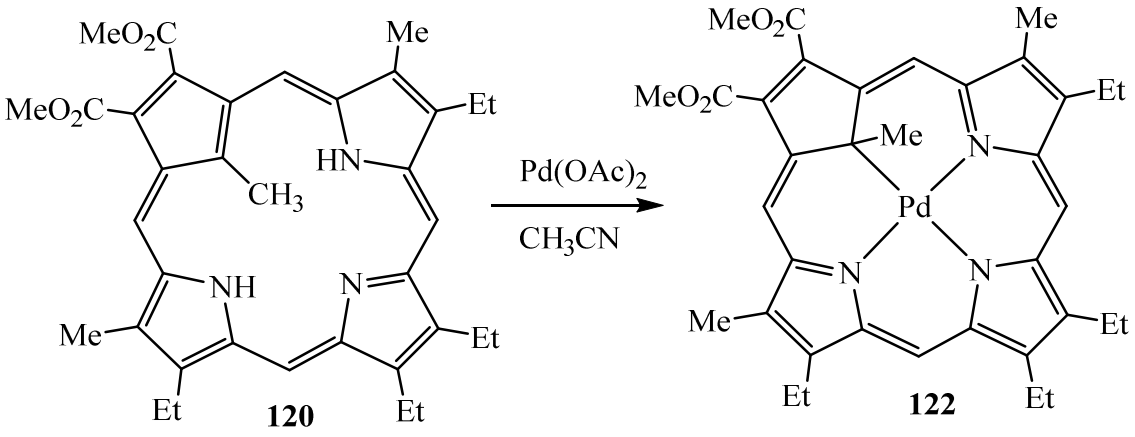

Scheme 62 Metalation of C-methylcarbaporphyrin with Palladium(II) Acetate

The proton NMR spectrum of **122** (Figure 36) gave two 2H singlets at 9.85 and 10.81 ppm in the downfield region for the four *meso*-protons, confirming that compound **122** has a plane of symmetry. Moreover, the presence of a singlet at -4.12 ppm (3H) indicated that the internal methyl group was strongly shielded. As the symmetry of the alkylation product after complexation is still maintained, the results indicate that no rearrangement has taken place. The UV-Vis spectrum for the Pd complex shows a strong Soret band at 306 nm and Q bands at 410, 460, 602 and 639 nm (Figure 37) that further support its aromatic character. The structure of palladium complex **122** was also confirmed using X-ray crystallography (Figure 38).

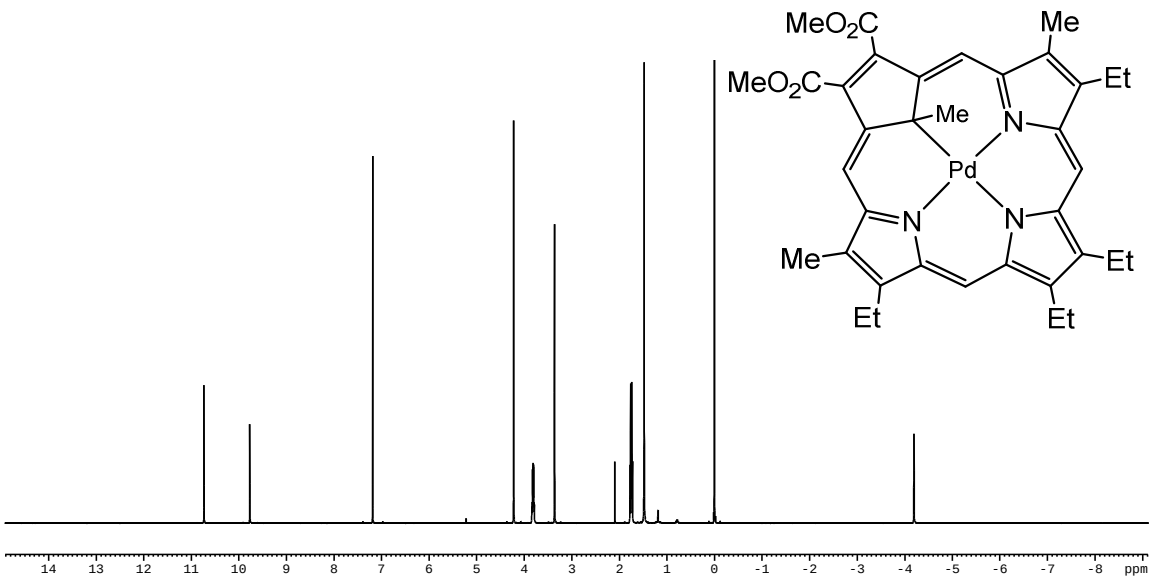

Figure 36 500 MHz ^{1}H NMR Spectrum of **122** in $CDCl_3$

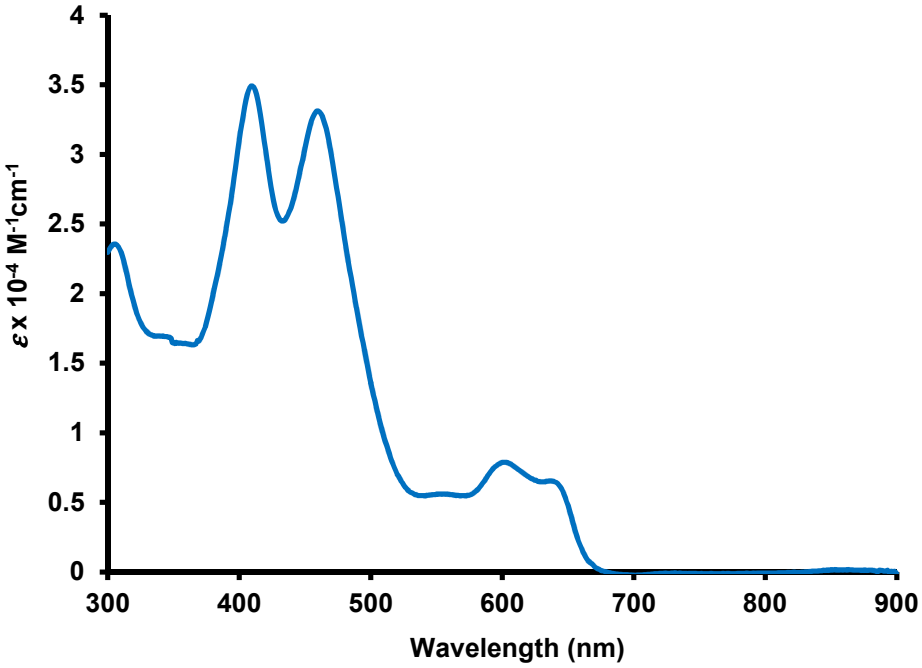

Figure 37 UV-vis Spectrum of Palladium(II) Carbaporphyrin in Chloroform

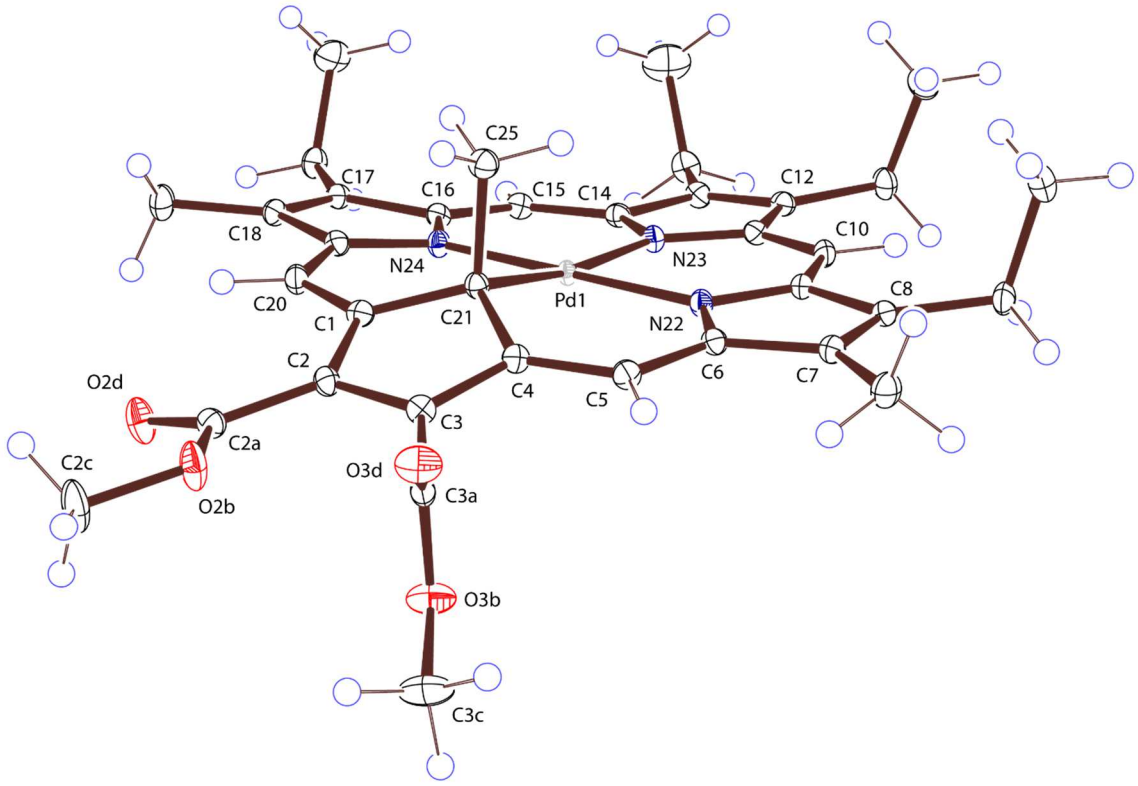

Figure 38 POV-Ray rendered ORTEP III Drawing of **122**

Nickel complexes of carbaporphyrins have not been previously reported and attempts were made to prepare a similar complex from nickel(II) acetate. Under the same set of conditions, no formation of a nickel complex was observed. However, when **120** was refluxed with nickel(II) acetate in DMF, the solution rapidly turned from brown to dark green as soon as it started to reflux. After 5 minutes of refluxing, it was determined by TLC analysis that all of the starting carbaporphyrin **120** had reacted with the nickel(II) acetate. After column chromatography, a green colored fraction was obtained that corresponded to nickel(II) complex **123.** After recrystallization from methanol and chloroform, the pure complex was obtained in 71% yield. (Scheme 63).

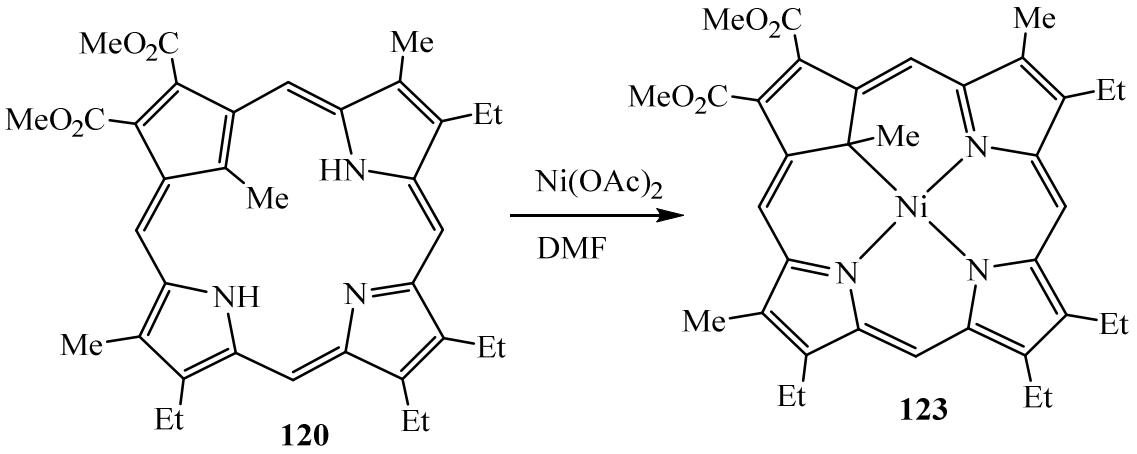

Scheme 63 Metalation of C-methylcarbaporphyrin with Nickel(II) Acetate

The proton NMR spectrum of **123** (Figure 39) showed two singlets at 9.59 and 10.56 ppm in the downfield region for the four *meso*-protons, suggesting that compound **123** has retained the plane of symmetry. Moreover, the presence of a singlet at -3.89 ppm (3H) indicated that an internal methyl group was still present. Clearly, the macrocycle still retained fully aromatic characteristics. The structure was also confirmed by X-ray crystallography (Figure 40).

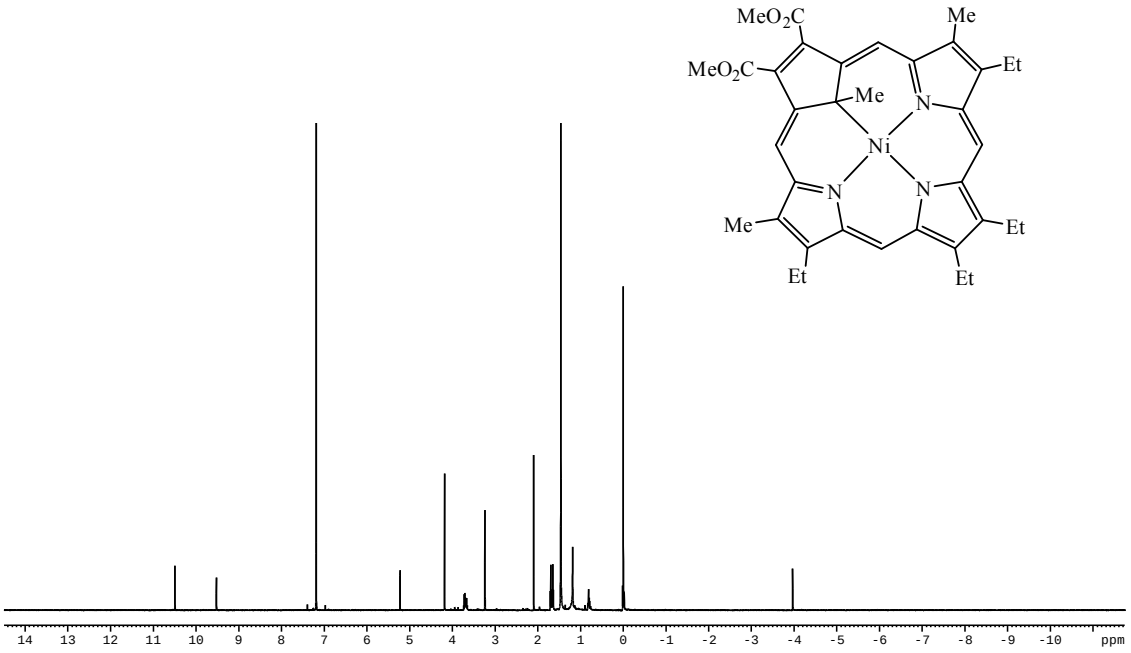

Figure 39 500 MHz ^{1}H NMR Spectrum of **123** in $CDCl_3$

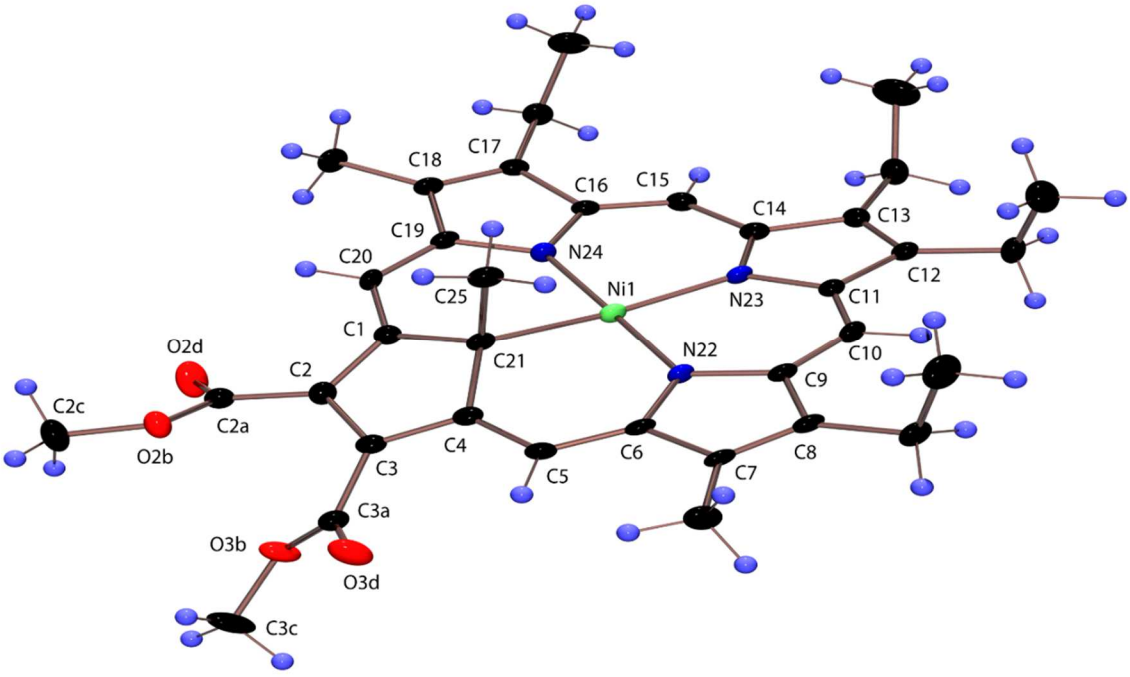

Figure 40 POV-Ray rendered ORTEP III Drawing of **123**

Conclusions

A cyclopentane dialdehyde was prepared in two steps from the Diels–Alder adduct of dimethyl fumarate and cyclopentadiene. The '3+1' condensation of dialdehyde **99** and tripyrrane dicarboxylic acid **62** led to the formation of carbaporphyrin **98** in 40% yield together with some carbachlorin **117** byproduct. This newly synthesized carbaporphyrin system proved to be highly aromatic. Protonation of this system can readily occur, forming both mono- and dications. Alkylation and metalation products were also synthesized and characterized.

Carbachlorin **117** can also readily form a monocation **117**H^+ when TFA is added, but no dication formation was observed. Reaction between carbaporphyrin **98** and silver(I) acetate gave a silver(III) organometallic complex. Similarly, reaction between carbaporphyrin **98** and gold(III) acetate afforded a gold(III) organometallic complex, albeit in low yield. Alkylation of carbaporphyrin **98** gave a C-methylated product **120** when refluxed with methyl iodide for 1 hr, but a dimethylated product predominated when the reaction was carried out overnight. Protonation of the monoalkylated carbaporphyrin with TFA gave both monocationic and dicationic species, but the dimethylated species only formed a monocation. Metalation of **120** with palladium(II) acetate afforded palladium(II) carbaporphyrin, while reaction with nickel(II) acetate afforded a related nickel(II) carbaporphyrin in good yields.

The straightforward synthesis of carbaporphyrin **98** will allow further studies on this system to be conducted. It is anticipated that the ester moieties can be reduced to give carbaporphyrin alcohols. Initial investigations with $LiAlH_4$ led to decomposition, but reaction with diisobutylaluminium hydride (DIBAL-H) selectively reduced one of the ester units. At -70 ℃, the related monoaldehyde **124** was generated but at room temperature monoalcohol **125** was formed (Scheme 64). So far attempts to reduce both ester moieties have been unsuccessful.

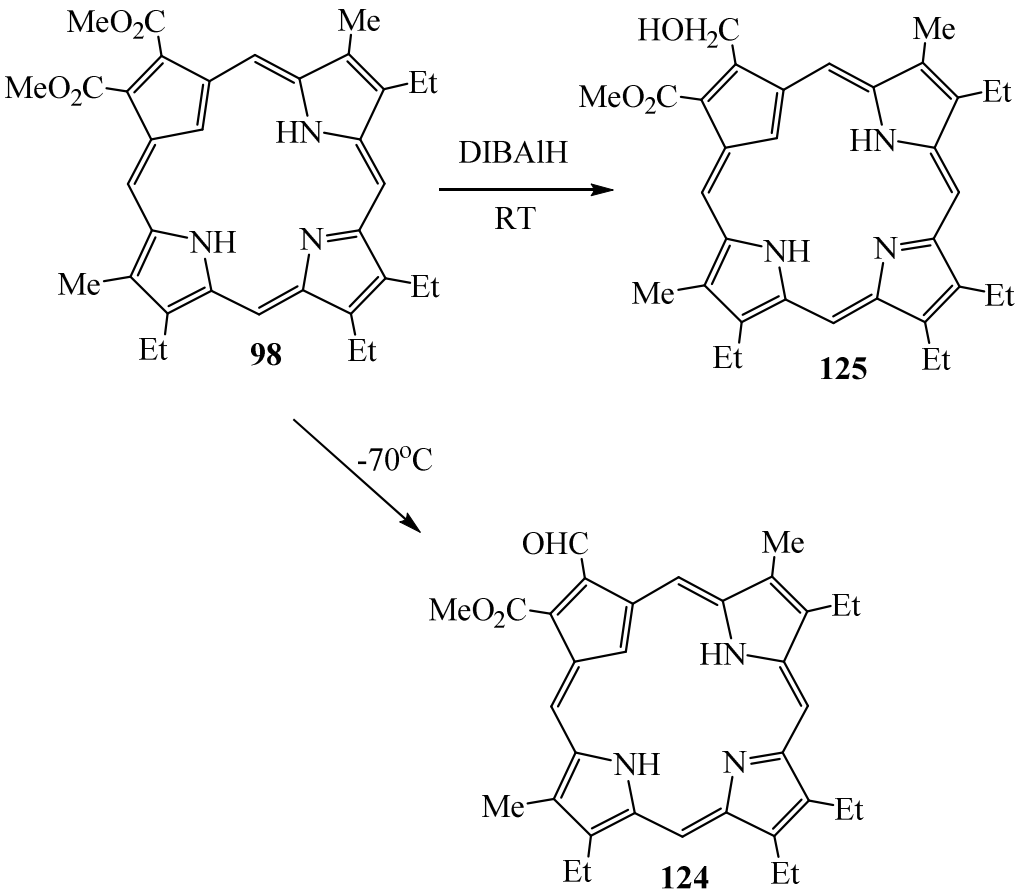

Scheme 64 Reduction of Carbaporphyrin **98**

Reduction to diol **126** could enable novel cycloaddition chemistry to be investigated. Conversion to the related dibromide **127** might be accomplished by reaction with phosphorus tribromide. Treatment with sodium iodide may result in the formation of a transient diene **128** that could undergo a Diels–Alder cycloaddition with suitable dienophiles such as dimethyl acetylenedicarboxylate to generate **129** (Scheme 65). This chemistry will make new classes of carbaporphyrin derivatives accessible.

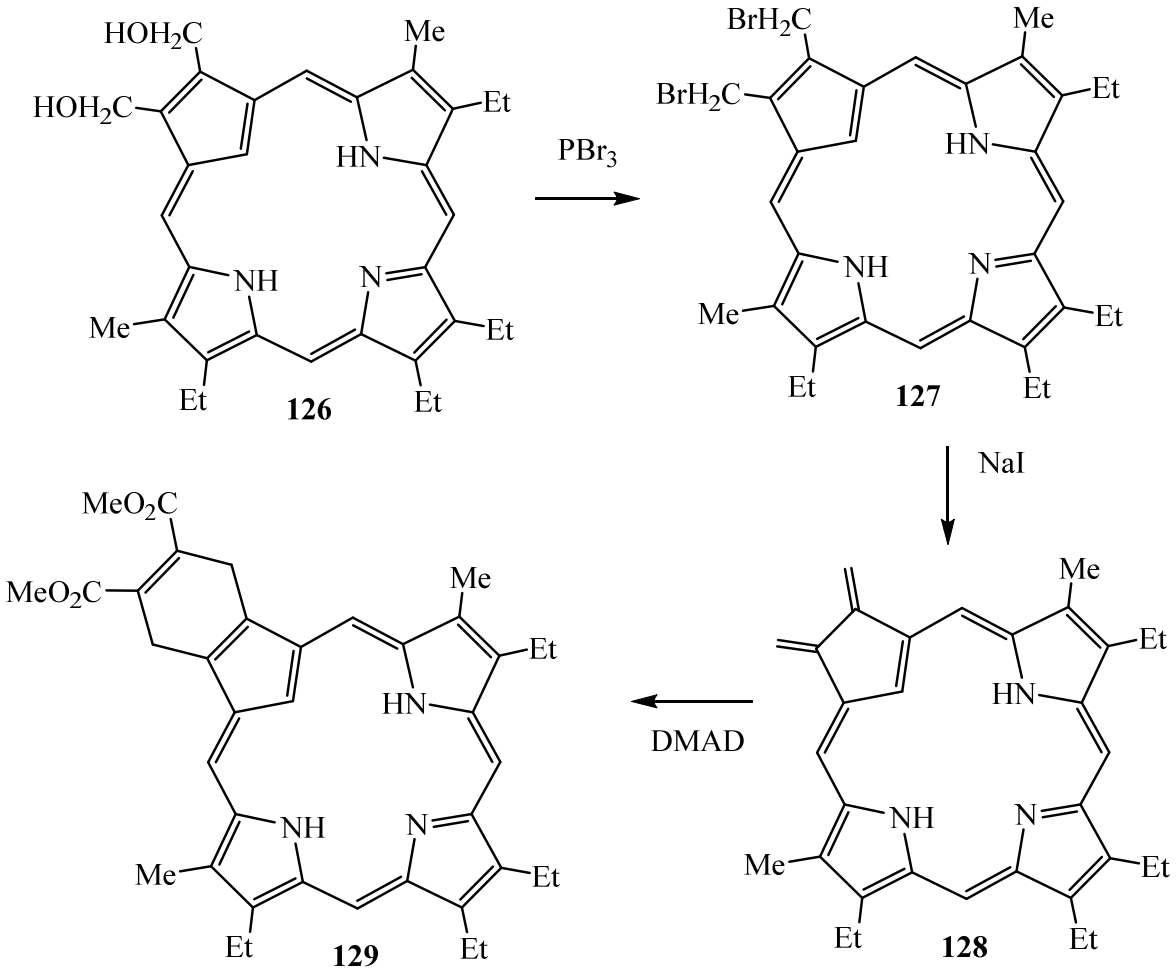

Scheme 65 New Class of Carbaporphyrin Derivatives

Experimental

All chemicals were purchased from Sigma Aldrich or Acros Organic. Grade III neutral alumina and silica gel were used to perform column chromatography. The ^{1}H and ^{13}C-NMR spectra were obtained either using Bruker Avance III 500 MHz NMR spectrometer or Bukner 400 MHz NMR spectrometer at 302 K. Chemical shifts were recorded, relative to $CDCl_3$ (residual chloroform at δ 7.26 ppm) in proton NMR spectra and the $CDCl_3$ triplet at δ 77.23 ppm in ^{13}C-NMR spectra, in parts per million (ppm). 2D experiments were performed by using standard

software. The UV-vis spectra for the compounds were collected by Cary 100 Bio spectrophotometer. Melting point were gathered using a Mel-Temp apparatus. High-resolution mass spectra (HRMS) were carried out by using a double focusing magnetic sector instrument Mass spectrometry data was obtained from the Mass Spectral Laboratory, School of Chemical Sciences, University of Illinois, Urbana-Champaign.

Dimethyl bicyclo[2.2.1]hept-5-ene-2-endo-3-exo-dicarboxylate (**114**)

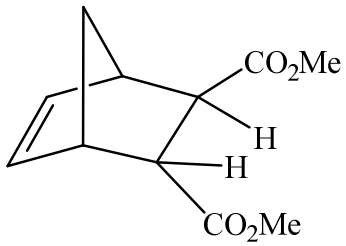

Freshly distilled cyclopentadiene (6.6 ml, 78 mmol) was added to a suspension of dimethyl fumarate (10 g, 69.3 mmol) in water (400 mL) and the suspension was stirred vigorously for 120 minutes. Ethyl acetate (150 mL) was added and the phases were separated, the organic phase was dried over Na_2SO_4 and the solvent evaporated to give the title compound (10.7 g, 50.9 mmol, 73%) as a colorless oil. ^{1}H NMR (400 MHz, $CDCl_3$): δ 1.46 (1H, dq, *J* = 8.8, 1.7 Hz), 1.62 (1H, br t, *J* = 8.8 Hz), 2.69 (1H, dd, *J* = 4.5, 1.7 Hz), 3.11-3.14 (1H, m), 3.25-3.28 (1H, m), 3.38 (1H, t, *J* = 4.1 Hz), 3.65 (3H, s), 3.72 (3H, s), 6.07 (1H, dd, *J* = 5.6, 2.8 Hz), 6.28 (1H, dd, *J* = 5.6, 3.1 Hz). ^{13}C NMR (100 MHz, $CDCl_3$): δ 45.9, 47.3, 47.5, 47.8, 48.1, 52.0, 52.3, 135.4, 137.8, 173.9, 175.1

Dimethyl 5,6-dihydroxybicyclo [2.2.1] heptane-2,3-dicarboxylate (**115**)

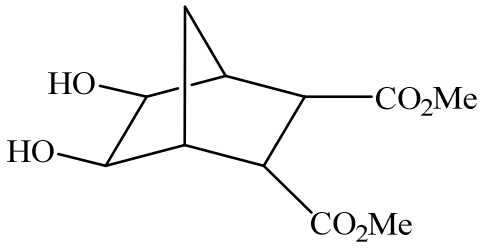

To a solution of norbornene **114** (10.83 g, 51.5 mmol) in *tert*-butyl alcohol (200 mL) and water (50 mL) at 0 °C was added dropwise a solution of potassium permanganate (12.0 g, 76.0 mmol) and sodium hydroxide (2.61 g, 65.3 mmol) in water (250 mL). After the addition was complete, the reaction mixture was stirred for 20 minutes and then quenched using a saturated aqueous solution of sodium metabisulphite ($Na_2S_2O_5$) until the solution turned colorless. The mixture was filtered and the *tert*-butyl alcohol was removed from the filtrate *in vacuo*. The solution was extracted with ethyl acetate (4 × 100 mL) and the combined organic layers dried over $MgSO_4$, filtered and concentrated *in vacuo* to furnish the diol **115** (6.85 g, 28.0 mmol, 55%) as a white crystalline solid, mp 84-86 °C (lit. mp[59] 81-84 °C). ^{1}H NMR (400 MHz, $CDCl_3$): δ 1.44 (1H, dp, *J* = 11.0, 1.5 Hz), 1.89 (1H, dq, *J* = 11.0, 1.5 Hz), 2.50 (1H, br s), 2.55-2.57 (1H, m), 2.62 (1H, br), 2.73 (1H, br s overlapping with dd, *J* = 5.7, 1.3 Hz), 3.20 (1H, t, *J* = 5.1 Hz), 3.70 (3H, s), 3.71 (3H, s), 3.76-3.79 (1H, br m), 3.86-3.89 (br m). ^{13}C NMR (100 MHz, $CDCl_3$): δ 31.9, 45.0, 46.4, 46.7, 48.5, 52.4, 52.5, 70.6, 73.7, 173.1, 174.2. HRMS (EI): calcd for $C_{11}H_{16}O_6$ + H 245.1025, found 245.1027.

Dimethyl 3,5-diformylcyclopentane-1,2-dicarboxylate (**99**)

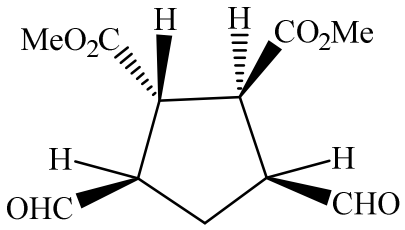

The foregoing diol **115** (4.15 g, 16.9 mmol) was mixed with water (5.0 ml), ether (10 ml) and potassium periodate (4.66 g, 20.3 mmol), and the reaction was stirred at room temperature for 1 hr. The excess potassium periodate was filtered off and the two phases were separated. The water layer was back extracted twice with ether. The ether layers were combined, dried over Na_2SO_4, and the ether removed under reduced pressure to gave dialdehyde as a clear oil **99** (2.08 g, 8.59 mmol, 50%). The unstable dialdehyde was not further purified but used immediately to prepare carbaporphyrin. ^{1}H NMR (400 MHz, $CDCl_3$): 2.17-2.26 (1H, m), 2.46 (1H, dt, J = 13.8, 5.9 Hz), 3.05-3.10 (1H, m), 3.26-3.32 (1H, m), 3.56-3.65 (2H, m), 3.70 (3H, s), 3.76 (3H, s), 9.65 (1H, d, J = 0.8 Hz), 9.68 (1H, d, J = 0.9 Hz). HRMS (EI): calcd for $C_{11}H_{14}O_6$ + H 243.0869, found 243.0871.

8,12,13,17-Tetraethyl-2,3-di(methoxycarbonyl)-7,18-dimethyl-21-carbaporphyrin (**98**)

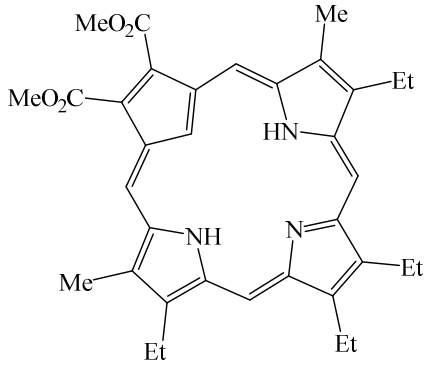

Tripyrrane dicarboxylic acid **62** (100 mg, 0.22 mol) was stirred with TFA (1 ml) under an atmosphere of nitrogen for 2 minutes in a 250 ml round bottom flask. Dichloromethane (99 ml) was added, followed immediately by dialdehyde **99** (56 mg, 0.23 mol), and the mixture was stirred under nitrogen overnight. The mixture was neutralized by the addition of triethylamine and the solvent removed under reduced pressure. The residue was taken up in toluene (50 ml), DDQ (150 mg, 0.66 mmol) was added and the resulting mixture was stirred under reflux for 1 hr. The solvent was removed under reduced pressure, then the residue was dissolved in CH_2Cl_2 and washed with water. The solution was concentrated under reduced pressure and the residue chromatographed on grade III neutral alumina column eluting with CH_2Cl_2 and hexane in a ratio of 60:40. The product was collected as a dark brown fraction that was the second fraction eluting from the column. Recrystallization from chloroform and methanol gave carbaporphyrin (52 mg, 0.091 mmol, 42%) as purple crystals, mp 234-236ºC; UV-Vis (1% Et_3N-CH_2Cl_2): λ_{max} (log ε) 368 (4.73), 436 (5.00), 526 (4.04), 566 (4.24), 648 (3.31), 717 nm (3.43). UV-Vis (5% DBU-CH_2Cl_2): λ_{max} (log ε) 361 (4.59), 450 (4.80), 530 (sh, 3.55), 572 (sh, 3.80), 625 nm (4.01). UV-Vis (100 eq TFA-CH_2Cl_2): λ_{max} (log ε) 315 (4.46), 392 (4.77), 446 (4.91), 549 nm (4.05). UV-Vis (50% TFA-CH_2Cl_2): λ_{max} (log ε) 315 (4.15), 407 (5.17), 425 (5.12), 549 (3.79), 597 (3.96), 656 nm (3.27). ^{1}H NMR (500

MHz, $CDCl_3$): δ -6.27 (1H, s), -3.12 (2H, br), 1.77-1.83 (12H, 2 overlapping triplets), 3.51 (6H, s), 3.84 (4H, q, *J* = 7.6 Hz), 3.95 (4H, q, *J* = 7.6 Hz), 4.27 (6H, s), 9.51 (2H, s), 10.24 (2H, s). ^{13}C NMR (125 MHz, $CDCl_3$): δ 11.5, 17.3, 18.4, 19.5, 19.9, 52.6, 94.6, 100.7, 107.2, 130.5, 131.6, 135.5, 136.0, 137.7, 139.4, 145.4, 156.1, 167.6. ^1H NMR (500 MHz, 4µl TFA-$CDCl_3$): δ -5.95 (1H, s), -3.14 (1H, v br), -1.97 (2H, s), 1.65 (6H, t, *J* = 7.6 Hz), 1.80 (6H, t, *J* = 7.6 Hz), 3.44 (6H, s), 3.90-4.00 (8H, 2 overlapping quartets), 4.26 (6H, s), 9.74 (2H, s), 10.40 (2H, s). ^{13}C NMR (125 MHz, 4µl TFA-$CDCl_3$): δ 11.7, 16.6, 17.4, 19.78, 19.81, 53.2, 94.2, 111.8, 113.8, 132.7, 134.1, 138.5, 140.2, 140.4, 140.5, 141.5, 142.9, 167.3. ^1H NMR (500 MHz, 50% TFA-$CDCl_3$): δ -7.65 (1H, s), 1.82 (12H, t, *J* = 7.6 Hz), 3.79 (6H, s), 4.22-4.32 (8H, m), 4.69 (6H), 11.10 (2H, s), 11.86 (2H, s). ^{13}C NMR (125 MHz, 50% TFA-$CDCl_3$): δ 11.7, 16.3, 17.4, 20.6, 29.2, 55.5, 105.1, 115.0, 142.7, 144.1, 144.8, 146.1, 147.1, 148.2, 148.2, 148.3, 149.0, 149.3, 167.3. HRMS (ESI): calcd for $C_{35}H_{39}N_3O_4$ + H 566.3019, found 566.3047.

trans–8,12,13,17-Tetraethyl-2,3-di(methoxycarbonyl)-7,8-dimethyl-2,3-dihydro-21-carbaporphyrin (**117)**

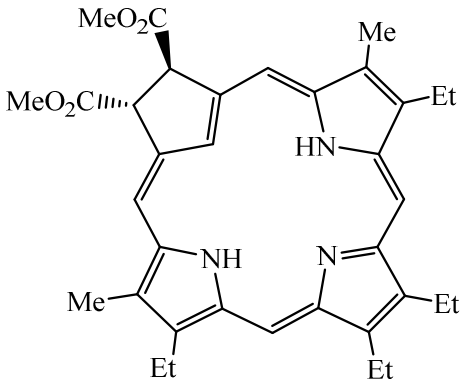

A third green fraction from the previous procedure was evaporated and the residue recrystallized from chloroform-methanol to give the carbachlorin (12 mg; 0.02 mmol, 9%) as a green powder, mp 232-234 ºC; UV-Vis (5% DBU-CH_2Cl_2): λ_{max} (log ε): 398 (4.86), 437 (4.59), 450 (sh, 4.52), 464 (sh, 4.44), 569 (sh, 3.74), 587 (sh, 3.75), 619 (sh, 3.90), 645 (sh, 3.98); UV-Vis (CH_2Cl_2): λ_{max} (log ε): 398 (5.31), 490 (4.17), 588 (3.41), 645 (4.23); UV-Vis (5% TFA-CH_2Cl_2): λ_{max} (log ε): 348 (4.21), 405 (5.24), 422 (5.15), 527 (3.84), 544 (sh, 3.84), 582 (3.88), 635 (3.91); ^{1}H NMR (500MHz, $CDCl_3$): δ -7.14 (1H, s, 21-H), 1.82 (6H, t, *J* = 7.7 Hz), 1.86 (6H, t, *J* = 7.7 Hz), 3.53 (6H, s), 3.92 (6H, s), 3.98 (4H, q, *J* = 7.7 Hz), 4.06 (4H, q, *J* = 7.7 Hz), 6.34 (2H, s), 9.48 (2H, s), 9.85 (2H, s). ^{13}C NMR (125 MHz $CDCl_3$): δ 11.5, 17.6, 18.8, 19.8, 20.1, 53.0, 56.0, 96.6, 97.9, 119.7, 130.0, 133.0, 135.7, 138.0, 139.6, 143.4, 150.5, 173.7. ^{1}H NMR (500 MHz, TFA-$CDCl_3$): δ -6.96 (1H, s), -6.00 (1H, br s), -5.56 (2H, br s), 1.72 (6H, t, *J* = 7.7 Hz), 1.82 (6H, t, *J* = 7.7 Hz), 3.53 (6H, s), 4.01 (6H, s), 4.12 (4H, q, *J* = 7.7 Hz), 4.19 (4H, q, *J* = 7.7 Hz), 6.34 (2H, s), 9.84 (2H, s), 10.30 (2H, s). ^{13}C NMR (125 MHz, TFA-$CDCl_3$): δ 11.4, 16.6, 17.5, 20.2, 20.3, 54.8, 56.9, 94.9, 103.3, 128.4, 134.8, 135.2, 136.2, 141.7, 142.3, 142.8, 143.3, 176.1. HRMS (ESI): Calcd for $C_{35}H_{41}N_3O_4$ + H 568.3175, found 568.3181.

(8,12,13,17-Tetraethyl-2,3-di(methoxycarbonyl)-7,18-dimethyl-21-carbaporphyrinato)silver(III) (**118**)

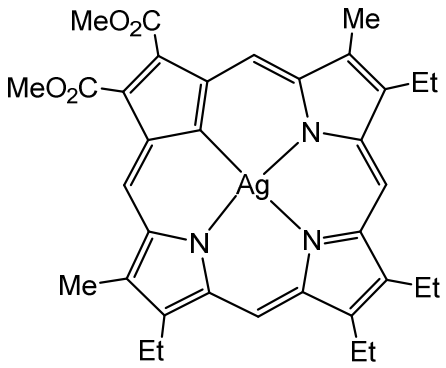

A solution of carbaporphyrin **98** (10.0 mg, 0.017 mmol) in dichloromethane (10 mL) was added to silver(I) acetate (11.0 mg, 0.066 mmol) dissolved in methanol (2.5 mL), and the mixture was stirred at room temperature overnight. The mixture was washed with water, and the solvent was removed under reduced pressure. The residue was chromatographed on grade III neutral alumina eluting with dichloromethane and hexane in a ratio of 60:40. A deep red fraction was collected and recrystallized from chloroform-methanol to give the silver(III) complex (7.2 mg, 0.011 mmol, 60%) as a red powder, mp >300°C; UV-Vis (CH_2Cl_2): λ_{max} (log ε): 309 (4.06), 352 (4.29), 376 (4.29), 407 (4.44), 449 (4.64), 515 (3.63), 567 (4.13); ^{1}H NMR (500 MHz, $CDCl_3$): δ 1.59 (12H, t, *J* = 7.7 Hz), 3.31 (6H, s), 3.59 (4H, q, *J* = 7.7 Hz), 3.64 (4H, q, *J* = 7.7 Hz) 4.40 (6H, s), 8.79 (2H, s), 9.91 (2H, s); ^{13}C NMR (125 MHz, $CDCl_3$): δ 11.5, 17.3, 18.1, 19.4, 20.0, 52.6, 96.1, 110.2, 118.3, 131.1, 134.51, 134.57, 137.2, 138.3, 139.6, 140.9, 167.5. HR MS (EI): calcd for $C_{35}H_{36}AgN_3O_4$ 669.1757, found 669.1752.

(8,12,13,17-Tetraethyl-2,3-di(methoxycarbonyl)-7,18-dimethyl-21-carbaporphyrinato)gold(III) (**119**)

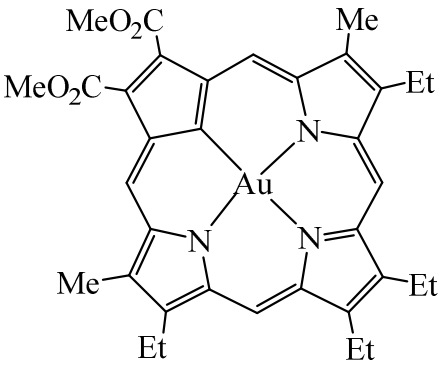

A solution of carbaporphyrin **98** (12 mg, 0.021 mmol) in pyridine (10 mL) was added to gold(III) acetate (12 mg, 0.032 mmol) dissolved in pyridine (2.0 mL), and the mixture was refluxed for 30 minutes. The mixture was washed with water, and the solvent removed under reduced pressure. The residue was chromatographed on Grade III neutral alumina eluting with dichloromethane and hexane in 60:40. A red fraction was collected and recrystallized from chloroform-methanol to give the gold(III) complex (2.6 mg, 0.004 mmol, 16%) as a red powder, mp 260-262 ^{o}C; UV-Vis (CH_2Cl_2): λ_{max} (log ε) 348 (4.38), 373 (4.35), 403 (4.41), 441 (4.43), 474 (sh, 3.83), 513 (3.76), 557 (4.41); ^{1}H NMR (500 MHz, $CDCl_3$): δ 1.63-1.68 (12H, t, *J* = 7.7 Hz), 3.36 (6H, s), 3.69 (4H, q, *J* = 7.7 Hz), 3.74 (4H, q, *J* = 7.7 Hz), 4.36 (6H, s), 9.02 (2H, s), 9.99 (2H, s). ^{13}C NMR (125 MHz, $CDCl_3$): δ 11.5, 17.3, 18.0, 19.4, 19.8, 52.5, 96.3, 111.4, 122.1, 134.07, 134.14, 135.1, 136.2, 137.3, 138.2 140.9, 167.5. HR MS (ESI): calcd for $C_{35}H_{36}AuN_3O_4$ 760.2450, found 760.2460.

8,12,13,17-Tetraethyl-2,3-di(methoxycarbonyl)-7,18,21-trimethyl-21-carbaporphyrin (**120)**

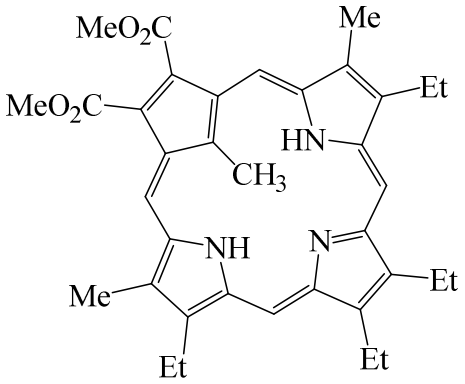

Carbaporphyrin **98** (12.0 mg, 0.021 mmol) was stirred with potassium carbonate (12 mg) and methyl iodide (6 drops) in acetone (18 mL) under reflux for 1 h. The mixture was washed with water and evaporated under reduced pressure. The residue was run through a grade III neutral alumina column, eluting with dichloromethane and hexane in a ratio of 60:40, and two colored fractions were collected. The later major red fraction was evaporated under reduced pressure and the residue recrystallized from chloroform-methanol to yield the *C*-methylcarbaporphyrin (9.1 mg, 0.016 mmol, 73%) as purple powder, mp 298-300ºC; UV-Vis (CH_2Cl_2): λ_{max} (log ε) 312 (4.17), 428 (4.67), 537 (sh, 3.64), 580 (3.92), 647 nm (sh, 3.33). UV-Vis (1% Et_3N-CH_2Cl_2): λ_{max} (log ε) 408 (4.64), 431 (sh, 4.61), 468 (sh, 4.45), 576 (sh, 3.73), 649 (3.90), 701 nm (sh, 3.37). UV-Vis (5% DBU-CH_2Cl_2): λ_{max} (log ε) 405 (4.67), 432 (sh, 4.62), 467 (sh, 4.50), 564 (sh, 3.73), 648 (3.97), 700 nm (sh, 3.38). UV-Vis (5 equiv TFA-CH_2Cl_2): λ_{max} (log ε) 316 (4.16), 411 (4.76), 556 (sh, 3.65), 581 (3.75), 629 nm (sh, 3.45). UV-Vis (25% TFA-CH_2Cl_2): λ_{max} (log ε) 320 (3.78), 414 (5.08), 430 (sh, 4.89), 550 (3.46), 606 nm (3.79). UV-Vis (50% TFA-CH_2Cl_2): λ_{max} (log ε) 316 (3.97), 413 (5.11), 432 (4.92), 529 (sh, 3.50), 549 (sh, 3.48), 598 (3.80), 620 nm (3.80). ^{1}H NMR (500 MHz, $CDCl_3$): δ -4.68 (3H, s), -3.19 (2H, v br), 1.76-1.80 (12H, 2 overlapping triplets), 3.43

(6H, s), 3.71-3.79 (4H, m), 3.86 (4H, q, J = 7.6 Hz), 4.02 (6H, s), 9.28 (2H, s), 9.90 (22H, s). ^{13}C NMR (125 MHz, $CDCl_3$): δ 10.7, 11.5, 17.2, 18.2, 19.5, 19.8, 52.3, 94.4, 101.6, 109.9, 118.3, 135.0, 135.1, 135.4, 137.8, 139.8, 145.6, 157.2, 167.0. ^{1}H NMR (500 MHz, DBU-$CDCl_3$): δ -4.78 (1H, s), 9.22 (2H, s), 9.83 (2H, s); ^{1}H NMR (500 MHz, 2 equiv. TFA-$CDCl_3$): δ -5.41 (3H, s), -1.5 (1H, v br), -1.42 (2H, s), 1.69 (6H, t, J = 7.7 Hz), 1.80 (6H, t, J = 7.7 Hz) 3.31 (6H, s), 3.74-3.88 (6H, m), 3.88-3.96 (2H, m), 3.98 (6H, s), 9.49 (2H, s), 10.03 (2H, s). ^{13}C NMR (125 MHz, 2 equiv. TFA-$CDCl_3$): δ 11.1, 11.6, 16.7, 17.3, 19.66, 19.72, 52.3, 95.0, 113.4, 115.0, 121.8, 135.4, 138.0, 138.8, 139.7, 140.3, 141.3, 142.5, 166.4. ^{1}H NMR (500 MHz, excess TFA-$CDCl_3$): δ -8.67 (1H, q, J = 7.6 Hz), -6.55 (3H, d, J = 7.6 Hz), 1.94 (6H, t, J = 7.6 Hz), 1.97 (6H, t, J = 7.7 Hz), 3.85 (6H, s), 4.30-4.41 (8H, m), 4.66 (6H, s), 11.16 (2H, s), 11.80 (2H, s). ^{13}C NMR (125 MHz, excess TFA-$CDCl_3$): δ 11.0, 12.0, 16.6, 17.7, 20.7, 20.8, 31.9, 55.5, 105.5, 114.4, 143.3, 144.3, 144.7, 145.9, 146.3, 149.2, 149.7, 150.6, 155.3, 166.9. HRMS (ESI): calcd for $C_{36}H_{41}N_3O_4$ + H 580.3175, found 580.3153.

8,12,13,17-Tetraethyl-2,3-di(methoxycarbonyl)-7,18,21,22-tetramethyl-21-carbaporphyrin (**121**)

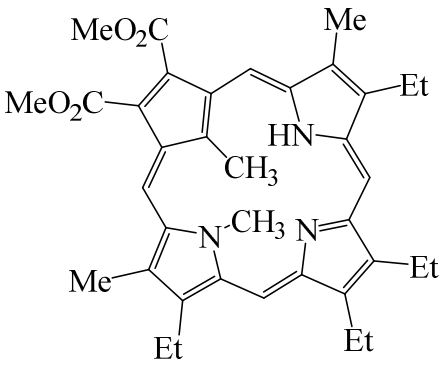

Carbaporphyrin **98** (12.0 mg, 0.021 mmol) was stirred with potassium carbonate (12 mg) and excess of methyl iodide (10 drops) in acetone (12 mL) under reflux for 16 h. The mixture was washed with water and evaporated under reduced pressure. The residue was run through a grade III neutral alumina column, eluting with dichloromethane and hexane in a ratio of 60:40, and a brown colored fraction was collected. The solvent was evaporated under reduced pressure and the residue recrystallized from chloroform-methanol to yield **121** (8.7 mg, 0.015 mmol, 69%) as purple crystals, mp 222-224 ^{o}C; UV-Vis (CH_2Cl_2): λ_{max} (log ε) 316 (4.41), 376 (4.59), 441 (5.89), 545 (3.93), 589 (4.01), 736 nm (3.30). UV-Vis (CH_2Cl_2): λ_{max} (log ε) 320 (4.34), 412 (4.77), 429 (sh, 4.73), 567 (3.85), 607 nm (sh, 3.76). ^{1}H NMR (500 MHz, $CDCl_3$): δ -5.27 (3H, s), -3.91 (3H, s), 1.39 (3H, t, J = 7.6 Hz), 1.70 (3H, t, J = 7.7 Hz), 1.73-1.78 (6H, 2 overlapping triplets, J = 7.6 Hz), 2.95 (3H, s), 3.32 (3H, s), 3.37-3.43 (2H, m), 3.55-3.66 (3H, m), 3.68-3.76 (3H, m), 4.02 (3H, s), 4.06 (3H, s), 8.90 (1H, s), 9.05 (1H, s), 9.52 (1H, s), 9.54 (1H, s) (5,20-H). ^{13}C NMR (125 MHz, $CDCl_3$): δ 9.6, 11.4, 11.7, 16.2, 17.1, 18.0, 18.1, 19.3, 19.57, 19.61, 19.8, 31.7, 52.1, 52.3, 93.7, 98.0, 108.9, 109.5, 112.5, 116.4, 123.3, 128.1, 131.2, 132.5, 134.4, 135.7, 136.1, 137.5, 141.8, 144.3, 145.8, 146.4, 150.6, 154.8, 158.2, 166.5, 167.7. ^{1}H NMR (500 MHz, TFA-$CDCl_3$): δ -4.91

(3H, s), -4.18 (1H, br s), -4.02 (1H, br s), -3.54 (3H, s), 1.46 (3H, t, *J* = 7.7 Hz), 1.72 (3H, t, *J* = 7.7 Hz), 1-80-1.85 (6H, 2 overlapping triplets, *J* = 7.7 Hz), 3.03 (3H, s), 3.37 (3H, s), 3.46-3.53 (2H, m), 3.82 (2H, q, *J* = 7.7 Hz), 3.86-3.97 (4H, m), 4.15 (3H, s), 4.19 (3H, s), 9.45 (1H, s), 9.46 (1H, s), 9.86 (1H, s), 9.92 (1H, s). ^{13}C NMR (125 MHz, 2 μL TFA-$CDCl_3$): δ 10.9, 11.8, 12.2, 15.8, 16.4, 17.17, 17.23, 19.6, 19.7, 19.8, 31.1, 53.0, 53.1, 92.9, 96.3, 113.3, 114.5, 117.4, 123.1, 134.3, 135.5, 136.5, 138.6, 138.9, 139.4, 141.1, 141.88, 141.94, 142.5, 144.6, 145.2, 150.6, 152.6. HRMS (ESI): calcd for $C_{37}H_{43}N_3O_4$ + H 594.3332, found 594.3326.

(8,12,13,17-Tetraethyl-2,3-di(methoxycarbonyl)-7,18,21-trimethyl-21-carbaporphyrinato)palladium(II) (**122**)

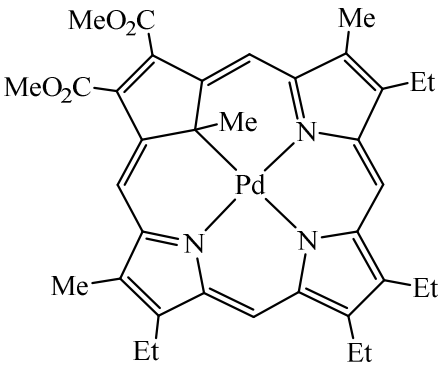

Palladium(II) acetate (10 mg, 0.044 mmol) was added to a solution of C-methylcarbaporphyrin **120** (10.0 mg, 0.017 mmol) in acetonitrile (10 mL), and the solution was stirred under reflux for 30 min. The solution was cooled, diluted with chloroform, washed with water, and the organic layer separated and then evaporated to dryness. The residue was chromatographed with grade III neutral alumina, eluting with 30% dichloromethane-hexanes, and the product was collected as a green band. The solvent was evaporated to dryness and the residue recrystallized from chloroform-methanol to yield the palladium(II) complex (7.4 mg, 0.011mmol, 63%) as dark green crystals, mp 282-284 ^{o}C; UV-Vis ($CHCl_3$): λ_{max} (log ε) 306 (4.37), 410 (4.54), 460 (4.52), 602 (3.90), 639 nm (sh, 3.81). ^{1}H NMR (500 MHz, $CDCl_3$): δ -4.12 (3H, s), 1.81 (6H, t, J = 7.7 Hz), 1.83 (6H, t, J = 7.7 Hz), 3.44 (6H, s), 3.86-3.92 (8H, 2 overlapping quartets), 4.30 (6H, s), 9.85 (2H, s), 10.81 (2H, s). ^{13}C NMR (125 MHz $CDCl_3$): δ 11.9, 17.6, 18.4, 19.8, 20.1, 21.8, 36.4, 52.9, 101.7, 113.0, 131.3, 136.9, 143.4, 143.9, 145.5, 145.6, 149.2, 158.6, 167.6. HRMS (ESI): calcd for $C_{36}H_{39}N_3O_4Pd$ + H 683.1851, found 683.1955.

(8,12,13,17-Tetraethyl-2,3-di(methoxycarbonyl)-7,18,21-trimethyl-21-carbaporphyrinato)nickel(II) (**123**)

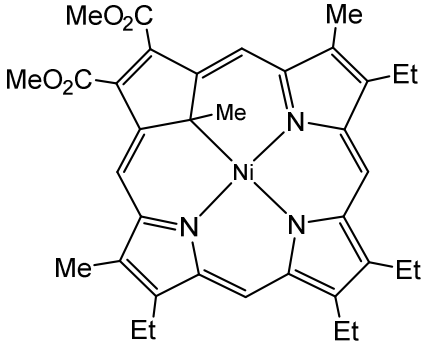

Nickel(II) acetate tetrahydrate (10 mg, 0.057 mmol) was added to a solution of C-methylcarbaporphyrin **120** (10.0 mg, 0.017 mmol) in dimethylformamide (10 mL), and the solution was stirred under reflux for 30 min. The solution was cooled, diluted with chloroform, washed with water, and the organic layer separated and then evaporated to dryness. The residue was chromatographed with grade III neutral alumina, eluting with 60% dichloromethane-hexanes, and the product was collected as a green band. The solvent was evaporated to dryness and the residue recrystallized from chloroform-methanol to yield the nickel(II) complex (7.6 mg, 0.012 mmol, 71%) as dark green crystals, mp 267-269 ^{o}C; UV-Vis ($CHCl_3$): λ_{max} (log ε) 348 (4.51), 420 (4.72), 456 (sh, 4.38), 612 nm (3.96). ^{1}H NMR (500 MHz, $CDCl_3$): δ -3.89 (3H, s), 1.72 (6H, t, *J* = 7.7 Hz), 1.77 (6H, t, *J* = 7.7 Hz), 3.31 (6H, s), 3.72-3.81 (8H, m), 4.26 (6H, s), 9.59 (2H, s), 10.56 (2H, s). ^{13}C NMR (125 MHz, $CDCl_3$): δ 11.8, 17.5, 18.2, 19.7, 19.8, 19.9, 26.7, 52.8, 99.8, 111.0, 131.3, 138.3, 144.3, 145.9, 146.1, 148.7, 150.9, 167.6. HRMS (ESI): calcd for $C_{36}H_{39}N_3O_4Ni$ + H 635.2294, found 635.2285.

CHAPTER III

SYNTHESIS OF A CARBACHLORIN

Introduction

Chlorins (2,3-dihydroporphyrins) are an important group of tetrapyrroles that provide the parent structure for many of the chlorophylls and other biological pigments present in nature.[2] Chlorins tend to have a green coloration in solution because of their strong absorptions near 650 nm in the long wavelength region of visible spectrum. It is this absorption which is in part responsible for their potential application as photosensitizers in photodynamic therapy,[29] and this property has led to numerous investigations into their synthesis.[53] However, there have been very few studies on the preparation of analogous systems, such as carbachlorins, that may have equally useful properties.[14] It was in 1998 that the first synthesis of carbachlorins was carried out by Hayes and Lash. For this synthesis, a "3 + 1" variant on the MacDonald condensation was used.[15] Bicyclic dialdehydes were found to condense with a tripyrrane in the presence of TFA to give, following oxidation with DDQ, carbachlorins **130** in moderate yields. These chlorin analogues were found to retain the aromatic properties as the proton NMR spectra showed the inner CH protons upfield around -7 ppm.[35] The UV-vis spectra were also very porphyrin-like, showing a Soret band at 404 nm and three smaller absorptions between 490 and 650 nm. The band at 650 nm was of medium intensity and resembles the characteristic absorptions of tetrapyrrolic chlorins.[15]

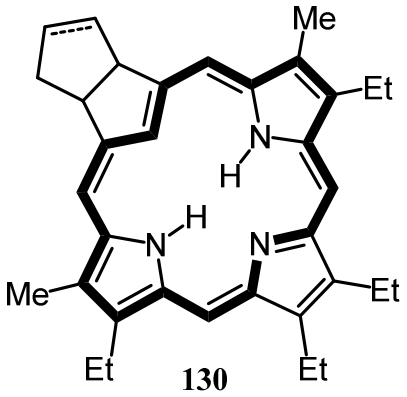

130

In 2014, Li and Lash, in their attempts to further explore carbachlorin chemistry, synthesized a carbachlorin **131** using 3-ethoxymethylenecyclopentene-1-carbaldehyde. This was condensed with a tripyrrane, and following oxidation with aqueous ferric chloride solutions, generated moderate yields of a carbachlorin **131**. Also, oxidation of the carbachlorin **131** with DDQ gave the first example of a carbaporphyrin **132** that was unsubstituted on the carbocyclic ring.[55]

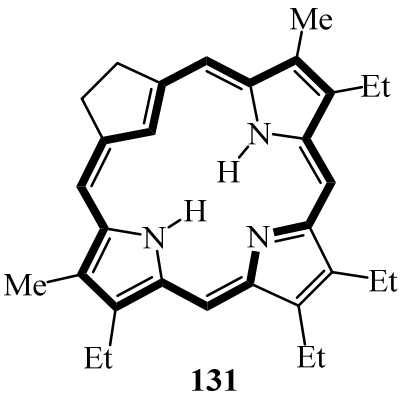

131

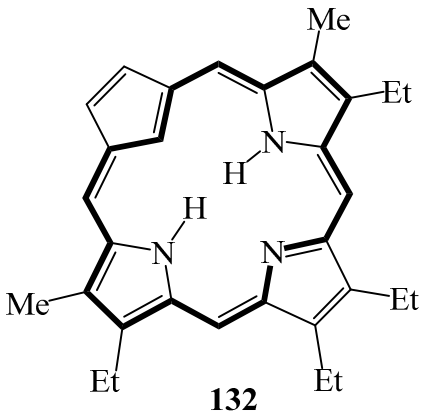

132

However, compared to studies on other core modified porphyrins, for instance carbaporphyrins, our knowledge of carbachlorins is still very limited. Questions such as whether these core-modified chlorins (carbachlorins) share similar properties with core-modified

porphyrins (carbaporphyrins) is still open. Therefore, to further investigate the chemistry of carbachlorins, it was necessary to develop an improved synthesis of a carbachlorin.

In the previous chapter, the synthesis of a carbaporphyrin with two methyl ester groups on adjacent carbons was performed. It was interesting to note that carbachlorin **117** was also formed as the minor fraction in this synthesis. However, this compound was prone to oxidation and carbaporphyrin was always the major product in these reactions. In the case of carbachlorins **130**, the presence of a fused five-membered ring appeared to inhibit further oxidation. We speculated that carbachlorins could be generated as the major products if the site of oxidation was blocked by geminal substitution. Carbachlorin **133** was an appealing target molecule, where the methyl esters were placed on the same carbon rather than at vicinal positions. It was anticipated that the synthesis and study of carbachlorin **133** would increase our understanding of the chlorin system and could allow the formation of new porphyrinoids and their metal complexes.

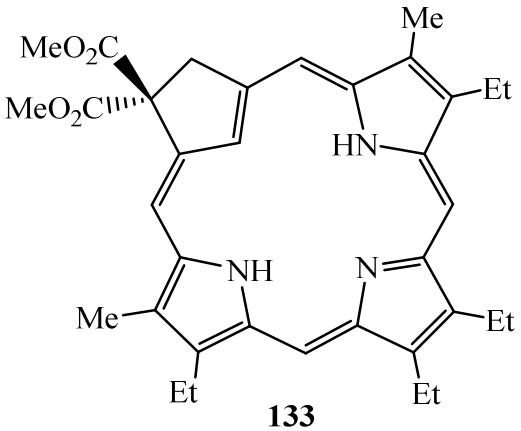

133

Results and Discussion

A retrosynthetic analysis suggested that carbachlorin **133** could be obtained from cyclopentane dialdehyde **134** and the known tripyrrane **62**. A straightforward acid catalyzed '3+1' condensation of dialdehyde **134** with tripyrrane **62** in the presence of trifluoroacetic acid, followed by oxidation with DDQ, would afford the targeted carbachlorin (Scheme 66).

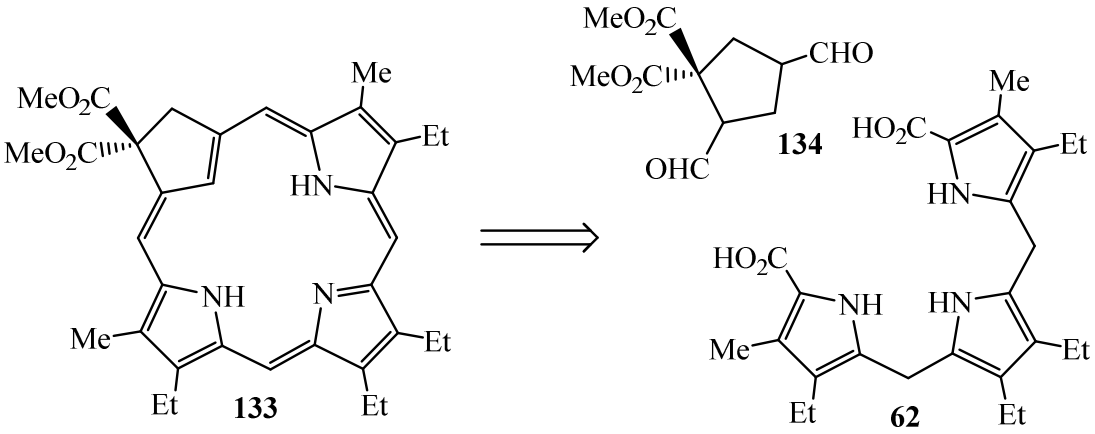

Scheme 66 Retrosynthetic Analysis of Carbachlorin **133**

In order to accomplish this goal, a synthesis of dialdehyde **134** had to be developed. This was accomplished using a similar strategy to the one described in Chapter 2. Initially, norbornene diester **135** was required and this could be generated using the Diels-Alder reaction. This required dienophile **136**, which was prepared by adapting a literature procedure reported by Harada and coworkers.[63] Copper(II) acetate was added to a solution of glacial acetic acid, paraformaldehyde and dimethyl malonate. After stirring at 100 °C for 3 h, the reaction mixture was cooled to room temperature and the excess acetic acid was removed under reduced pressure. The residue was later distilled under reduced pressure to afford the colorless distillate **136** (Scheme 67). This distillate was immediately diluted with CH_2Cl_2 and used for the following Diels-Alder reaction.[57]

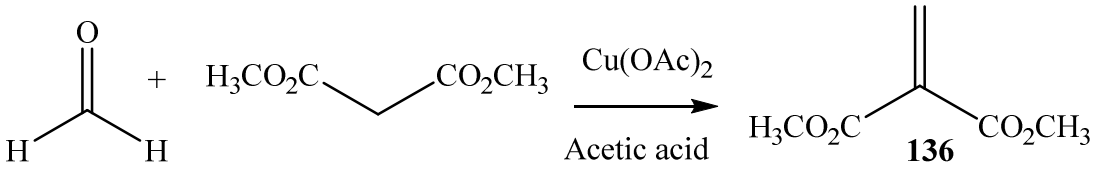

Scheme 67 Formation of **136**

In order to form the bicyclic adduct **135**, freshly cracked 1,3-cyclopentadiene was added dropwise to the solution of dimethyl 2-methylenemalonate **136** dissolved in CH_2Cl_2 whilst stirring. The temperature of the reaction was controlled with a water bath. The reaction mixture was stirred at room temperature for almost 60 min and purified by column chromatography on silica gel using hexane/EtOAc (19:1, *v*/*v*) as the eluent to give bicyclic adduct **135** as a colorless oil (Scheme 68).[57]

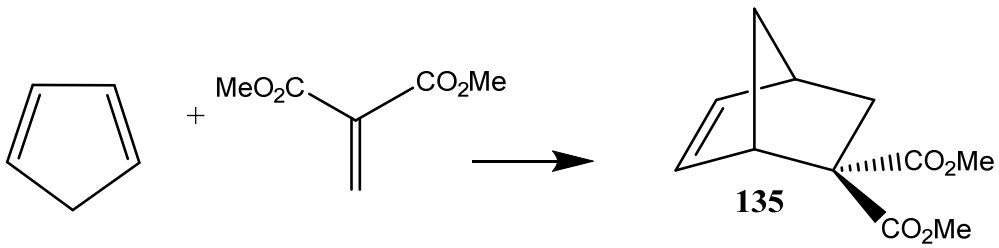

Scheme 68 Formation of **135**

Once the norbornene was generated, the next step was to oxidize the compound to dialcohol **137**. Several different procedures were attempted to carry out the transformation, and it was observed that the best results were obtained using $KMnO_4$ and NaOH for oxidation. For this reaction, a solution of potassium permanganate and sodium hydroxide in water was added dropwise to a solution of norbornene in *tert*-butyl alcohol and water while maintaining the

temperature at 0° C. After the addition was completed, the reaction mixture was stirred for 40 minutes and quenched with a saturated aqueous solution of sodium metabisulfite until the solution turned colorless. The mixture was filtered and the *tert*-butyl alcohol was removed from the filtrate *in vacuo*. The remaining solution was extracted with ethyl acetate which was filtered and concentrated *in vacuo* to yield dialcohol **137** as white crystalline solid (Scheme 69).[59] Compound **137** had not been prepared previously and was synthesized for the first time.

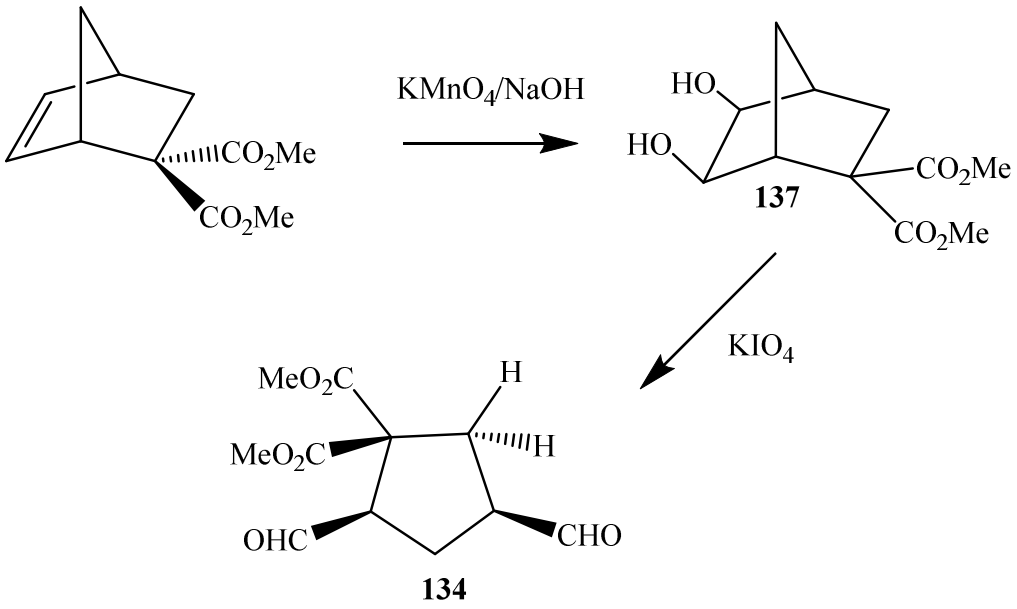

Scheme 69 Formation of Dialdehyde **134**

Diol **137** could be oxidatively ring opened using potassium periodate as an oxidizing agent to give dialdehyde **134**. Dialdehyde **134** was immediately condensed with tripyrrane dicarboxylic acid **62** in the presence of TFA/CH_2Cl_2 and the reaction mixture stirred overnight under the atmosphere of nitrogen**.** After stirring overnight, oxidation with DDQ in refluxing toluene was performed and carbachlorin **133** was isolated as the major product (Scheme 70).[35]

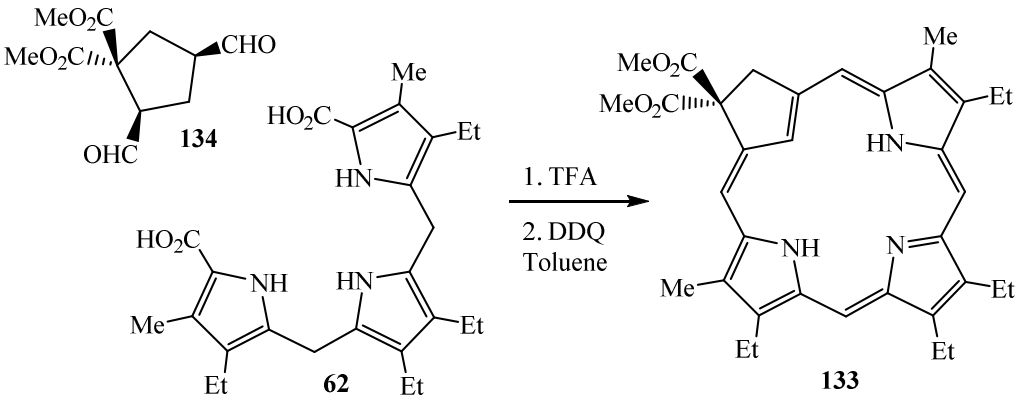

Scheme 70 Preparation of Carbachlorin **133**

Carbachlorin **133**, like other chlorin analogues, proved to be aromatic in the free base form. The proton NMR spectrum for **133** (Figure 41) in $CDCl_3$ showed the presence of a strong diamagnetic ring current. The internal CH proton was found at -7.08 ppm, while the *meso*-protons were shifted downfield to 9.86, 9.84, 9.58 and 9.25 ppm. As there were four signals for the four *meso*-protons, the molecule must be asymmetrical. The UV-Vis spectrum of carbachlorin **133**, shows a strong Soret band at 398 nm along with small Q bands at 491, 588 and 646 nm. The slightly stronger absorption at 646 nm is characteristic of chlorin-type structures (Figure 42).

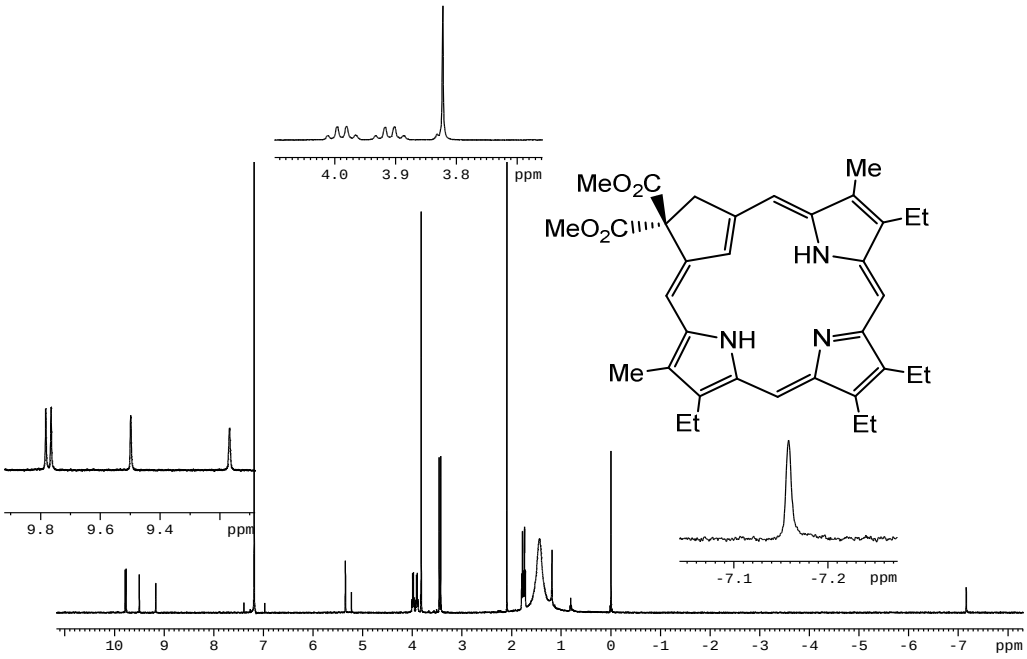

Figure 41 500 MHz Proton NMR Spectrum of Carbachlorin **133** in $CDCl_3$

s

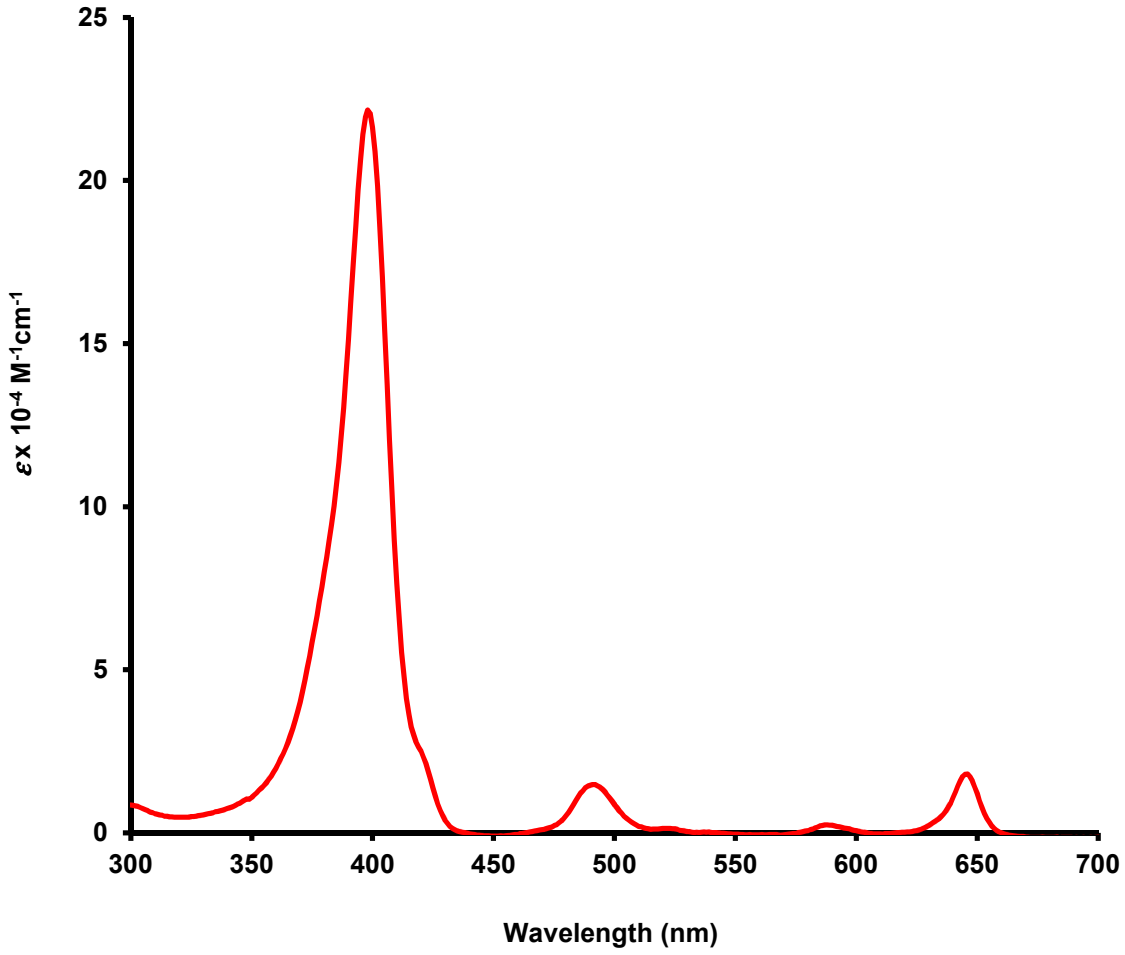

Figure 42 UV-Vis Spectrum of Carbachlorin **133**

When carbachlorin **133** was exposed to a trace amount of TFA, a deep purple solution corresponding to monocation **133**H^+ (Scheme 71) was generated. The proton NMR spectrum for **133**H^+ (Figure 43) showed that the addition of acid to the carbachlorin system had slightly increased its aromatic nature, as the internal CH was shifted upfield to -7.10 ppm, while the *meso*-protons were shifted further downfield to 10.23, 10.22, 9.96 and 9.71 ppm (Figure 43). The appearance of broad singlets at -4.95 ppm (2H) and -5.96 ppm (1H) confirmed the presence of an additional NH due to protonation. Unlike the related carbaporphyrins, further addition of TFA to

133H^+ did not give a diprotonated species, as aromatic character would be disrupted if protonation occurred at the inner carbon.

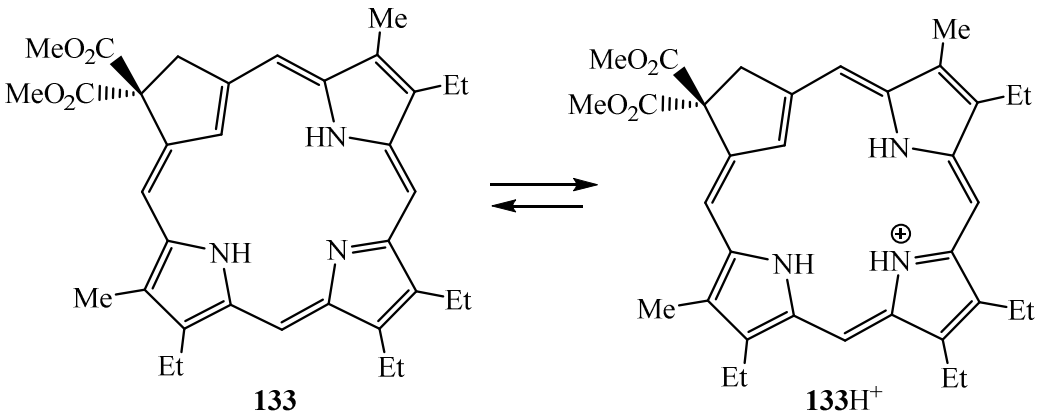

Scheme 71 Protonation of **133**

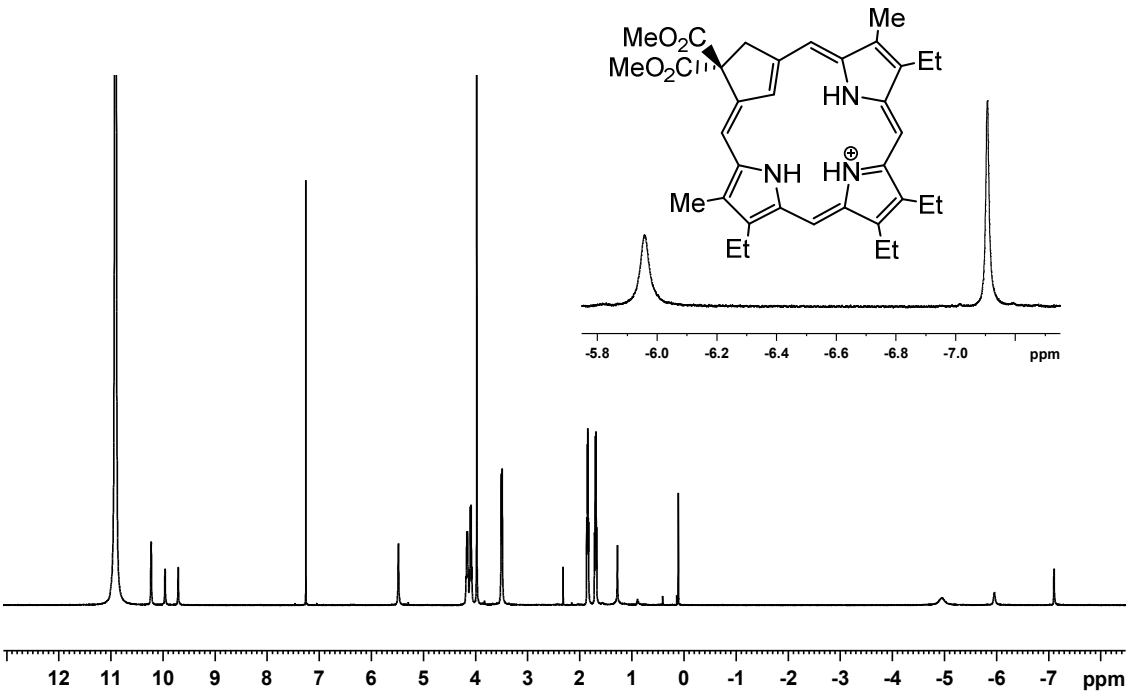

Figure 43 500 MHz Proton NMR Spectrum of Carbachlorin **133**H^+ in $CDCl_3$

In order to further understand the reactivity of carbachlorin **133**, a few more experiments were performed to observe how the exchange of protons takes place with addition of acid to **133**. As expected, when d-TFA was added to a solution of **133** in $CDCl_3$ the resulting monocation did not show any exchange of the inner CH proton, in contrast to carbaporphyrins which exhibit rapid deuterium exchange. However, exchange of the *meso*-protons was evident. After 20 minutes, the intensities for two of the *meso*-resonances were reduced by 15%, while the remaining two peaks were reduced by more than 50%. After several hours, proton-deuterium exchange was virtually 100% for all four *meso*-positions (Figure 44). The results imply that *meso*-substituted monocations such as **133a-d**H^+ are in equilibria with **133** and **133**H^+ (Scheme 72). It is also possible that related dications could also be involved. It is noteworthy that the exchange rate for chlorin **133** is far greater than the exchange rates noted for carbaporphyrins such as **98.**

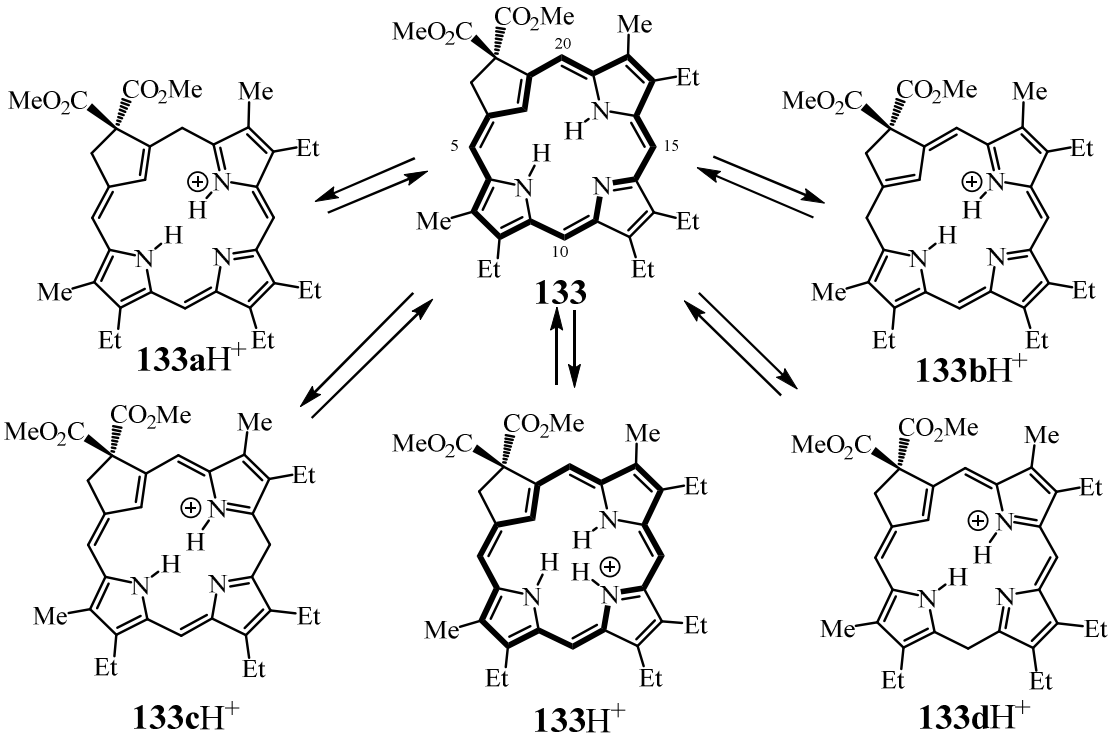

Scheme 72 Proposed Equilibrium of Different Cationic Species for Carbachlorin **133**

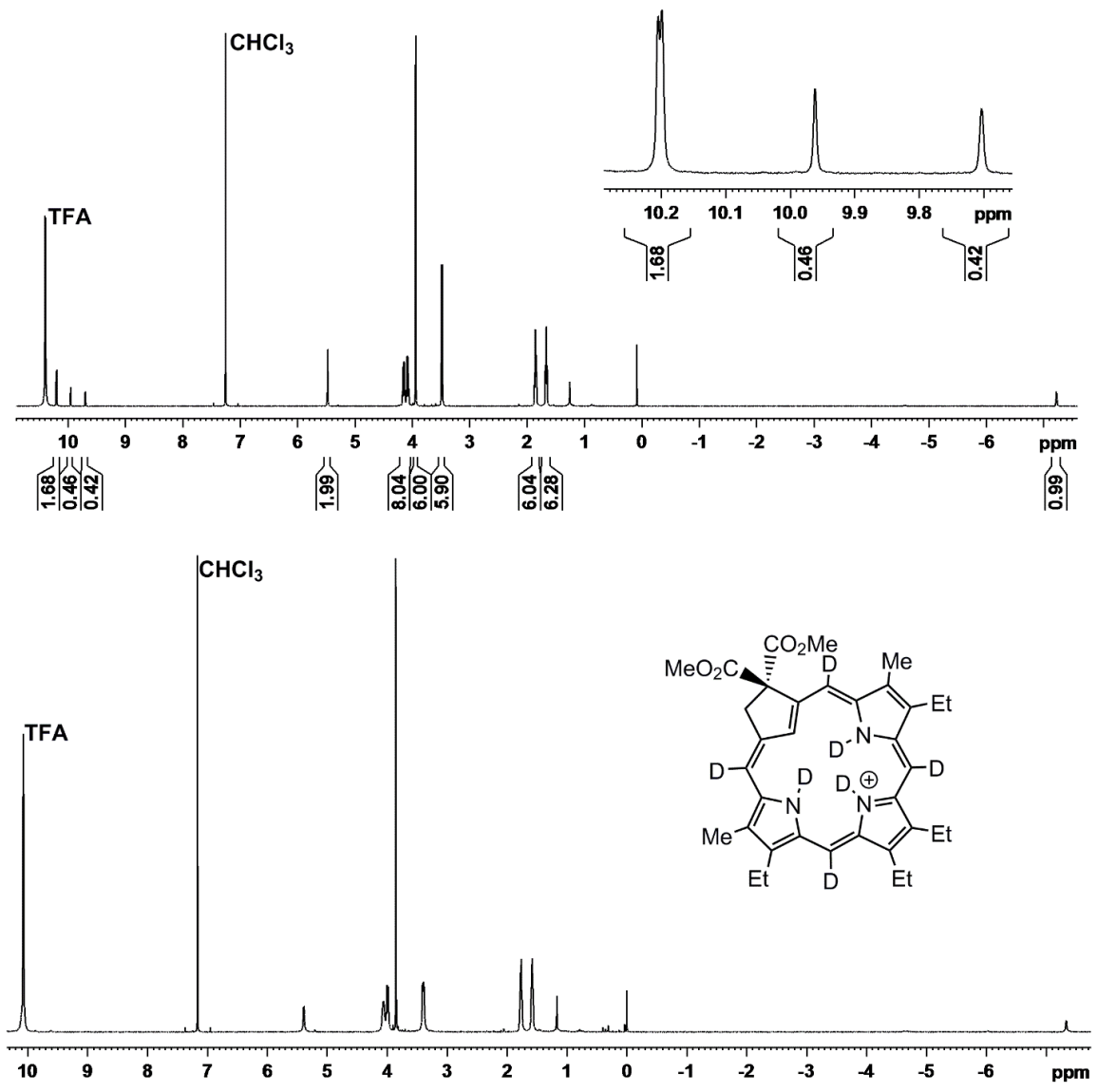

Figure 44 Proton NMR spectra of Carbachlorin **133** in $CDCl_3$ with Two Drops of d-TFA after 20 min (upper spectrum) and 7 hours (lower spectrum).

Metalation of carbachlorin **133** with silver acetate was also briefly investigated. A solution of carbachlorin **133** in CH_2Cl_2 was added to a suspension of silver(I) acetate in methanol, and the resulting mixture was stirred overnight at room temperature. After purification by column chromatography, a red fraction was collected and recrystallized from chloroform and methanol to yield organometallic complex **138** as a dark red powder in 62% yield (Scheme 73). Silver complex

138 retains aromatic characteristics as indicated by proton NMR spectrum (Figure 45). The UV-Vis spectrum of **138** (Figure 46) has a strong absorptions at 386 and 410 nm in the Soret region, along with three absorptions at 490, 522 and 546 nm. Moreover, the stronger band at 592 nm is reminiscent of chlorin systems.

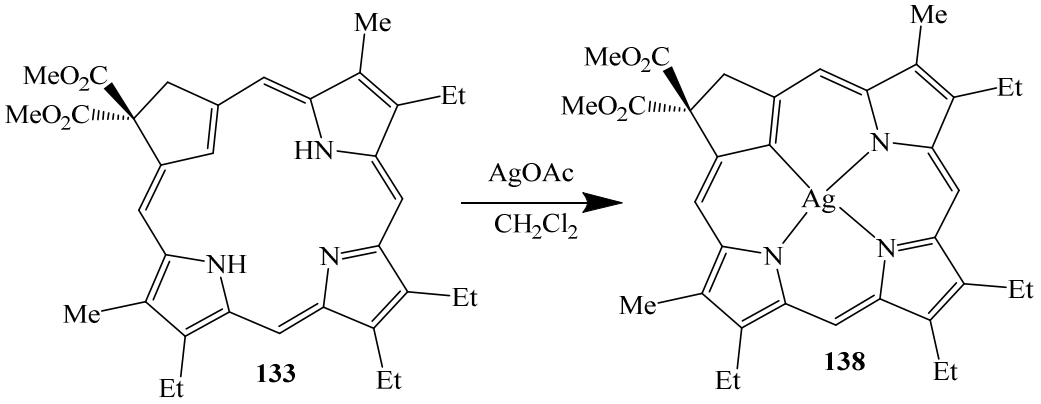

Scheme 73 Formation of Silver(III) Chlorin **138**

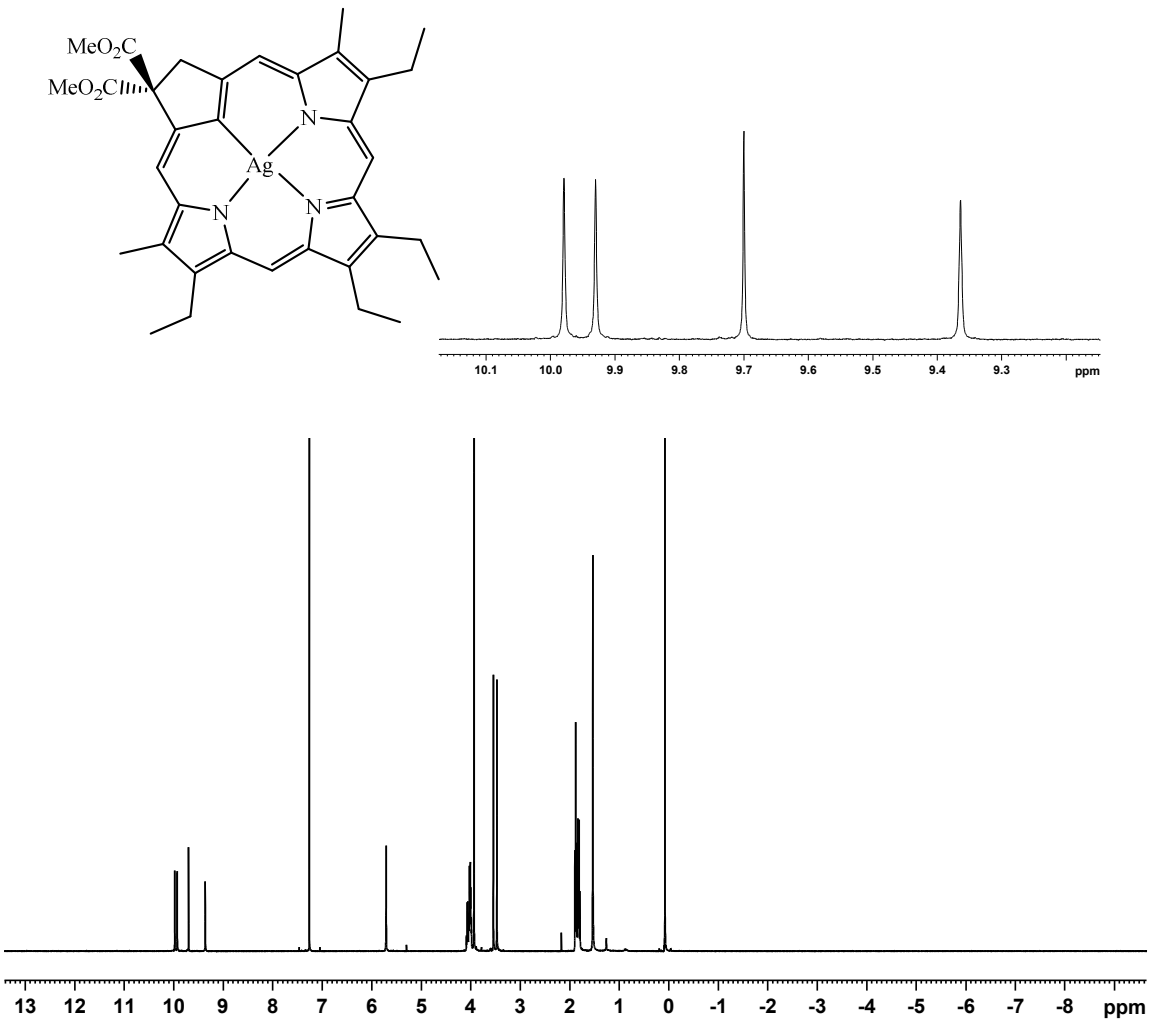

Figure 45 500 MHz Proton NMR spectrum of **138** in $CDCl_3$

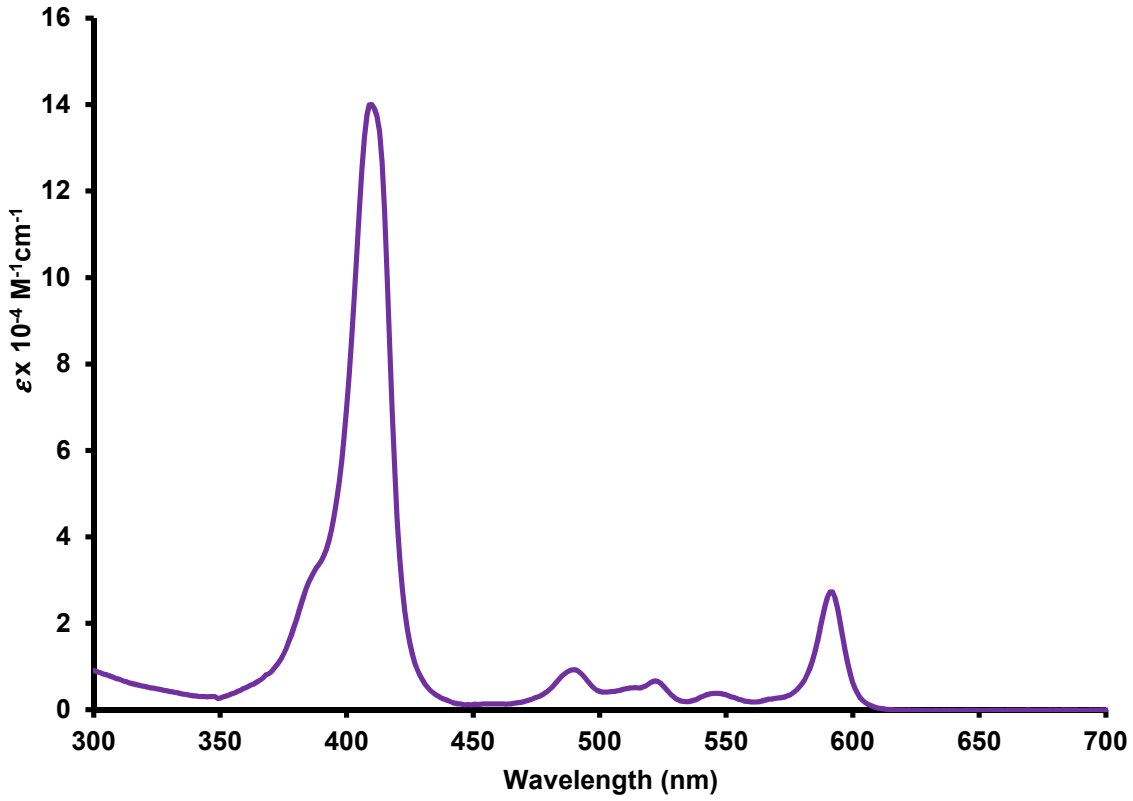

Figure 46 UV-Vis Spectrum of Silver(III) Chlorin **138** in Dichloromethane

Conclusions

A cyclopentane dialdehyde was prepared in three steps, starting with the formation of dimethyl 2-methylenemalonate **135** from paraformaldehyde and dimethyl malonate. This dienophile then underwent Diels-Alder chemistry with cyclopentadiene to generate the bicyclic compound **136**. Norbornene **136** was then oxidized in two steps to generate dialdehyde **134**. Although difficulties were initially encountered in preparing dialdehyde precursor **134**, careful adjustments of the reaction conditions allowed the five-memebered ring dialdehyde to be isolated in good yields. The '3+1' condensation of dialdehyde **134** and tripyrrane dicarboxylic acid **62** led to the formation of carbachlorin **133** in 30% yield. This newly synthesized carbachlorin system

proved to be highly aromatic. Protonation of this system can readily occur, forming an aromatic monocation.

Reaction between carbachlorin **133** and silver(I) acetate gave a silver(III) organometallic complex. The straightforward synthesis of carbachlorin **133** will allow further studies on this system to be conducted. It is anticipated that further coordination chemistry could be performed on this system as the yields are quite good.

Experimental

All chemicals were purchased from Sigma Aldrich or Acros Organic. Grade III neutral alumina and silica gel were used to perform column chromatography. The ^{1}H and ^{13}C-NMR spectra were obtained either using Bruker Avance III 500 MHz NMR spectrometer or Bukner 400 MHz NMR spectrometer at 302K. Chemical shifts were recorded, relative to $CDCl_3$ (residual chloroform at δ 7.26 ppm) in proton NMR spectra and the $CDCl_3$ triplet at δ 77.23 ppm in ^{13}C-NMR spectra, in parts per million (ppm). The UV-vis spectra for the compounds were collected by Cary 100 Bio spectrophotometer. Melting point were gathered using a Mel-Temp apparatus. Mass spectrometry data was obtained from the Mass Spectral Laboratory, School of Chemical Sciences, University of Illinois, Urbana-Champaign.

Dimethyl 2-methylenemalonate (**136)**[63]

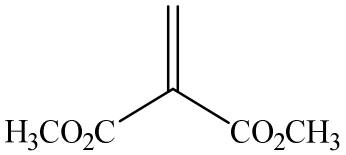

Paraformaldehyde (20 g, 133 mmol), dimethyl malonate (50 mL, 87.5 mmol), and copper(II) acetate (3.25g, 1.64 mmol) were added to glacial acetic acid (100 ml). The reaction mixture was stirred at 100 °C for 3 h, then cooled to room temperature, and the acetic acid removed under reduced pressure. The residue was distilled under reduced pressure using a vacuum pump and a colorless fraction was obtained between 90 ºC to 97 ºC (the external temperature was held between 152 ºC to 160 ºC) corresponding to **137** (3.6 g, 0.025mmol, 28%). This product was immediately diluted with CH_2Cl_2 and the solution used for the following Diels-Alder reaction. ^{1}H NMR (500 MHz, $CDCl_3$): δ 6.60 (2H, s), 4.02 (6H, s).

5,5-Dimethoxycarbonyl-2-norbornene (**135)**[57]

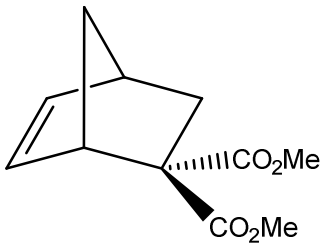

A solution of dimethyl 2-methylenemalonate **137** in dichloromethane (1.37 g, 0.021mmol) was added slowly to freshly cracked 1,3-cyclopentadiene (3.00 g, 0.021 mol) whilst stirring and maintaining temperature at 25^{o}C with the aid of water bath. The reaction mixture was stirred at room temperature for 60 min and purified by chromatography on silica gel using hexane/EtOAc (19:1) to give the Diels-Alder adduct as a colorless oil (2.97 g, 0.0141 mmol, 80%). ^{1}H NMR (500MHz, $CDCl_3$): δ 1.48-1.52 (1H, m), 1.65 (1H, br d, *J* = 8.9 Hz), 1.99 (1H, dd, *J* = 12.4, 2.9 Hz), 2.10 (1H, dd, *J* = 12.4, 3.6 Hz), 2.90 (1H, br), 3.37-3.39 (1H, br m), 3.65 (3H, s), 3.72 (3H, s), 5.97 (1H, dd, *J* = 5.6, 2.9 Hz), 6.24 (1H, dd, *J* = 5.6, 3.1 Hz). ^{13}C NMR (125 MHz, $CDCl_3$): δ 36.1, 42.2, 48.9, 50.0, 52.5, 52.9, 60.4, 133.7, 140.0, 171.6, 173.2. HRMS (EI): calcd for $C_{11}H_{14}O_4$ 210.0892, found 210.0896.

Dimethyl 5,6-dihydroxybicyclo[2.2.1]heptane-2,2-dicarboxlate (**137)**

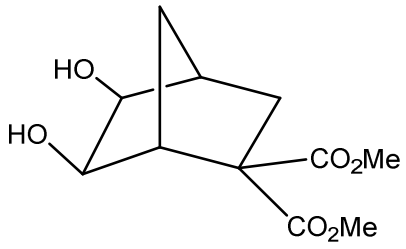

To a solution of norbornene **137** (10.80 g, 53.1 mmol) in *tert*-butyl alcohol (200 mL) and water (50 mL) at 0 °C was added dropwise a solution of potassium permanganate (12.0 g, 76.0 mmol) and sodium hydroxide (2.61 g, 65.3 mmol) in water (250 mL). After the addition was complete, the reaction mixture was stirred for 20 minutes and then quenched using a saturated aqueous solution of sodium metabisulphite ($Na_2S_2O_5$) until the solution turned colorless. The mixture was filtered and the *tert*-butyl alcohol was removed from the filtrate *in vacuo*. The solution was extracted with ethyl acetate (4 × 100 mL) and the combined organic layers dried over $MgSO_4$, filtered and concentrated *in vacuo* to furnish the diol **138** (6.23 g, 0.025 mmol, 61%) as a white crystalline solid, mp 86-88 ^oC. ^1H NMR (500 MHz, $CDCl_3$): δ 1.43 (1H, dq, *J* = 11.0, 1.6 Hz), 1.88 (1H, dq, *J* = 11.0, 1.6 Hz), 2.49-2.50 (1H, m), 2.54-2.56 (1H, m), 2.72 (1H, dd, *J* = 5.6, 1.5 Hz), 2.86 (1H, br), 2.96 (1H, br), 3.20 (1H, dd, *J* = 5.6, 4.7 Hz), 3.69 (3H, s), 3.71 (3H, s), 3.75-3.77 (1H, m), 3.85-3.87 (1H, m). ^{13}C NMR (125 MHz, $CDCl_3$): δ 31.9, 45.0, 46.4, 46.7, 48.5, 52.4, 52.5, 70.5, 73.6, 173.2, 174.3. HRMS (EI): calcd for $C_{11}H_{16}O_6$ + H 245.1025, found 245.1017.

Dimethyl 3,5-diformylcyclopentane-1,1-dicarboxylate **(134)**

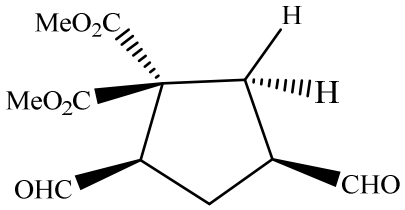

The foregoing diol **138** (3.05 g, 0.021 mole) was mixed with water (5.0 ml), ether (10 ml) and potassium periodate (4.16 g, 0.018 mol) and the reaction stirred at room temperature for 1 hr. The excess potassium periodate was filtered off and the two phases were separated. The water layer was back extracted twice with ether. The ether layers were combined, dried over sodium sulfate and the ether removed under reduced pressure to form the dialdehyde (1.67 g, 0.021 mmol, 60%) as a clear oil. The unstable dialdehyde was not further purified but used immediately to prepare carbachlorin. ^{1}H NMR (500 MHz, $CDCl_3$): 2.17-2.25 (1H, m), 2.47 (1H, dt, J = 13.8, 5.9 Hz), 3.05-3.11 (1H, m), 3.27-3.32 (1H, m), 3.57-3.66 (2H, m), 3.70 (3H, s), 3.76 (3H, s), 9.65 (1H, d, J = 0.8 Hz), 9.68 (1H, d, J = 0.9 Hz). HRMS (EI): calcd for $C_{11}H_{14}O_6$ + H 243.0869, found 243.0870.

8,12,13,17-Tetraethyl-2,3-dimethoxycarbonyl-7,18-dimethyl-21-carbaporphyrin (**133**)

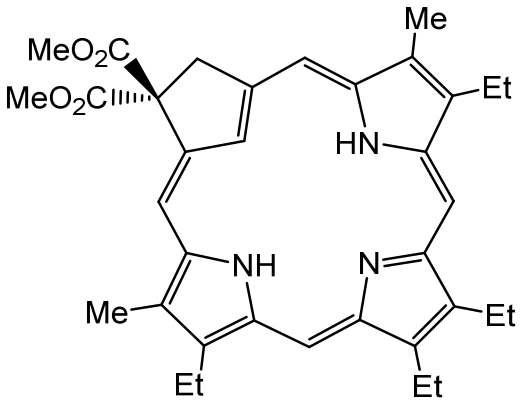

Tripyrrane dicarboxylic acid **62** (100 mg, 0.220 mmol) was stirred with TFA (1 ml) under an atmosphere of nitrogen for 2 minutes in a 250 ml round bottom flask. Dichloromethane (99 ml) was added, followed immediately by dialdehyde **140** (55 mg, 0.23 mmol) and the mixture was stirred under nitrogen overnight. The mixture was neutralized by the addition of triethylamine and the solvent removed under reduced pressure. The residue was taken up in toluene (50 ml), DDQ (100 mg, 0.44 mmol) was added, and the resulting mixture was stirred under reflux for 1 hr. The solvent was removed under reduced pressure, then the residue was dissolved in CH_2Cl_2 and washed with water. The solution was concentrated under reduced pressure and the residue chromatographed on grade III neutral alumina column eluting with CH_2Cl_2 and hexane in a ratio of 60:40.The product was collected as a dark green fraction. Recrystallization from chloroform and methanol gave the carbachlorin (37 mg, 0.065 mmol, 30%) as purple crystals, mp 228-230 ºC. UV-Vis (1% Et_3N-CH_2Cl_2): λ_{max} (log ε) 398 (5.36), 491 (4.23), 588 (3.45), 646 nm (4.31). UV-Vis (5% TFA-CH_2Cl_2): λ_{max} (log ε) 406 (5.30), 423 (5.19), 527 (3.86), 543 (3.86), 583 (3.93), 635 nm (3.99). ^{1}H NMR (500 MHz, $CDCl_3$): δ -7.08 (1H, s), 1.80-1.84 (6H, 2 overlapping triplets, J = 7.7 Hz), 1.85-1.88 (6H, 2 overlapping triplets, J = 7.7 Hz), 3.50 (3H, s), 3.54 (3H, s), 3.90 (6H, s),

3.96-4.01 (4H, 2 overlapping quartets), 4.04-4.09 (4H, 2 overlapping quartets), 5.43 (2H, s), 9.25 (1H, s), 9.58 (1H, s), 9.84 (1H, s), 9.86 (1H, s). ^{13}C NMR (125 MHz, $CDCl_3$): δ 11.4, 11.6, 17.6, 18.8, 19.8, 20.2, 45.3, 53.5, 96.2, 96.5, 97.7, 99.3, 120.7, 129.7, 130.2, 132.95, 133.05, 135.5, 135.8, 137.8, 137.9, 139.8, 140.6, 143.3, 143.4, 150.5, 172.2. ^{1}H NMR (500 MHz, 5% TFA-$CDCl_3$): δ -7.10 (1H, s), -5.96 (1H, br s), -4.95 (2H, br s), 1.67-1.72 (6H, 2 overlapping triplets), 1.83-1.87 (2 overlapping triplets), 3.49 (3H, s), 3.51 (3H, s), 3.98 (6H, s), 4.09 (4H, q, J = 7.7 Hz), 4.16 (4H, q, J = 7.6 Hz), 9.71 (1H, s), 9.96 (1H, s), 10.226 (1H, s), 10.231 (1H, s). ^{13}C NMR (125 MHz, 5% TFA-$CDCl_3$): δ 11.44, 11.47, 16.6, 17.6, 20.1, 20.2, 45.7, 55.1, 68.4, 94.6, 94.7, 103.7, 103.9, 128.6, 134.5, 134.8, 134.9, 135.1, 135.6, 135.9, 141.4, 142.0, 142.1, 142.7, 142.9, 143.0, 145.0, 173.7. HRMS (ESI): calcd for $C_{35}H_{41}N_3O_4$ + H 568.3175, found 568.3177.

(8,12,13,17-Tetraethyl-2,2-dimethoxycarbonyl-7,18-dimethyl-21-carbaporphyrinato)silver(III)

(**138**)

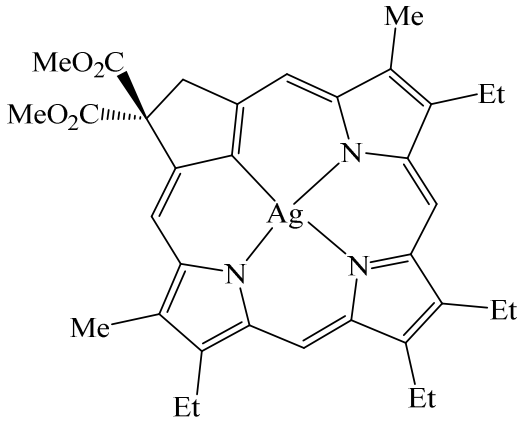

A solution of carbachlorin **133** (10.0 mg, 0.017 mmol) in dichloromethane (10 mL) was added to silver(I) acetate (12 mg, 0.019 mmol) dissolved in methanol (2.5 mL), and the mixture was stirred at room temperature overnight. The mixture was washed with water, and the solvent was removed under reduced pressure. The residue was chromatographed on grade III neutral alumina eluting with dichloromethane and hexane in a ratio of 60:40. A deep red fraction was collected and recrystallized from chloroform-methanol to give the silver(III) complex (7.3 mg, 0.011mmol, 62%) as a red powder, mp 266-268 ^{o}C. UV-Vis (CH_2Cl_2): λ_{max} (log ε) 386 (sh, 4.49), 410 (5.15), 490 (3.96), 522 (3.82), 546 (3.58), 592 nm (4.43). ^{1}H NMR (500 MHz, $CDCl_3$): 1.81 (3H, t, J = 7.7 Hz), 1.83 (3H, t, J = 7.7 Hz), 1.88 (6H, t, J = 7.7 Hz), 3.47 (3H, s), 3.54 (3H, s), 3.93 (6H, s), 3.98-4.09 (8H, m), 9.36 (1H, s), 9.70 (1H, s), 9.93 (1H, s), 9.98 (1H, s) (10,15-H). ^{13}C NMR (125 MHz $CDCl_3$): δ 11.8, 12.0, 17.82, 17.83, 18.58, 18.59, 19.9, 20.48, 20.52, 45.3, 53.5, 67.5, 98.2, 98.5, 101.3, 103.0, 130.8, 133.4, 133.5, 134.2, 134.4, 136.0, 136.5, 138.7, 138.8, 140.3, 140.6, 172.4. HRMS (ESI): calcd for $C_{35}H_{38}AgN_3O_4$ + H 672.1992, found 672.2007.

CHAPTER IV

SUMMARY AND CONCLUSIONS

Carbaporphyrins and carbachlorins are interesting molecules showing strong diatropic character and unusal coordination chemistry. In order to expand this important area, new routes to carbaporphyrins and carbachlorins have been developed. In Chapter II, it was shown that a carbaporphyrin could be synthesized from a cyclopentane dialdehyde in good yields and this porphyrin analogue proved to be a versatile precursor for alkylation and coordination chemistry. Initially, a Diels-Alder adduct was prepared from cyclopentadiene and dimethyl fumarate. This was converted in two steps to the cyclopentane dialdehyde, and subsequent condensation with a tripyrrane in the presence of TFA, followed by oxidation with DDQ in refluxing toluene, gave the novel carbaporphyrin in 40% yield together with a low yield of a related carbachlorin. The carbaporphyrin possesses macrocyclic aromaticity and afforded stable silver(III) and gold(III) complexes. In addition, alkylation with methyl iodide and potassium carbonate gave a C-methyl derivative and this underwent metalation with palladium(II) acetate and nickel(II) acetate to give the related organometallic species. These reactions involved both the formation of an organometallic species and an increase in aromaticity. On protonation, the new carbaporphyrin also exhibited enhanced diatropic character. Mono- and diprotonated species were characterized, and deuterium exchange studies also indicated that *meso*-protonated structures were present in equilibrium. In addition to characterization by UV-Vis, proton NMR and carbon-13 NMR spectroscopy, and mass spectrometry, the structures of the free base carbaporphyrin and two metalated derivatives were confirmed by X-ray crystallography.

The ‘3+1’ variant of the MacDonald condensation has been widely used to prepare

porphyrin analogues but only one example of using aliphatic dialdehydes has previously been reported for this synthetic strategy. Even in that case, only poor yields of porphyrinoid products were obtained. In this work, aliphatic cyclopentane dialdehydes bearing two ester substituents were shown to be superior precursors to carbaporphyrinoids. The efficient synthesis of a carbaporphyrin with ester substituents lays the foundation for further investigation.

Future work entailing this carbaporphyrin could include reductions to generate dicarbinols that could be converted into precursors for cycloaddition reactions. This strategy would provide access to further modified structures.

In Chapter III, it was demonstrated that an equally efficient synthesis of a carbachlorin could be facilitated using a cyclopentane dialdehyde with geminal diester substituents. The required dialdehyde was obtained from the Diels-Alder adduct of dimethyl methylenemalonate and cyclopentadiene. Condensation of the dialdehyde with a tripyrrane in the presence of trifluoroacetic acid, followed by oxidation with DDQ, produced a novel carbachlorin diester in 30% yield. This macrocycle was found to react with silver(III) acetate forming a silver(III) complex in good yields. The carbachlorin and its silver complex both exhibited strongly aromatic characteristics. Addition of acid to the carbachlorin resulted in the formation of a monocation with slightly enhanced diatropic character.

The methodology reported in the thesis provides the most convenient route available for preparing carbaporphyrins and carbachlorins. The availability of the new porphyrin analogues will allow further investigations into the reactivity of these systems. Furthermore, the presence of absorption bands near 650 nm for carbachlorins may allow this system to be utilized as a photosenitizers in photodynamic therapy.

REFERENCES

1. *Porphyrins and Metalloporphyrins*; Smith, K. M., ed.; Elsevier, **1975**.

2. Milgrom, L. R. *The Colours of Life: An Introduction to the Chemistry of Porphyrins and Related Compounds*; Oxford University Press, **1997**.

3. Kekulé, A. *Bull de la Societe Chimique de Paris*, **1865**, *3*, 98–110.

4. Loudon, G. M. *Organic Chemistry*; Roberts and Company, **2009**.

5. Hofmann, A. W. *Proc. R. Soc. Lond.* **1856**, *8*, 1–3.

6. Sondheimer, F.; Wolovsky, R.; Amiel, Y. *J Am. Chem. Soc.* **1962***, 84*, 274–284.

7. Lash, T. D. in *The Porphyrin Handbook: Heteroporphyrins, Expanded Porphyrins and Related Macrocycles*; Kadish, K. M.; Smith, K. M.; Guilard, R. Academic Press, **2000**; Vol. 2, pp 125–199.

8. Soret, J. L. *Compt. Rend.* **1883**, *97*, 1267.

9. Kuster, W.; Deihle, P. *Z. Physiol. Chem.* **1912**, 82.

10. Fischer, H.; Zeile, K. *Justus Liebigs Ann. Der Chem.* **1929**, *468*, 98–116.

11. Smith, K. M. in *The Porphyrin Handbook: Synthesis and Organic Chemistry*; Kadish, K. M.; Smith, K. M.; Guilard, R Academic Press, **2000**; Vol. 1, pp 2–43.

12. Rothemund, P. *J. Am. Chem. Soc.* **1936**, *58*, 625–627.

13. Adler, A. D.; Longo, F. R.; Finarelli, J. D.; Goldmacher, J.; Assour, J.; Korsakoff, L. *J. Org. Chem.* **1967**, *32*, 476–477.

14. Lindsey, J. S.; Schreiman, I. C.; Hsu, H. C.; Kearney, P. C.; Marguerettaz, A. M. *J. Org. Chem*. **1987**, *52*, 827–836.

15. Arsenault, G. P.; Bullock, E.; MacDonald, S. F. *J. Am. Chem. Soc.* **1960**, *82*, 4384–4389.

16. Broadhurst, M. J.; Grigg, R.; Johnson, A. W. *J. Chem. Soc.* **1971**, 3681–3690.

17. Cavaleiro, J. A. S.; Gonsalves, A. M. d'A R.; Kenner, G. W.; Smith, K. M. *J. Chem. Soc Perkin Trans.* **1973***, 1*, 2471.

18. Sessler, J. L.; Johnson, M. R.; Lynch, V. *J. Org. Chem.* **1987**, *52*, 4394–4397.

19. Lash, T. D.; Toney, A. M.; Castans, K. M.; Ferrence, G. M. *J. Org. Chem.* **2013**, *78*, 9143–9152.

20. Graham, S. R.; Colby, D. A.; Lash, T. D. *Angew. Chem. Int. Ed.* **2002**, *41*, 1371–1374.

21. Lash, T. D.; Chaney, S. T.; Richter, D. T. *J. Org. Chem.* **1998**, *63,* 9076–9088.

22. Sessler, J. L.; Cyr, M.; Burrell, A, K. *Tetrahedron*, **1992**, *48*, 9661–9672.

23. Lash, T. D. *Eur. J. Org. Chem.* **2007**, *33*, 5461–5481.

24. Muckey, M. A.; Szczepura, L. F.; Ferrence, G. M.; Lash, T. D. *Inorg. Chem.* **2002**, *41*, 4840 – 4842.

25. Xue, Z.-L.; Shen, Z.; Mack, J.; Kuzuhara, D.; Yamada, H.; Okujima, T.; Ono, N.; You, X.-Z.; Kobayashi, N. *J. Am. Chem. Soc.* **2008**, *130*, 16478–16479.

26. Broadhurst, M. J.; Grigg, R.; Johnson, A. W. *J. Chem. Soc. Perkin Trans. 1* **1972**, 2111.

27. Sessler, J. L.; Murai, T.; Lynch, V.; Cyr, M. *J. Am. Chem. Soc*. **1988**, *110*, 5586–5588.

28. Amao, T.; Okura, I. *J. Porphyrins Phthalocyanines* **2009**, *13*, 1111–1122.

29. Malinski, T. in *The Porphyrin Handbook: Applications Past, Present, and Future*; Kadish, K. M, Smith, K. M.; Guilard, R. Academic Press, **2000**; Vol.6, pp 232–255.

30. Collman, J. P.; Brauman, J. I.; Meunier, B.; Raybuck, S. A.; Kodadek, T. *Proc Natl. Acad Sci.* **1984**, *81*, 3245–3248.

31. Anding, B. J.; Ellern, A.; Woo, L. K. *Organometallics,* **2012**, *31*, 3628–3635.

32. Kostas, I. D.; Coutsolelos, A G; Charalambidis, G; Skondra, A. *Tetrahedron Lett.* **2007**, *48*, 6688–6691.

33. Rambo, B. M.; Sessler, J. L. *Chem. –Eur. J.* **2011**, *17,* 4946–4959.

34. Groves, J. T.; Myers, R. S. *J. Am. Chem. Soc.* **1983**, *105*, 5791–5796.

35. Lash, T. D. *Chem. Rev*. **2017**, *117*, 2313–2446.

36. Toganoh, M.; Furuta, H. *Chem. Commun.* **2012**, *48*, 937−954.

37. Bergman, K. M.; Ferrence, G. M.; Lash, T. D. *J. Org. Chem*. **2004**, *69*, 7888−7897.

38. Lash, T. D. *Acc. Chem. Res.* **2016**, *49*, 471−482.

39. Lash, T. D. *Org. Biomol. Chem*. **2015**, *13*, 7846−7878.

40. Lash, T. D.; Hayes, M. J. *Angew. Chem., Int. Ed. Engl.* **1997**, *36*, 840−842.

41. AbuSalim, D. I.; Lash, T. D. *J. Org. Chem*. **2013**, *78*, 11535−11548.

42. Colby, D. A.; Lash, T. D. *Chem. - Eur. J*. **2002**, *8*, 5397−5402.

43. Lash, T. D.; Colby, D. A.; Ferrence, G. M. *Eur. J. Org. Chem*. **2003**, *2003*, 4533−4548.

44. Lash, T. D.; Hayes, M. J. *Angew. Chem., Int. Ed. Engl*. **1997**, *36*, 840−842.

45. Lash, T. D.; Hayes, M. J.; Spence, J. D.; Muckey, M. A.; Ferrence, G. M.; Szczepura, L. F. *J. Org. Chem*. **2002**, *67*, 4860−4874.

46. Muckey, M. A.; Szczepura, L. F.; Ferrence, G. M.; Lash, T. D. *Inorg. Chem*. **2002**, *41*, 4840−4842.

47. Lash, T. D.; Colby, D. A.; Szczepura, L. F. *Inorg. Chem.* **2004**, *43*, 5258−5267.

48. Adiraju, V. A. K.; Ferrence, G. M.; Lash, T. D. *Dalton Trans*. **2016**, *45*, 13691−13694.

49. Lash, T. D. *Org. Lett*. **2011**, *13*, 4632−4635.

50. Hayes, M. J.; Spence, J. D.; Lash, T. D. *Chem. Commun*. **1998**, *34*, 2409−2410.

51. Lash, T. D.; Muckey, M. A.; Hayes, M. J.; Liu, D.; Spence, J. D.; Ferrence, G. M. *J. Org. Chem.* **2003**, *68*, 8558−8570.

52. Lash, T. D.; Romanic, J. L.; Hayes, M. J.; Spence, J. D. *Chem. Commun*. **1999**, *35*, 819−820.

53. Taniguchi, M.; Lindsey, J. S. *Chem. Rev.* **2017**, *117*, 344–535.

54. Hayes, M. J.; Lash, T. D. *Chem. - Eur. J.* **1998**, *4*, 508−511.

55. Daming, Li.; Lash, T. D. *J. Org. Chem.* **2014**, *79*, 7112–7121.

56. Barton, D. H. R.; Zard, S. Z. *J. Chem. Soc.* **1985***, 16*, 1098.

57. Atkins, A. J.; Fairlamb, I. J. S.; Ward, J. S.; Lynam, J. M. *Organometallics* **2012**, *31*, 5896–5902.

58. Göksu, S.; Altundas, R.; Sütbeyaz, Y. *Syn. Comm*. **2000**, *9*, 1615–1621.

59. Donohoe, T.; Jahanshahi, A.; Tucker, M. J.; Bhatti, F. L.; Roslan, I. A.; Kabeshov, M.; Wrigley, G. *Chem. Commun*. **2011**, *47*, 5849–5851.

60. Henderson, L. C.; Li, J.; Nation, R. L.; Velkov, T.; Pfeffer, F. M.; *Chem. Commun*. **2010**, *46*, 3197–3199.

61. Hickey, S. M.; Ashton, T. D.; White, J. M.; Li, J.; Nation. R. L.; Yu, H. Y.; Elliott, A. G.; Butler, M. S.; Huang, J. X.; Cooper, M. A.; Pfeffer, F. M. *RSC Adv*. **2015**, *5*, 28582–28596.

62. Beare, K. D.; Yuen, A. K. L.; Masters, A. F.; Maschmeyer, T.; McErlean, C. S. P. *Chem. Commun*. **2013**, *49*, 8347–8349.

63. Harada, M.; Asaba, K. N.; Iwai, M.; Kogure, N.; Kitajima, M.; *Org. Lett.*, **2012**, *14*, 5800l.

APPENDIX A

SELECTED NMR SPECTRA

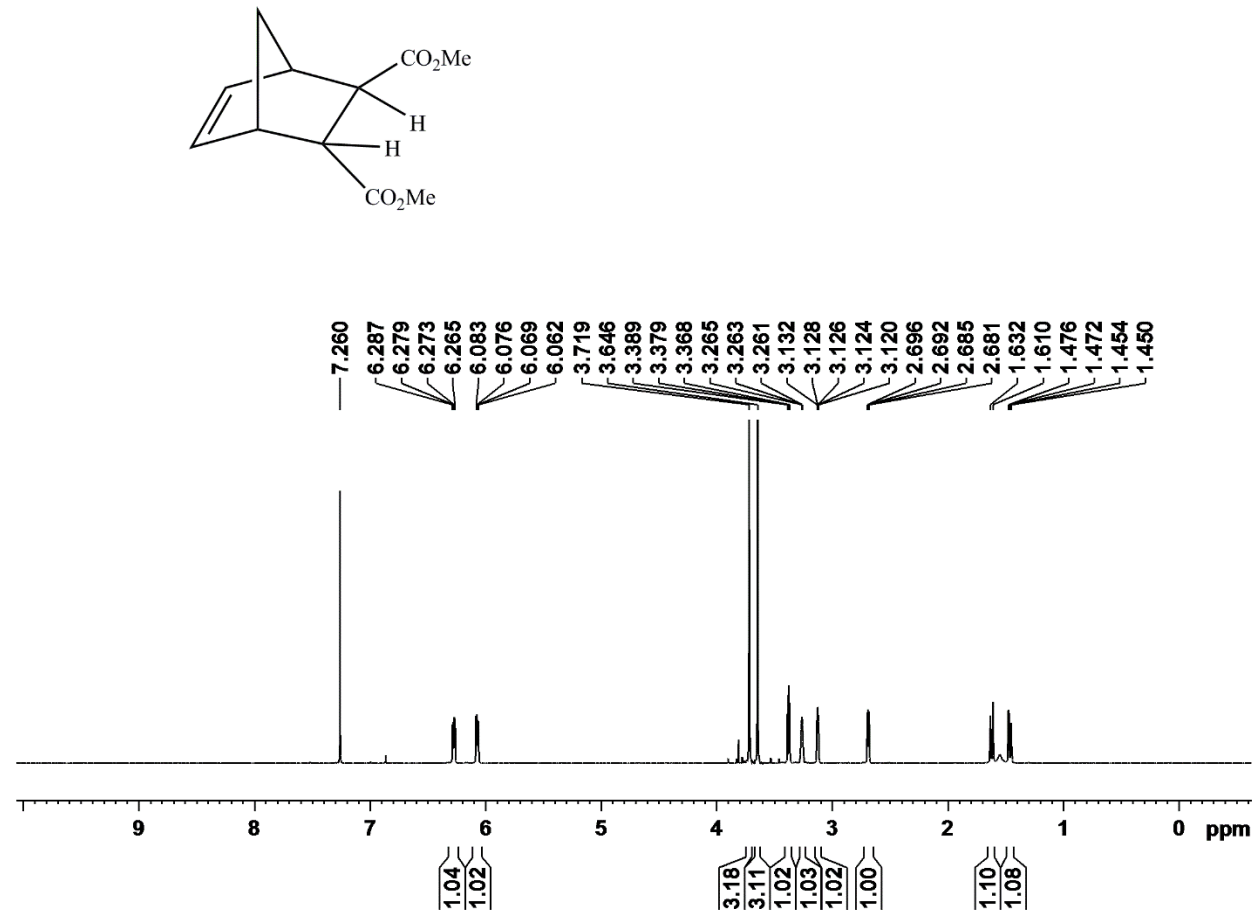

Figure A – 1: 400 MHz ^{1}H NMR Spectrum of **114** in $CDCl_3$

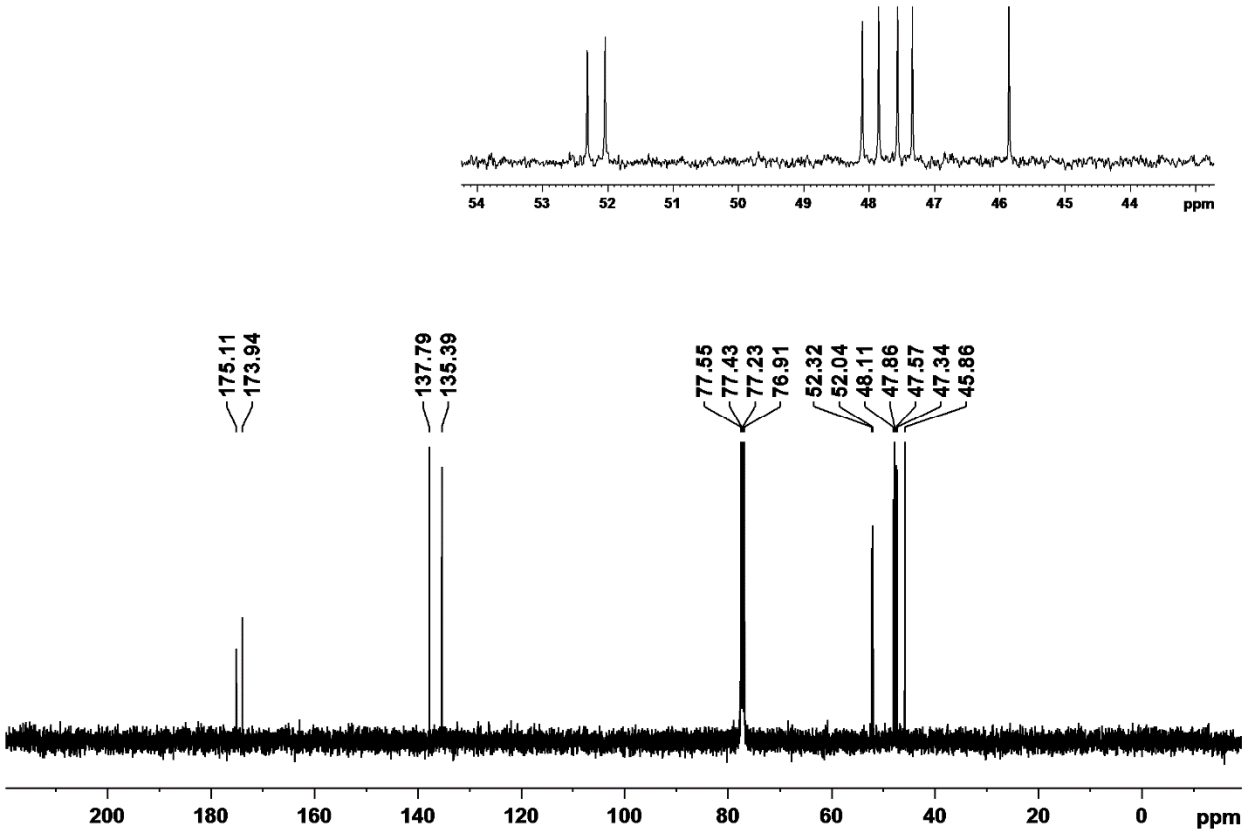

Figure A – 2: 100 MHz carbon-13 NMR spectrum of **114** in $CDCl_3$.

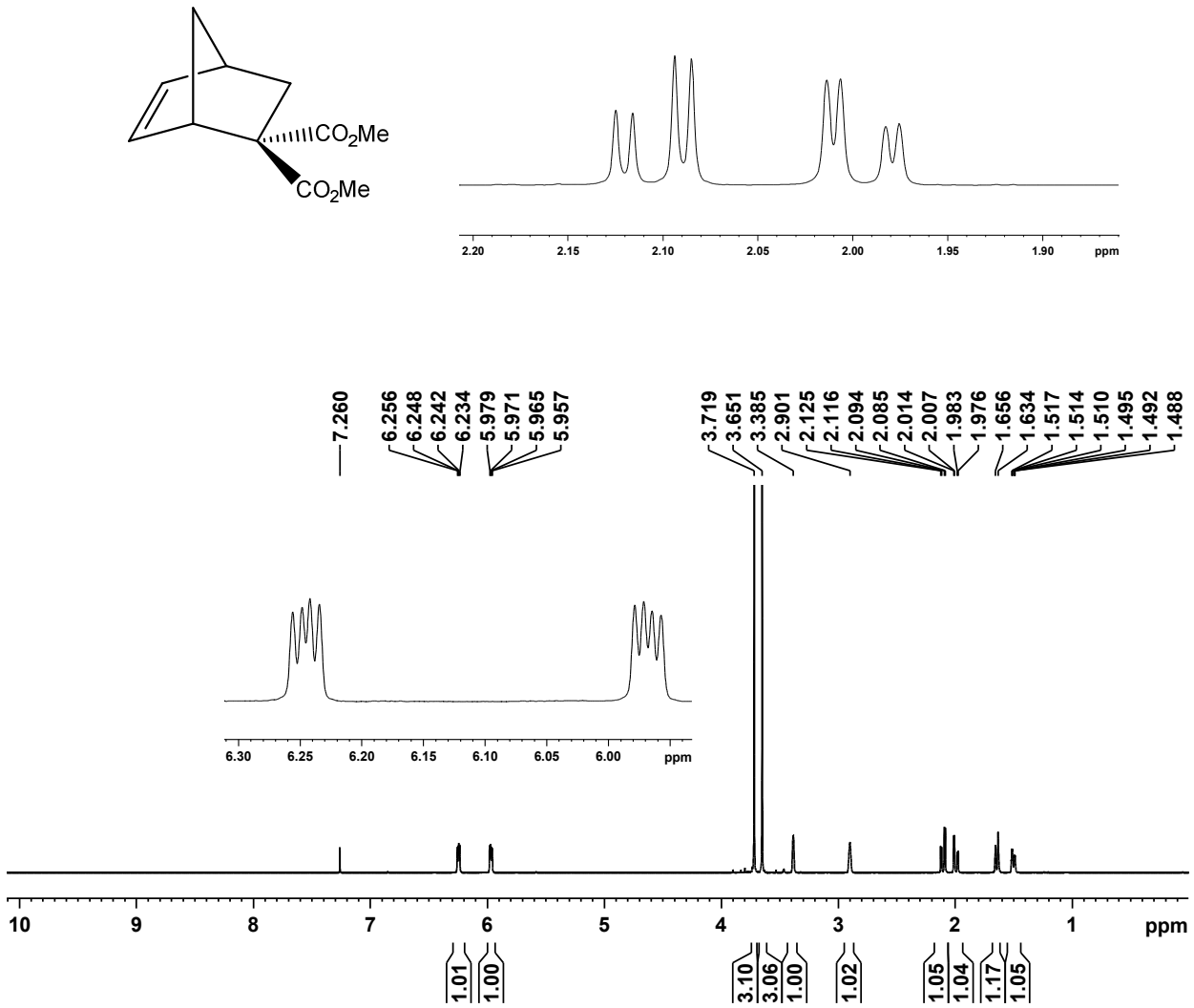

Figure A – 3: 400 MHz ^{1}H NMR Spectrum of **135** in $CDCl_3$

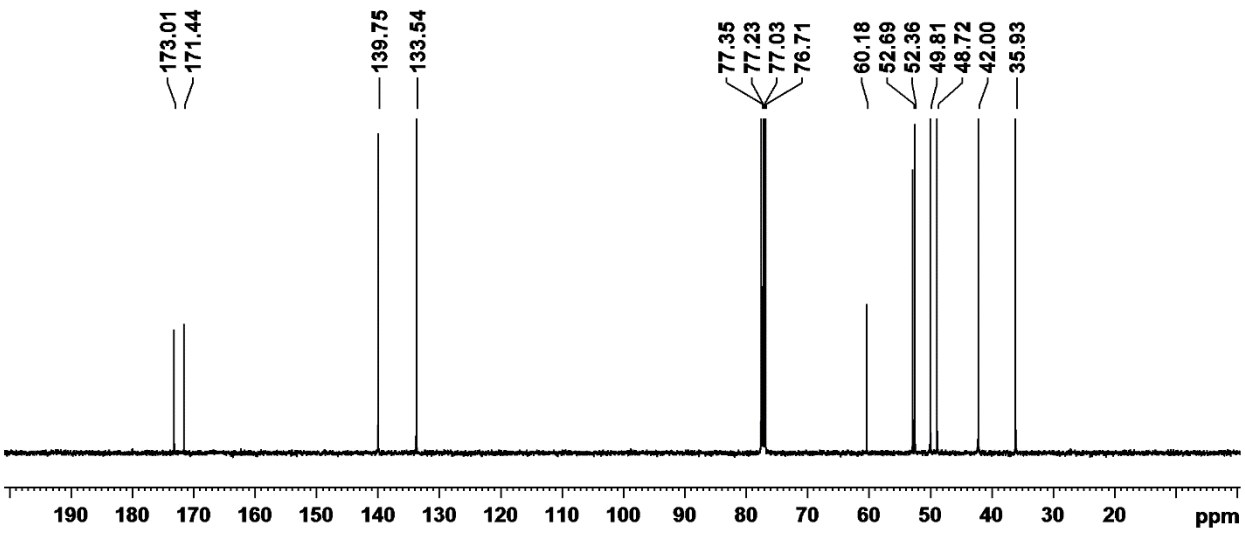

Figure A – 4: 100 MHz carbon-13 NMR spectrum of **135** in $CDCl_3$.

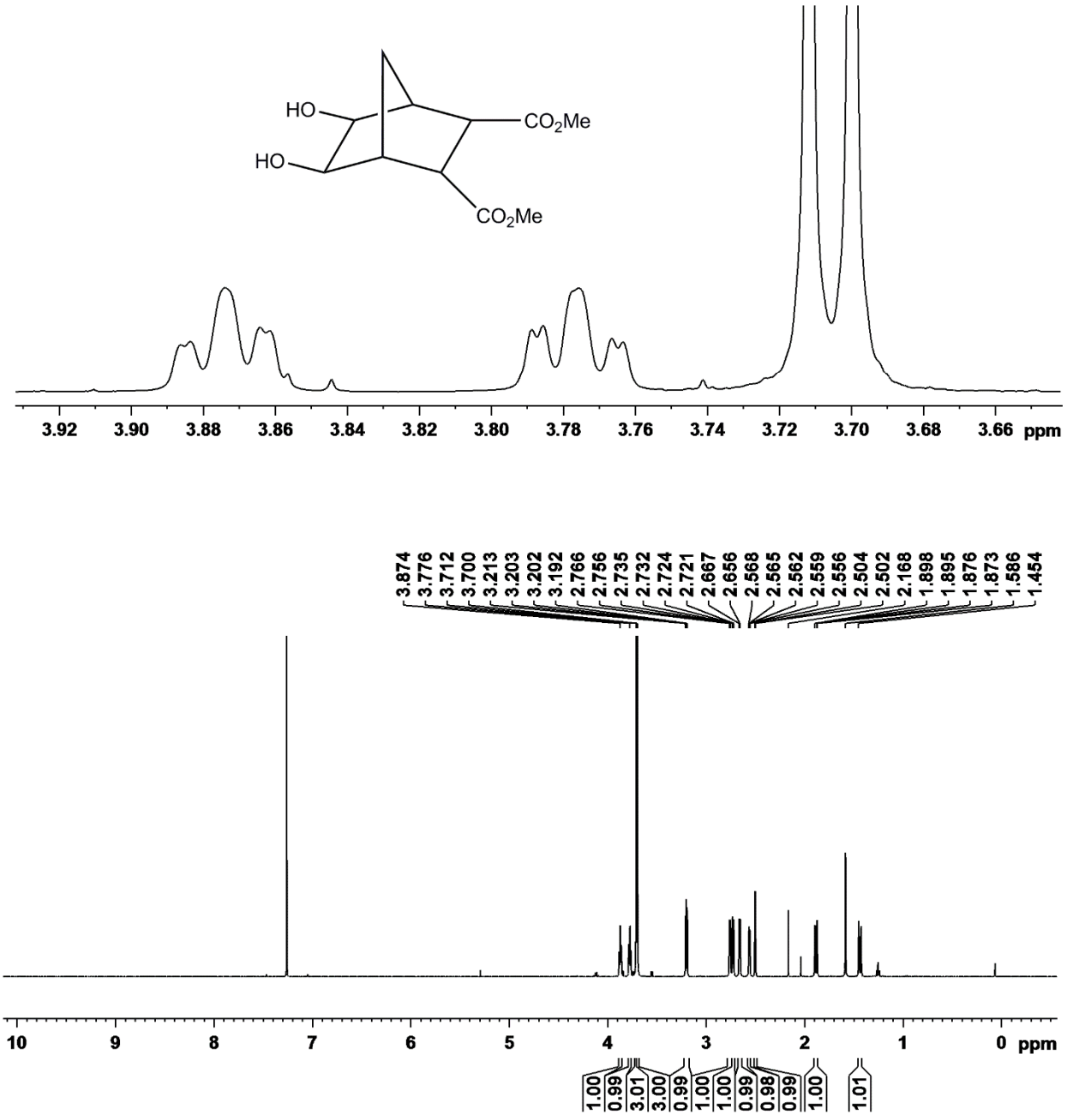

Figure A – 5: 400 MHz ^{1}H NMR Spectrum of **115** in $CDCl_3$

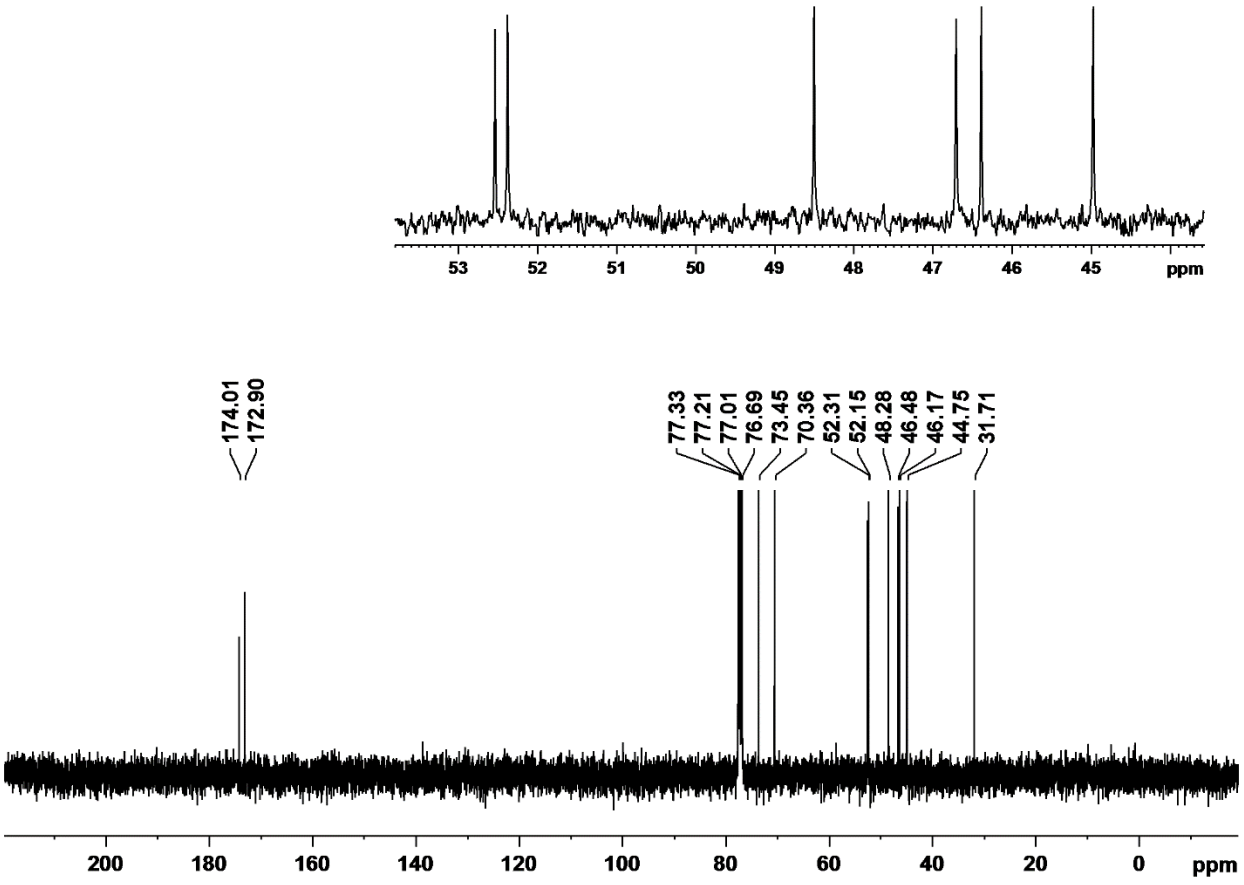

Figure A – 6: 100 MHz carbon-13 NMR spectrum of **115** in $CDCl_3$.

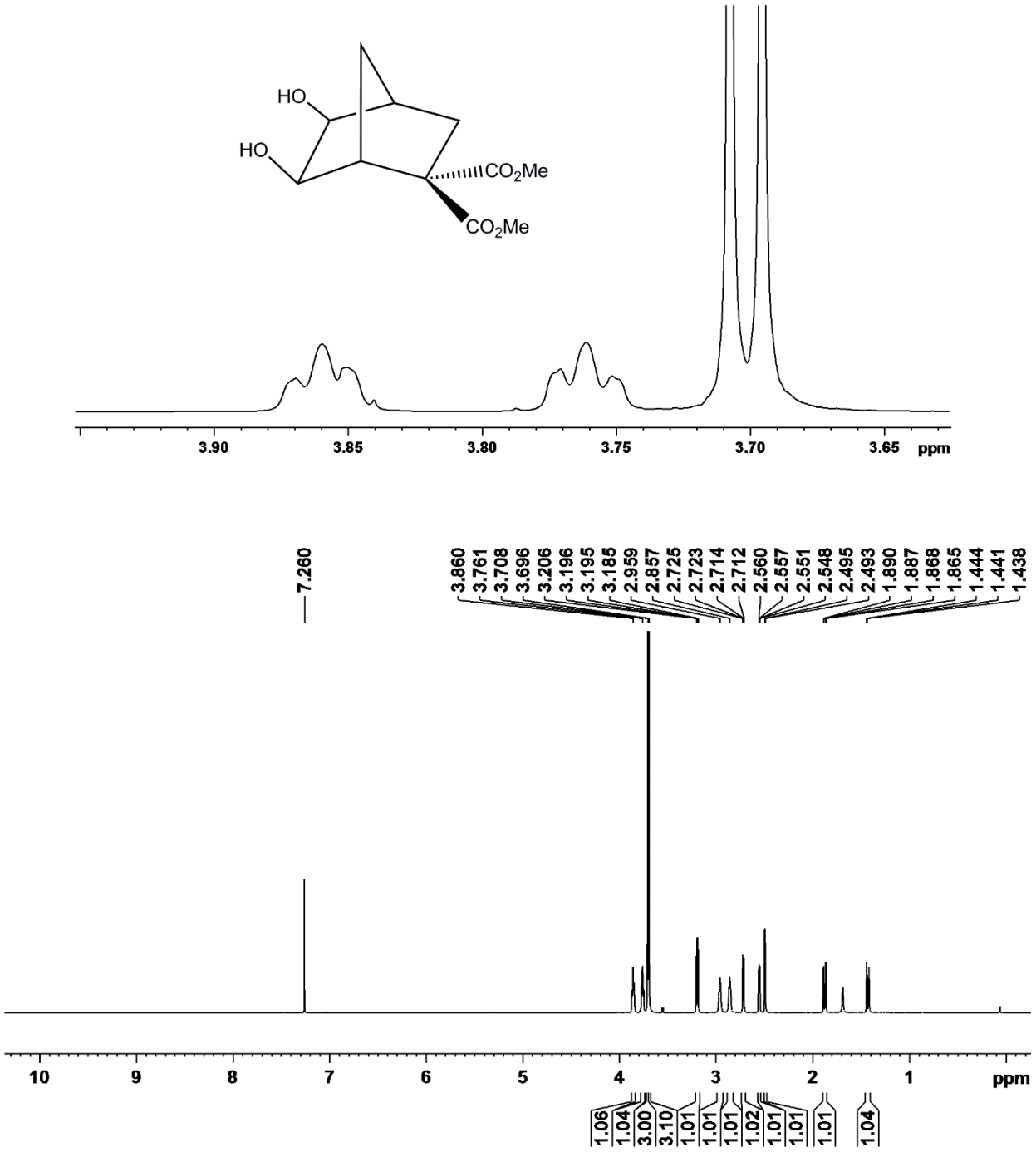

Figure A – 7: 400 MHz ^{1}H NMR Spectrum of **137** in $CDCl_3$

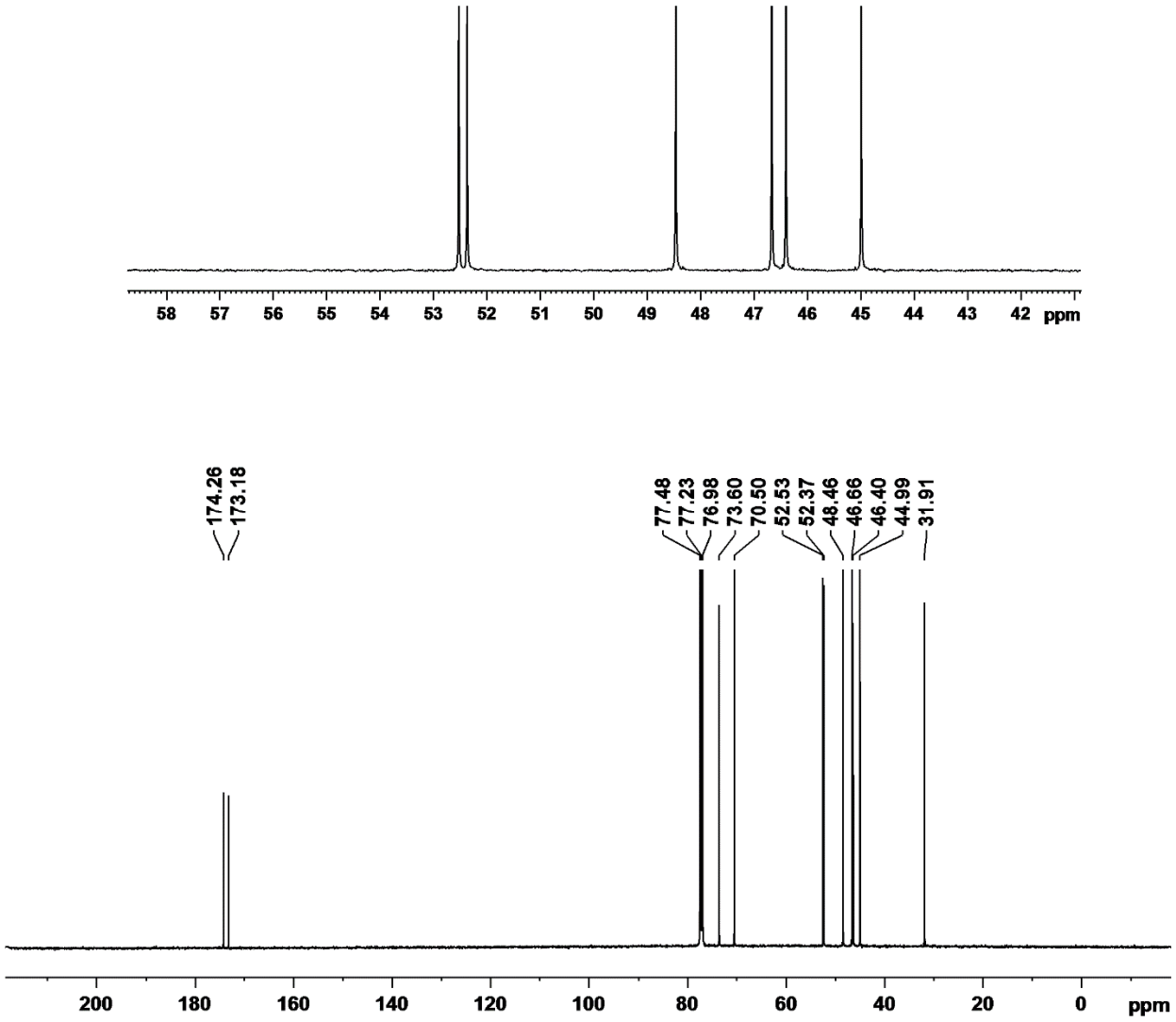

Figure A – 8: 100 MHz carbon-13 NMR spectrum of **137** in $CDCl_3$.

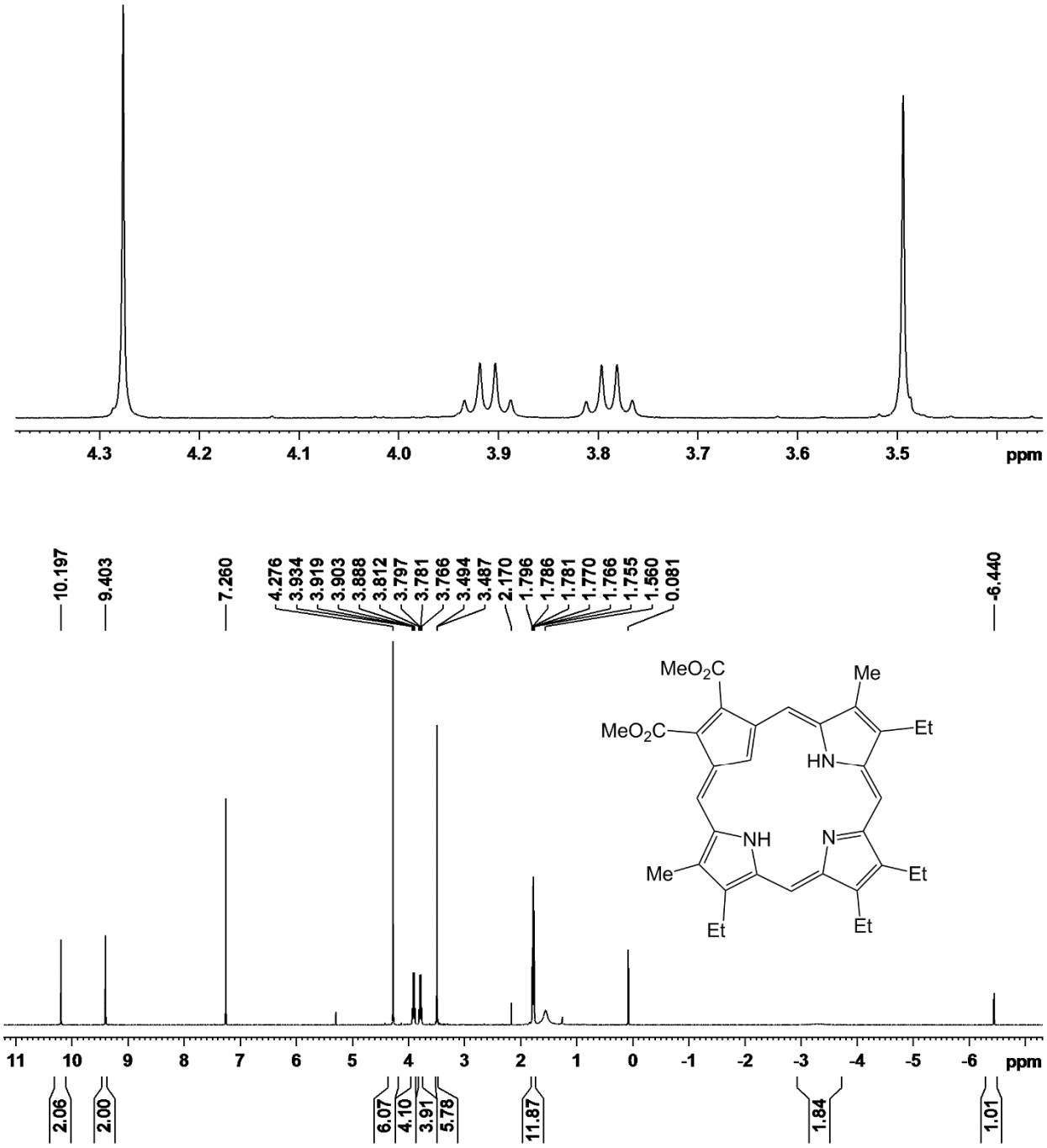

Figure A – 9: 500 MHz ^{1}H NMR Spectrum of Carbaporphyrin **98** in $CDCl_3$

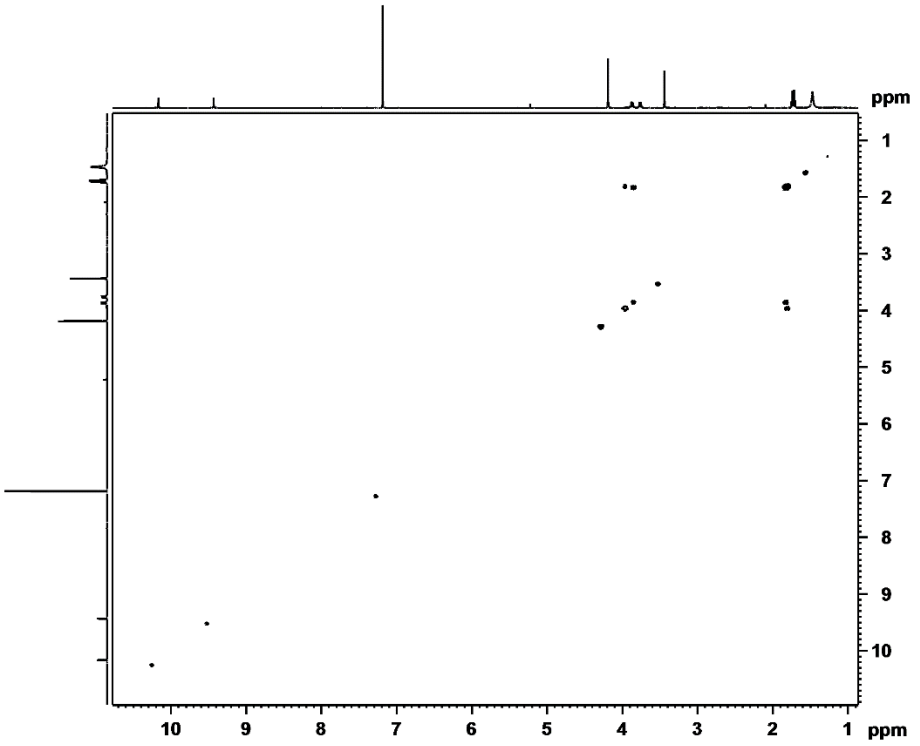

Figure A – 10: ^{1}H-^{1}H COSY NMR spectrum of carbaporphyrin diester **98** in $CDCl_3$

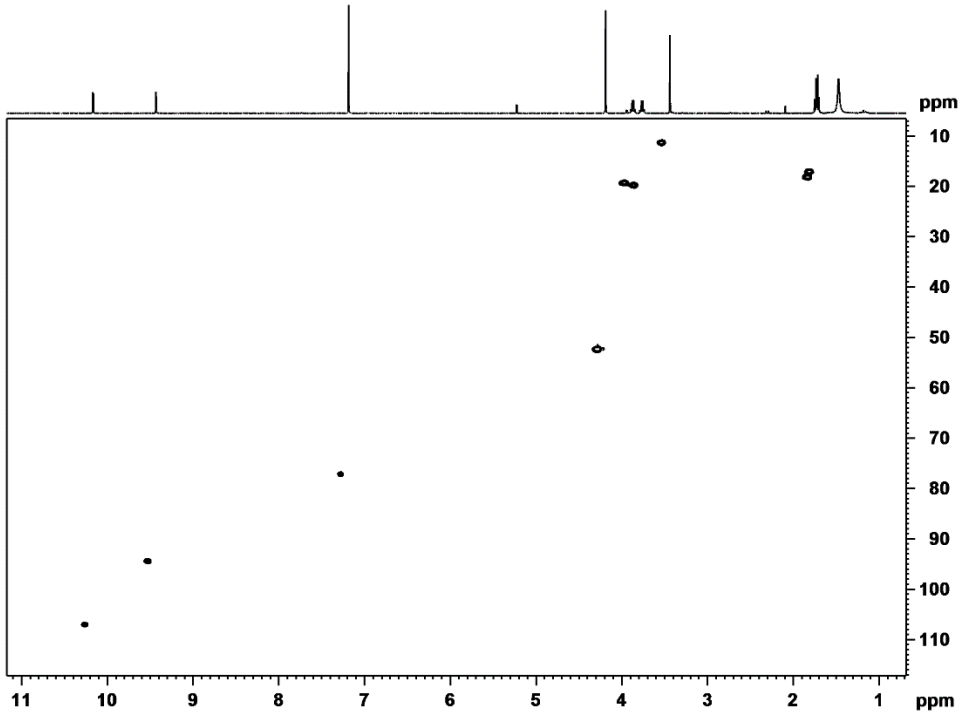

Figure A – 11: HSQC NMR spectrum of carbaporphyrin diester **98** in $CDCl_3$.

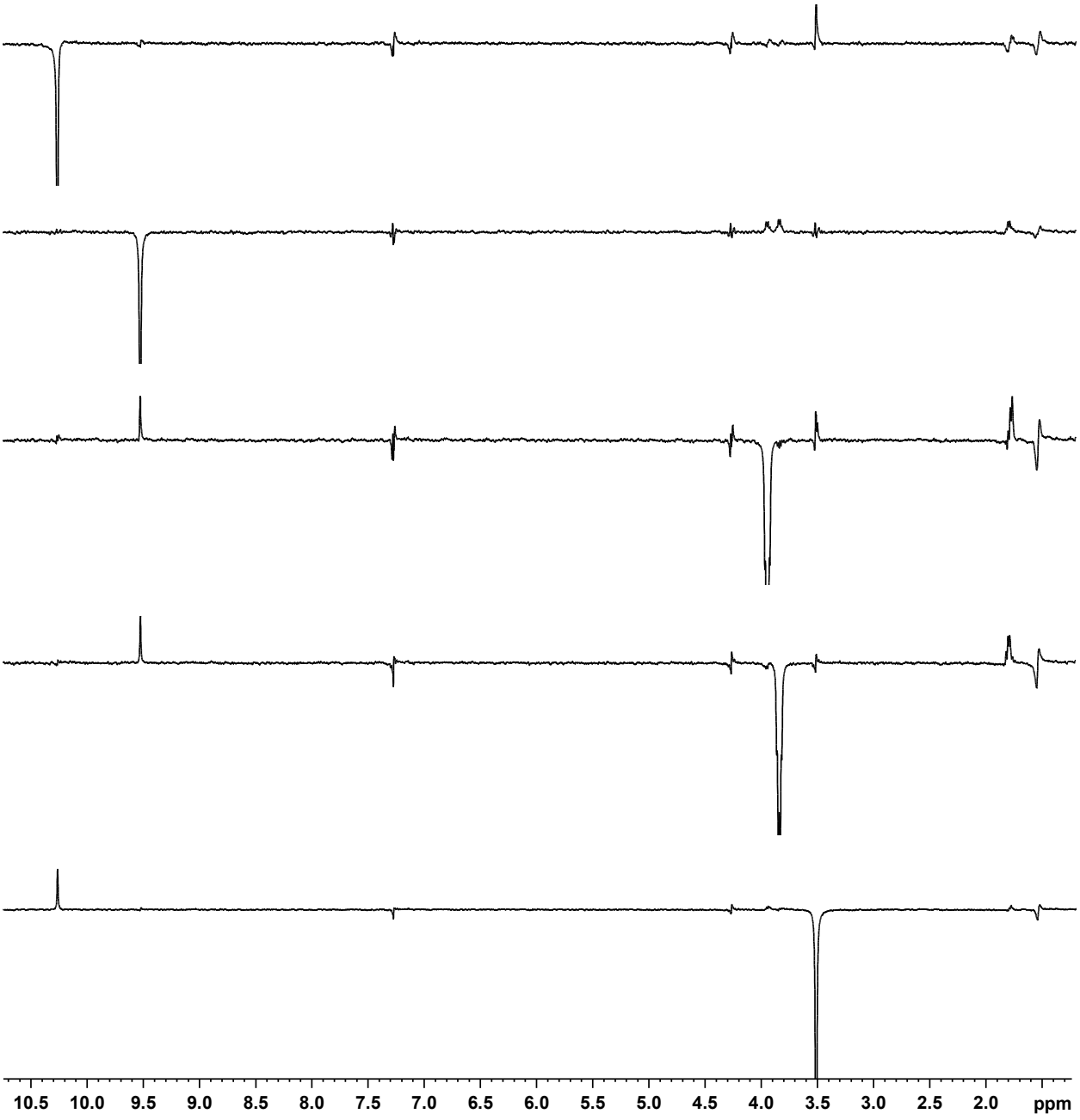

Figure A – 12: Selected nOe difference proton NMR spectra of carbaporphyrin diester **98** in $CDCl_3$.

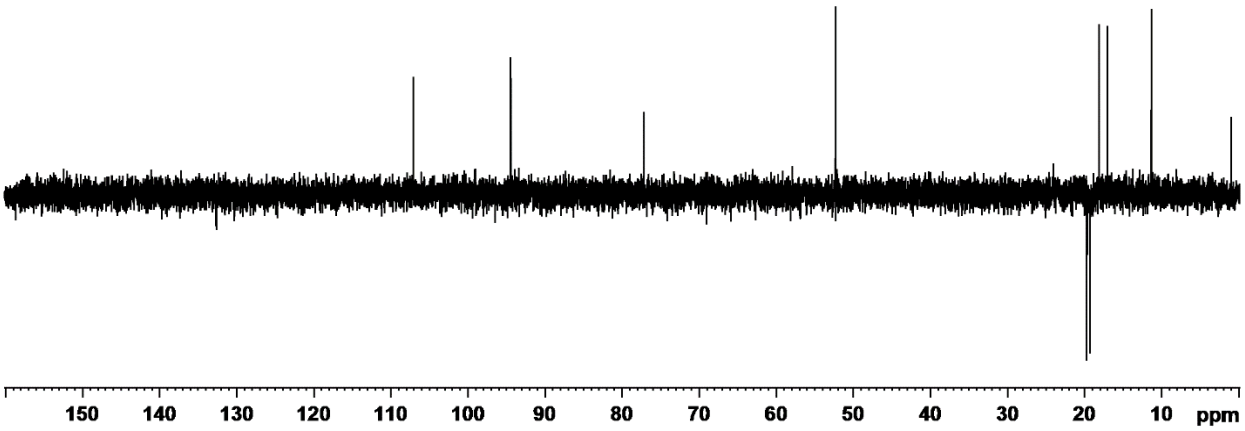

Figure A – 13: DEPT-135 NMR spectrum of carbaporphyrin diester **98** in $CDCl_3$.

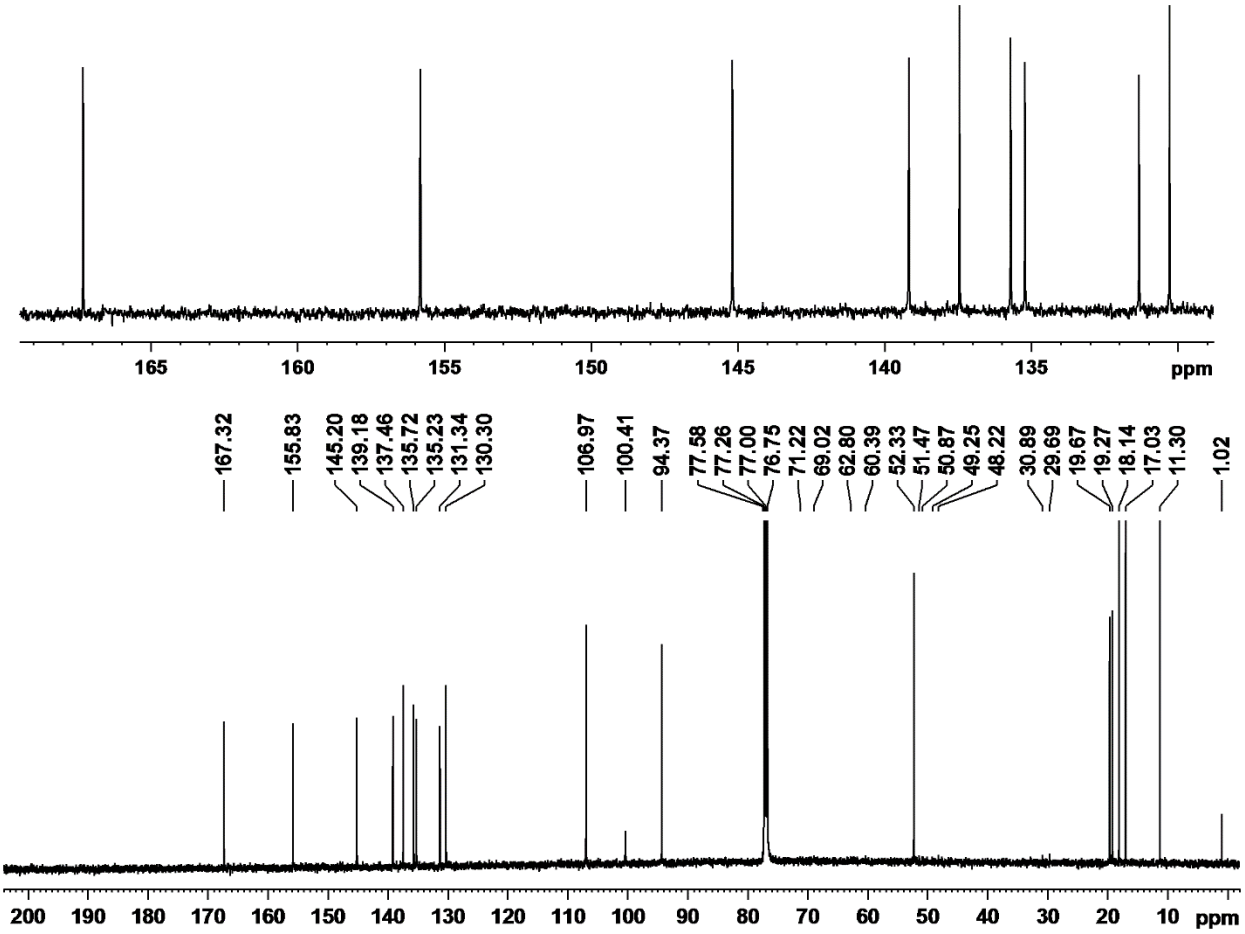

Figure A – 14: 125 MHz carbon-13 NMR spectrum of carbaporphyrin diester **98** in $CDCl_3$.

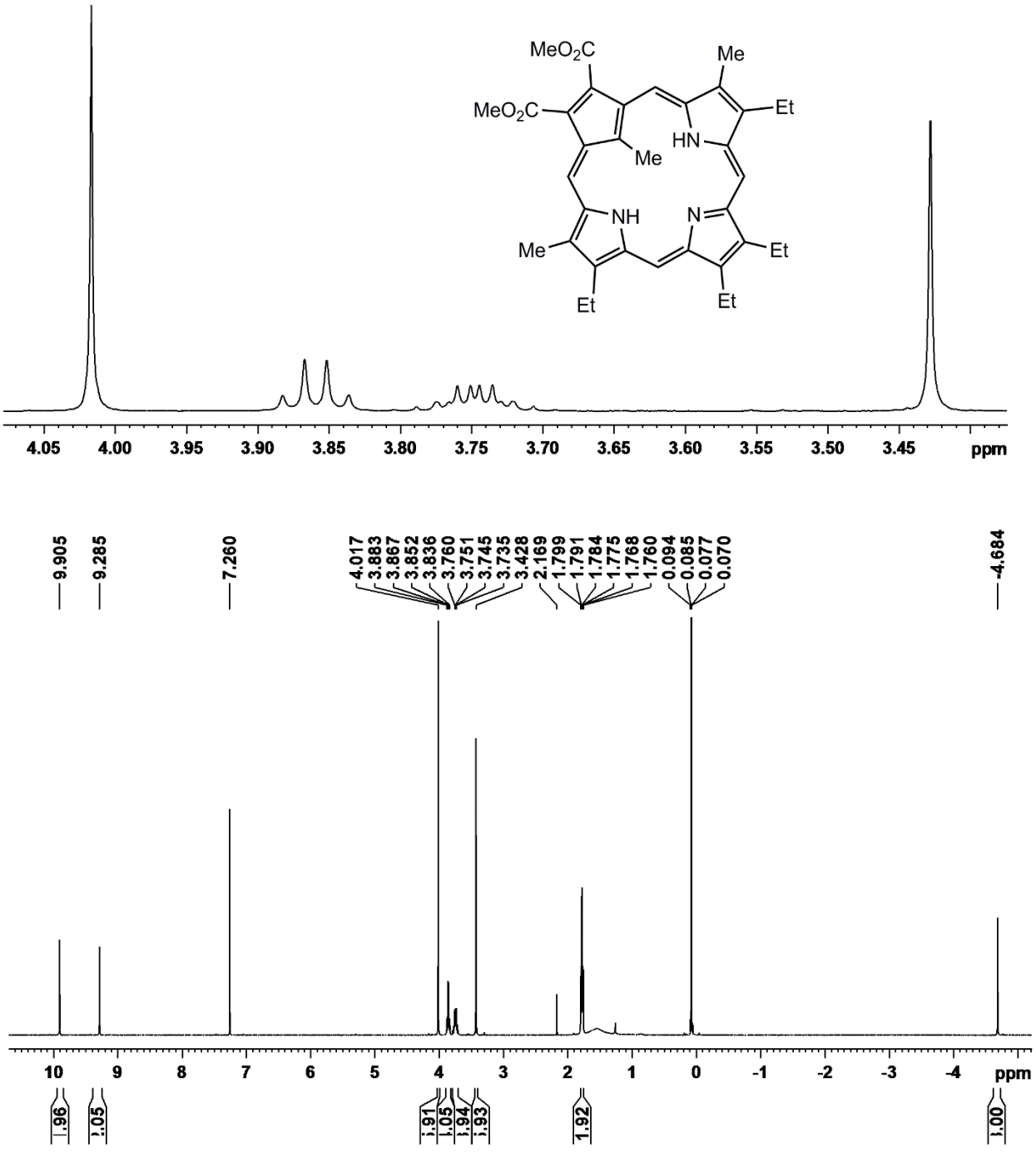

Figure A – 15: 500 MHz ^{1}H NMR Spectrum of C-methylated Carbaporphyrin **120** in $CDCl_3$

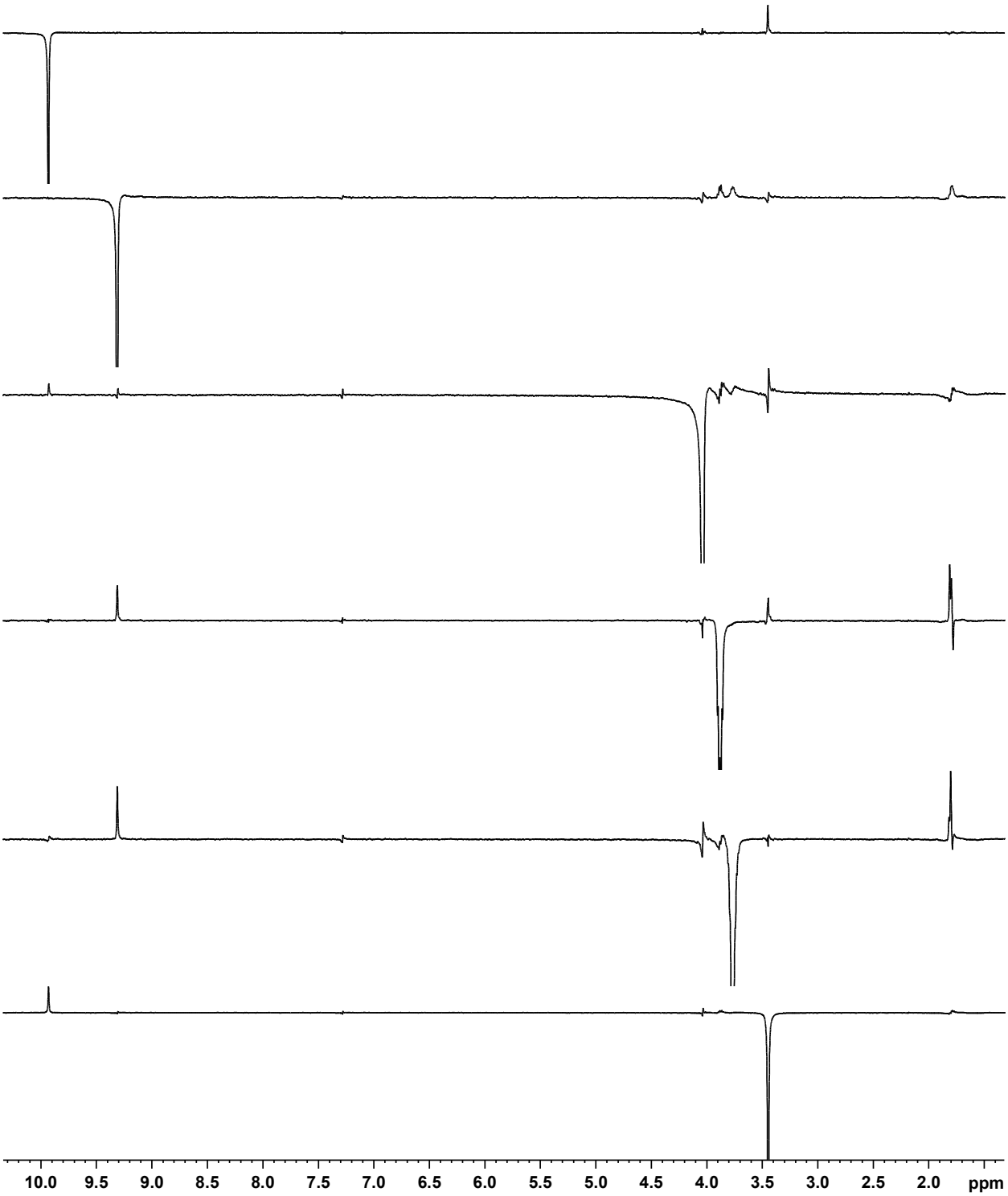

Figure A – 16: Selected nOe difference proton NMR spectra of **120** in $CDCl_3$

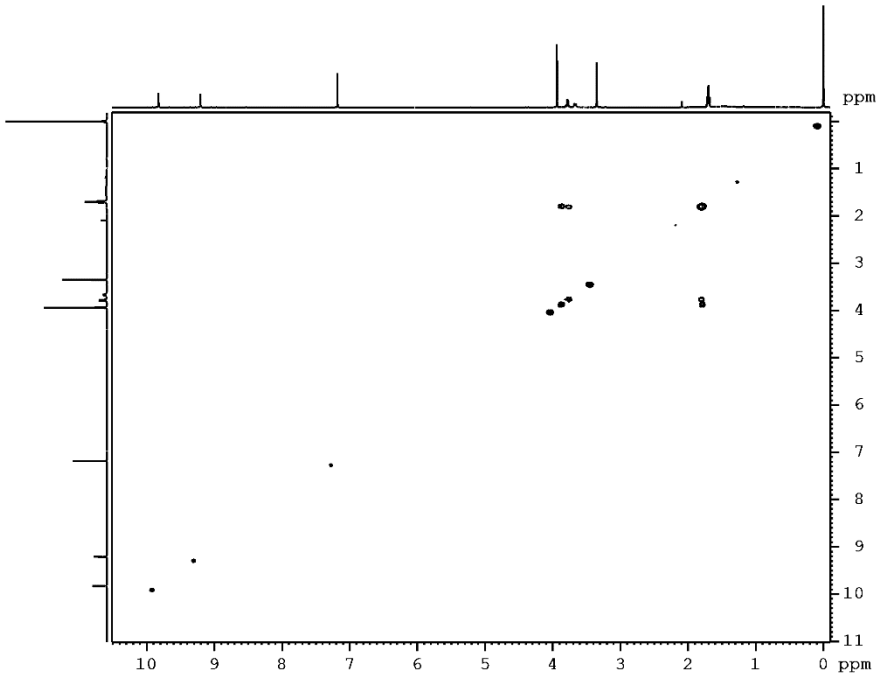

Figure A – 17: ^{1}H-^{1}H COSY NMR spectrum of **120** in $CDCl_3$

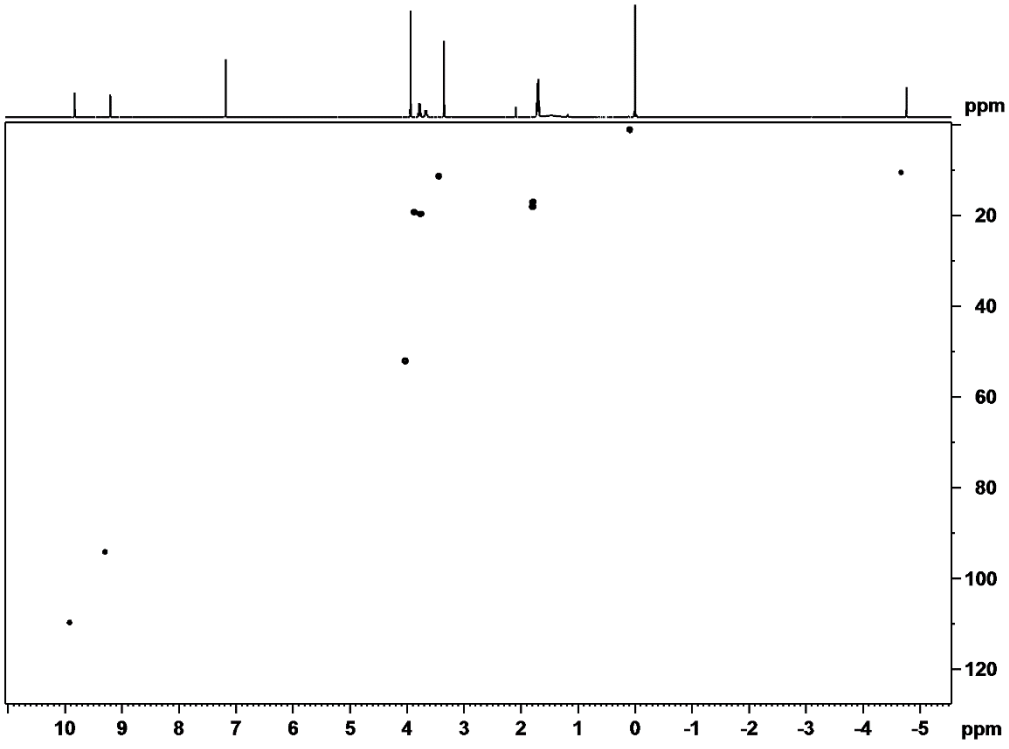

Figure A – 18: HSQC NMR spectrum of **120** in $CDCl_3$

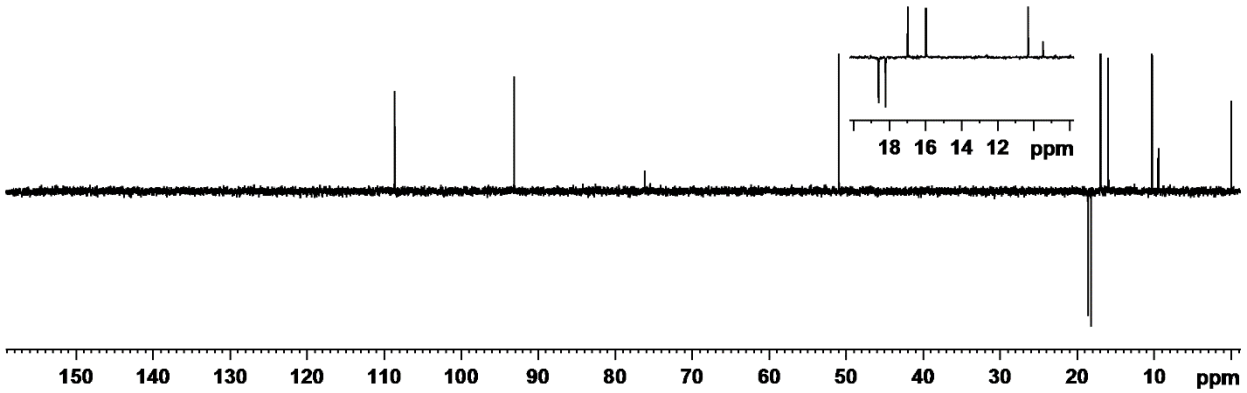

Figure A – 19: DEPT-135 NMR spectrum of **120** in $CDCl_3$.

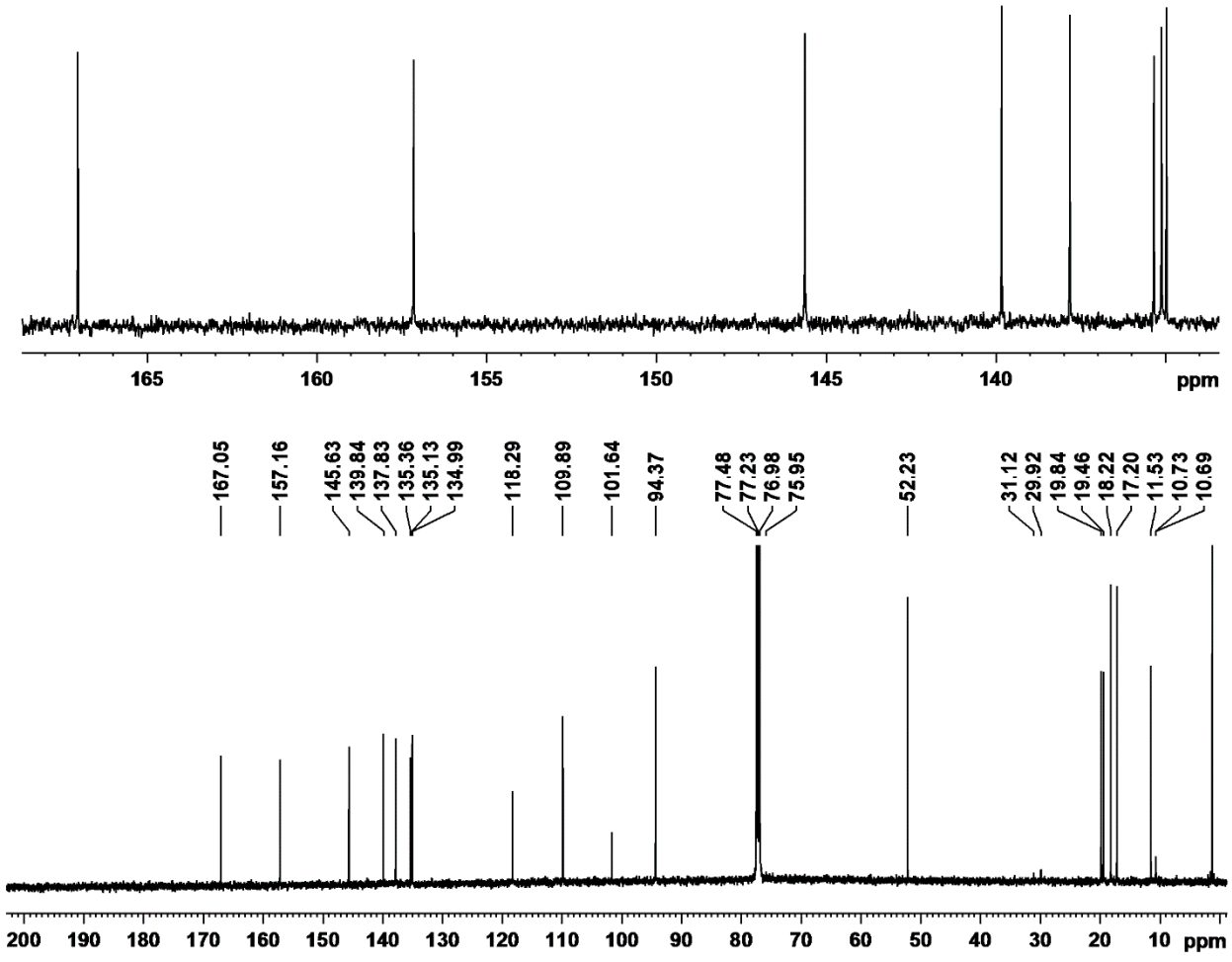

Figure A –20: 125 MHz carbon-13 NMR spectrum of **120** in $CDCl_3$.

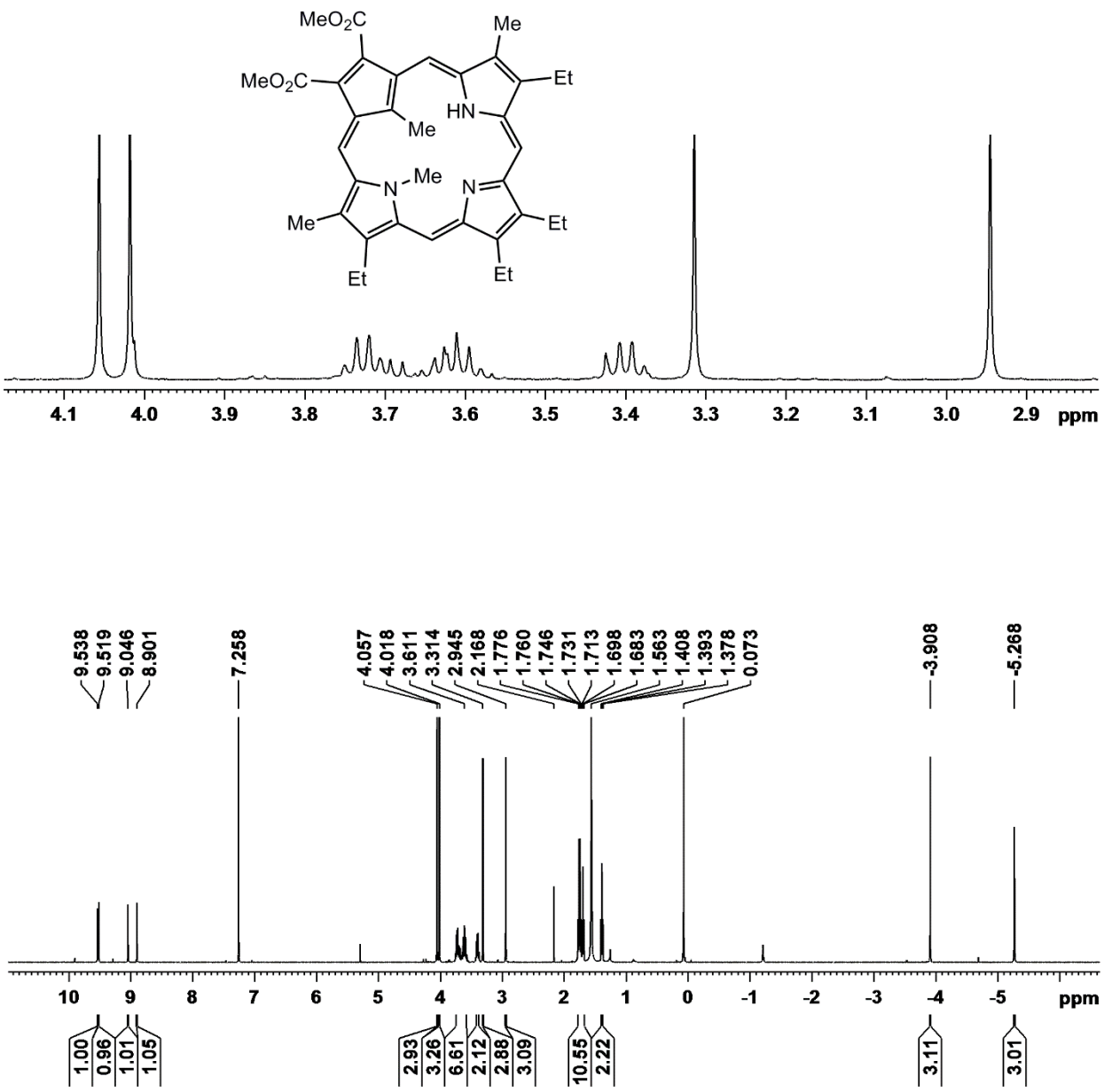

Figure A – 21: 500 MHz ^{1}H NMR Spectrum of **121** in $CDCl_3$.

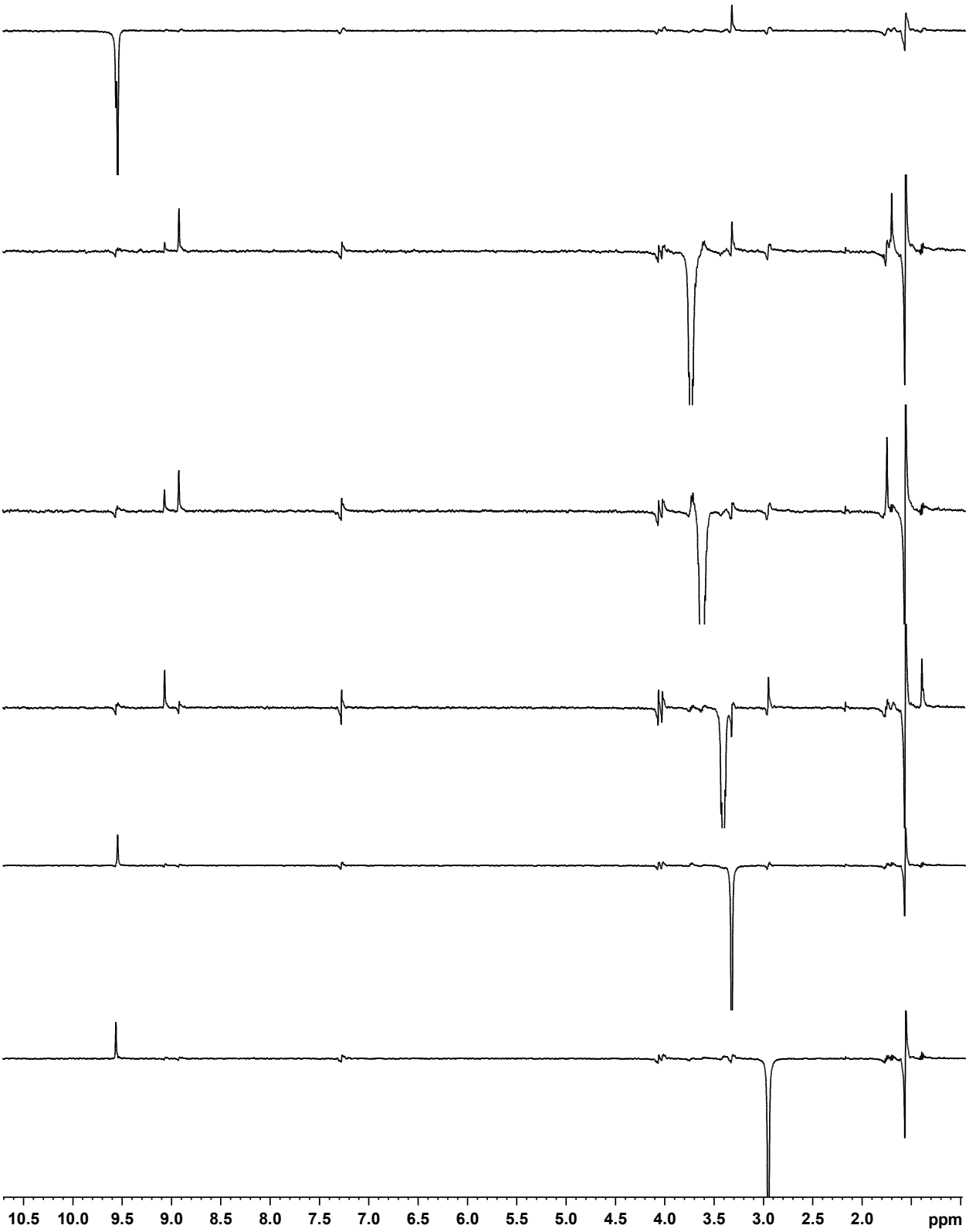

Figure A – 22: Selected nOe difference proton NMR spectra of **121** in $CDCl_3$

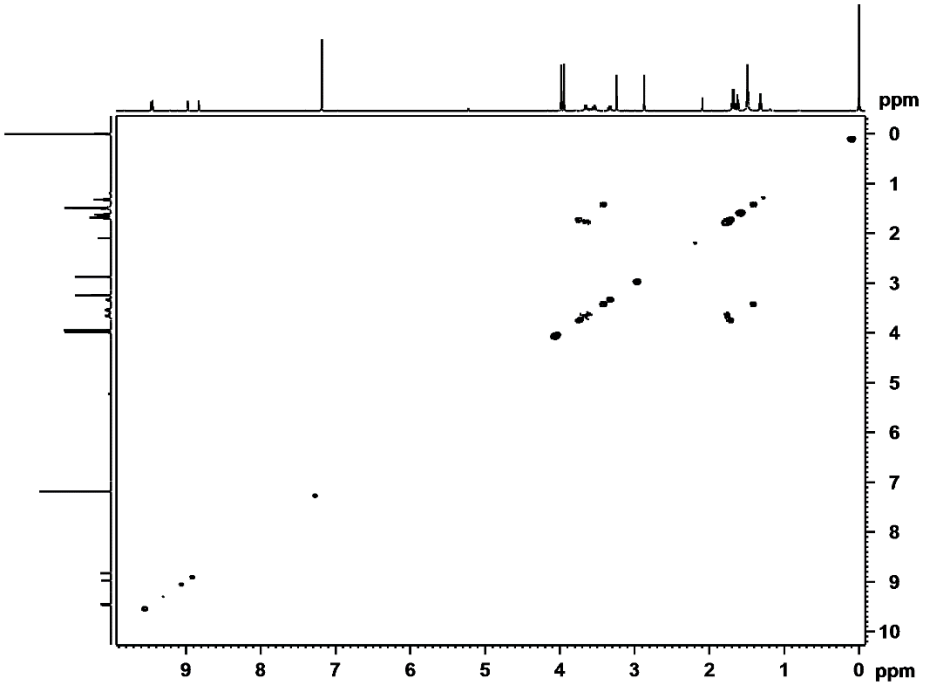

Figure A – 23: ^{1}H-^{1}H COSY NMR spectrum of **121** in $CDCl_3$

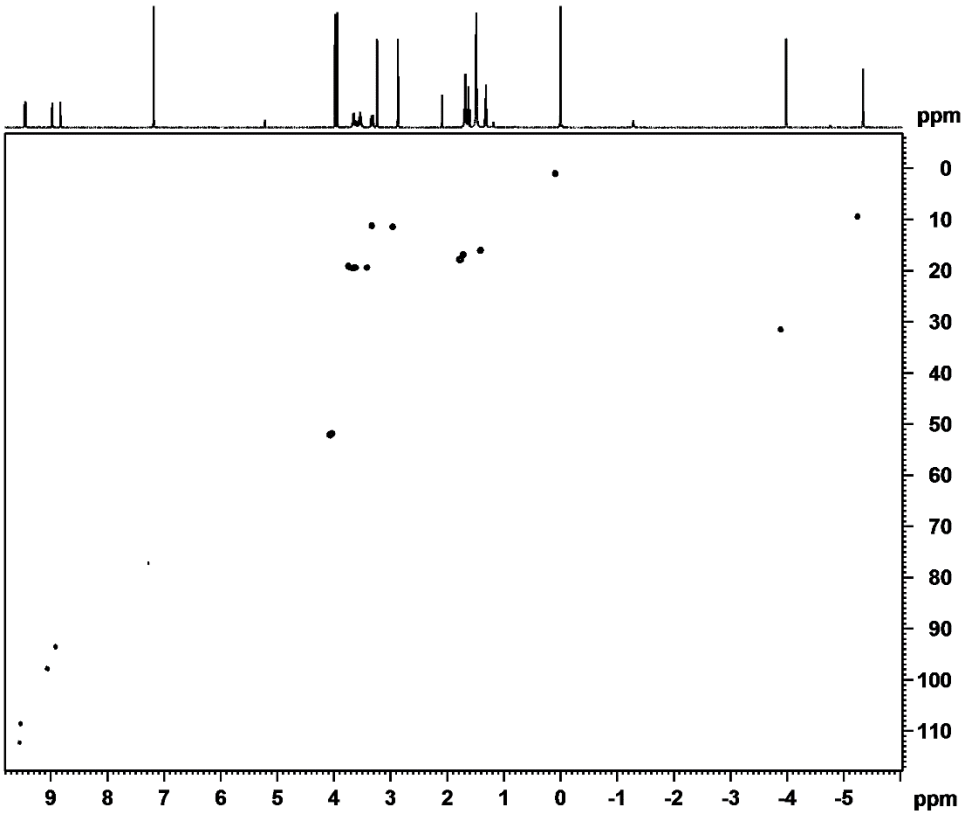

Figure A – 24: HSQC NMR spectrum of **121** in $CDCl_3$

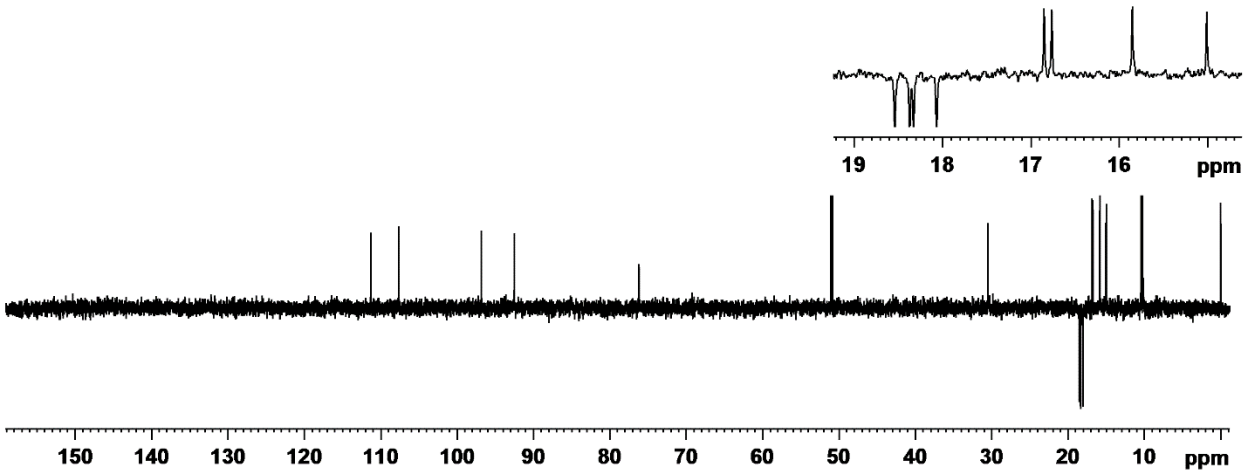

Figure A – 25: DEPT-135 NMR spectrum of **121** in $CDCl_3$

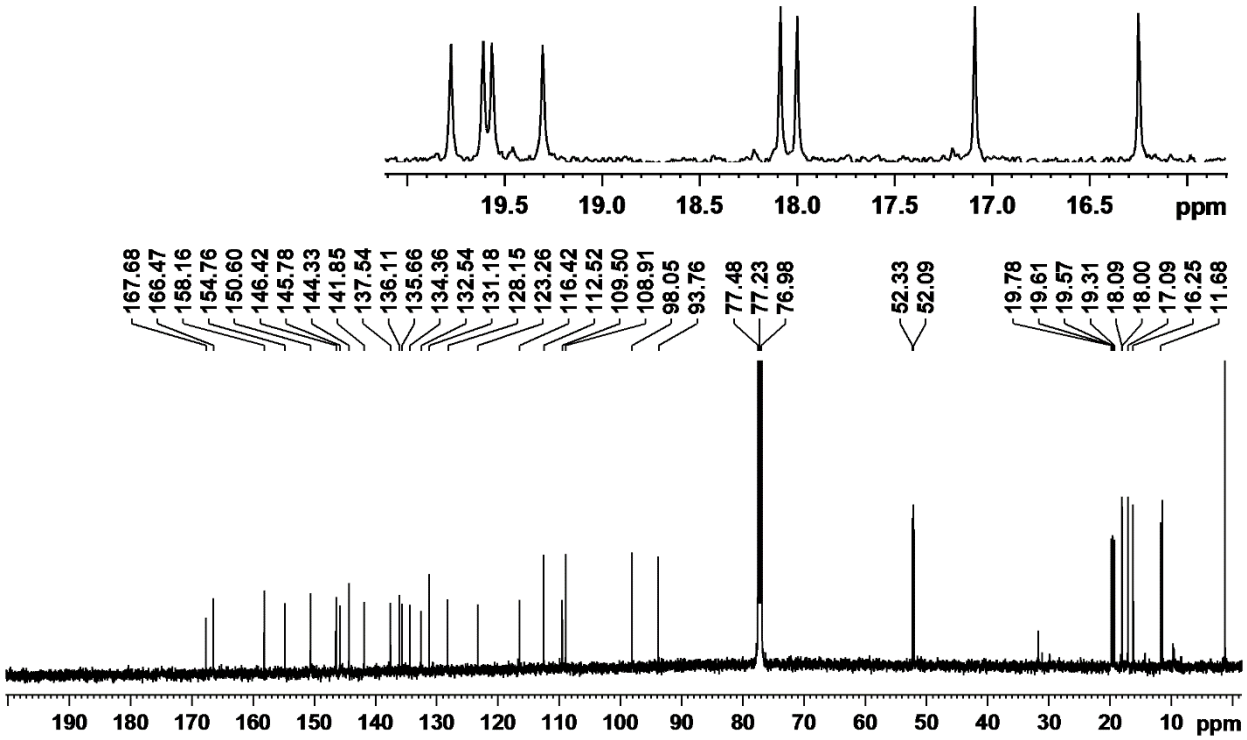

Figure A – 26: 125 MHz carbon-13 NMR spectrum of **121** in $CDCl_3$

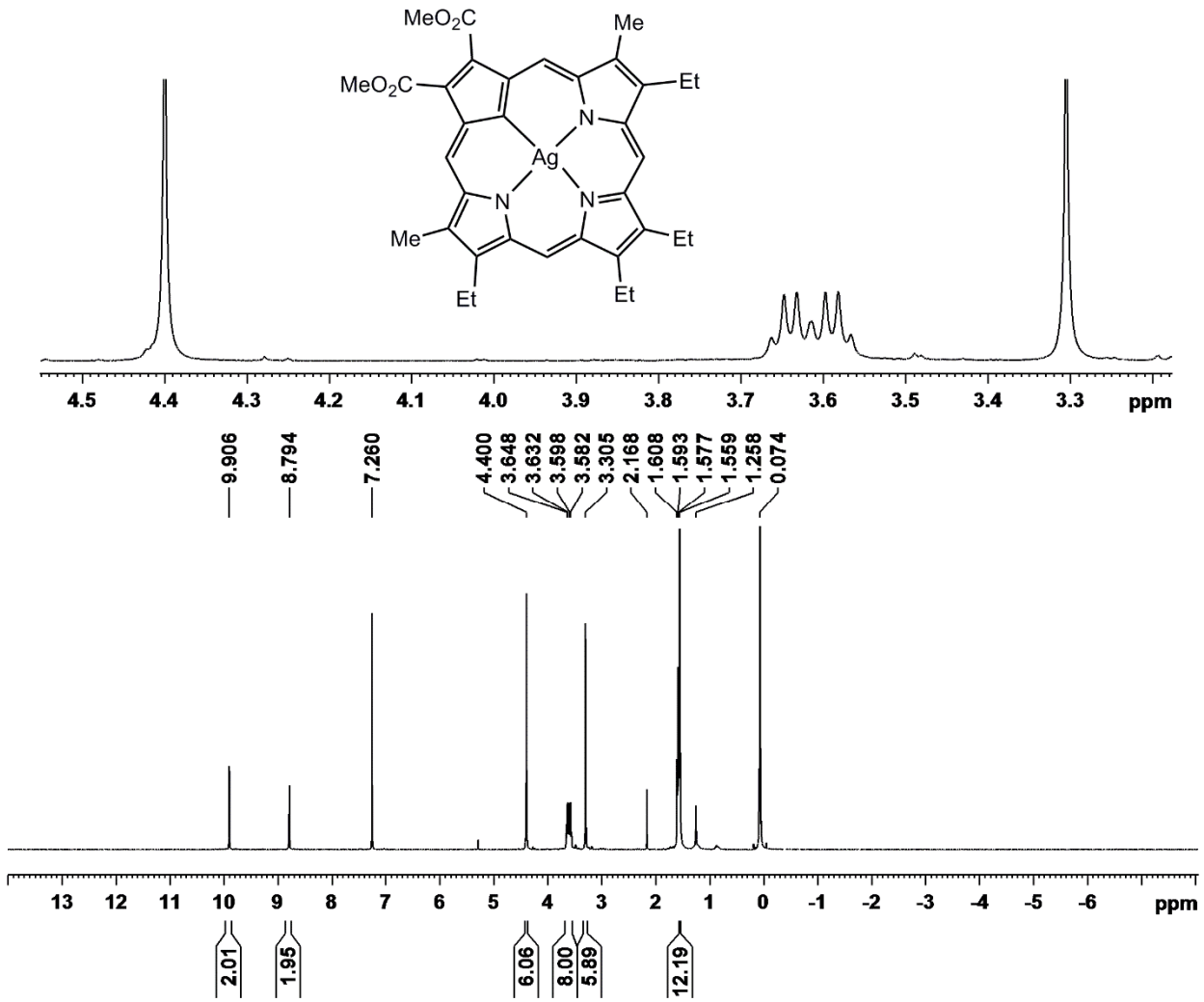

Figure A – 27: 500 MHz ^{1}H NMR Spectrum of **118** in $CDCl_3$

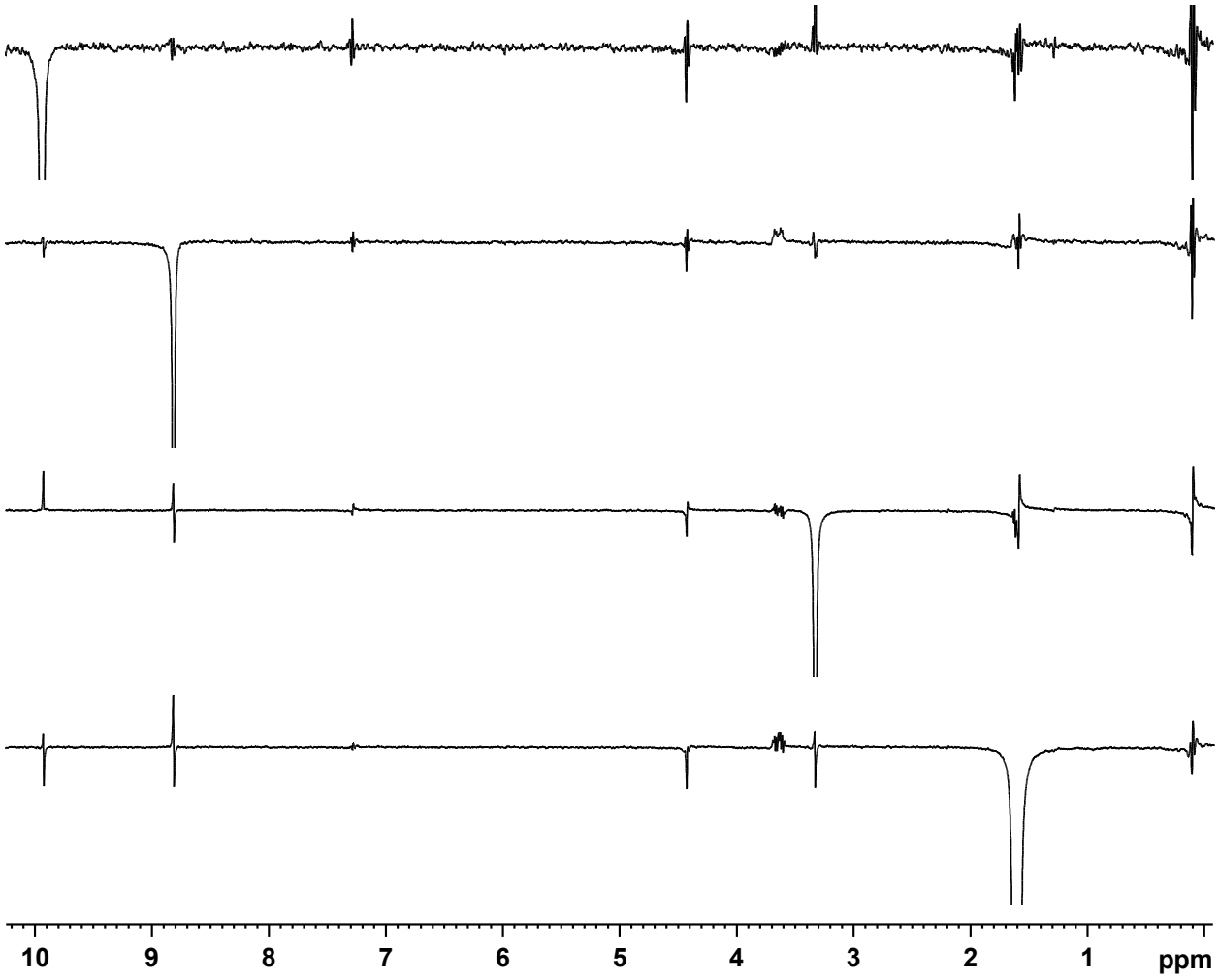

Figure A – 28: Selected nOe difference proton NMR spectra of **118** in $CDCl_3$

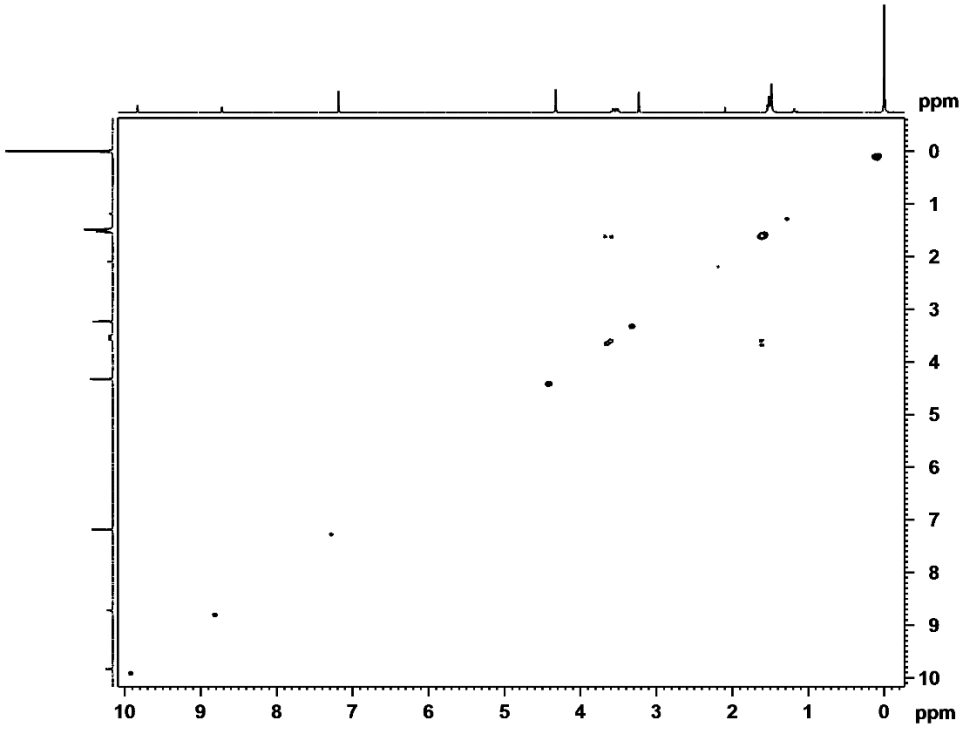

Figure A – 29: ^{1}H-^{1}H COSY NMR spectrum of **118** in $CDCl_3$

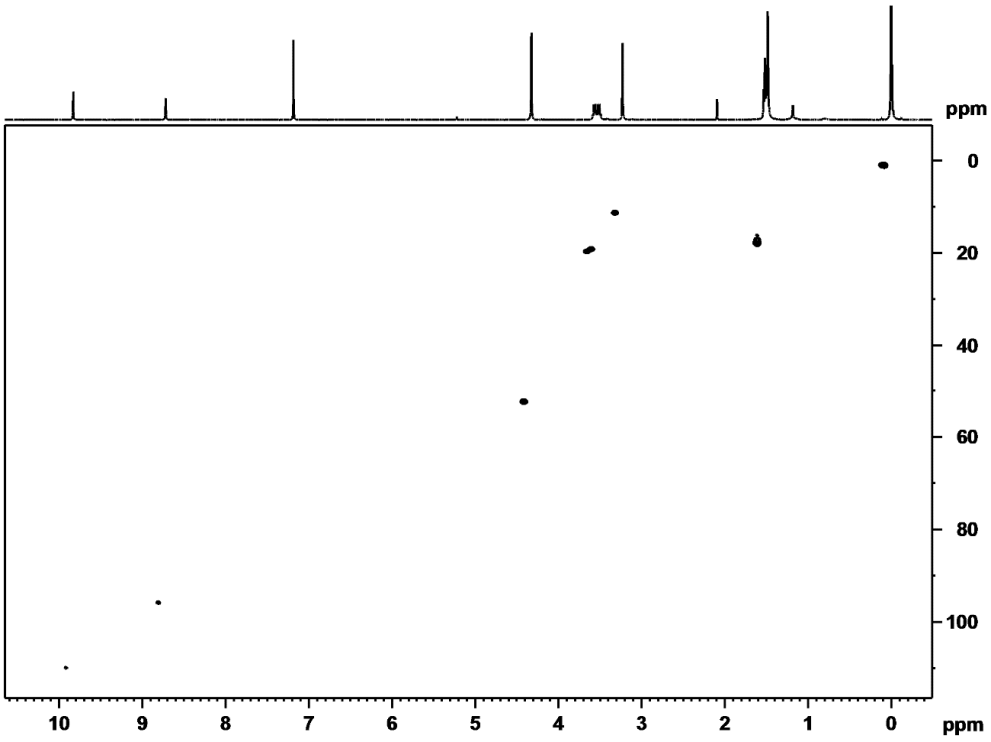

Figure A – 30: HSQC NMR spectrum of **118** in $CDCl_3$

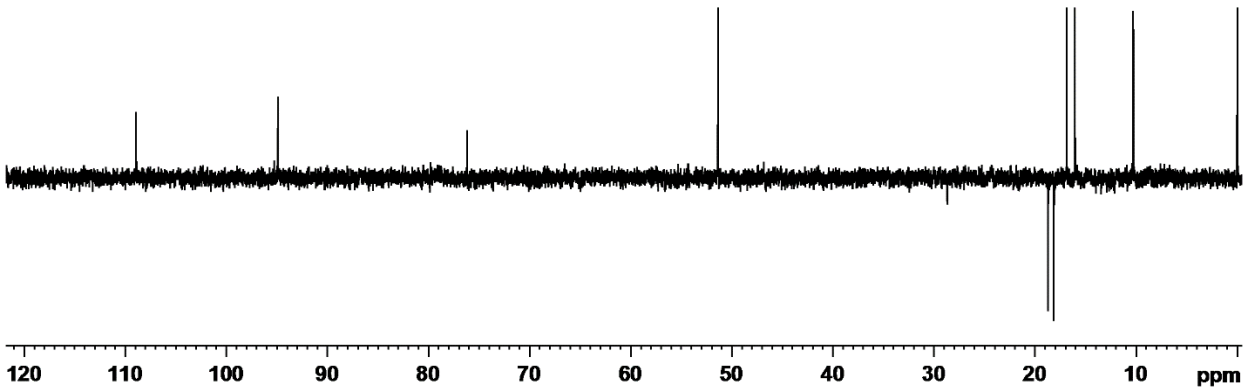

Figure A – 31: DEPT-135 NMR spectrum of **118** in $CDCl_3$

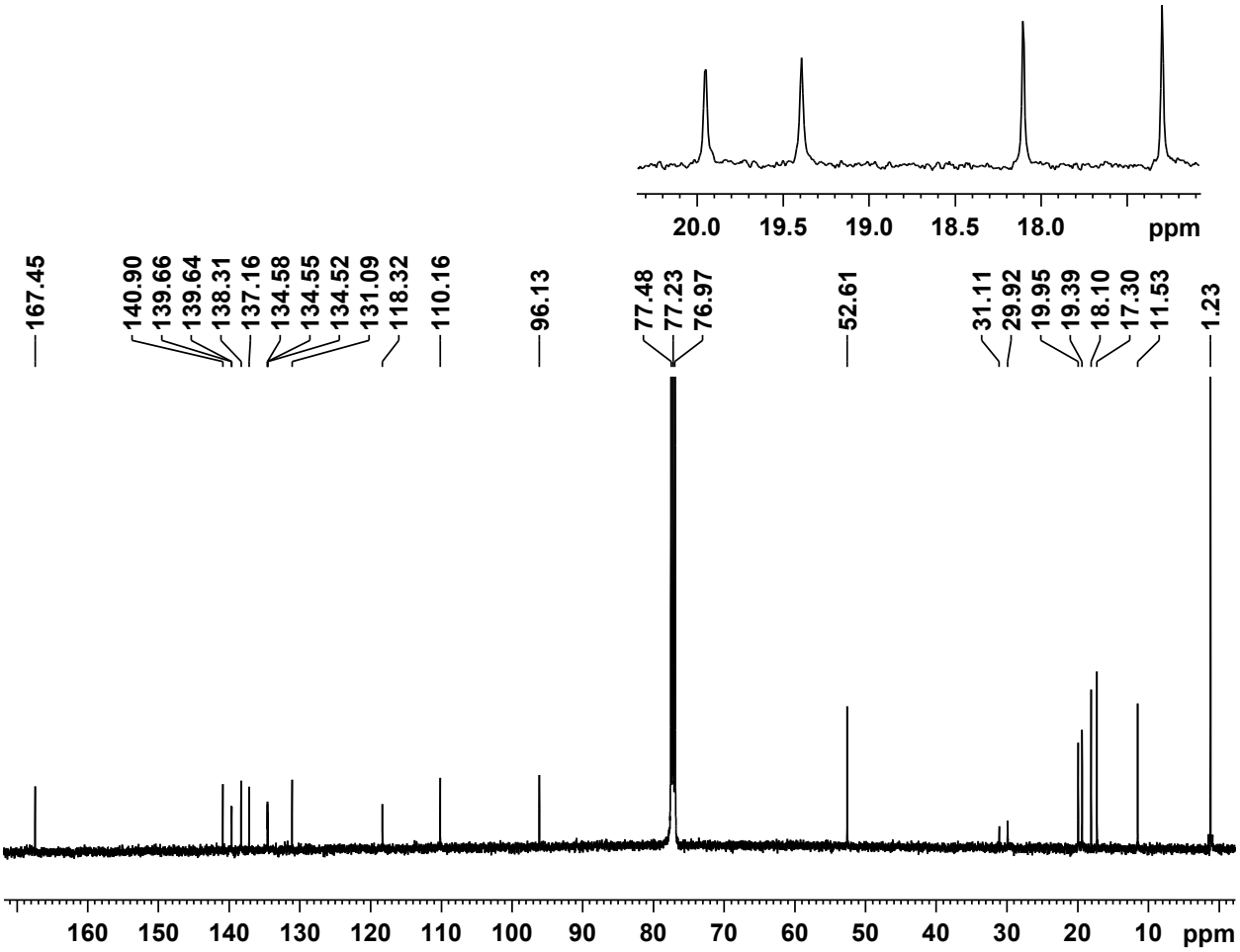

Figure A – 32: 125 MHz carbon-13 NMR spectrum of **118** in $CDCl_3$

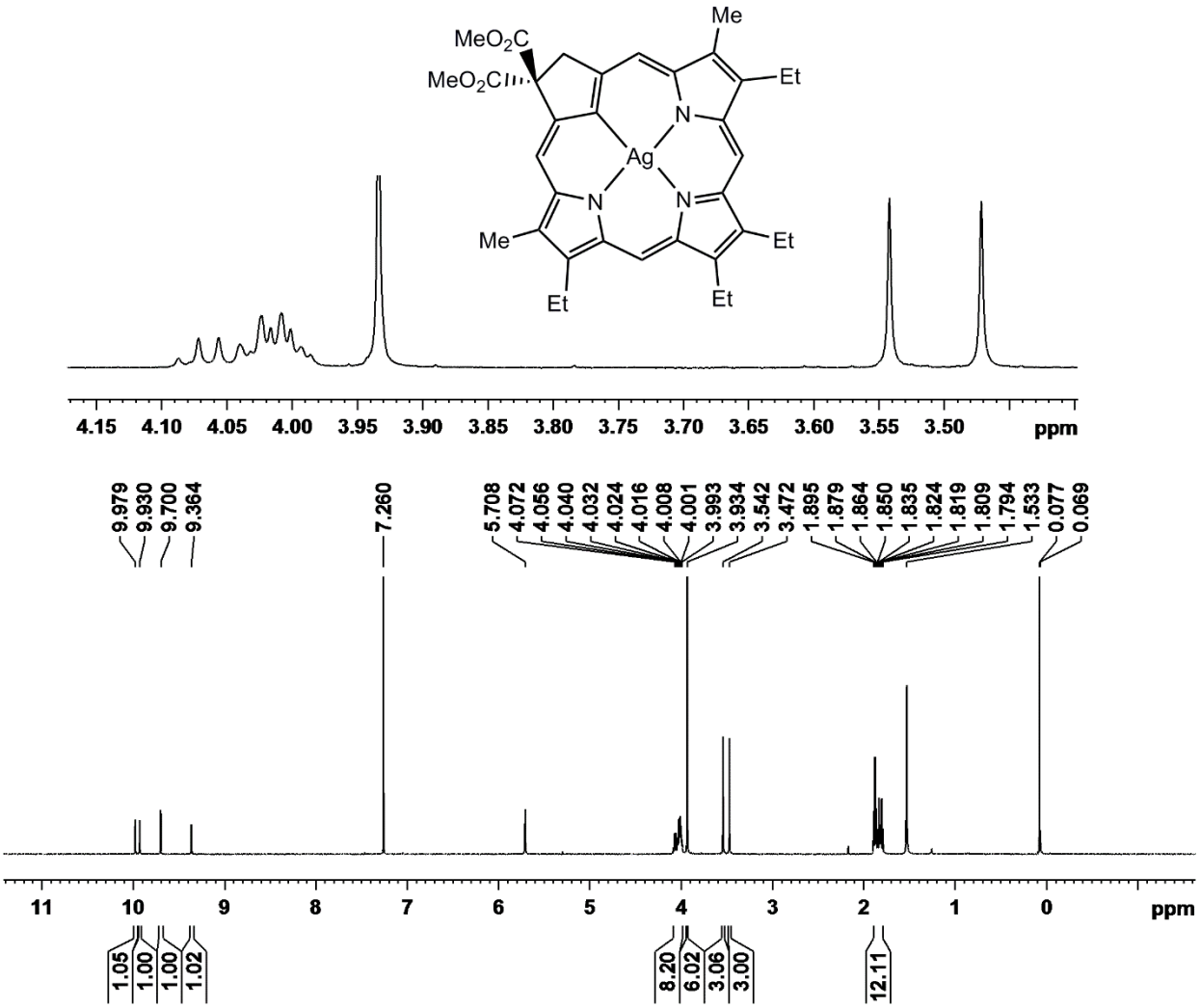

Figure A – 33: 500 MHz ^{1}H NMR Spectrum of **138** in $CDCl_3$

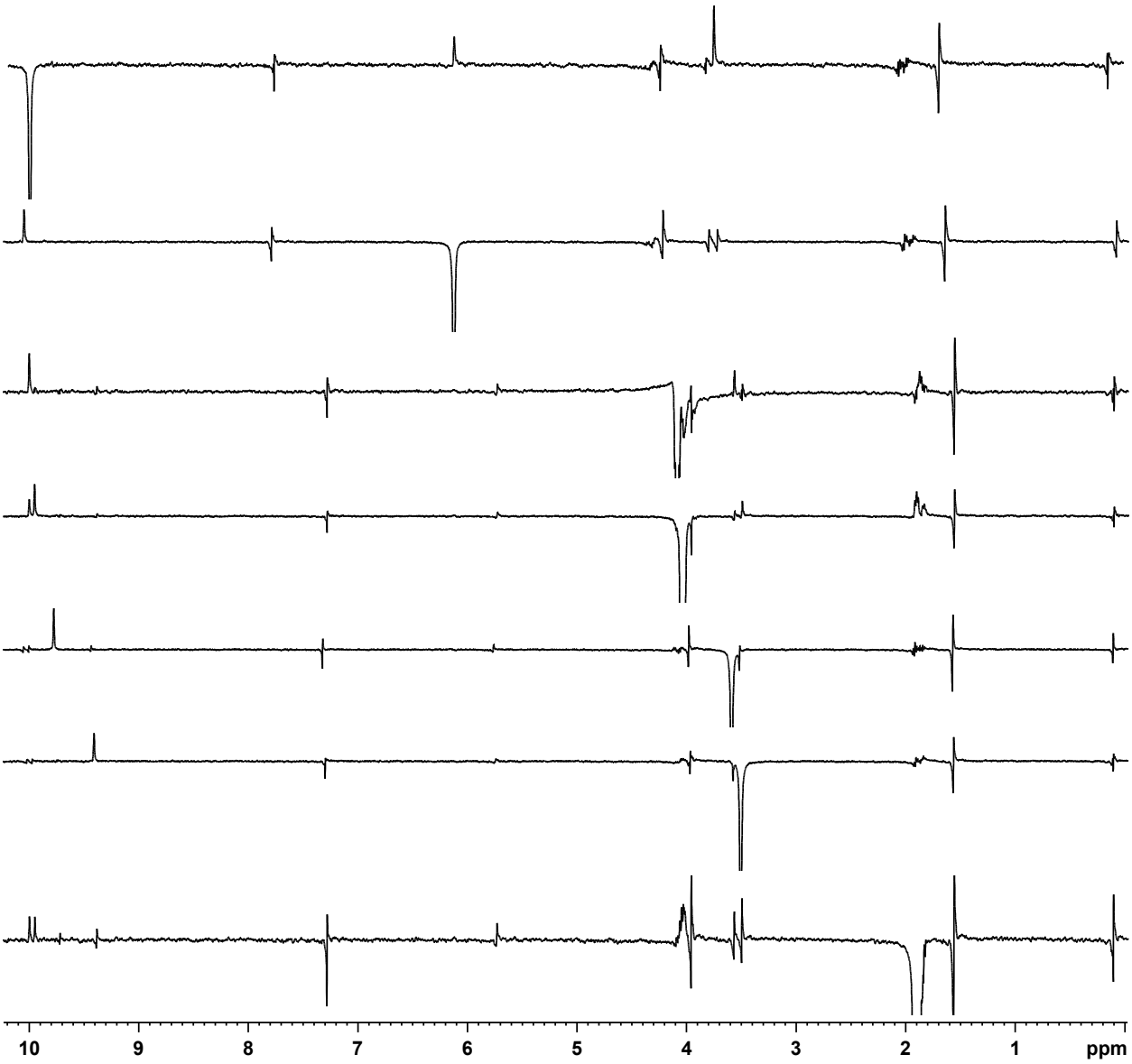

Figure A – 34: Selected nOe difference proton NMR spectra of **138** in $CDCl_3$

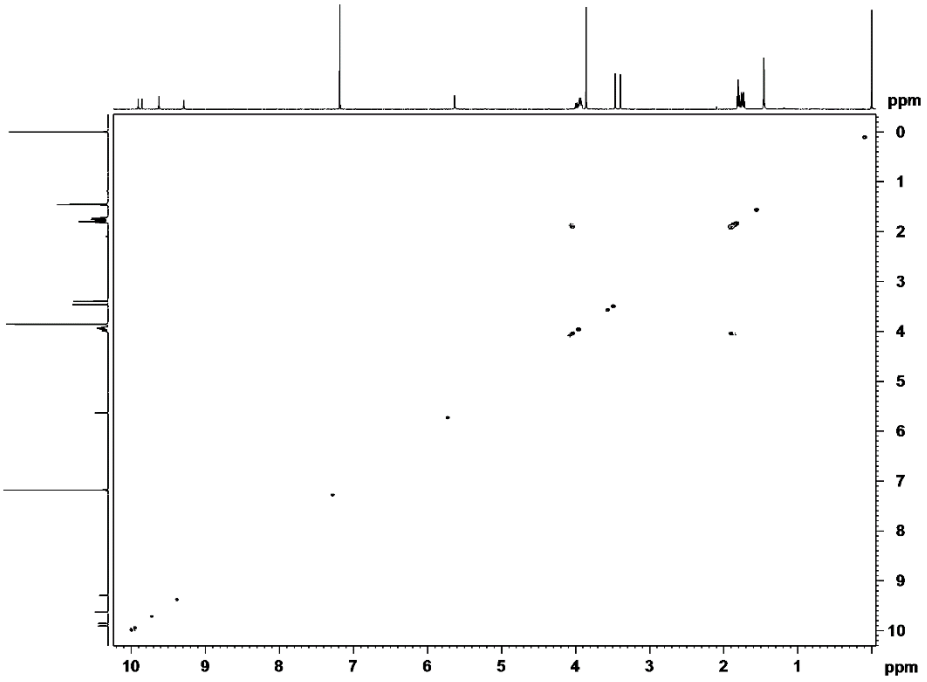

Figure A – 35: ^{1}H-^{1}H COSY NMR spectrum of **138** in $CDCl_3$

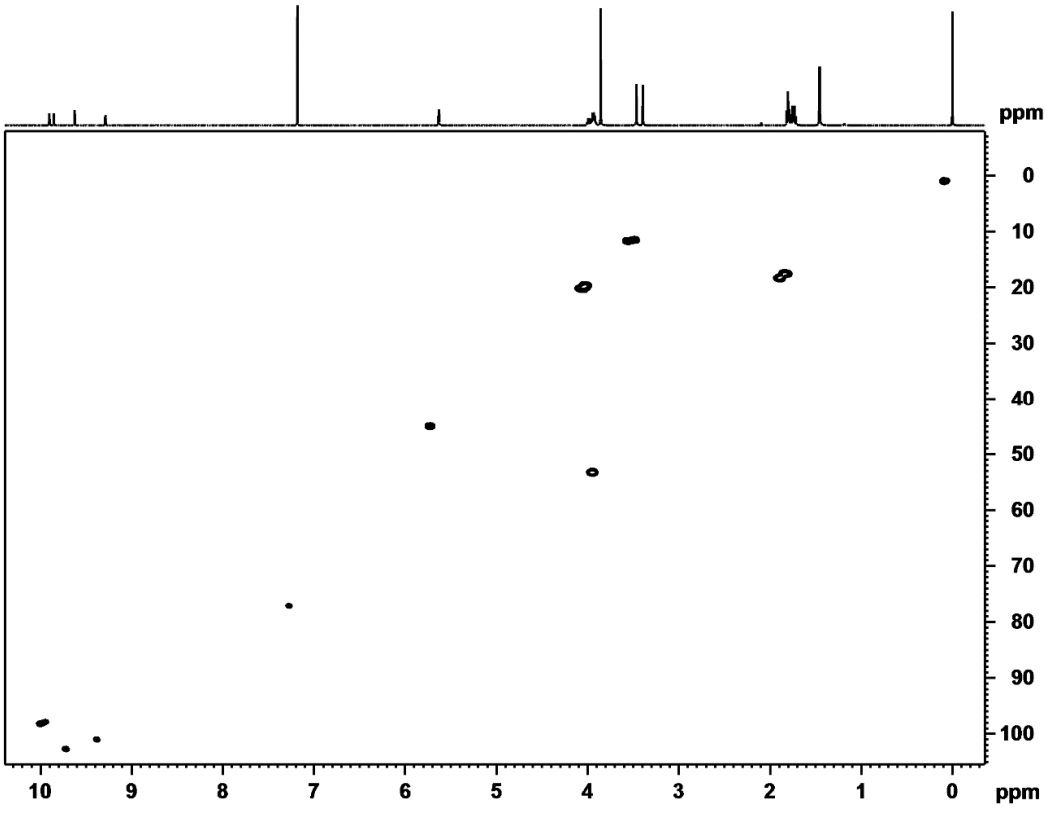

Figure A – 36: HSQC NMR spectrum of **138** in $CDCl_3$

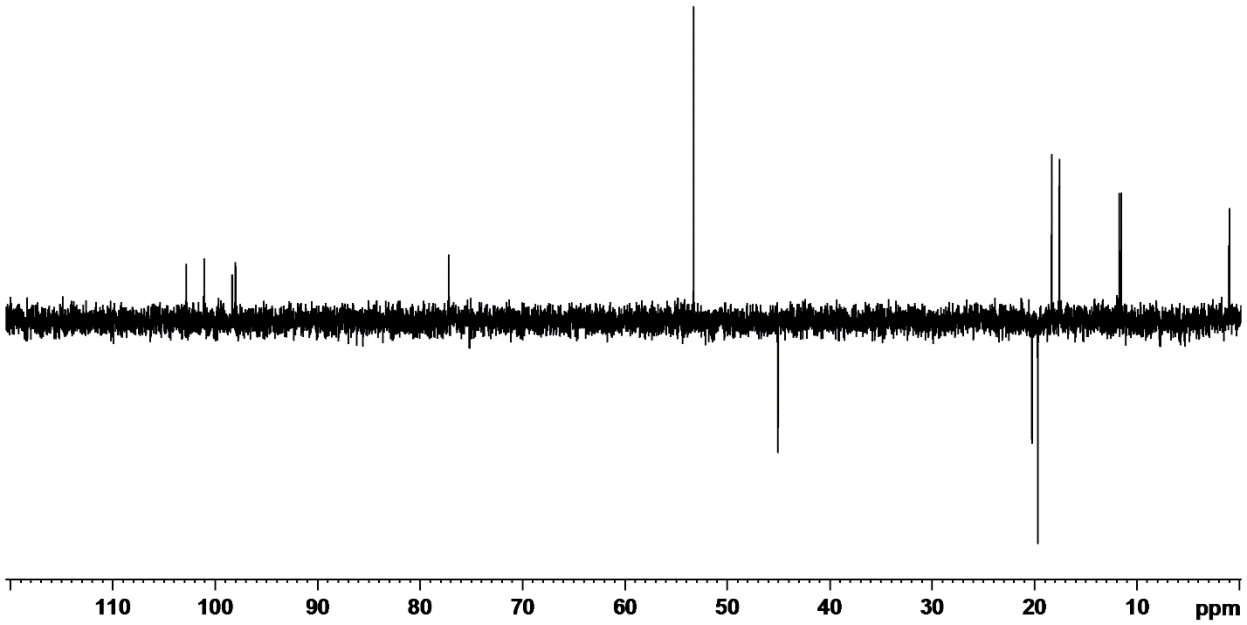

Figure A – 37: DEPT-135 NMR spectrum of **138** in $CDCl_3$

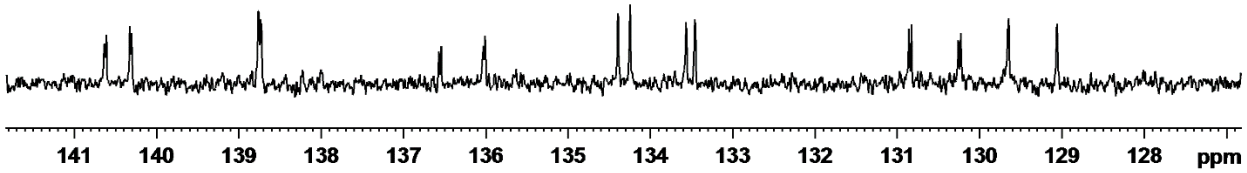

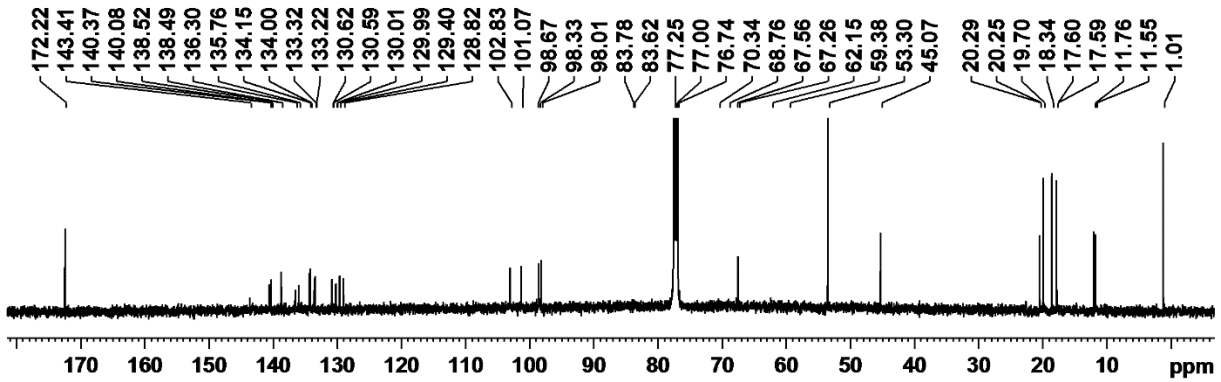

Figure A – 38: 125 MHz carbon-13 NMR spectrum of **138** in $CDCl_3$

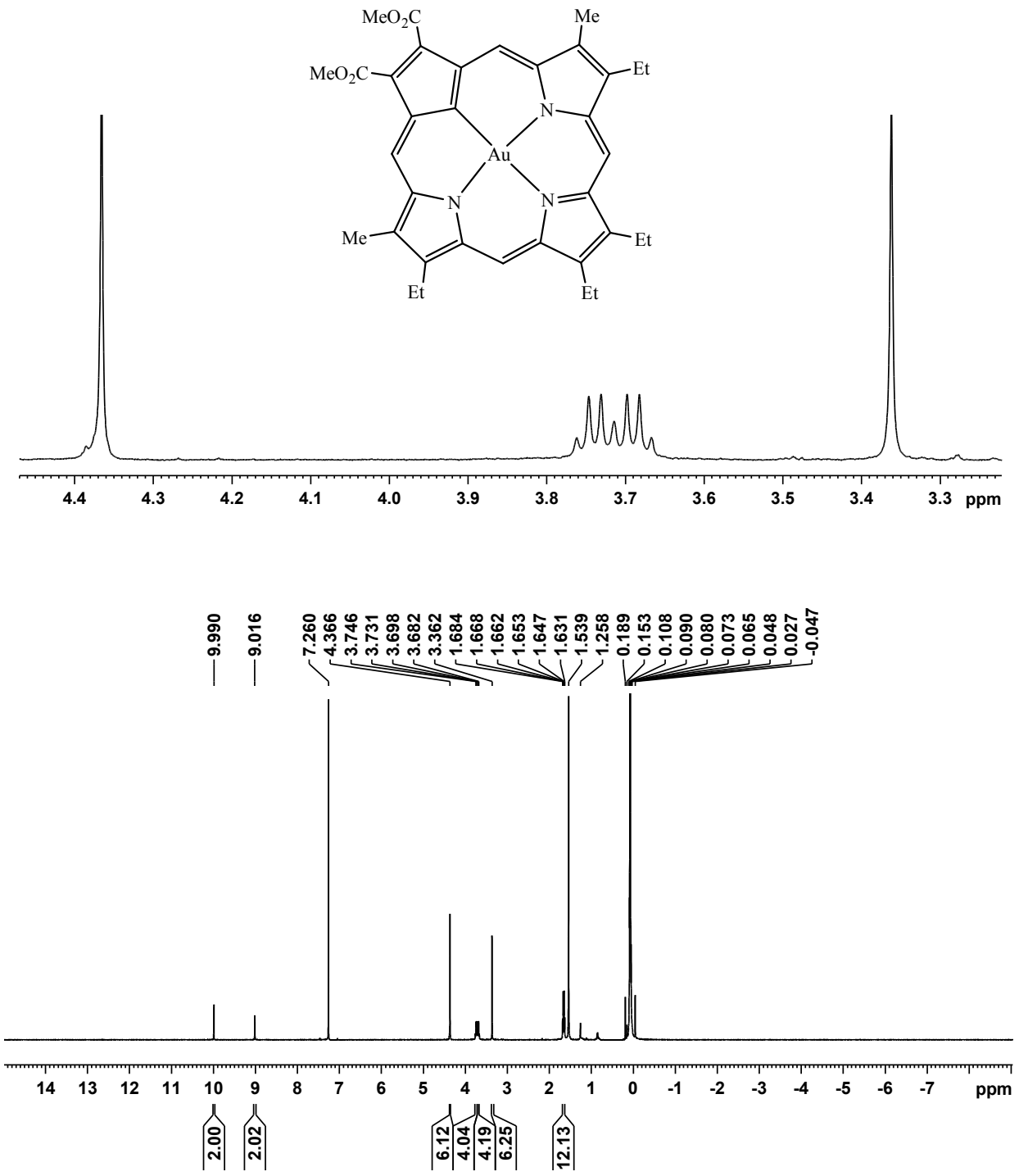

Figure A – 39: 500 MHz ^{1}H NMR Spectrum of **119** in $CDCl_3$

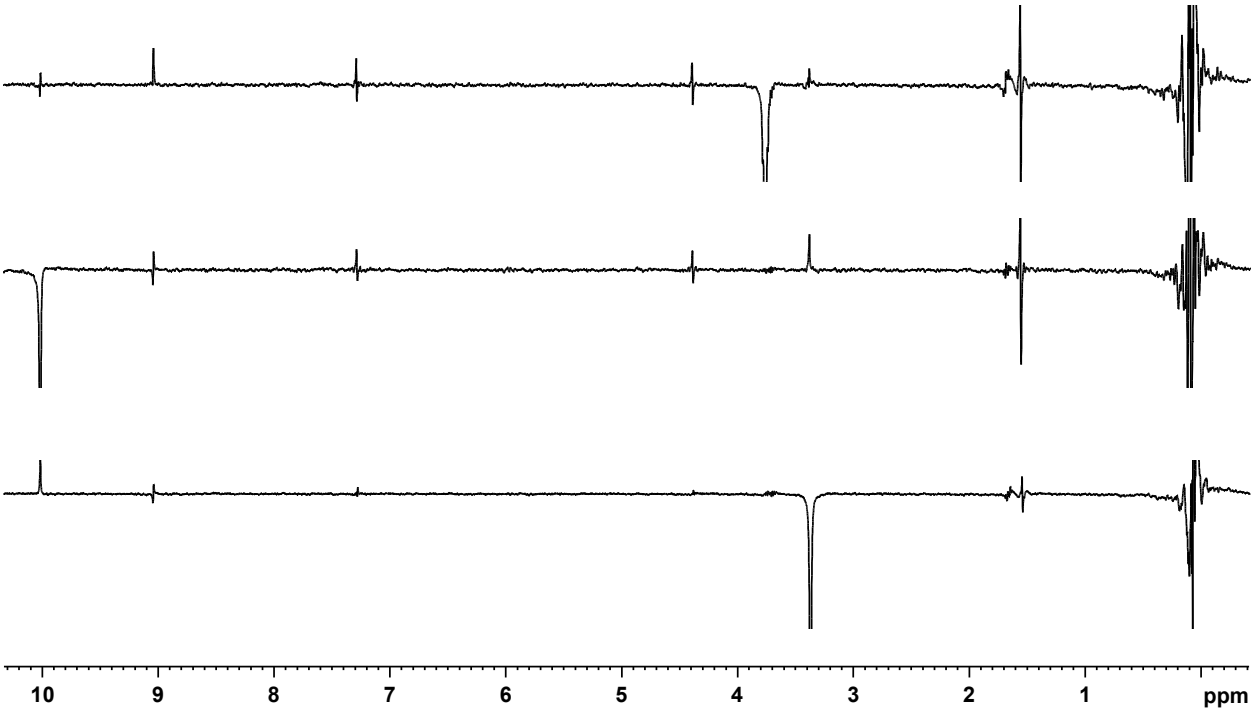

Figure A – 40: Selected nOe difference proton NMR spectra of **119** in $CDCl_3$

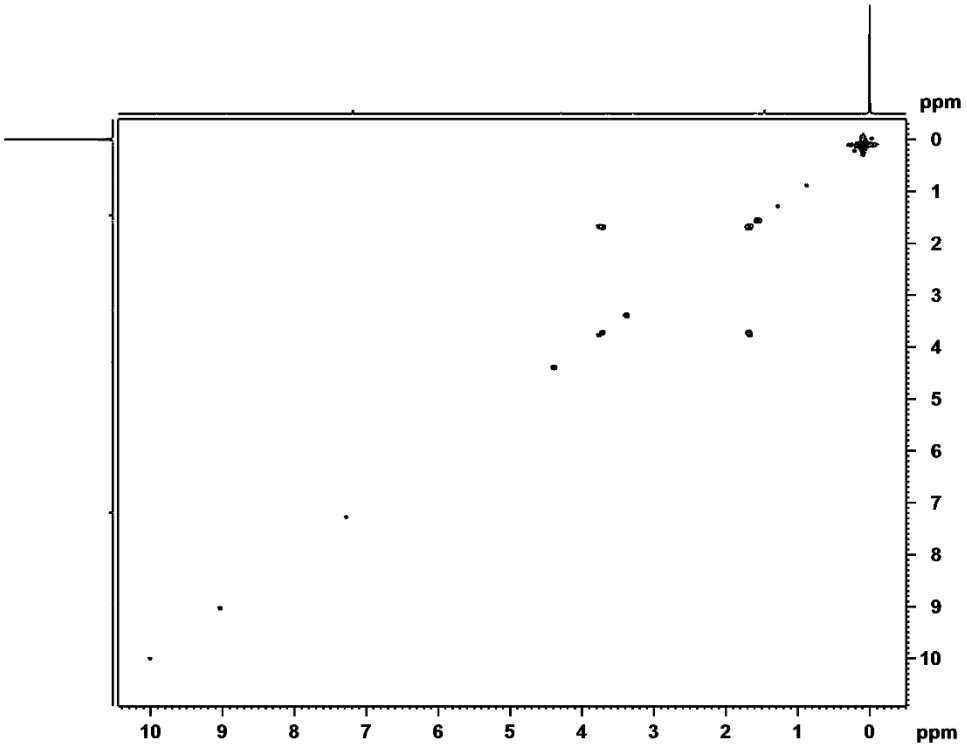

Figure A – 41: ^{1}H-^{1}H COSY NMR spectrum of **119** in $CDCl_3$

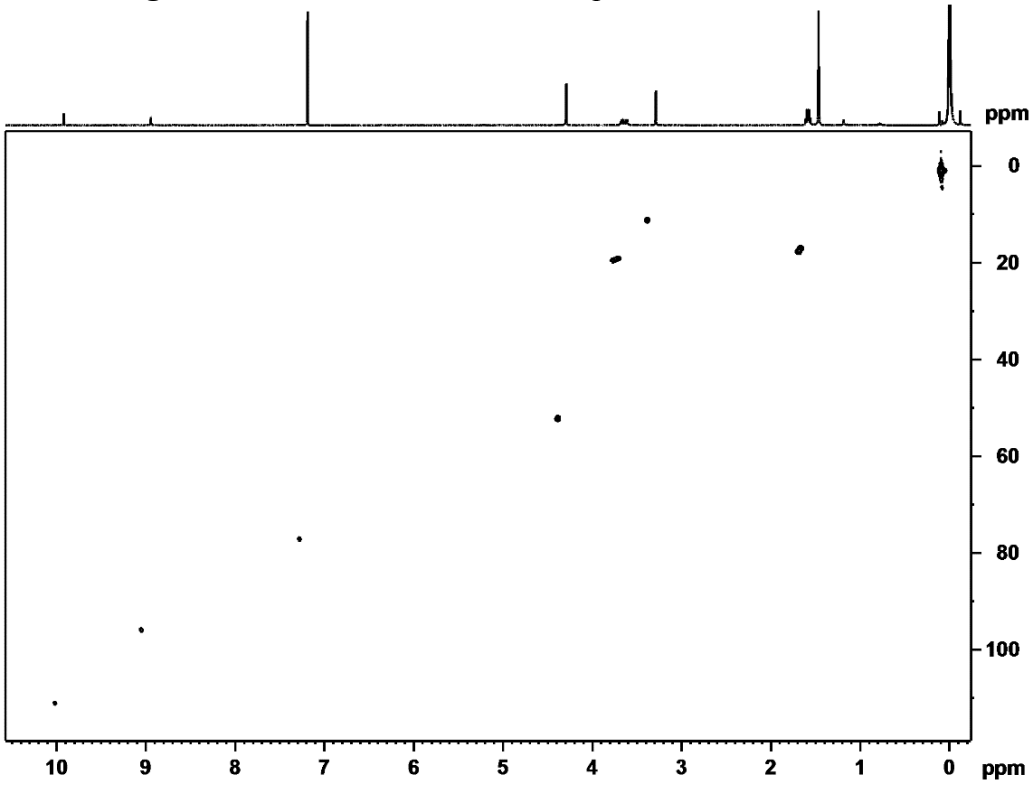

Figure A – 42: HSQC NMR spectrum of **119** in $CDCl_3$

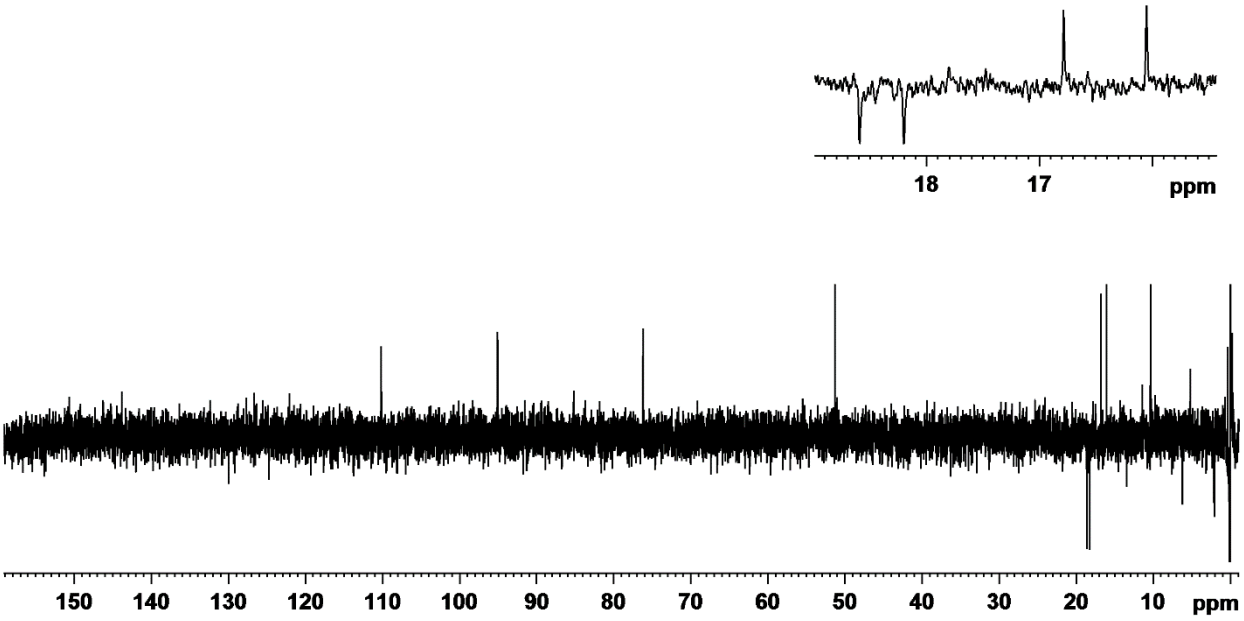

Figure A – 43: DEPT-135 NMR spectrum of **119** in $CDCl_3$

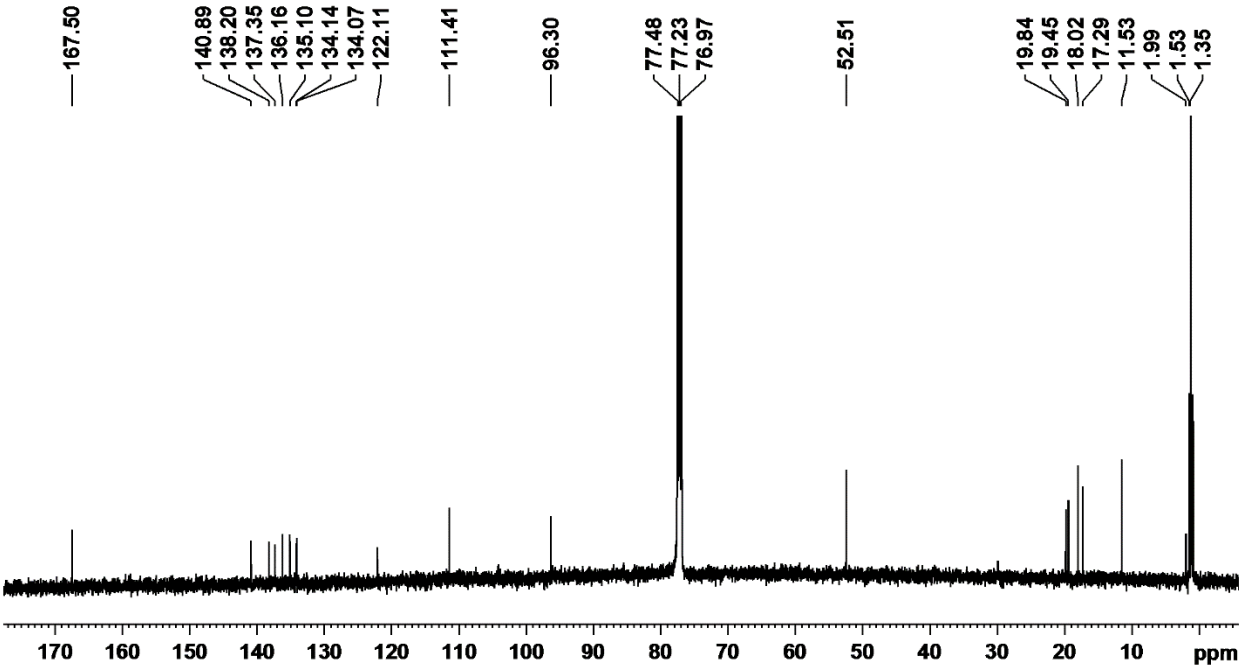

Figure A – 44: 125 MHz carbon-13 NMR spectrum of **119** in $CDCl_3$

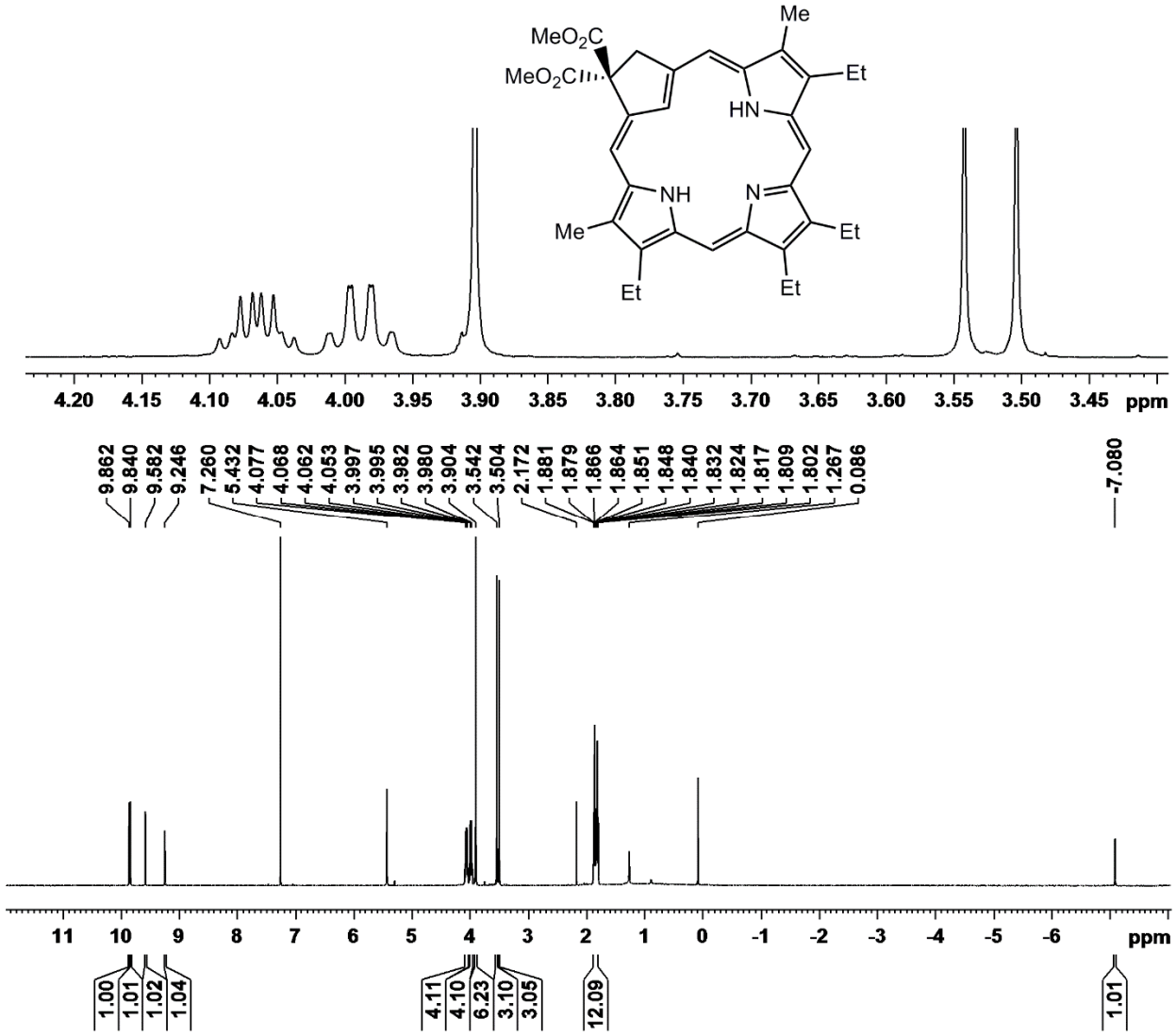

Figure A – 45: 500 MHz ^{1}H NMR Spectrum of **133** in $CDCl_3$

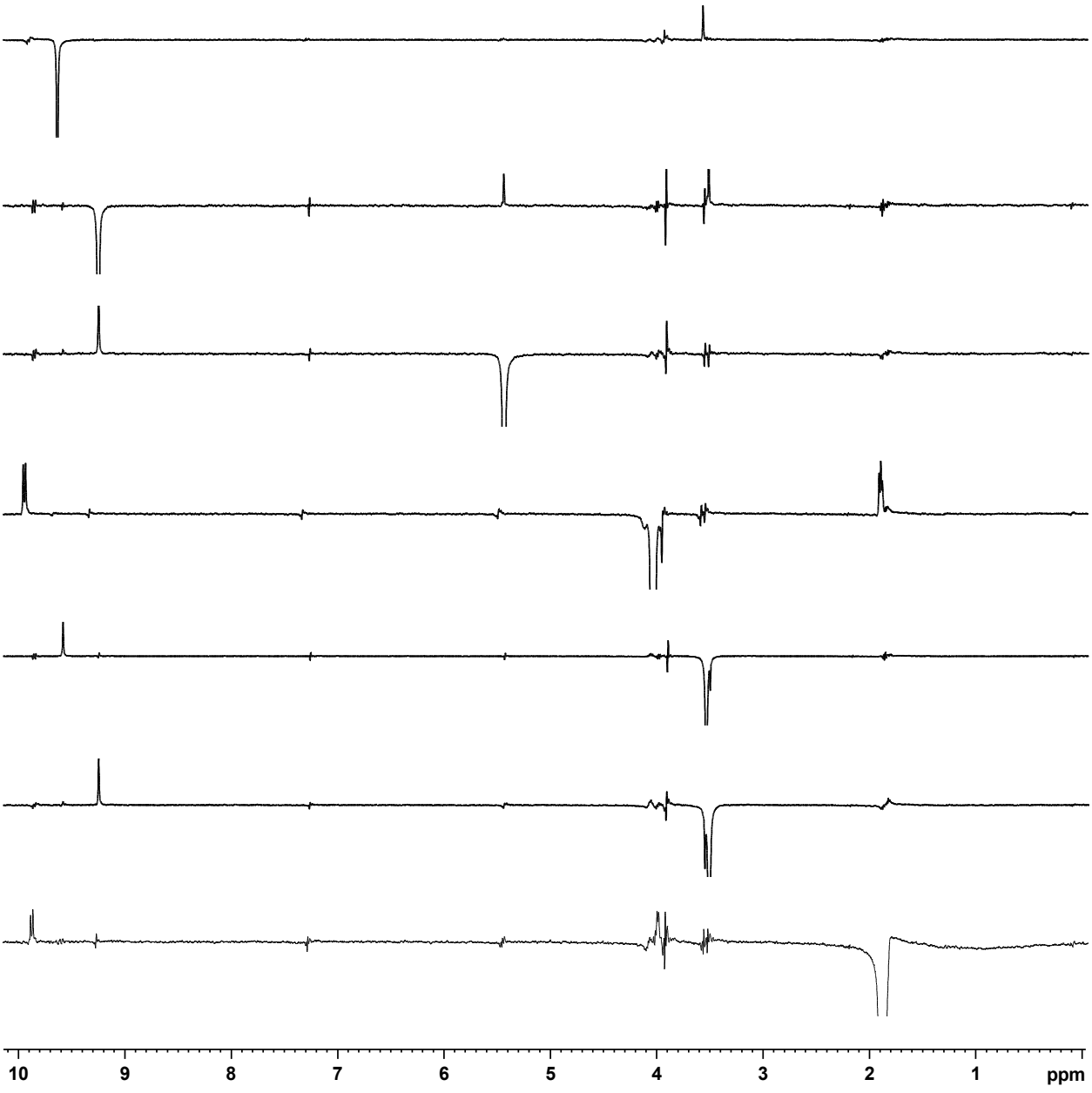

Figure A – 46: Selected nOe difference proton NMR spectra of **133** in $CDCl_3$

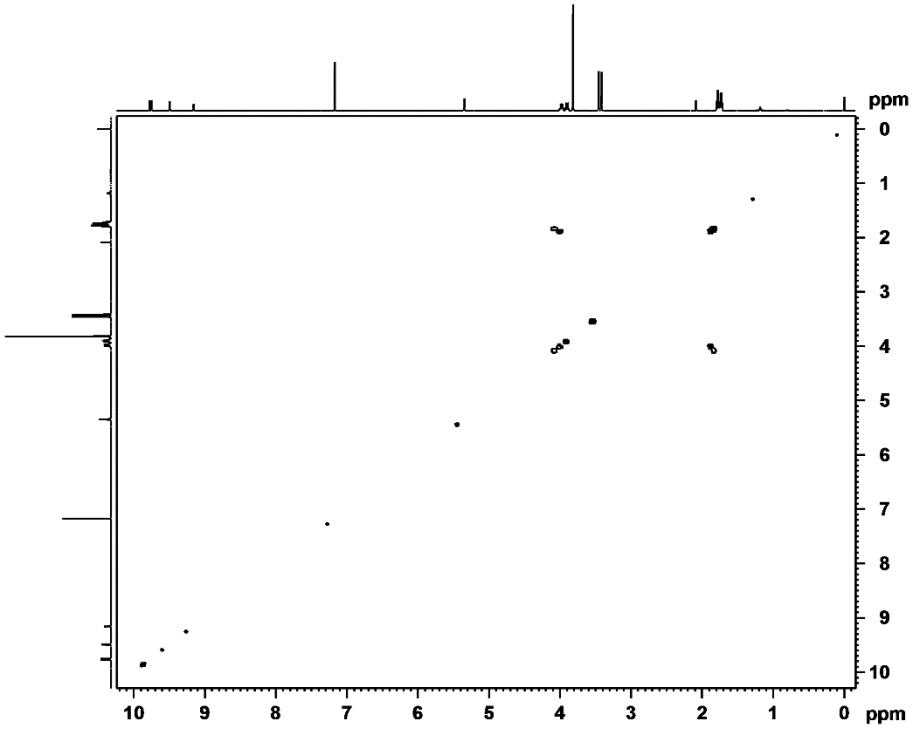

Figure A – 47: ^{1}H-^{1}H COSY NMR spectrum of **133** in $CDCl_3$

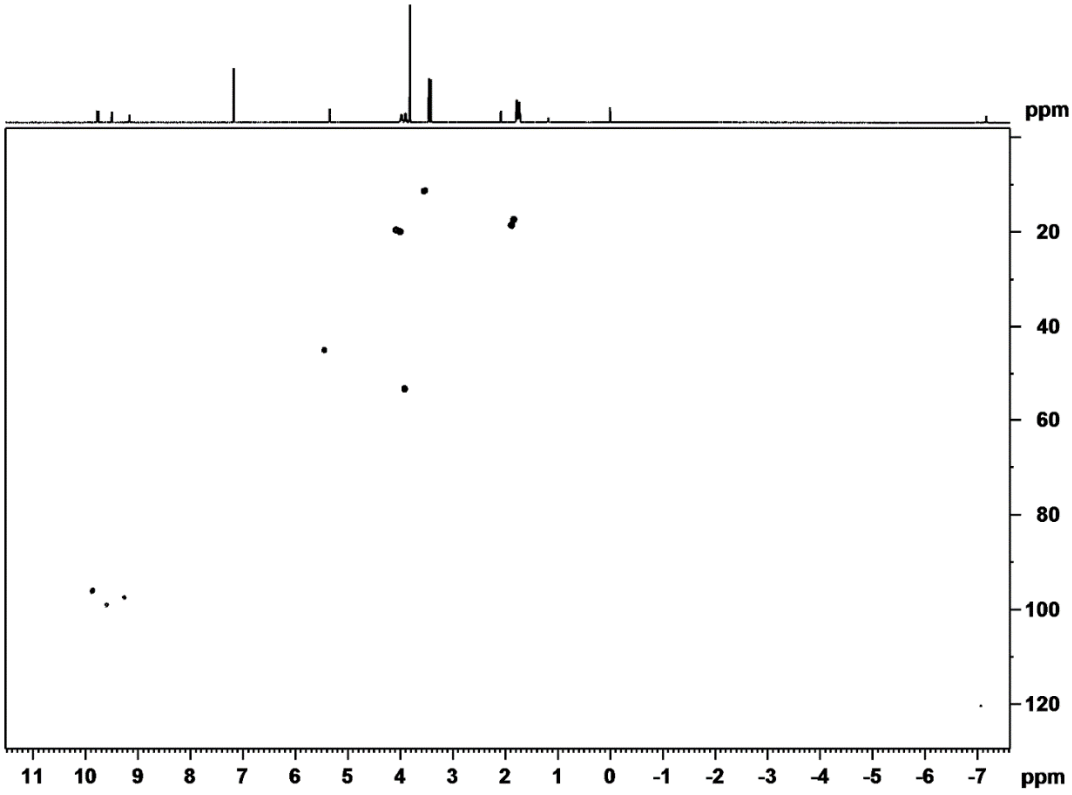

Figure A – 48: HSQC NMR spectrum of **133** in $CDCl_3$

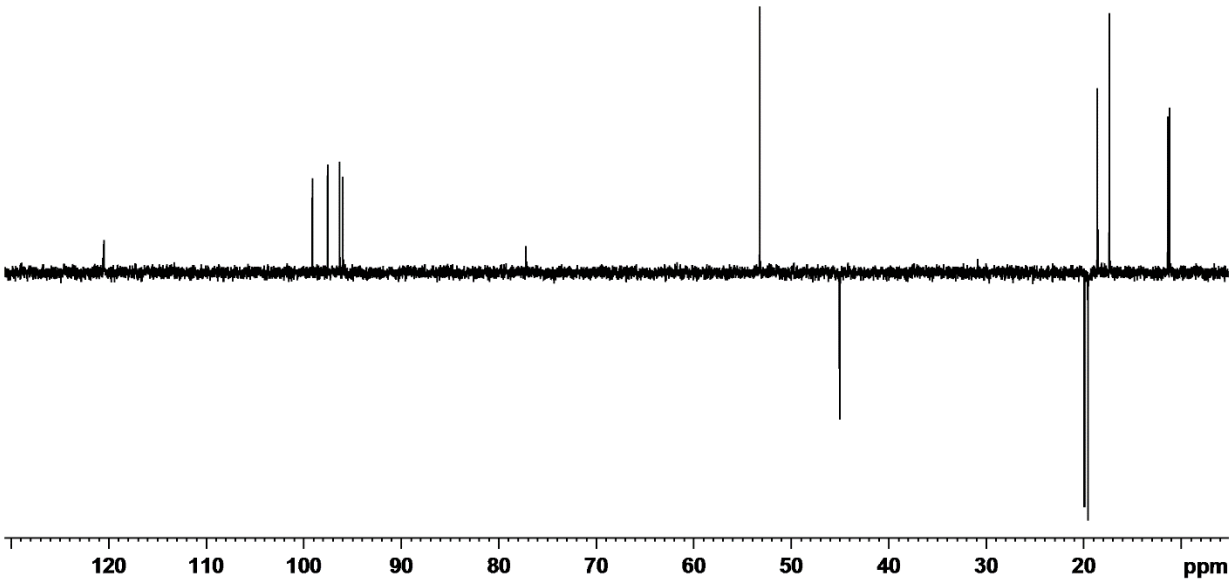

Figure A – 49: DEPT-135 NMR spectrum of **133** in $CDCl_3$

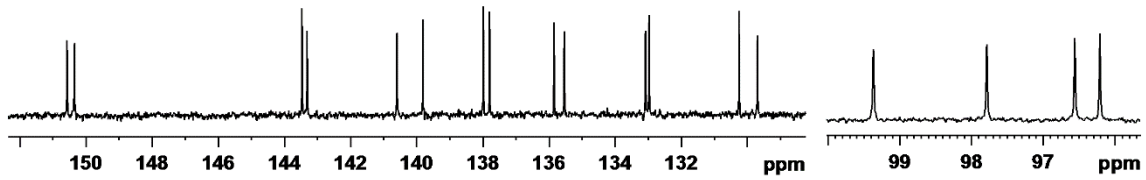

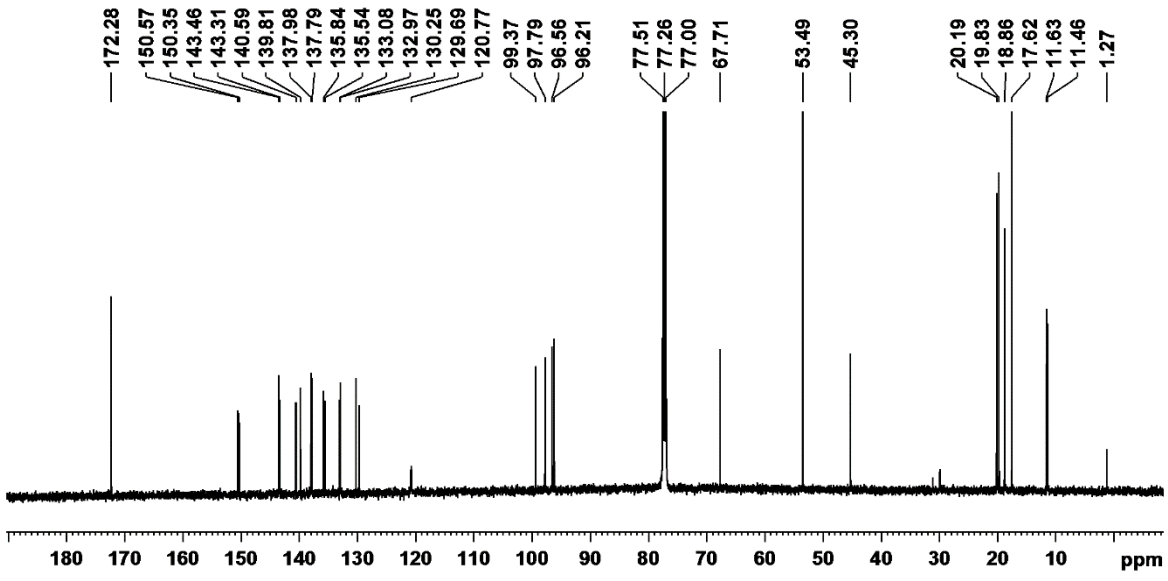

Figure A – 50: 125 MHz carbon-13 NMR spectrum of **133** in $CDCl_3$

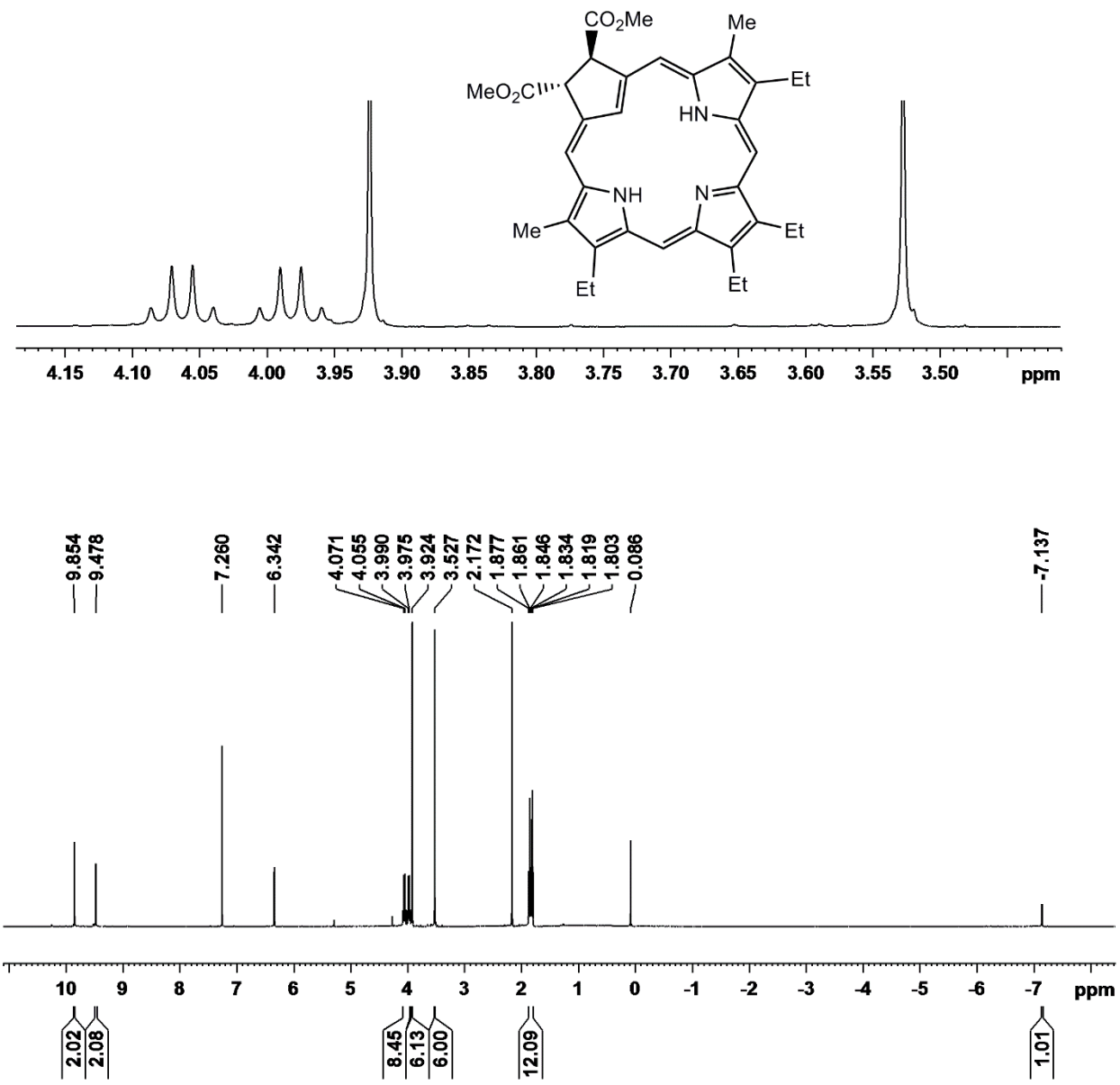

Figure A – 51: 500 MHz ^{1}H NMR Spectrum of **117** in $CDCl_3$

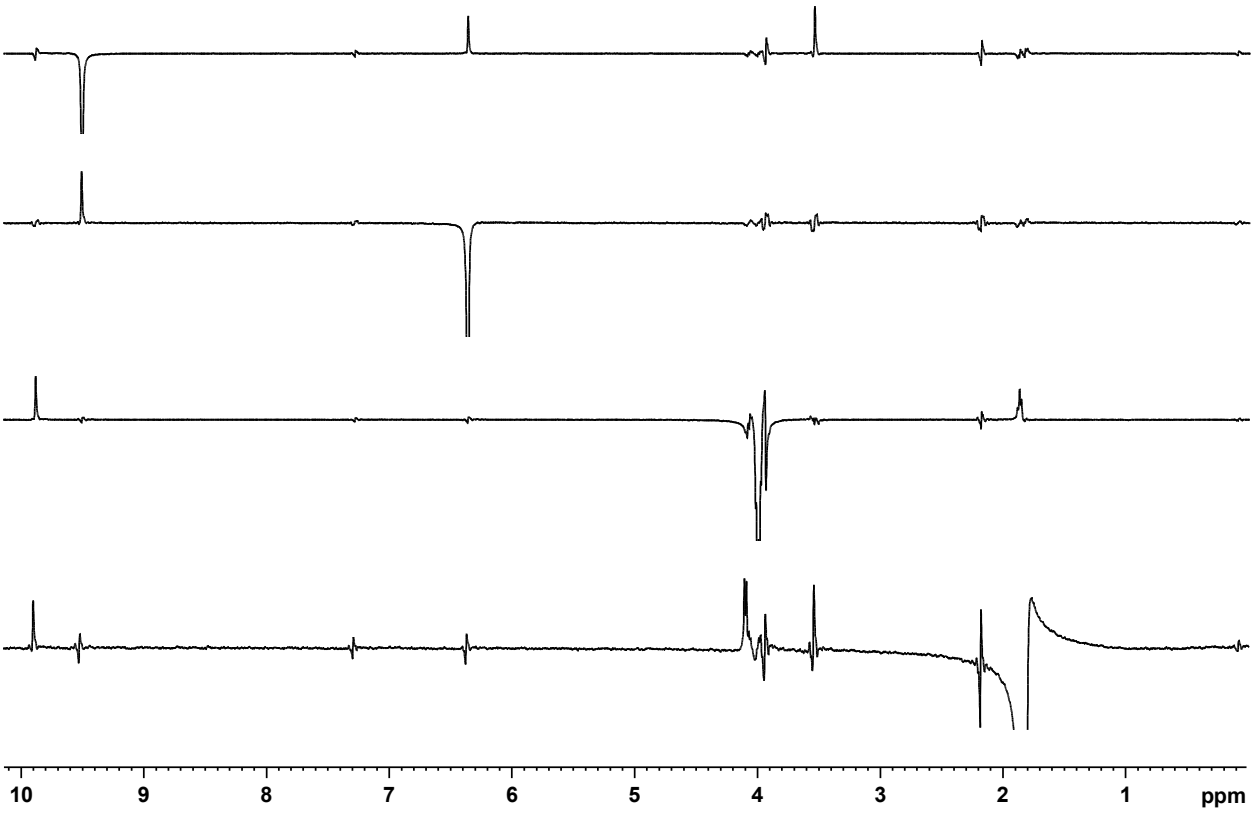

Figure A – 52: Selected nOe difference proton NMR spectra of **117** in $CDCl_3$

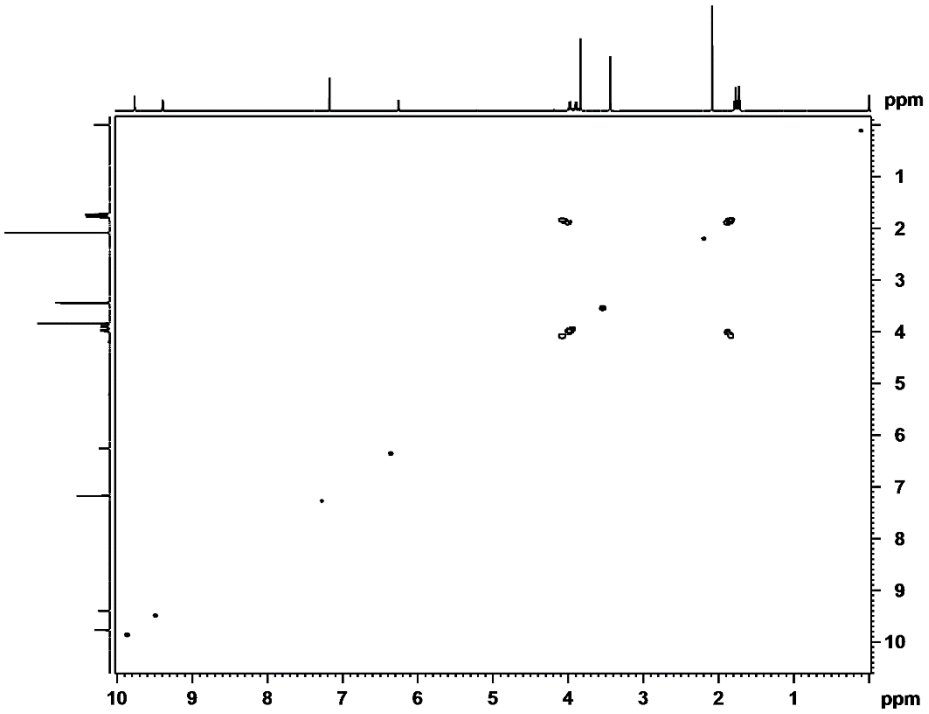

Figure A – 53: ^{1}H-^{1}H COSY NMR spectrum of **117** in $CDCl_3$

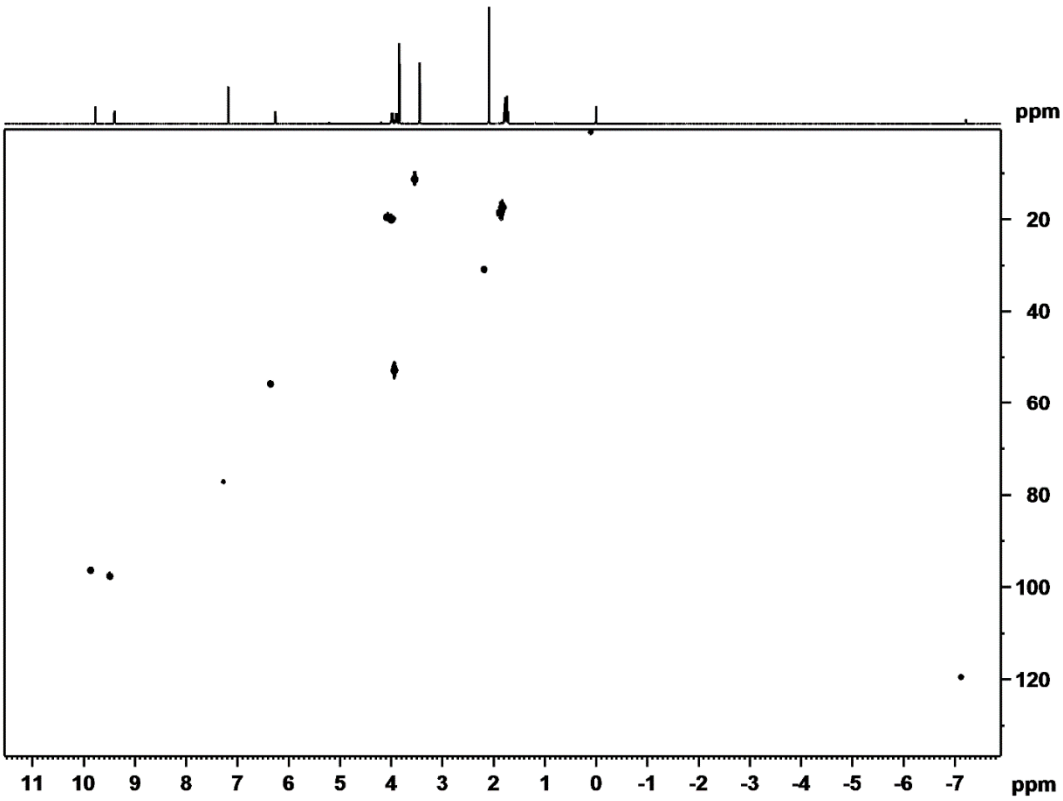

Figure A – 54: HSQC NMR spectrum of **117** in $CDCl_3$

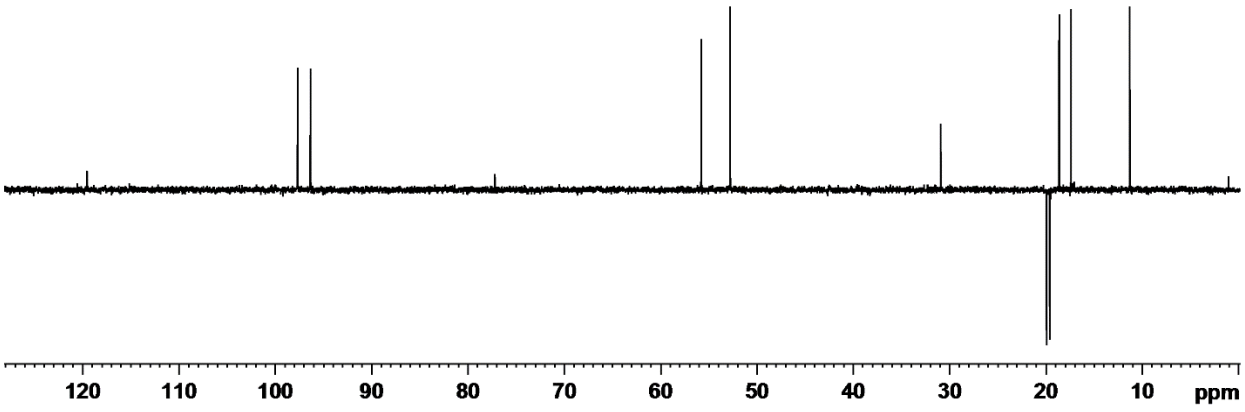

Figure A – 55: DEPT-135 NMR spectrum of **117** in $CDCl_3$

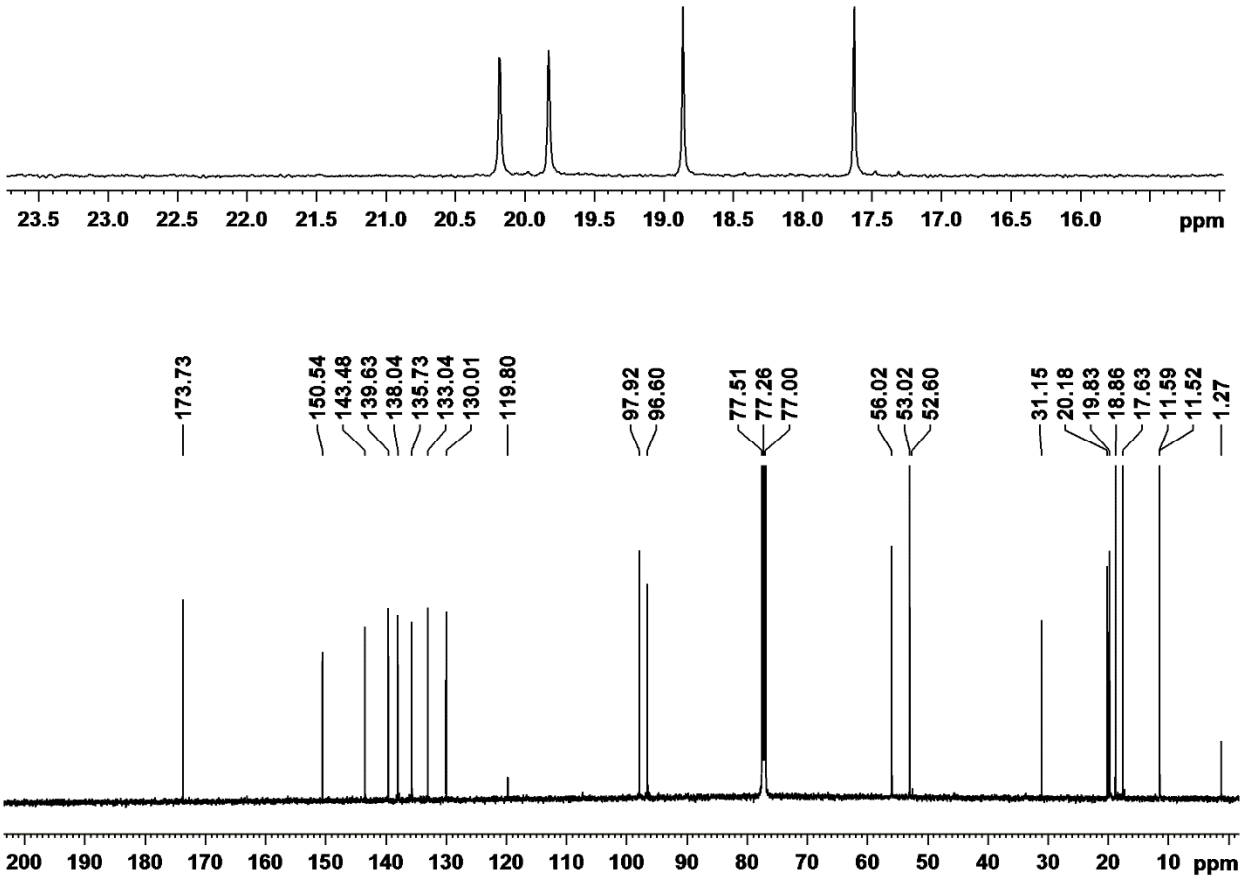

Figure A – 56: 125 MHz carbon-13 NMR spectrum of **117** in $CDCl_3$

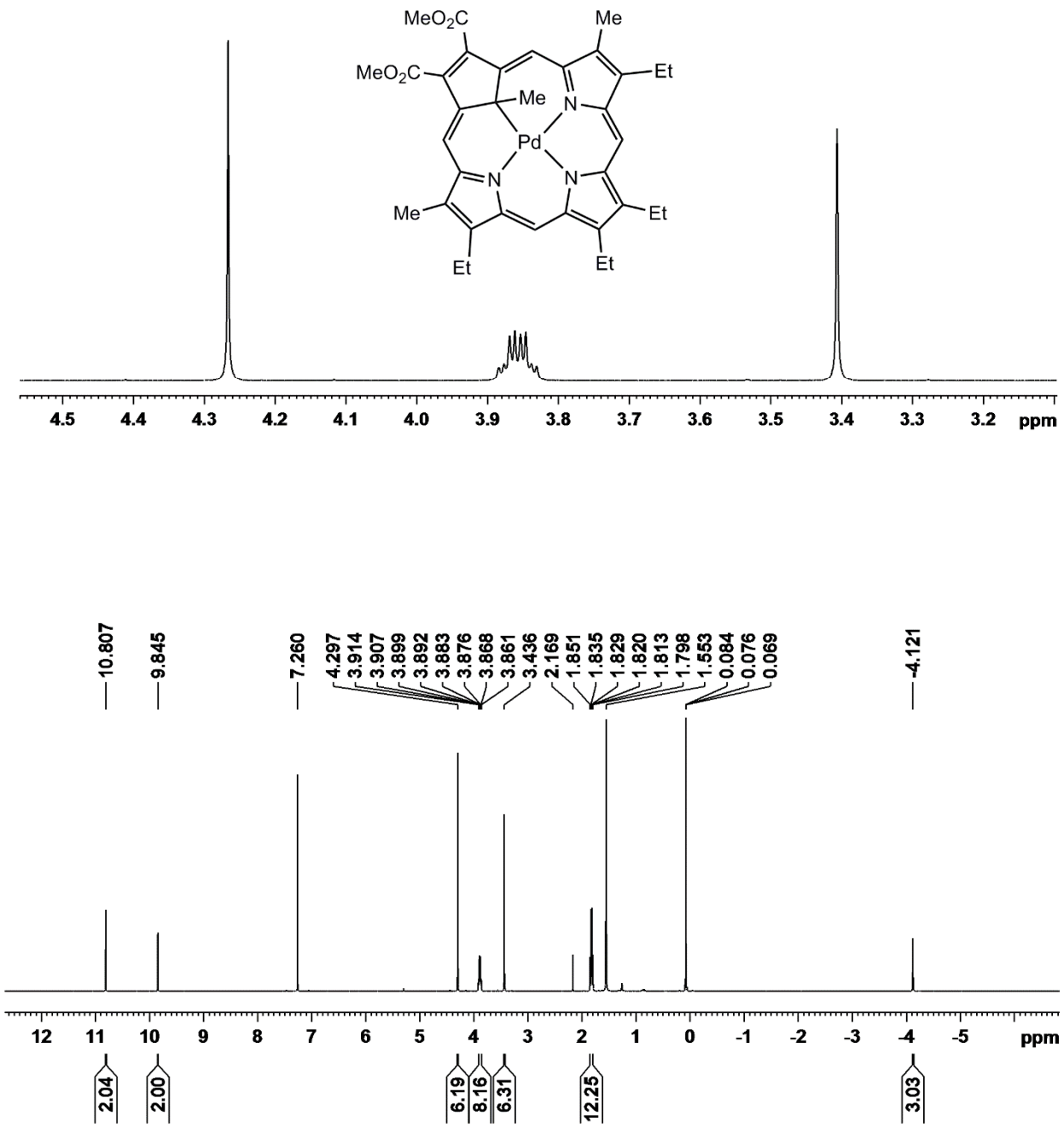

Figure A – 57: 500 MHz ^{1}H NMR Spectrum of **122** in $CDCl_3$

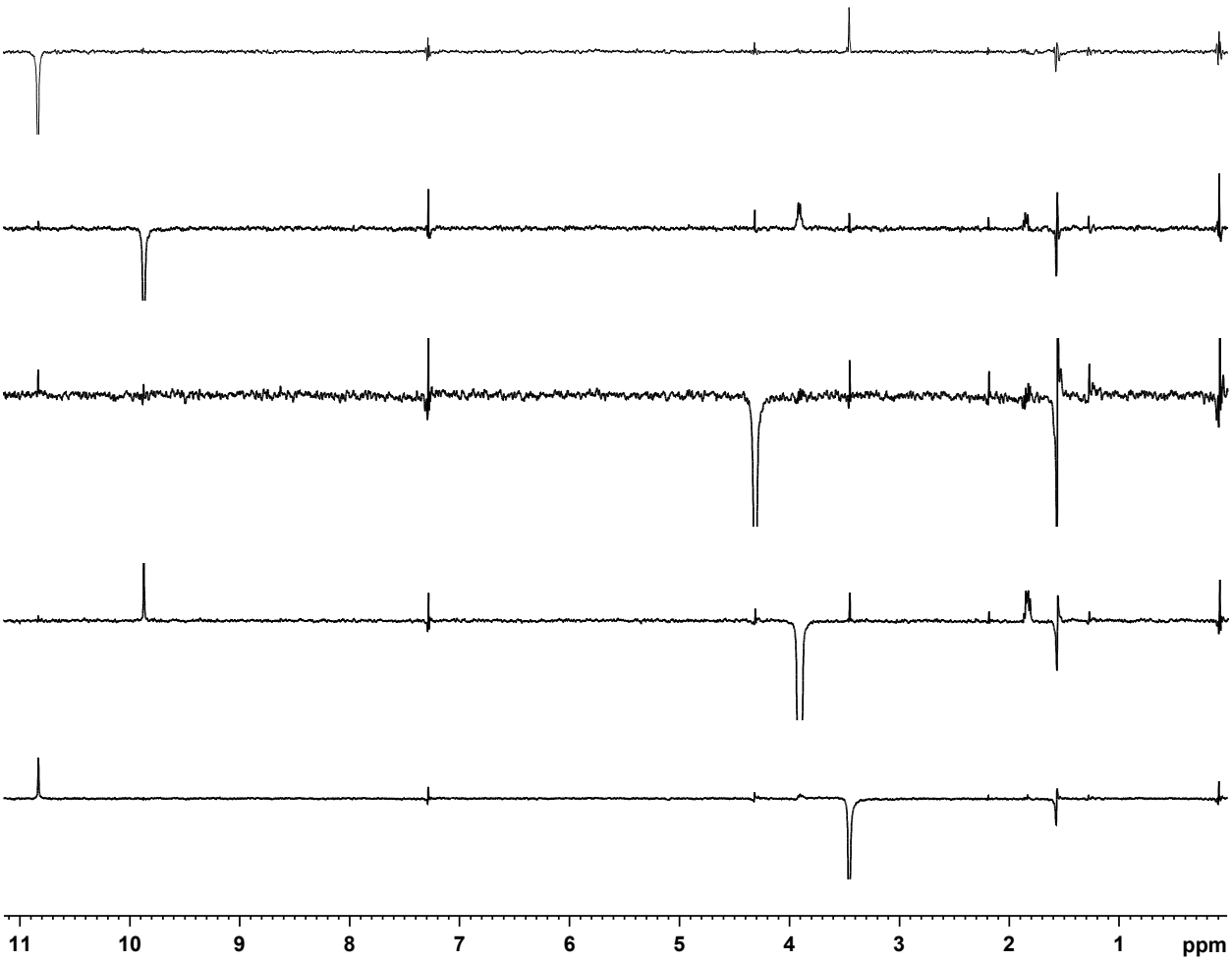

Figure A – 58: Selected nOe difference proton NMR spectra of **122** in $CDCl_3$

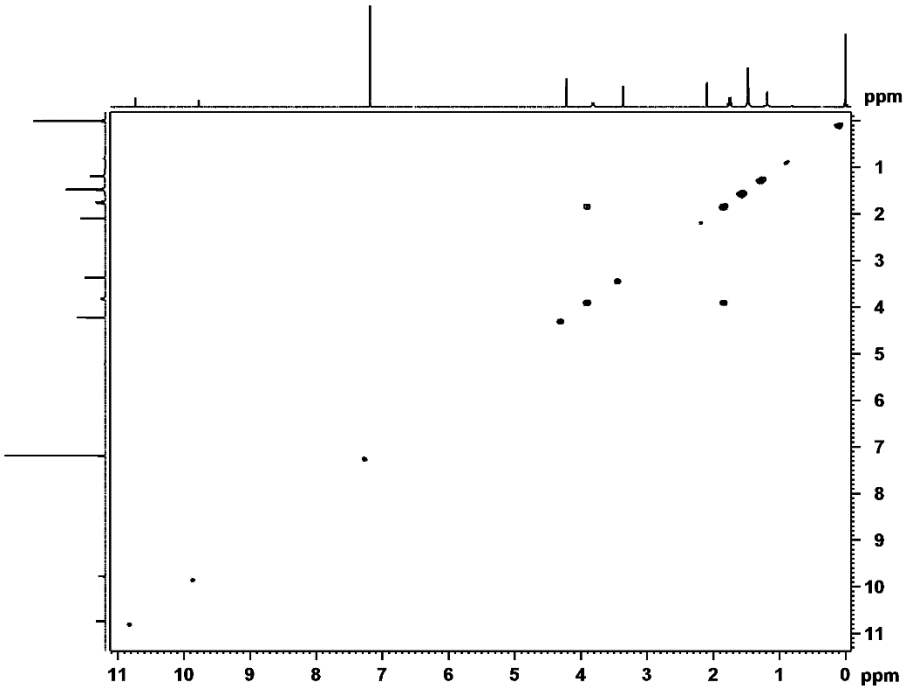

Figure A – 59: ^{1}H-^{1}H COSY NMR spectrum of **122** in $CDCl_3$

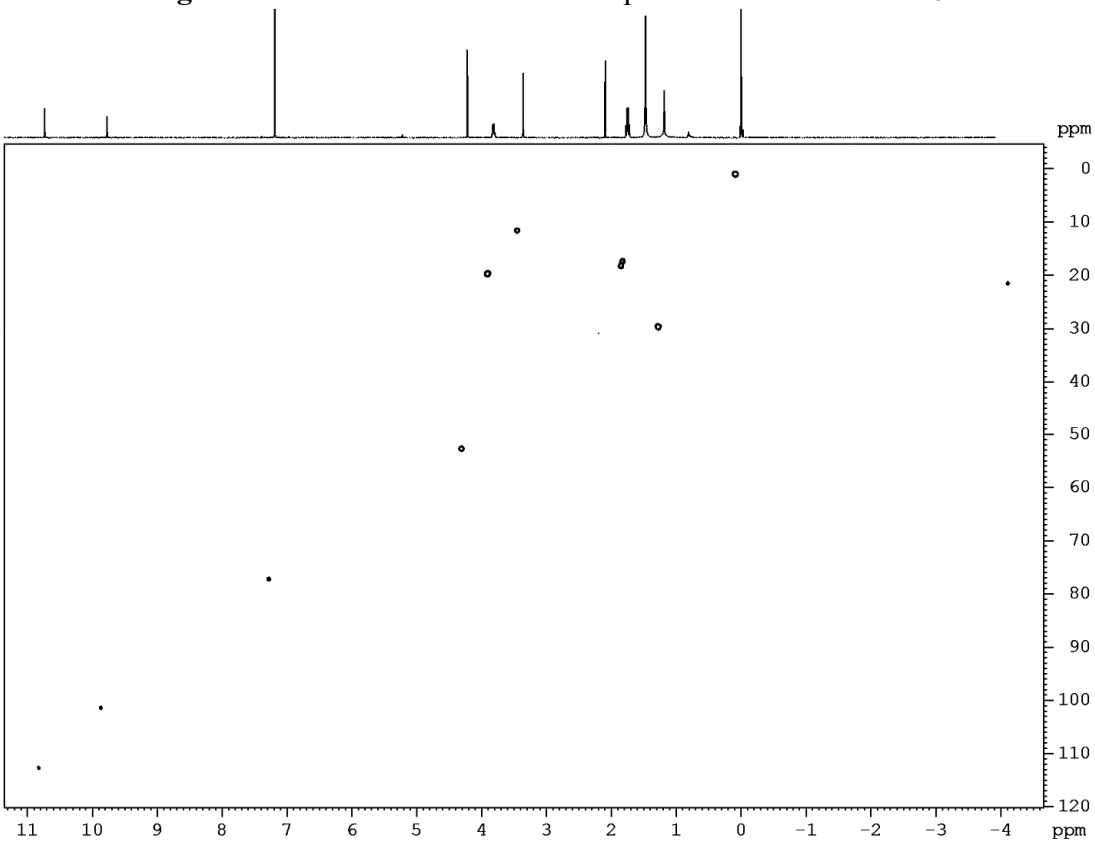

Figure A – 60: HSQC NMR spectrum of **122** in $CDCl_3$

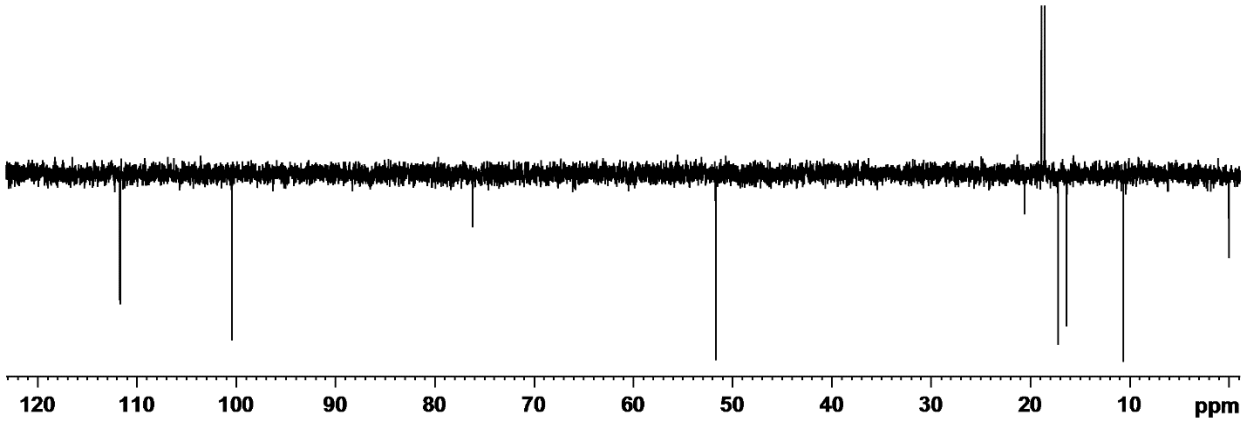

Figure A – 61: DEPT-135 NMR spectrum of **122** in $CDCl_3$

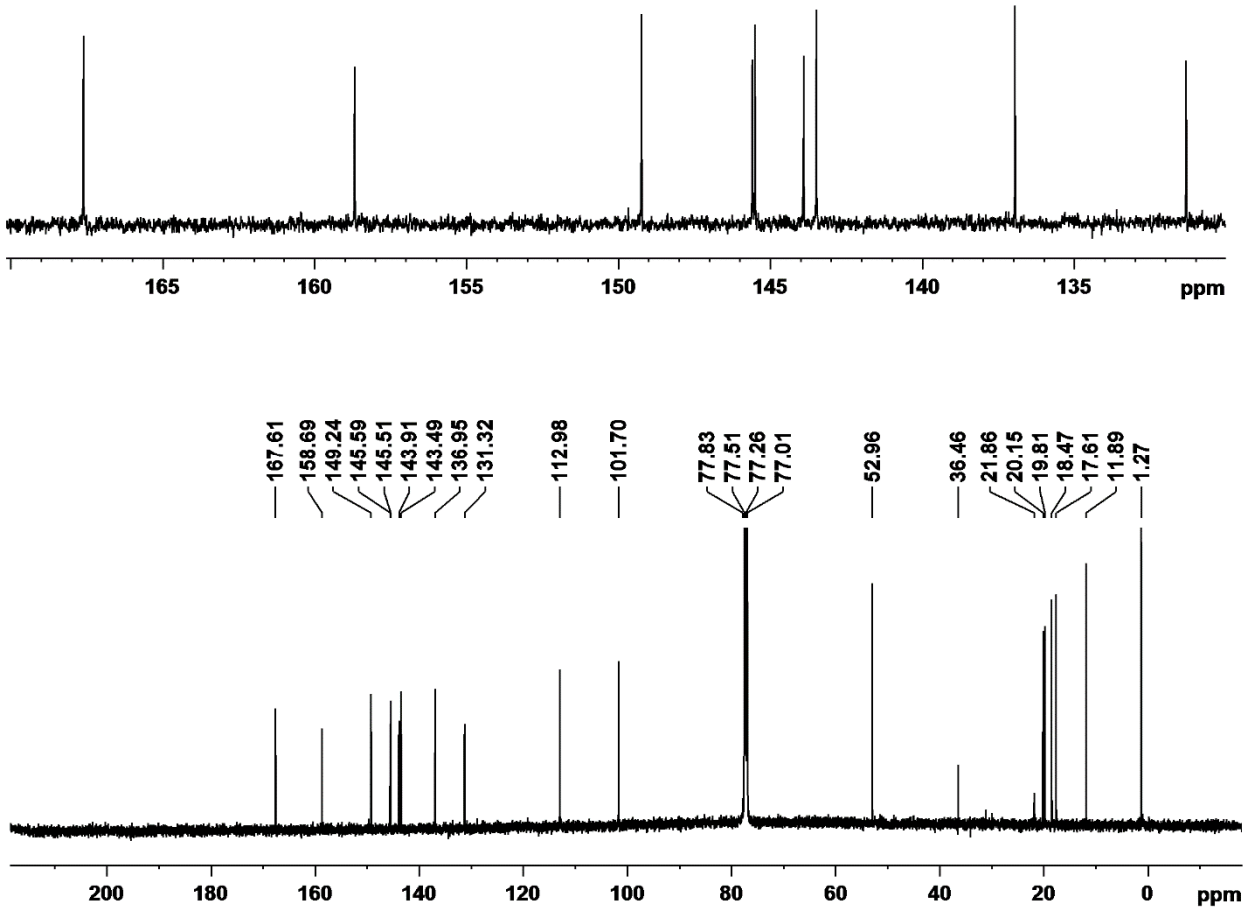

Figure A – 62: 125 MHz carbon-13 NMR spectrum of **122** in $CDCl_3$

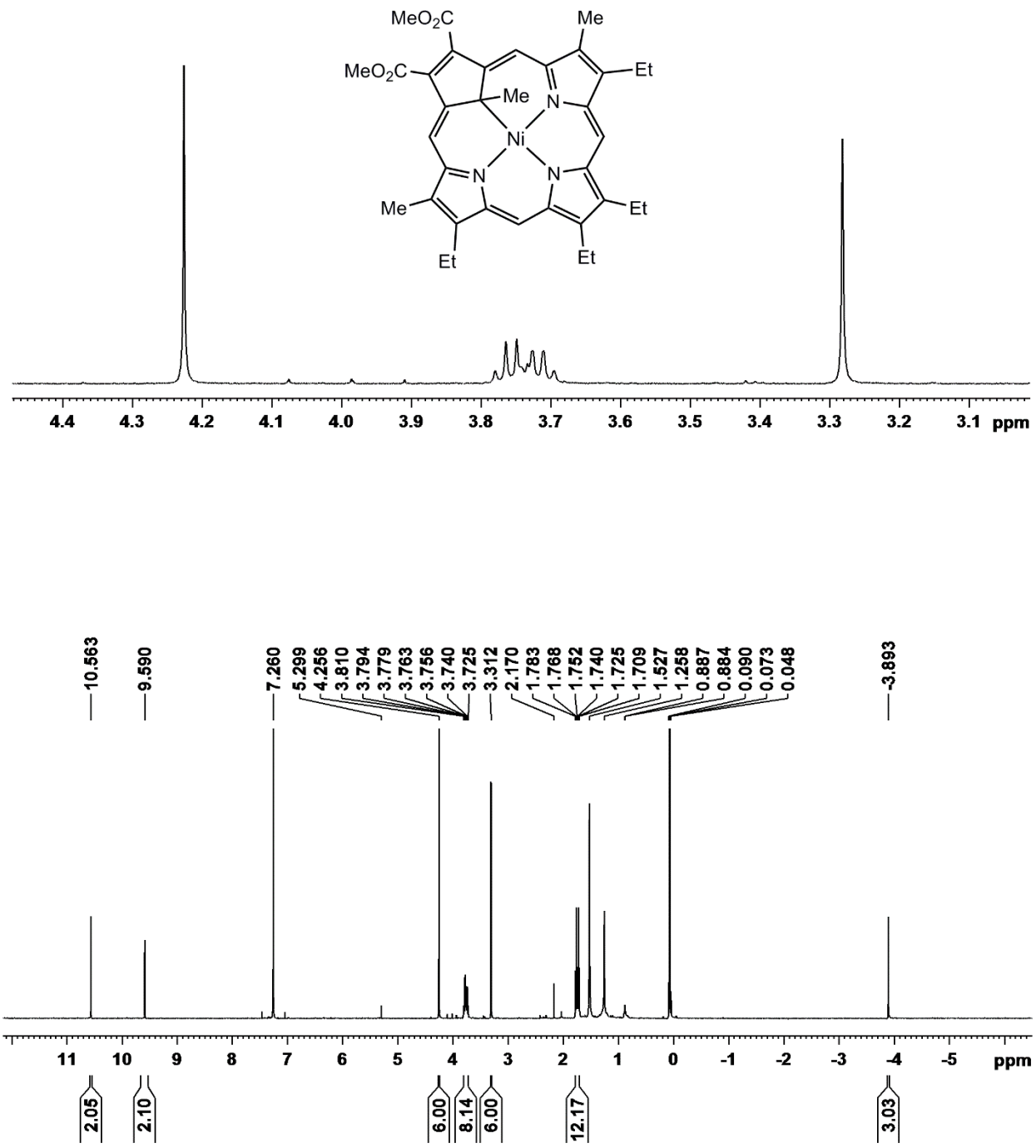

Figure A – 63: 500 MHz ^{1}H NMR Spectrum of **123** in $CDCl_3$

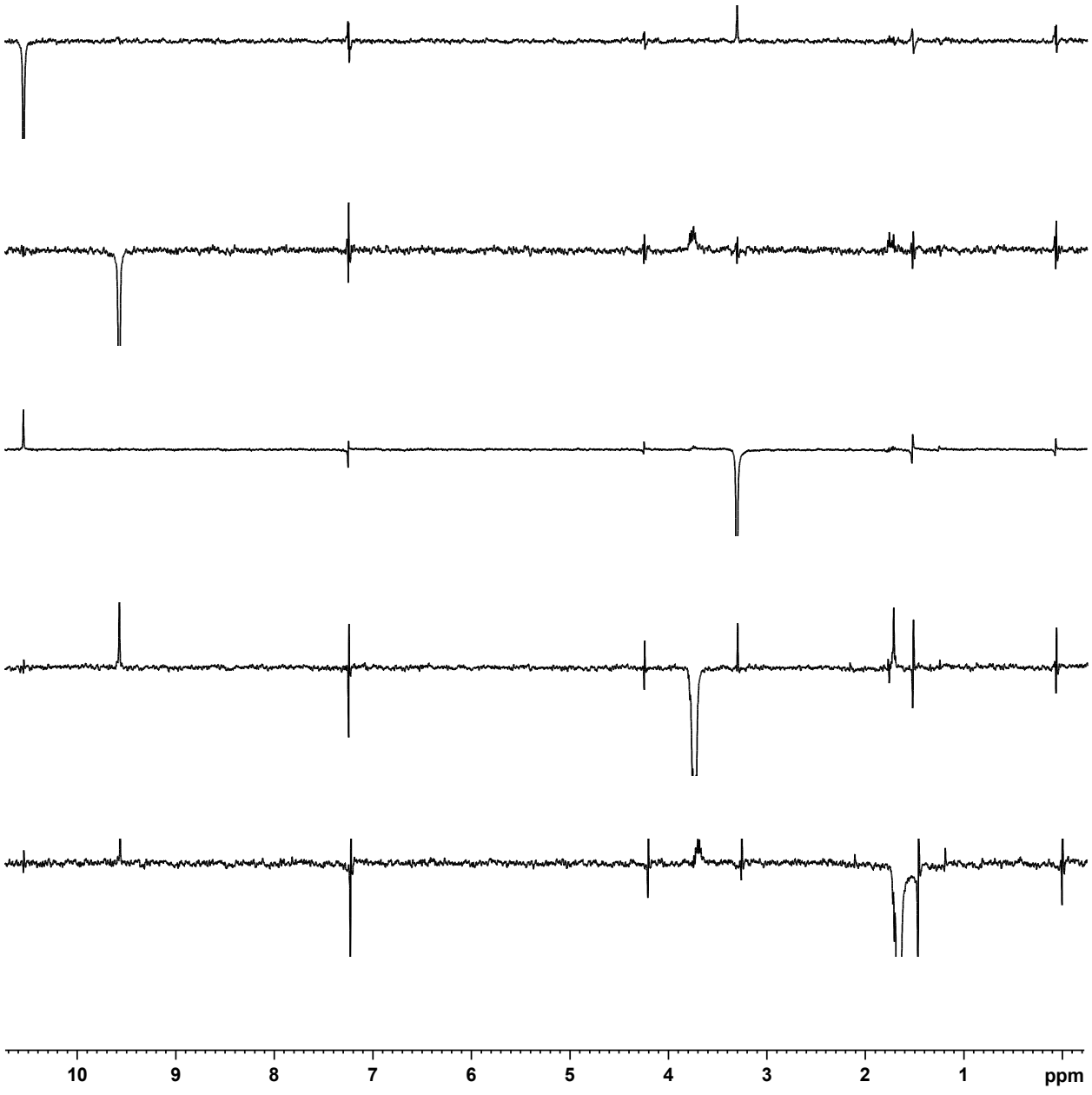

Figure A – 64: Selected nOe difference proton NMR spectra of **123** in $CDCl_3$

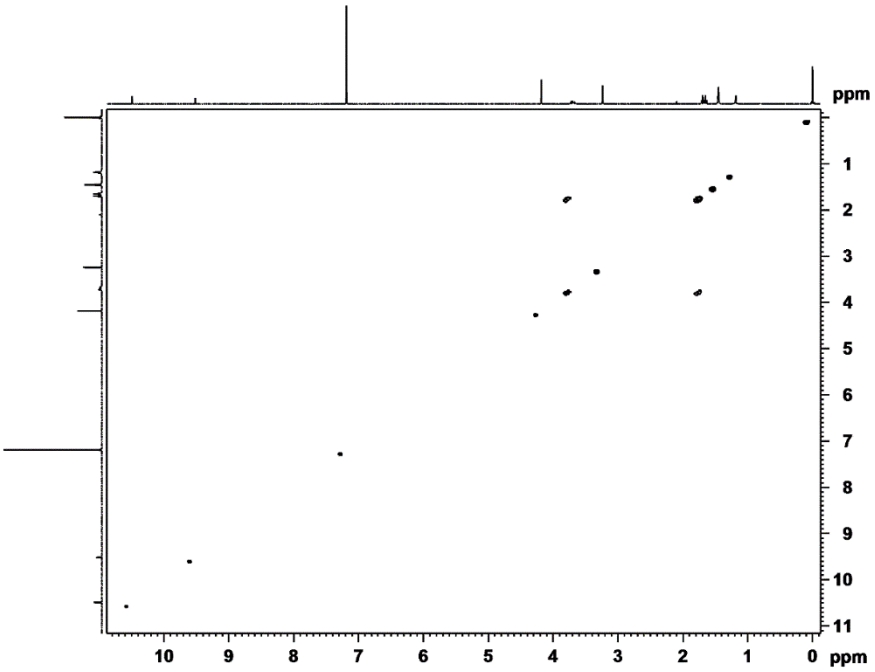

Figure A – 65: ^{1}H-^{1}H COSY NMR spectrum of **123** in $CDCl_3$

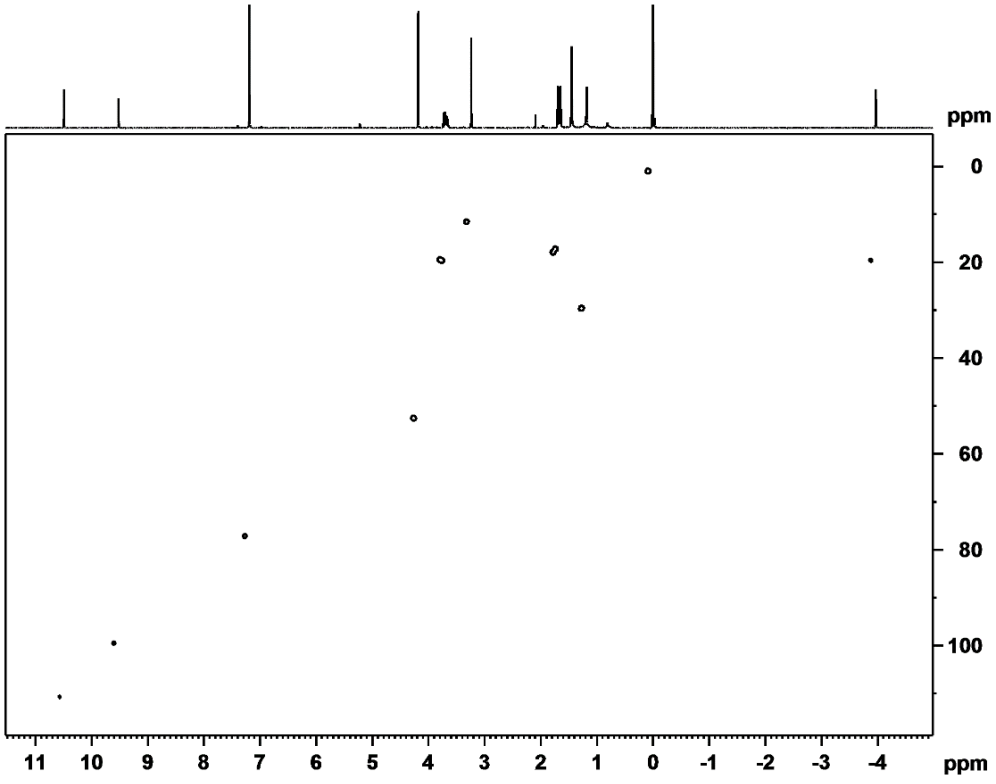

Figure A – 66: HSQC NMR spectrum of **123** in $CDCl_3$

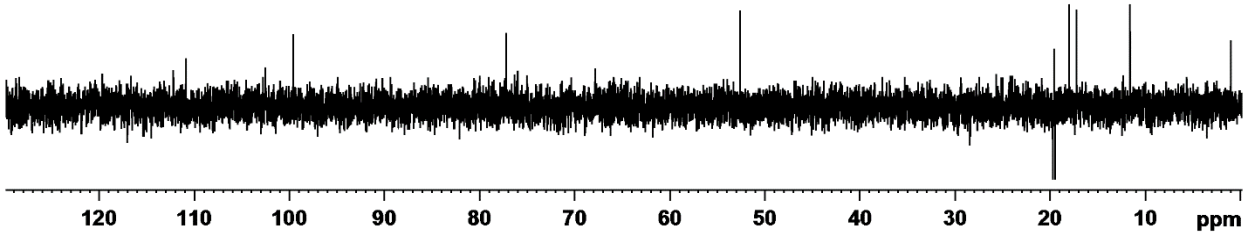

Figure A – 67: DEPT-135 NMR spectrum of **123** in $CDCl_3$

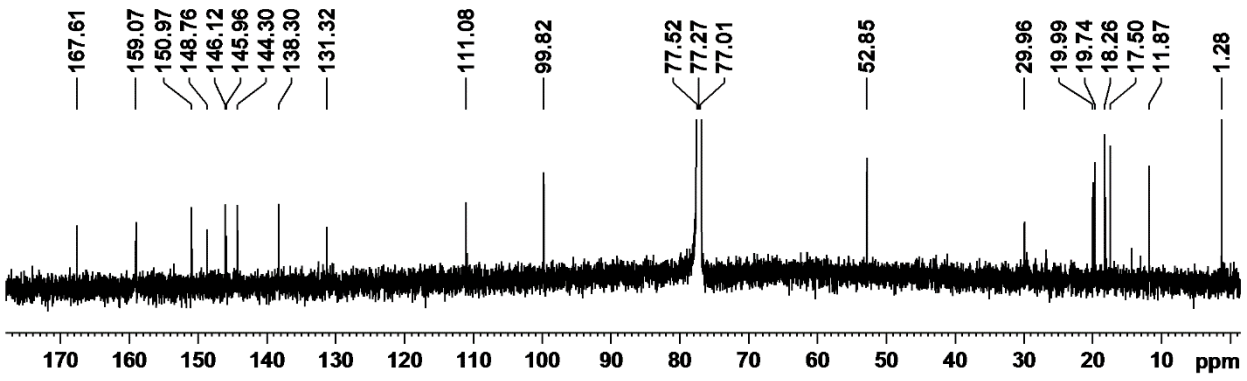

Figure A – 68: 125 MHz carbon-13 NMR spectrum of **123** in $CDCl_3$

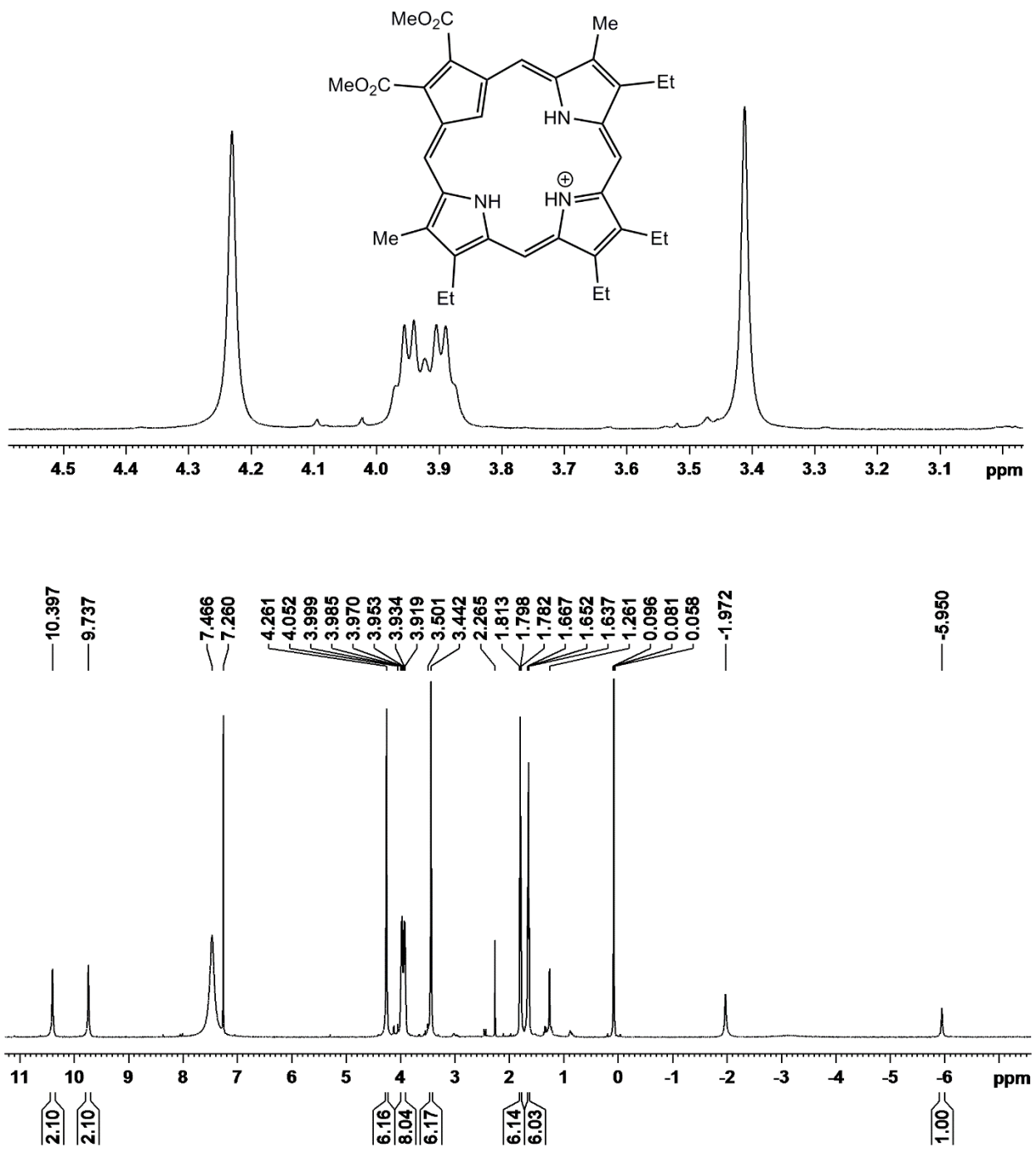

Figure A – 69: 500 MHz ^{1}H NMR Spectrum of **98**H^{+} in TFA-$CDCl_3$

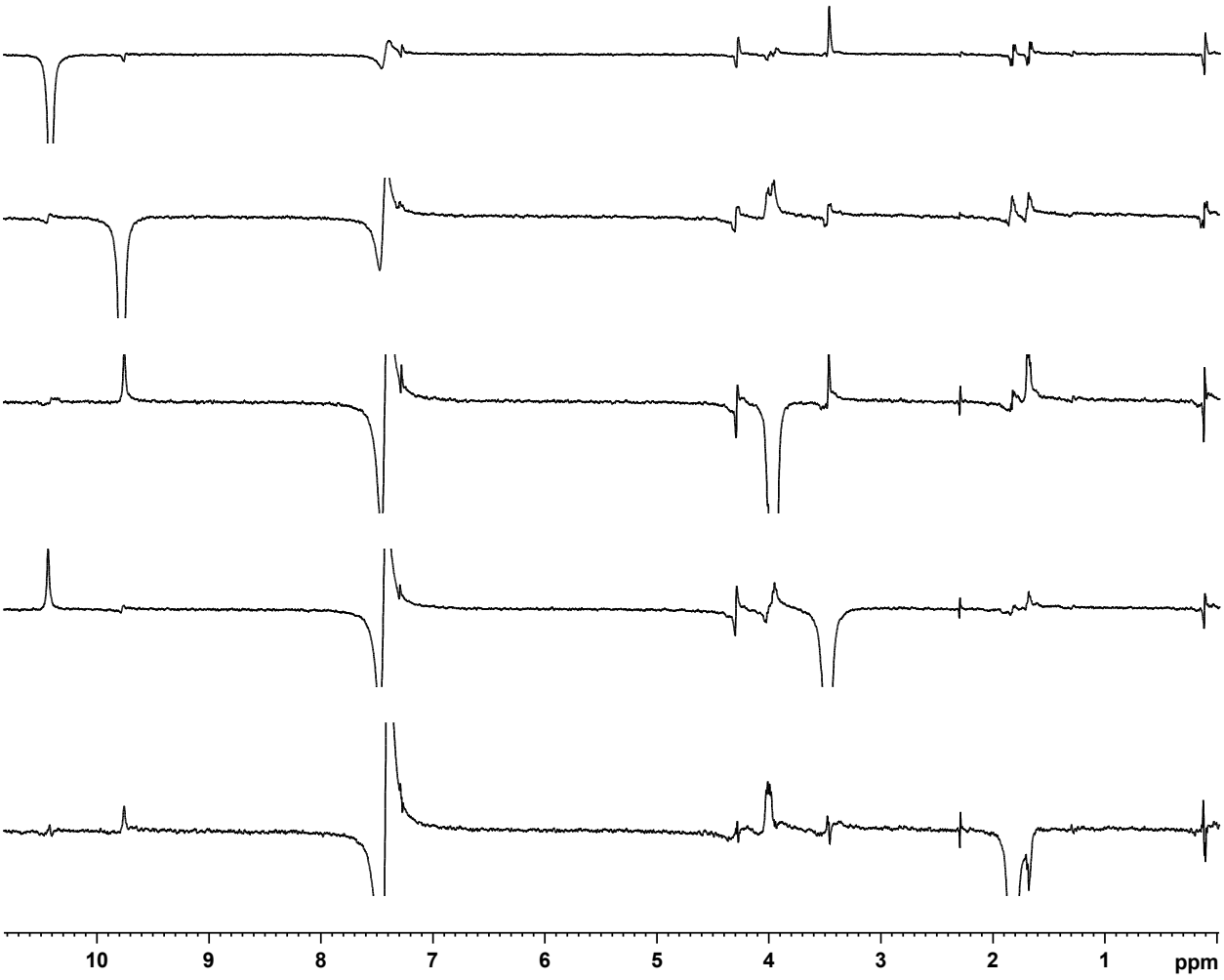

Figure A – 70: Selected nOe difference proton NMR spectra of **98**H^+ in TFA-$CDCl_3$

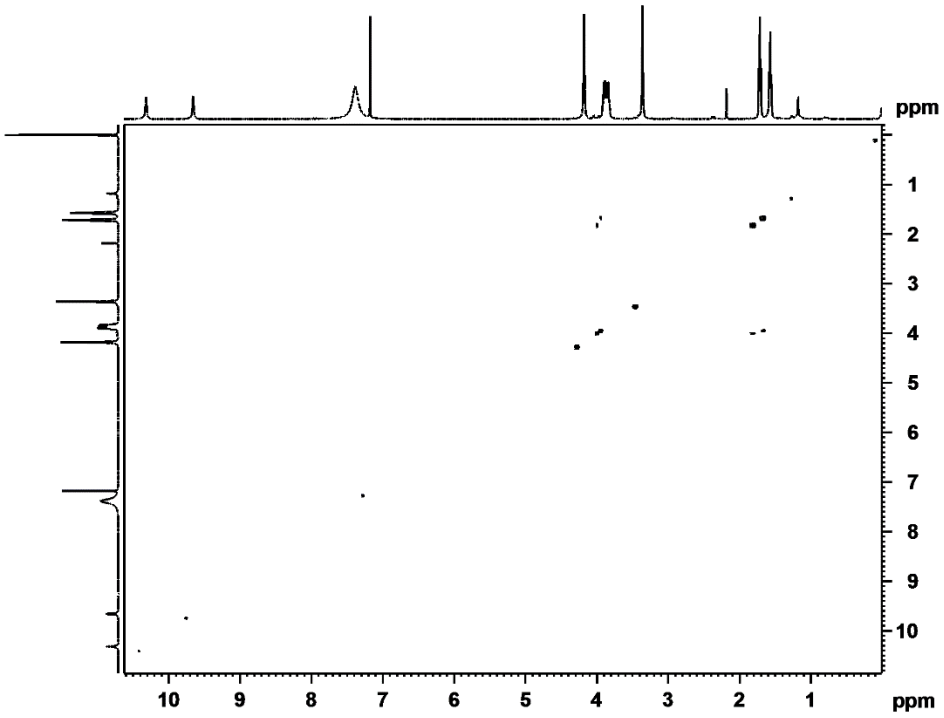

Figure A – 71: DEPT-135 NMR spectrum of **98**H^+ in TFA-$CDCl_3$

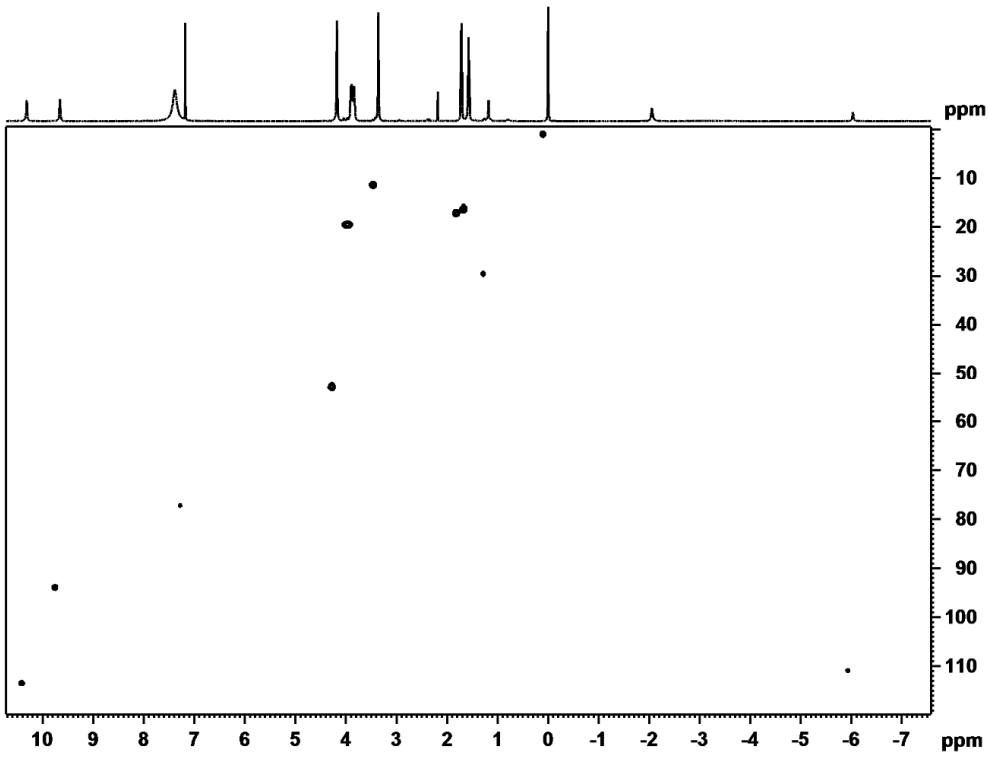

Figure A – 72: HSQC NMR spectrum of **98**H^+ in TFA-$CDCl_3$

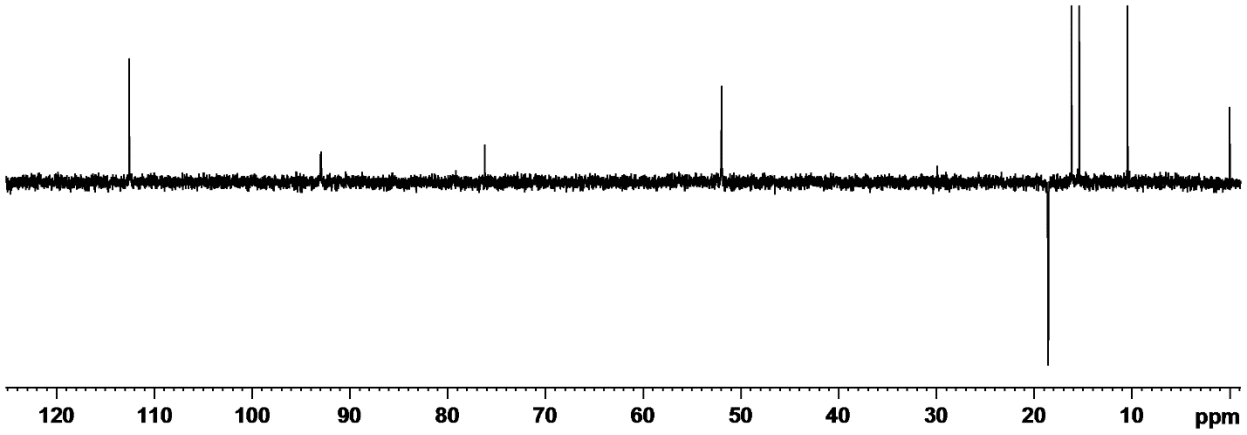

Figure A – 73: DEPT-135 NMR spectrum of **98**H^+ in TFA-$CDCl_3$

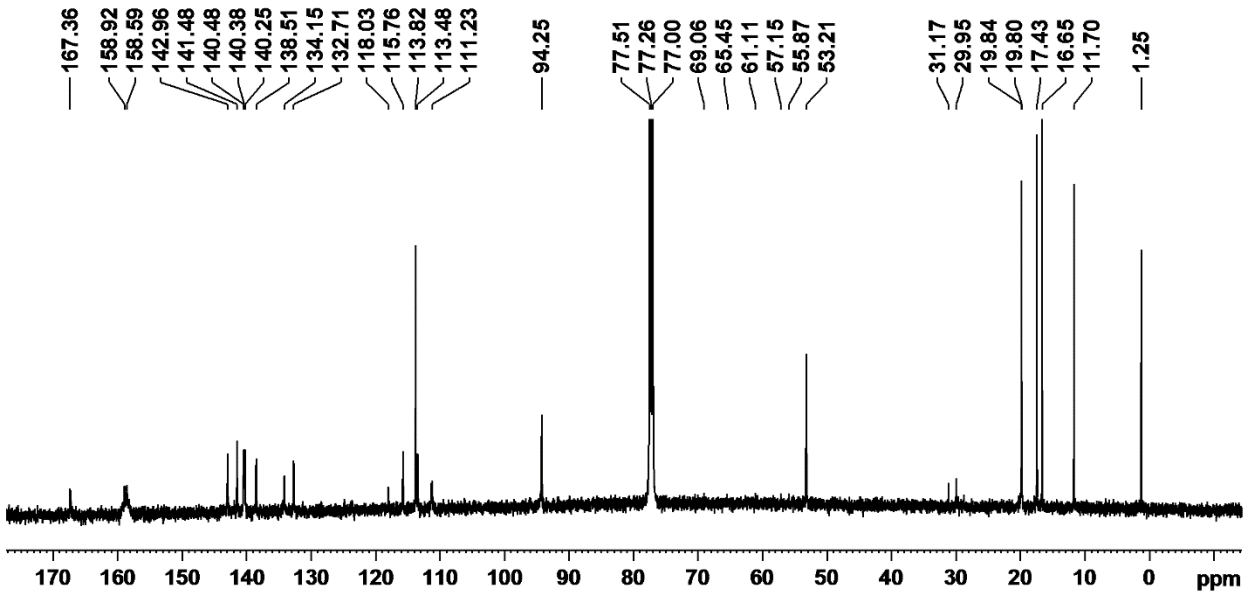

Figure A – 74: 125 MHz carbon-13 NMR spectrum of **98**H^+ in TFA-$CDCl_3$

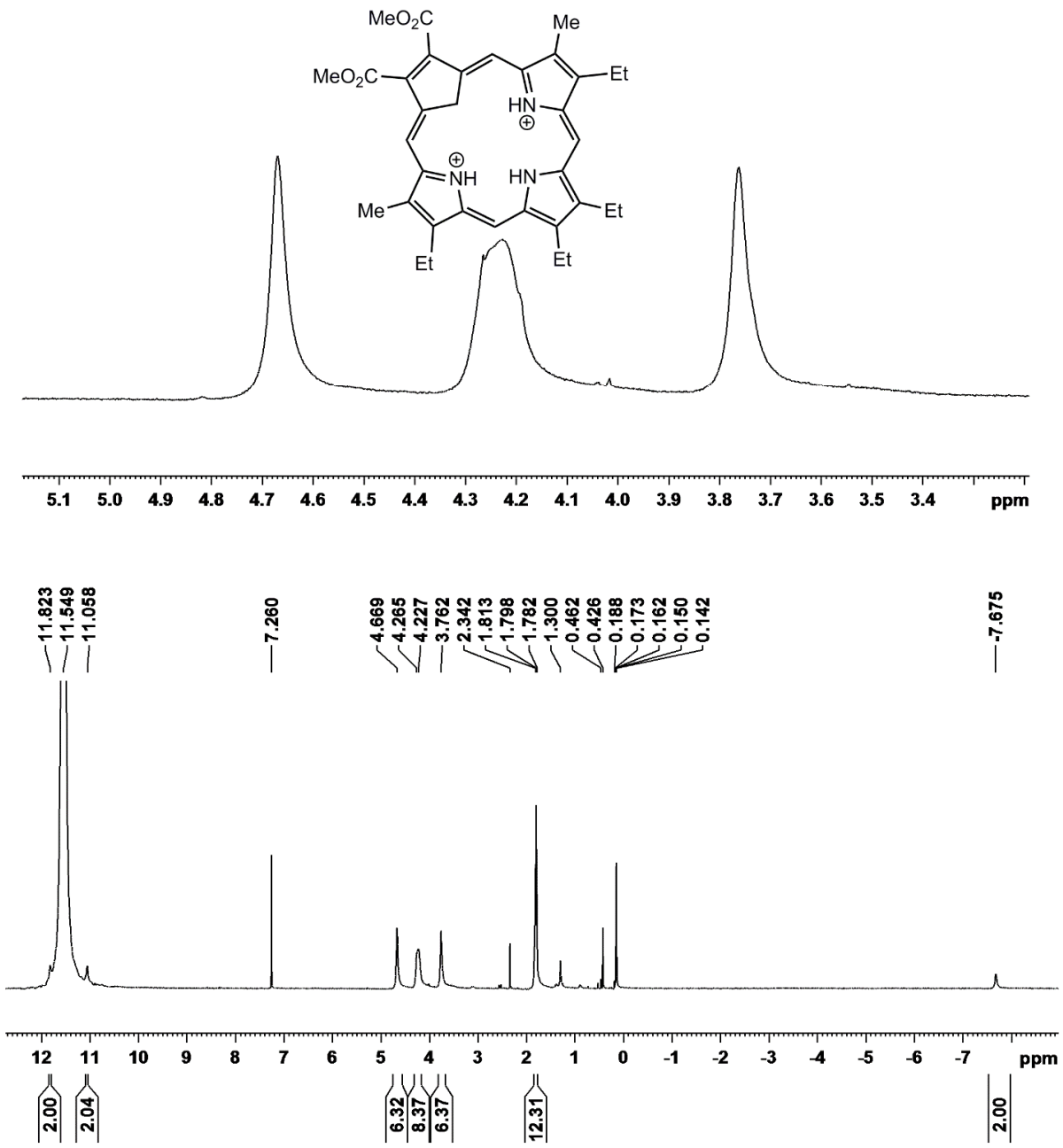

Figure A – 75: 500 MHz ^{1}H NMR Spectrum of **98**H_2^{2+} in TFA-$CDCl_3$

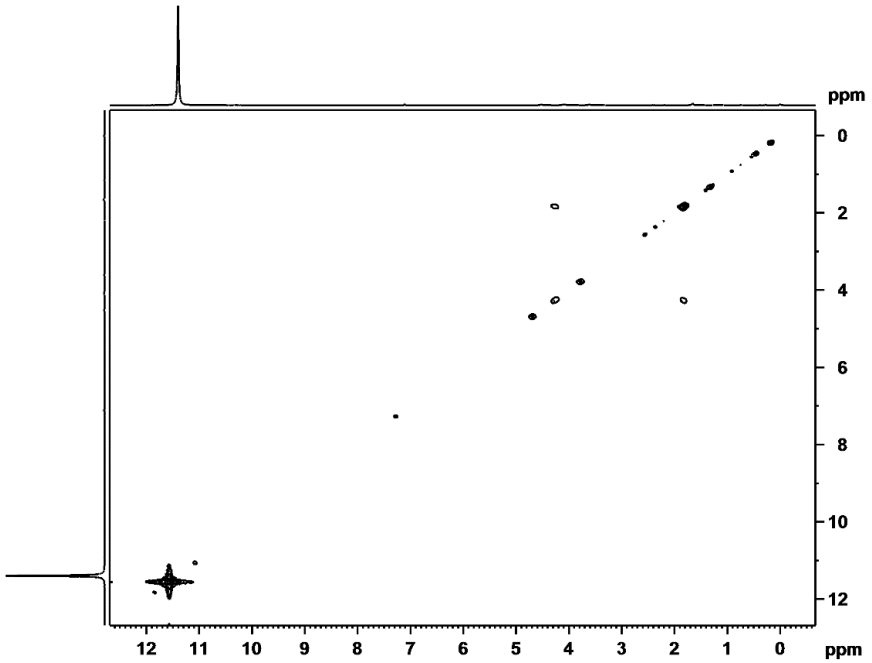

Figure A – 76: ^{1}H-^{1}H COSY NMR spectrum of **98**H_2^{2+} in TFA-$CDCl_3$

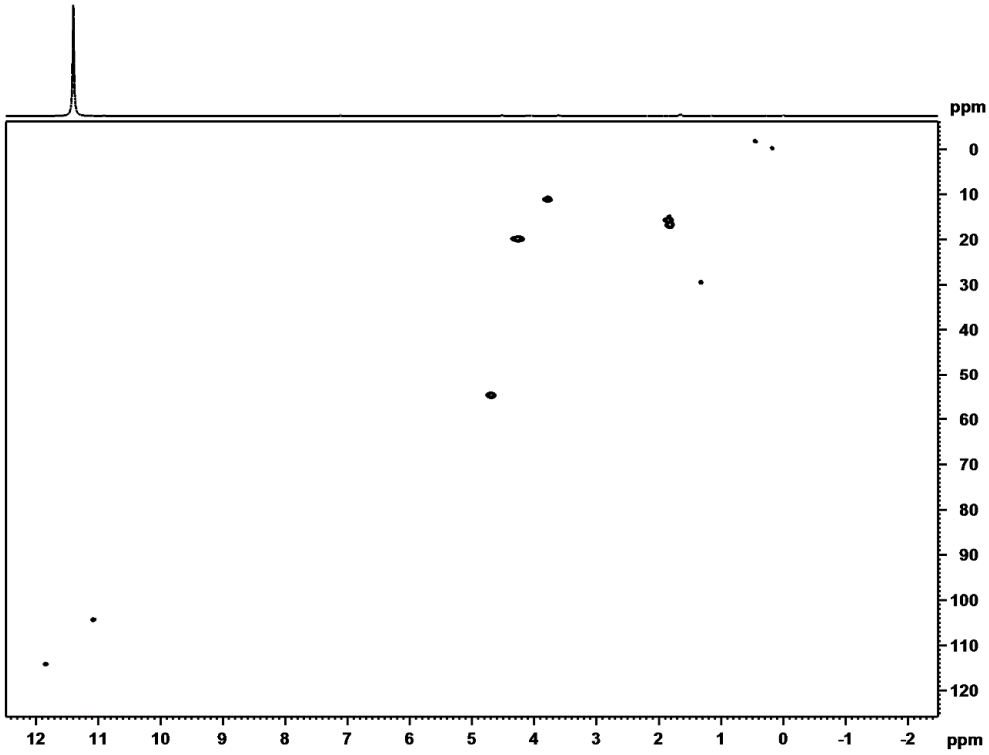

Figure A – 77: HSQC NMR spectrum of **98**H_2^{2+} in TFA-$CDCl_3$

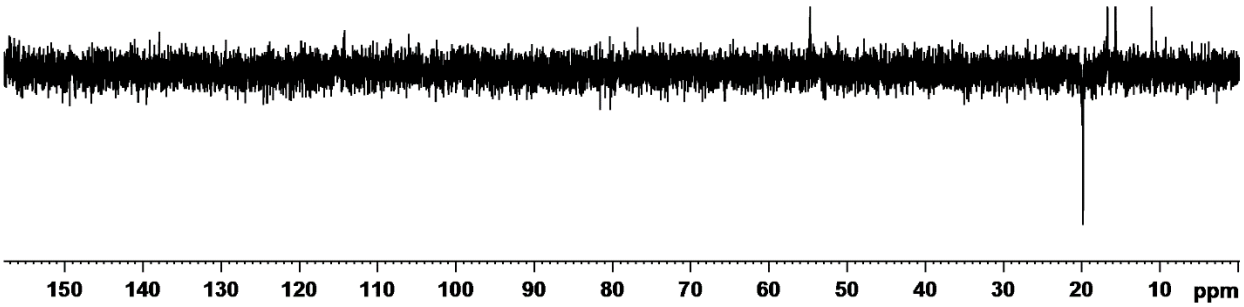

Figure A – 78: DEPT-135 NMR spectrum of **98**H_2^{2+} in TFA-$CDCl_3$

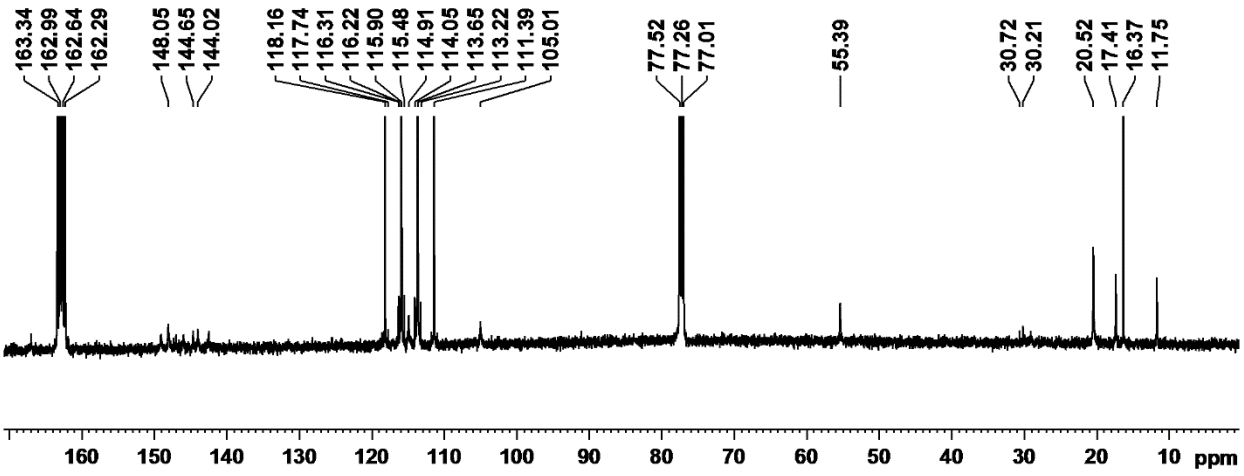

Figure A – 79: 125 MHz carbon-13 NMR spectrum of **98**H_2^{2+} in TFA-$CDCl_3$

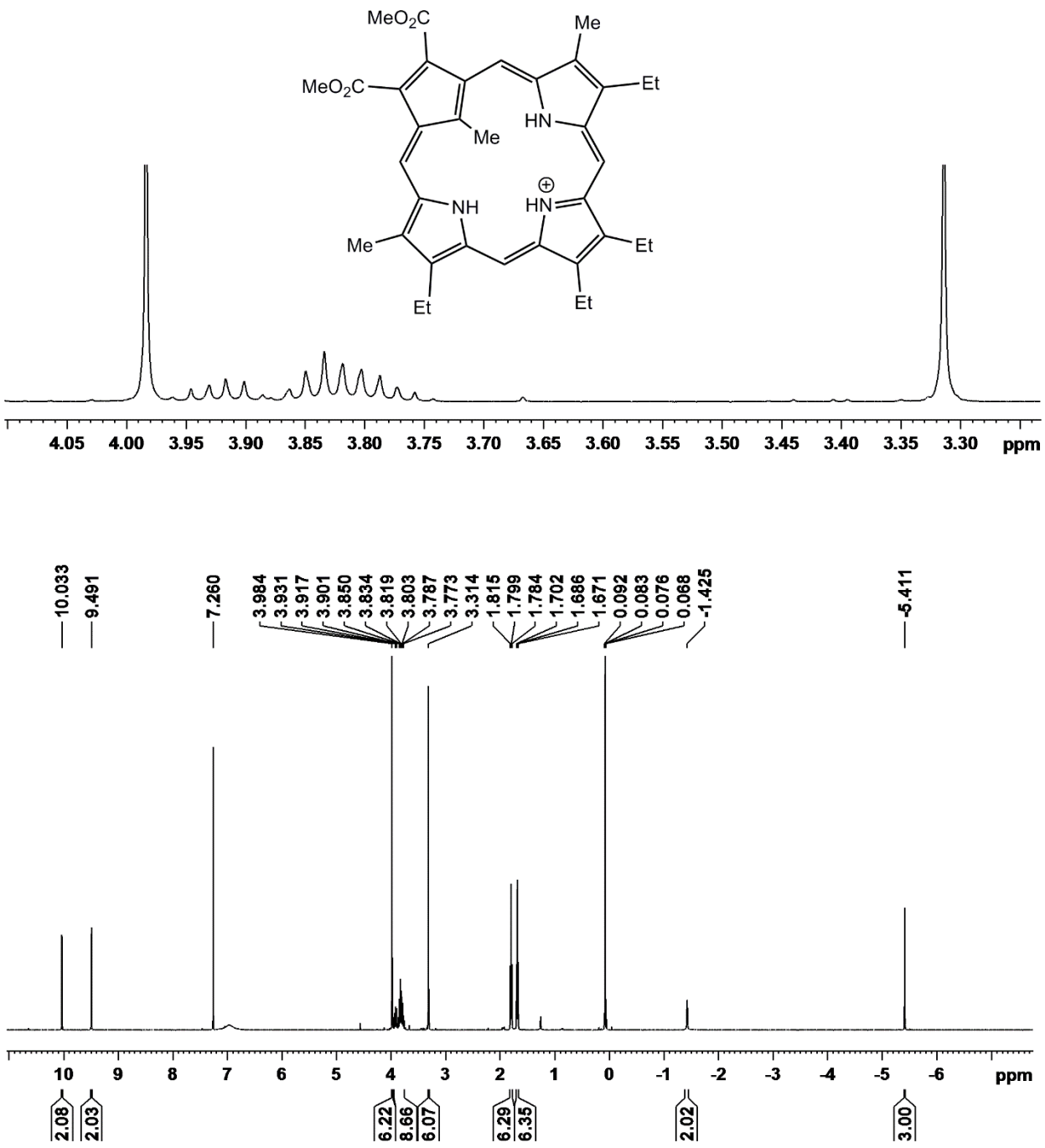

Figure A – 80: 500 MHz ^{1}H NMR Spectrum of **120**H^{+} in TFA-$CDCl_3$

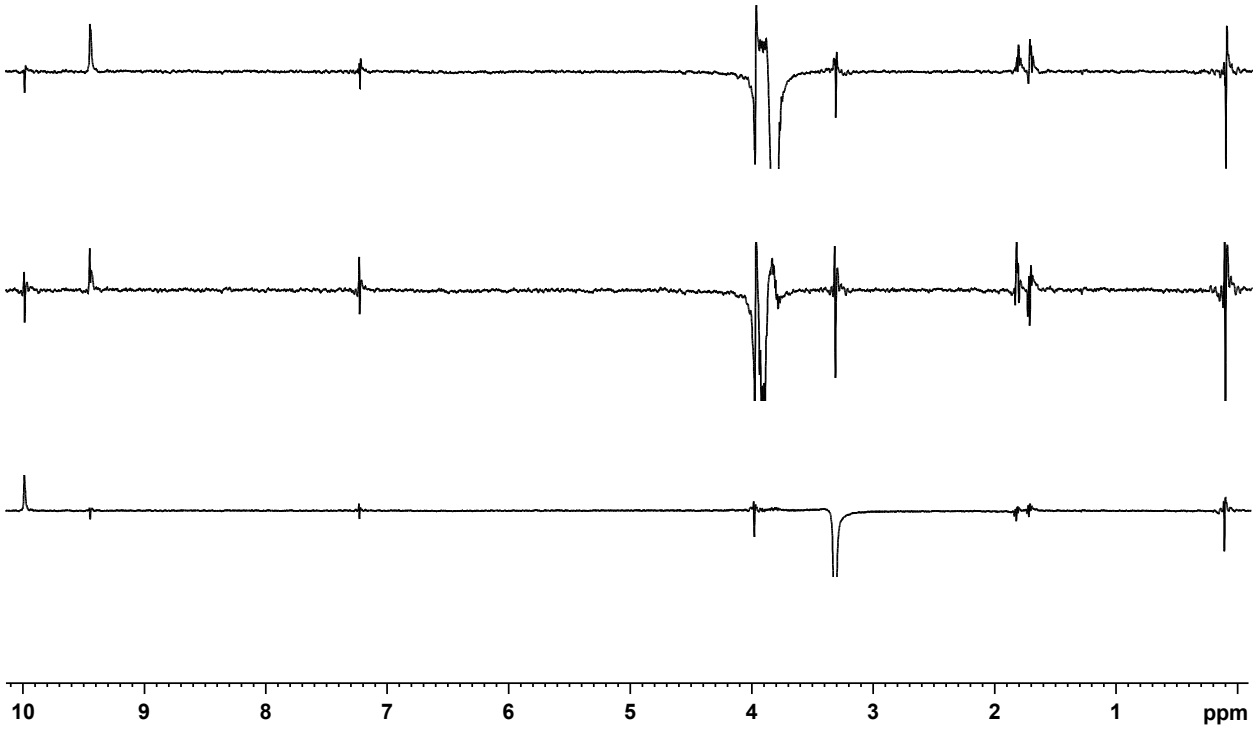

Figure A – 81: Selected nOe difference proton NMR spectra of **120**H^+ in TFA-$CDCl_3$

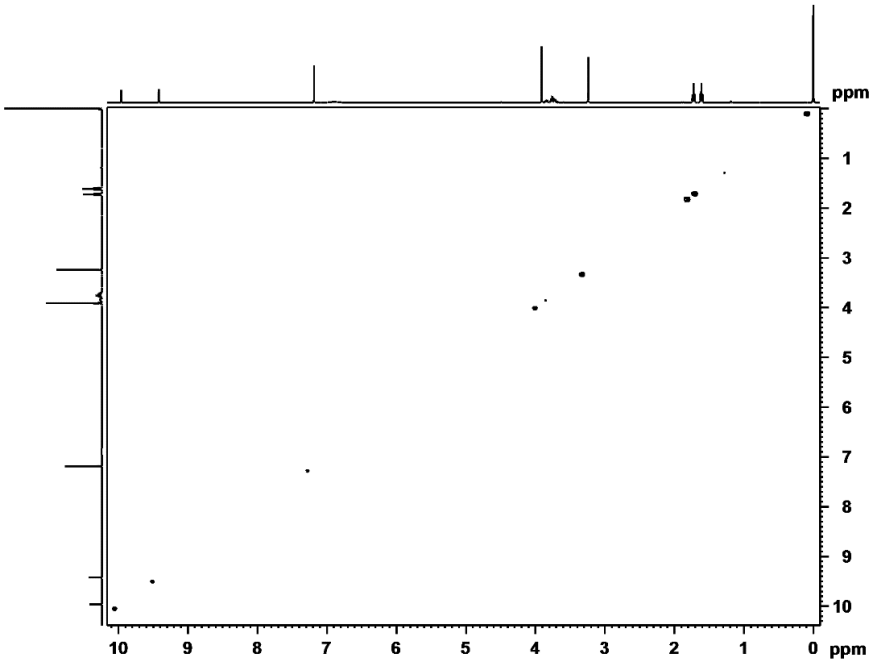

Figure A – 82: ^{1}H-^{1}H COSY NMR spectrum of **120**H^{+} in TFA-$CDCl_3$

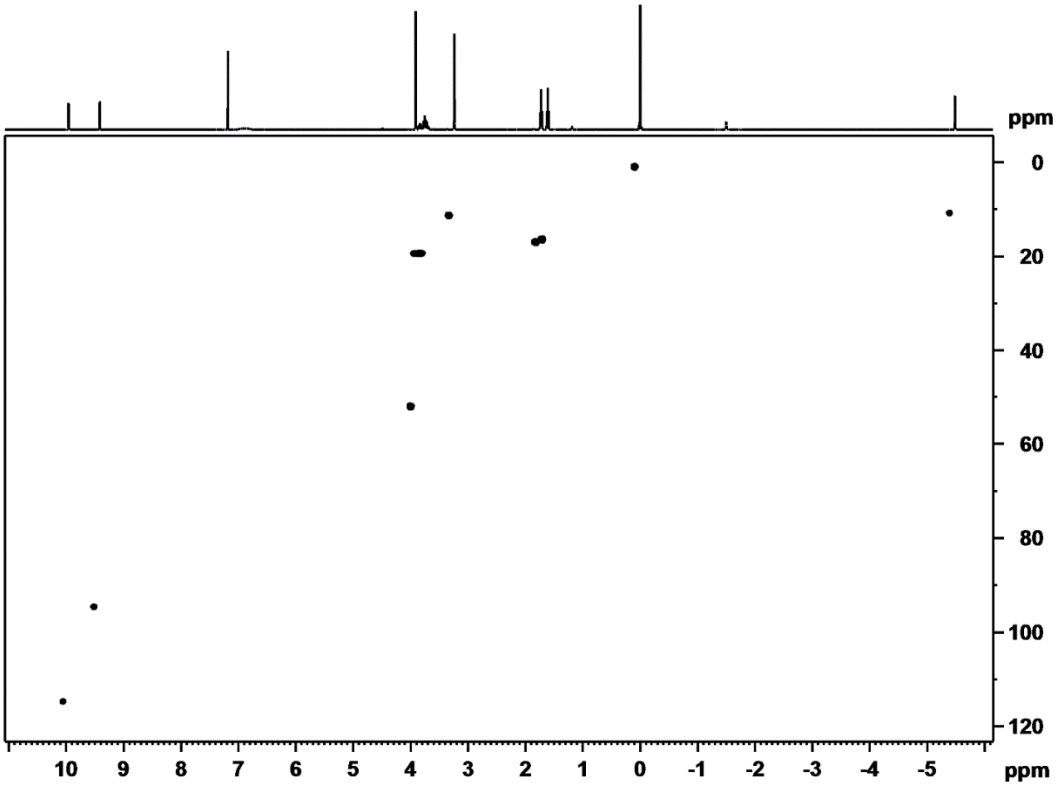

Figure A – 83: HSQC NMR spectrum of **120**H^{+} in TFA-$CDCl_3$

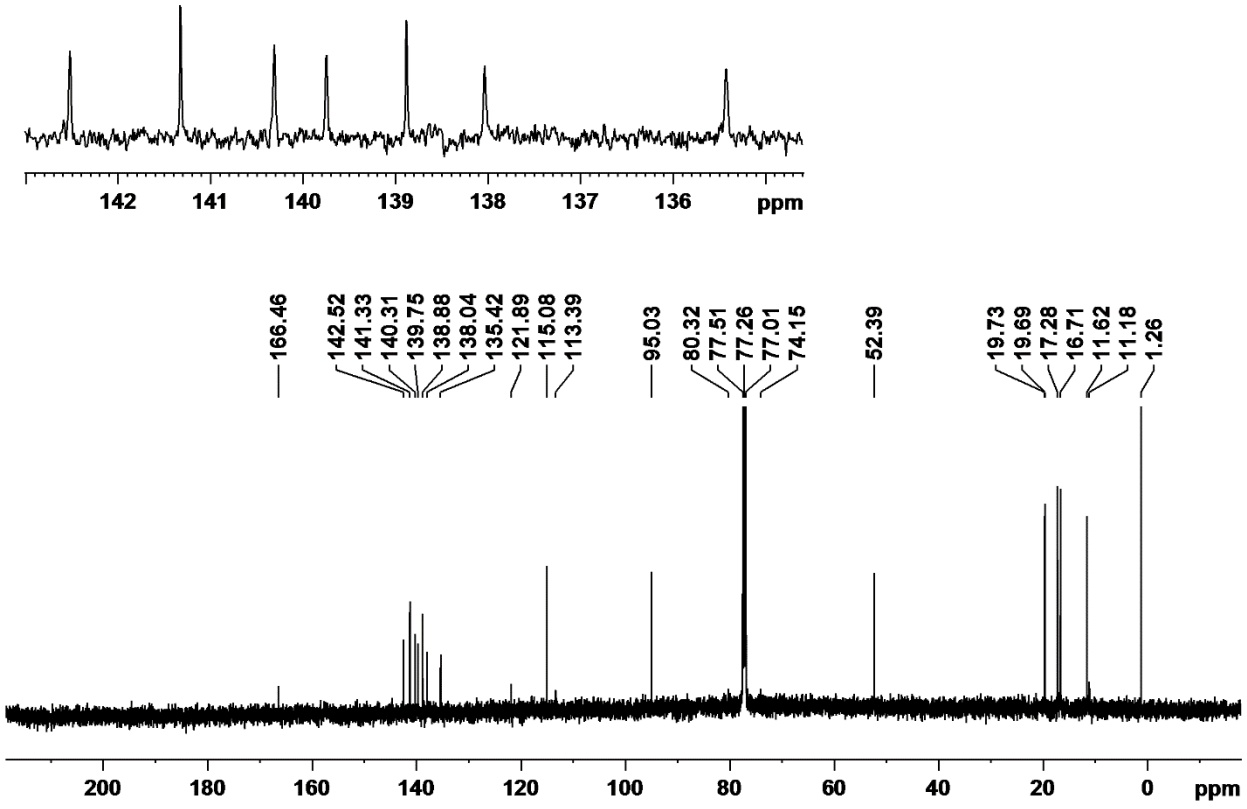

Figure A – 84: 125 MHz carbon-13 NMR spectrum of **120**H^+in TFA-$CDCl_3$

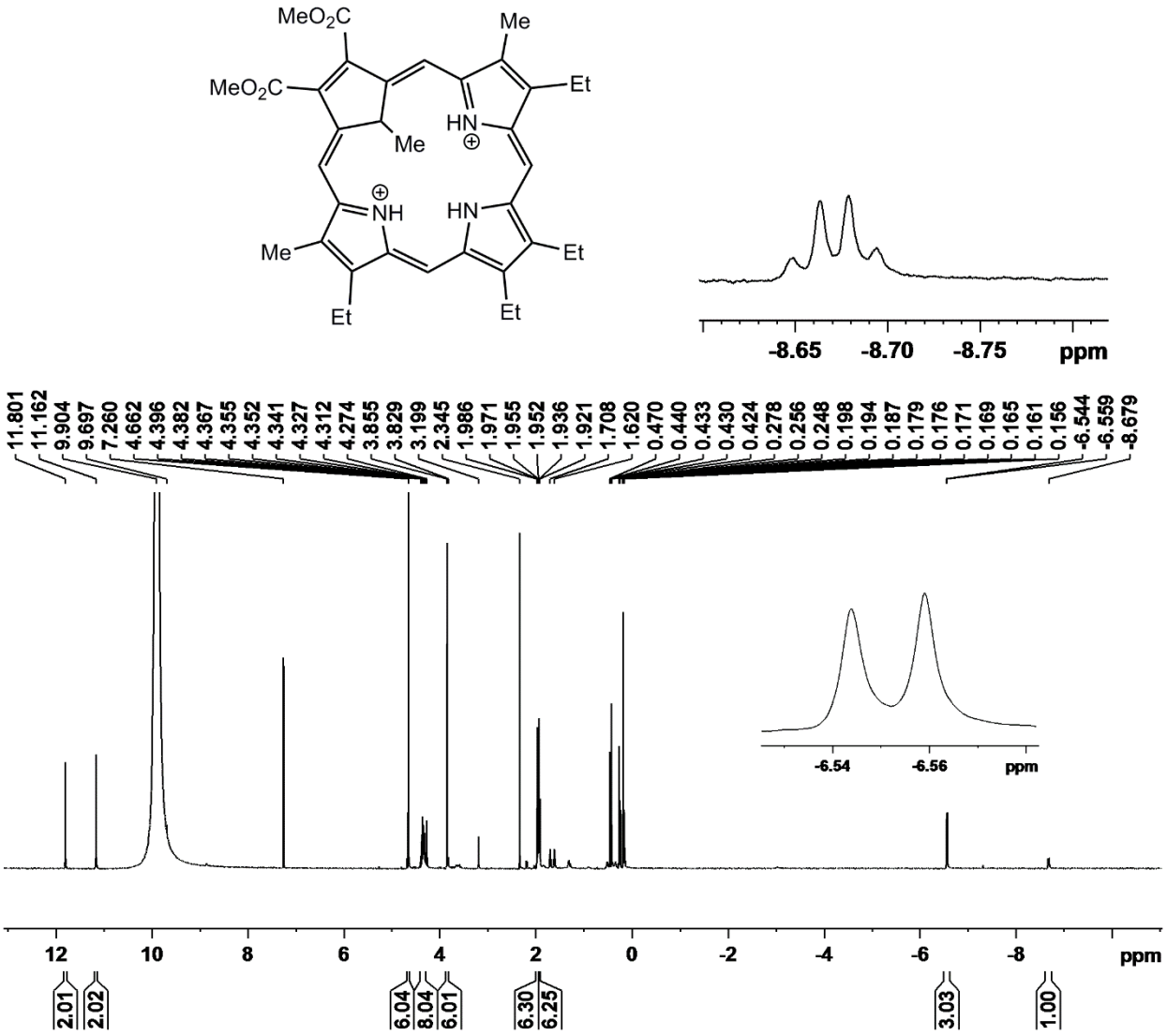

Figure A – 85: 500 MHz ^{1}H NMR Spectrum of **120**H_2^{2+} in TFA-$CDCl_3$

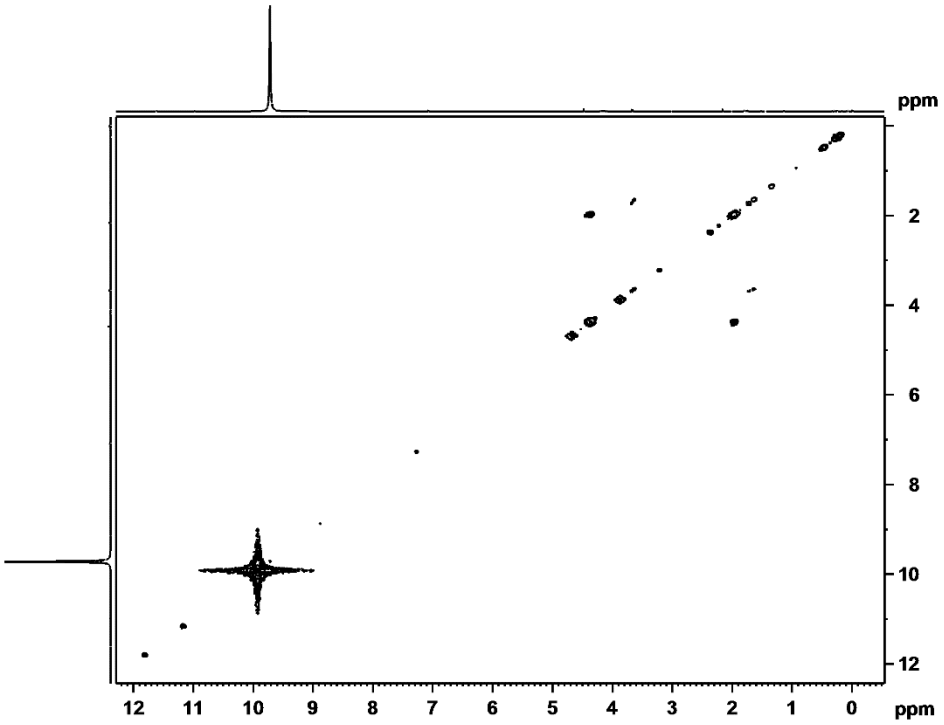

Figure A – 86: ^{1}H-^{1}H COSY NMR spectrum of **120**H_2^{2+} in TFA-$CDCl_3$

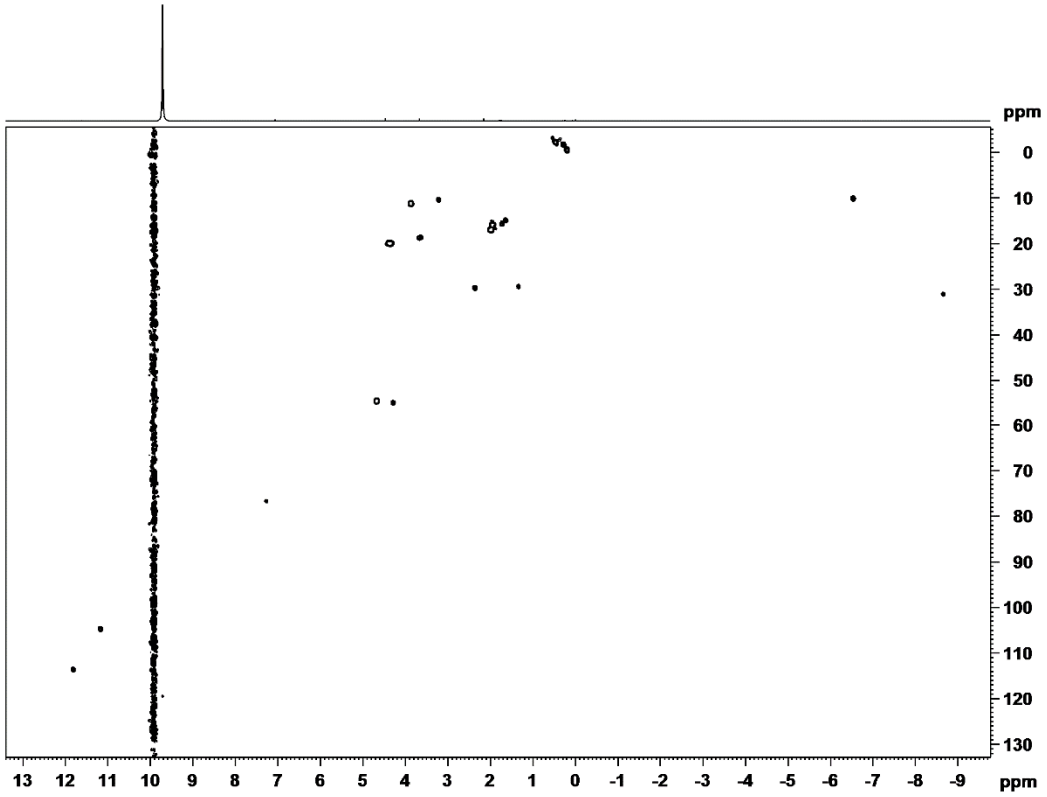

Figure A – 87: HSQC NMR spectrum of **120**H_2^{2+} in TFA-$CDCl_3$

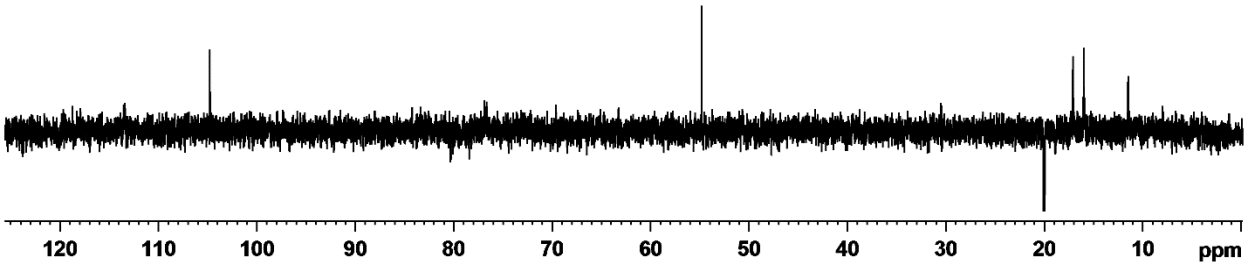

Figure A – 88: DEPT-135 NMR spectrum of **120**H_2^{2+} in TFA-$CDCl_3$

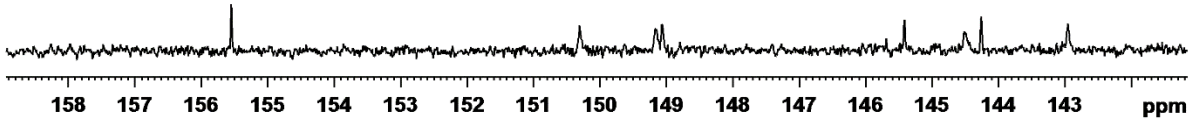

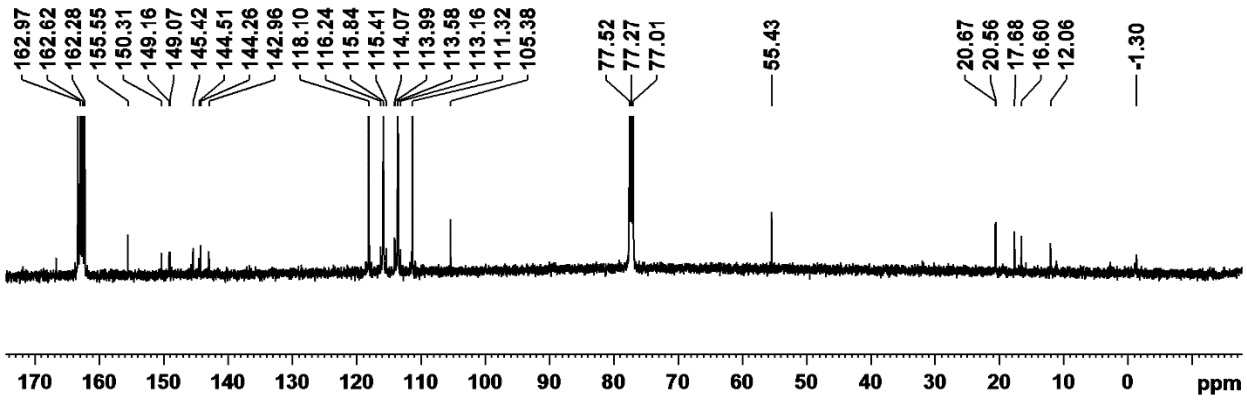

Figure A –89: 125 MHz carbon-13 NMR spectrum of **120**H_2^{2+} in TFA-$CDCl_3$

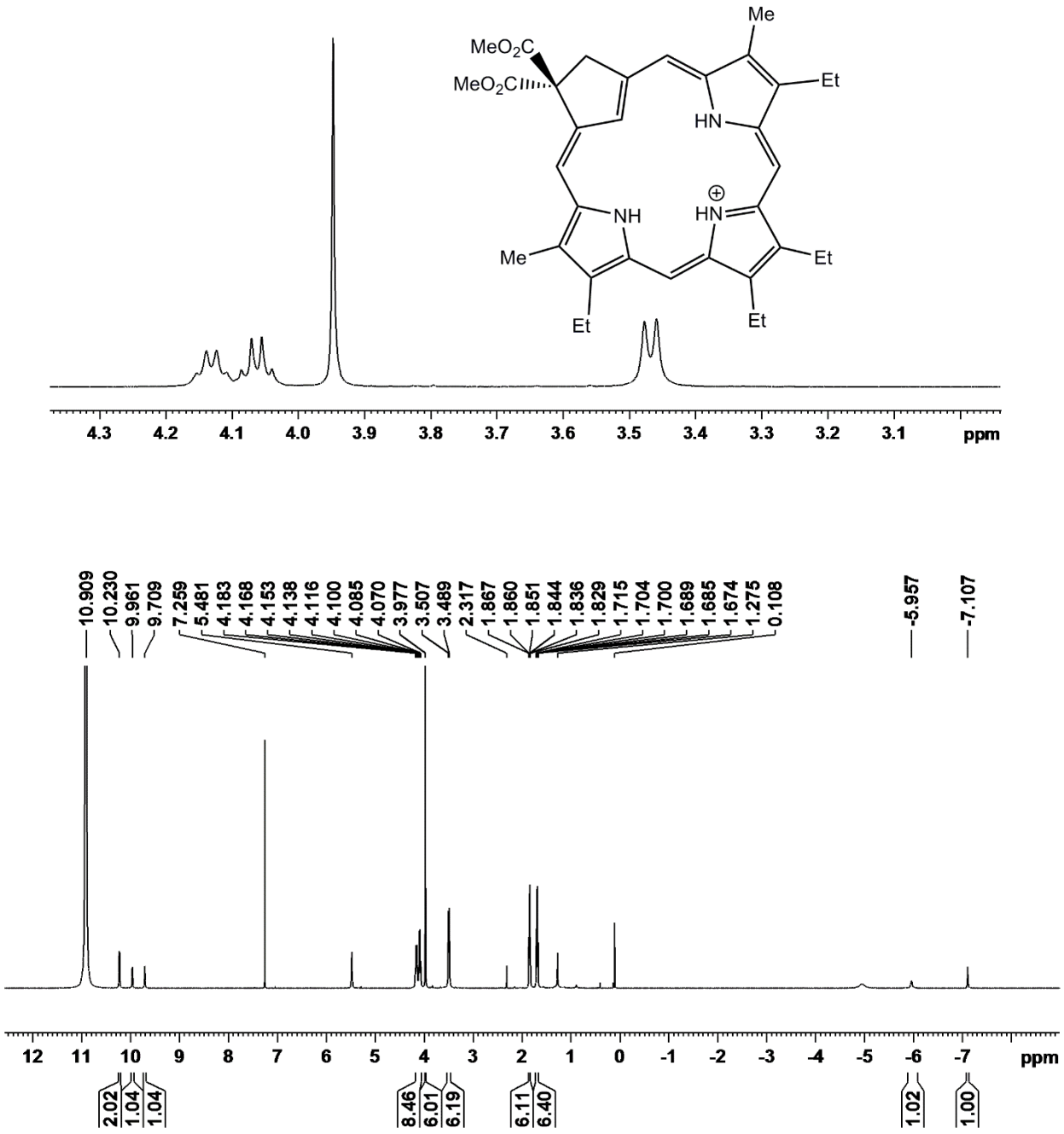

Figure A – 90: 500 MHz ^{1}H NMR Spectrum of **133**H^{+} in TFA-$CDCl_3$

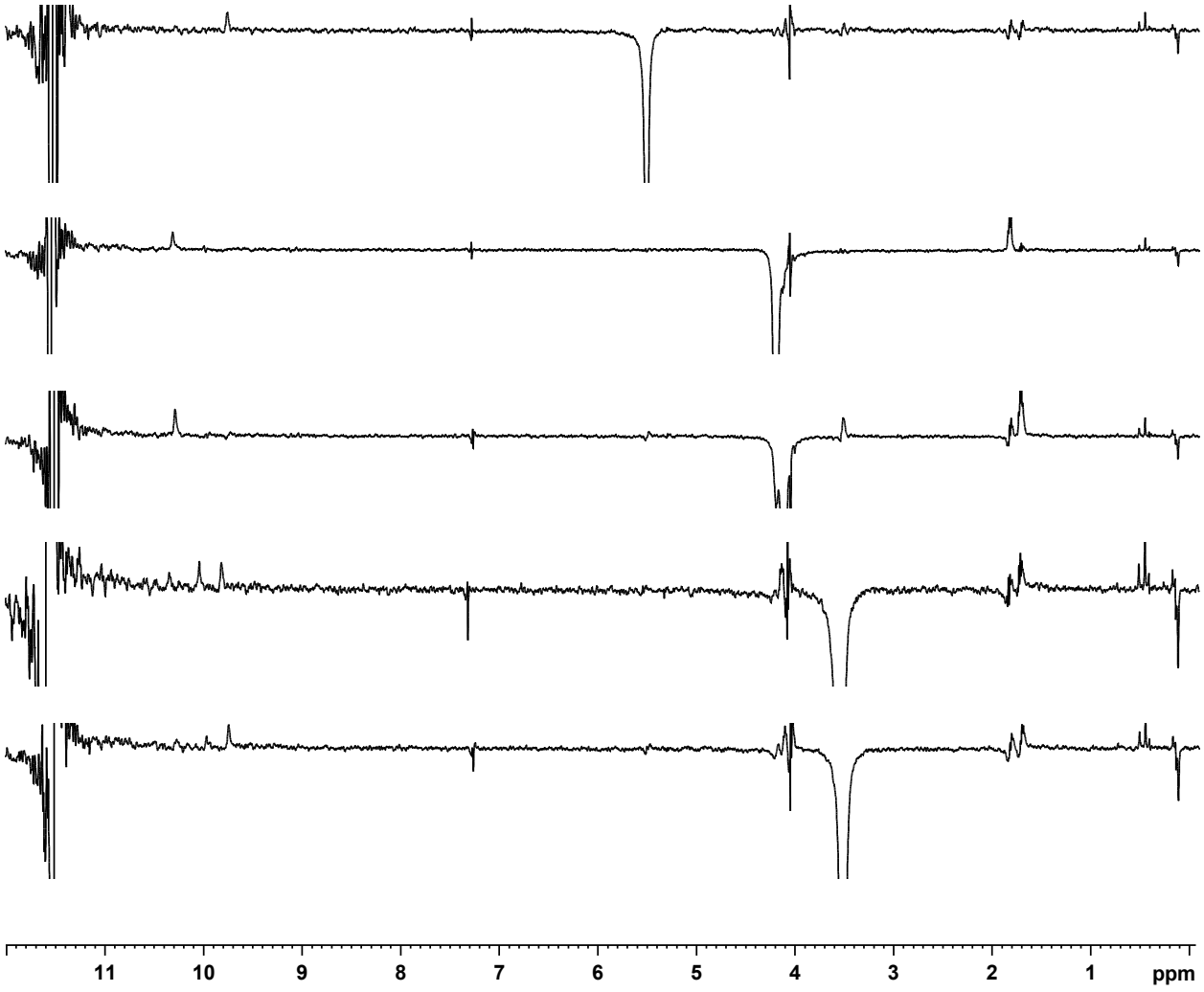

Figure A – 91: Selected nOe difference proton NMR spectra of **133**H^+ in TFA-$CDCl_3$

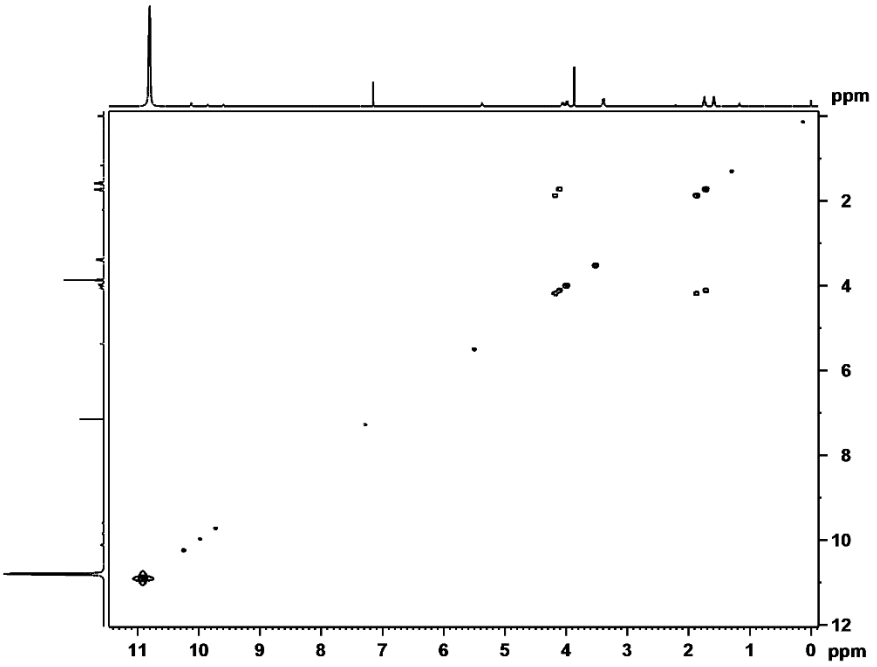

Figure A – 92: ^{1}H-^{1}H COSY NMR spectrum of **133**H^{+} in TFA-$CDCl_3$

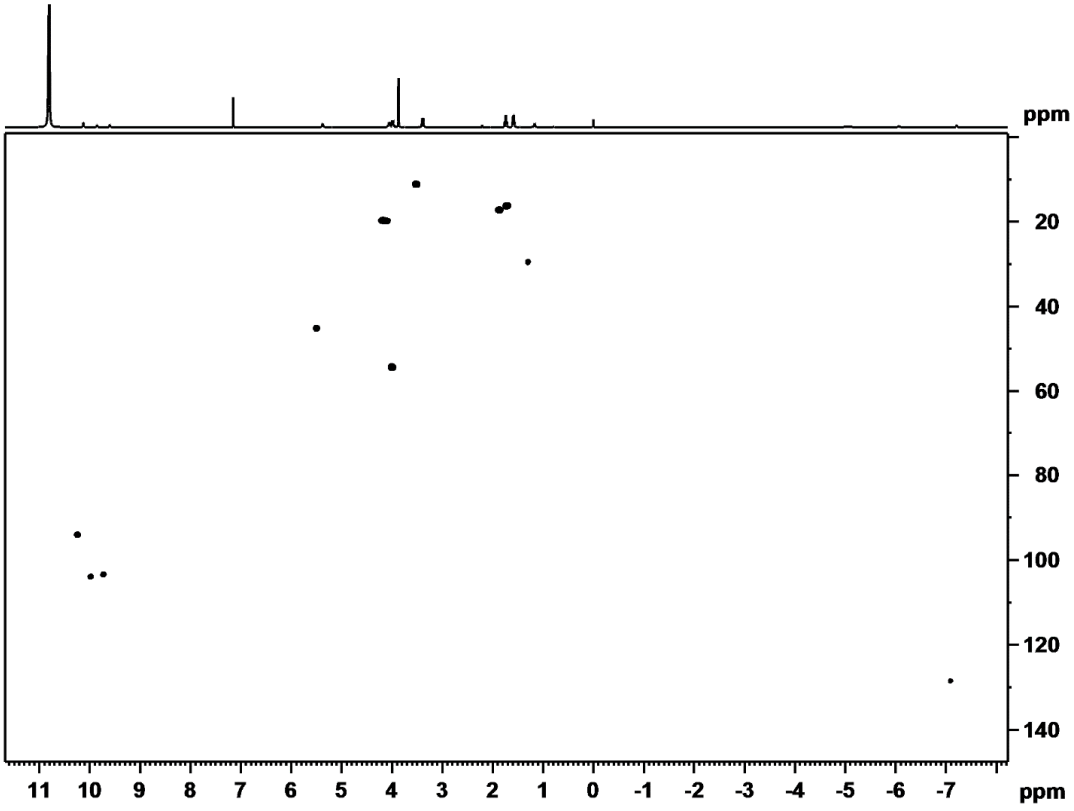

Figure A – 93: HSQC NMR spectrum of **133**H^{+} in TFA-$CDCl_3$

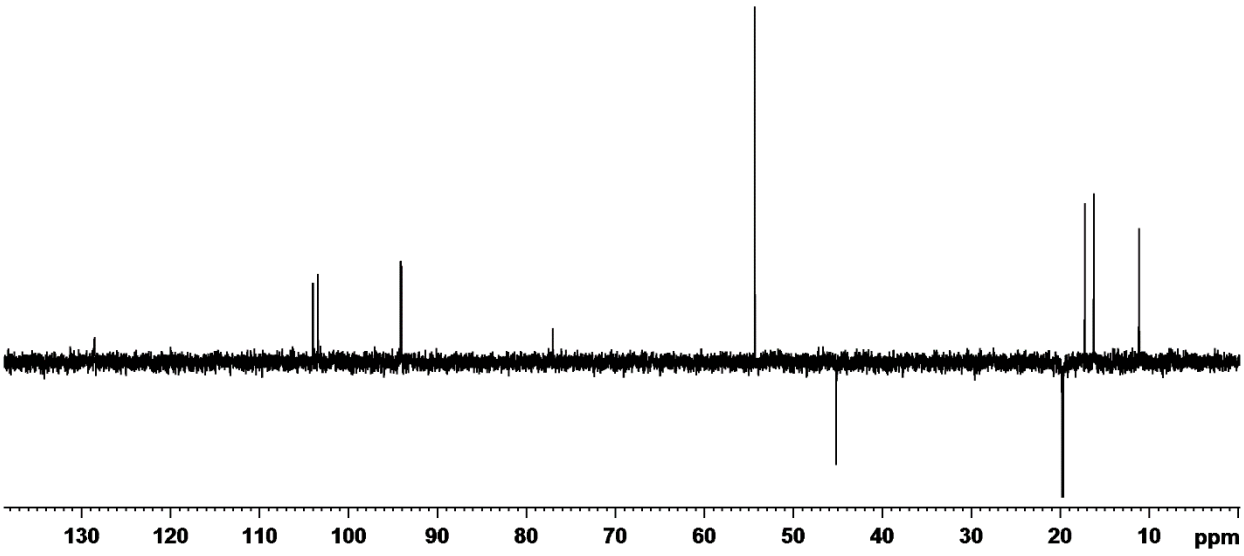

Figure A – 94: DEPT-135 NMR spectrum of **133**H^+ in TFA-$CDCl_3$

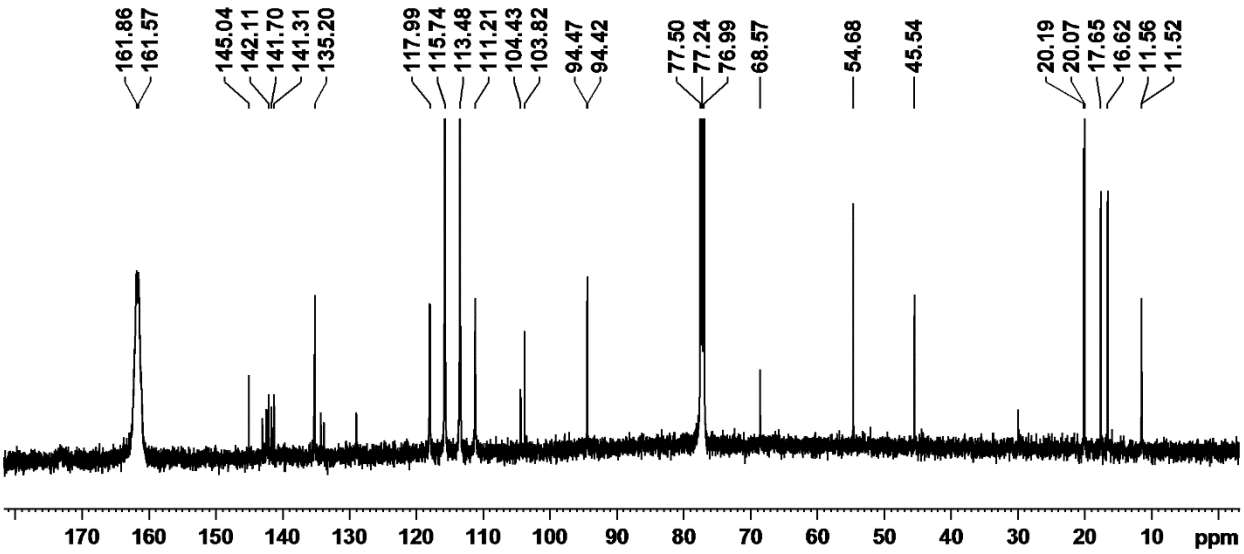

Figure A – 95: 125 MHz carbon-13 NMR spectrum of **133**H^+ in TFA-$CDCl_3$

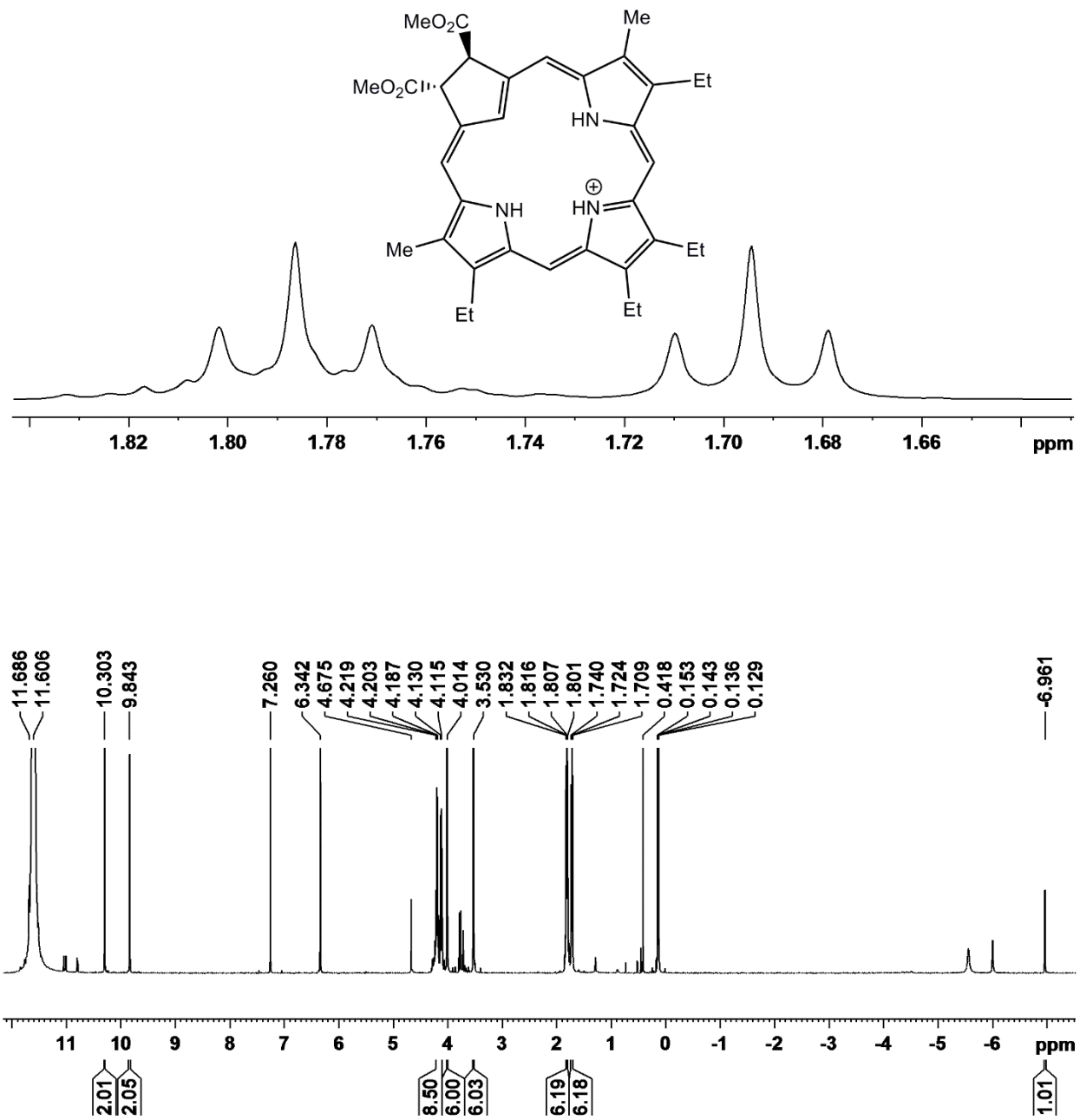

Figure A – 96: 500 MHz ^{1}H NMR Spectrum of **117**H^{+} in TFA-$CDCl_3$

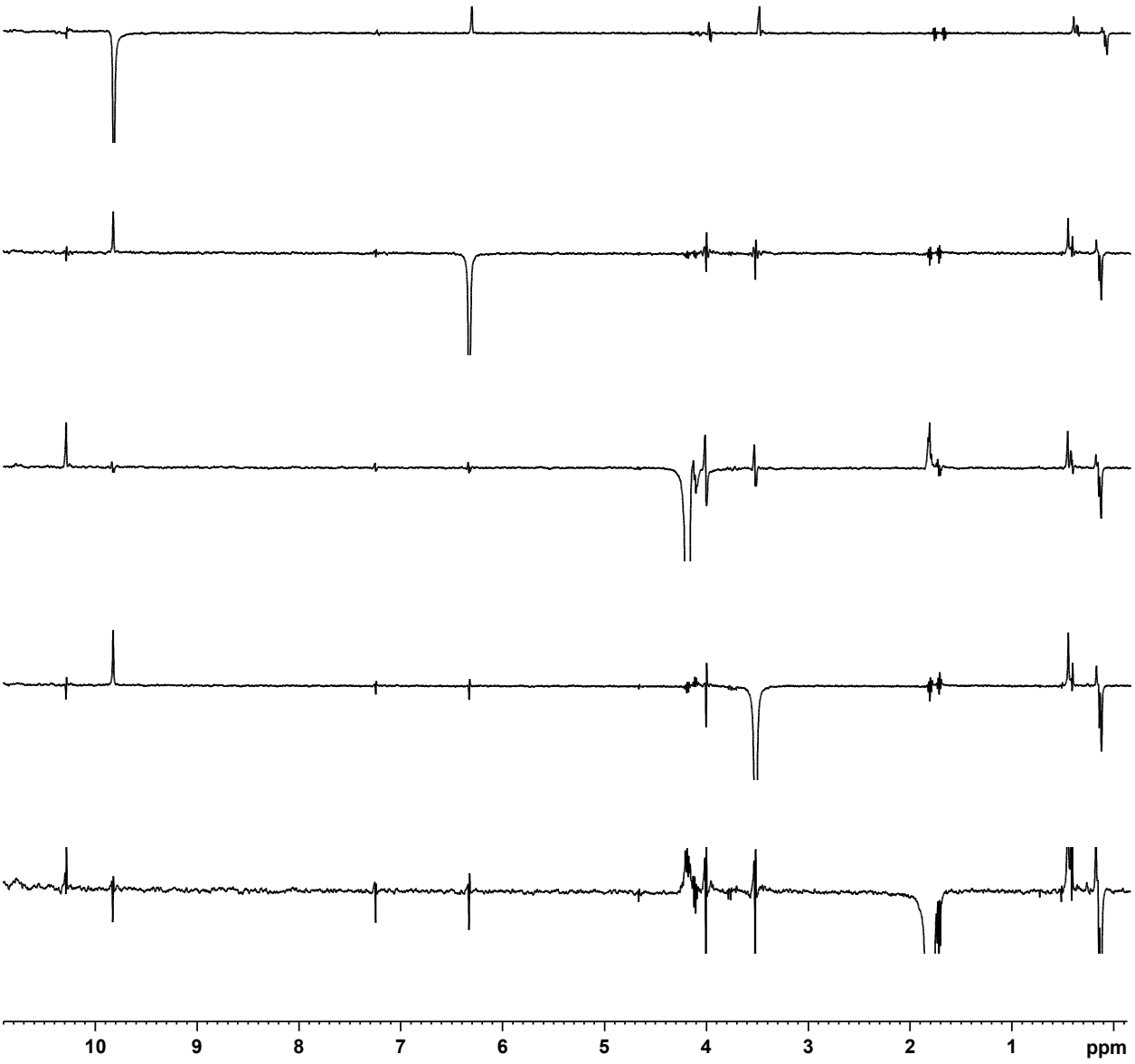

Figure A – 97: Selected nOe difference proton NMR spectra of **117**H^+ in TFA-$CDCl_3$

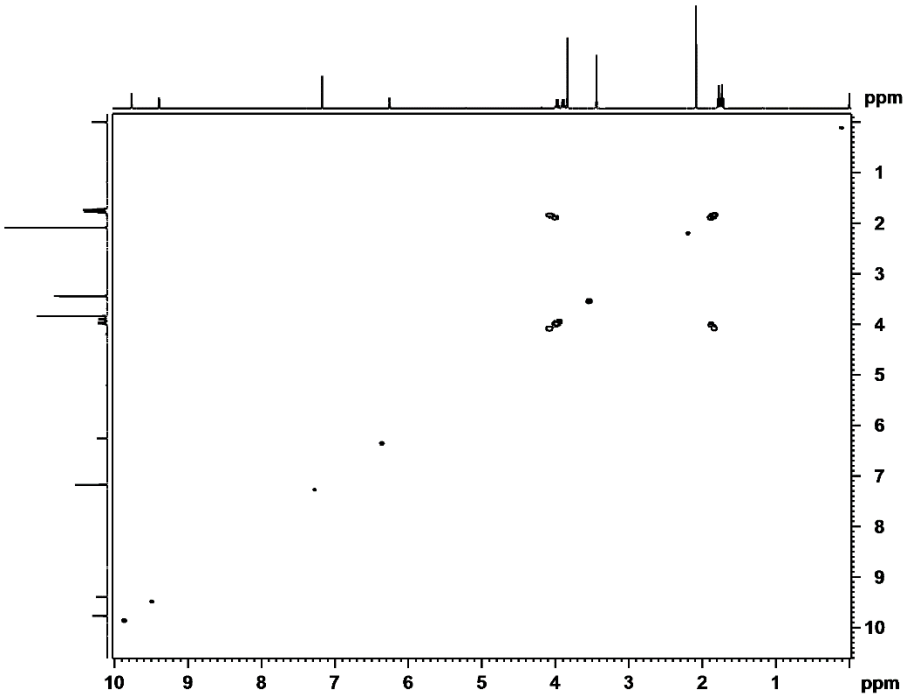

Figure A – 98: ^{1}H-^{1}H COSY NMR spectrum of **117**H^{+} in TFA-CDCl$_3$

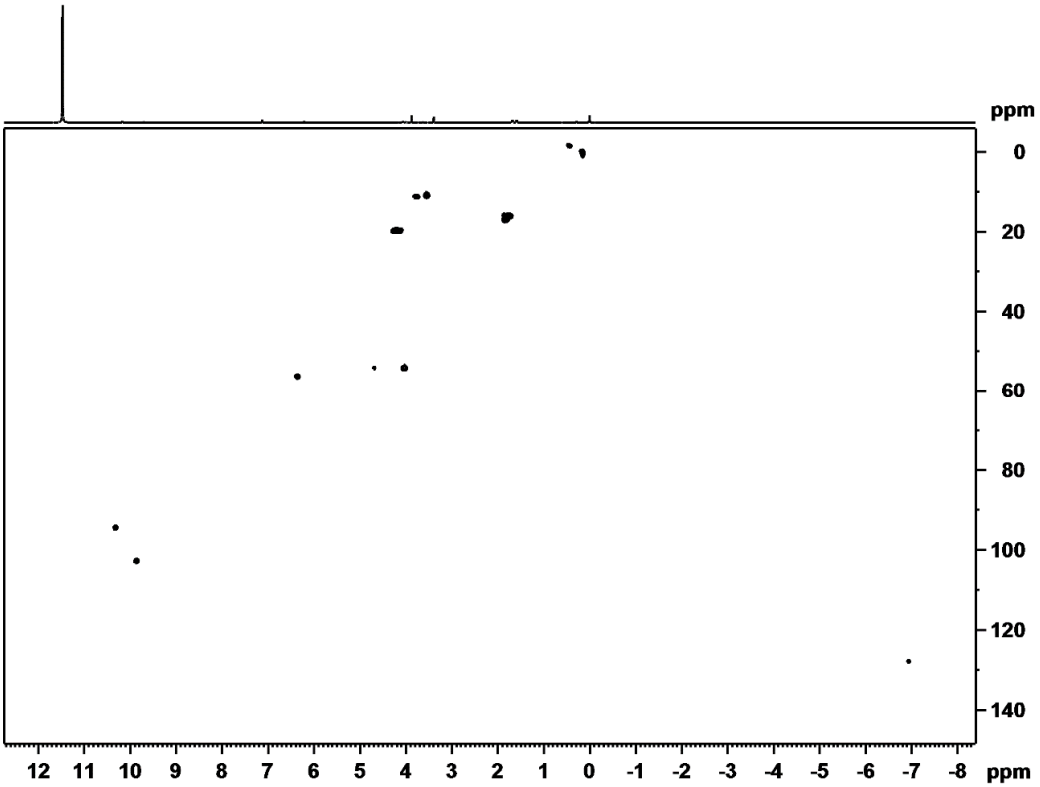

Figure A – 99: HSQC NMR spectrum of **117**H^{+} in TFA-CDCl$_3$

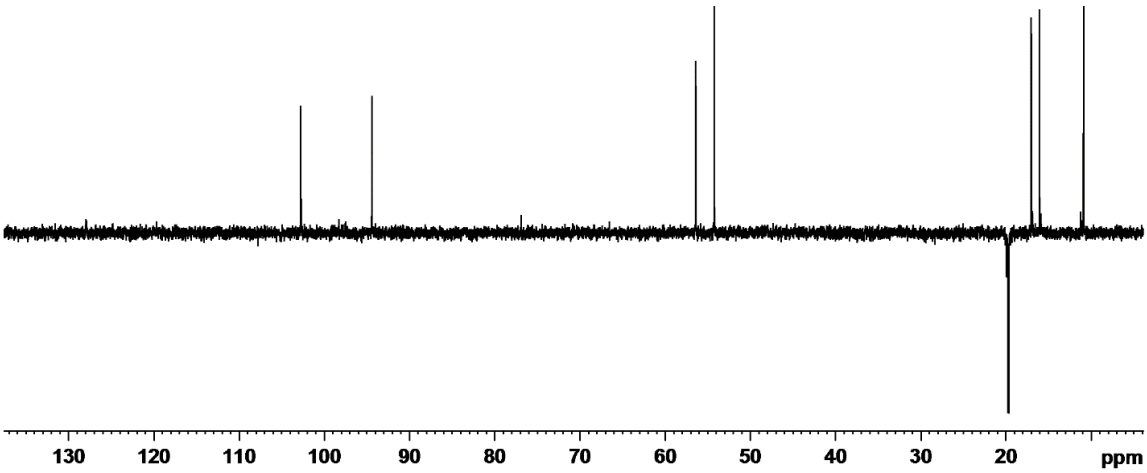

Figure A – 100: DEPT-135 NMR spectrum of **117**H^+ in TFA-$CDCl_3$

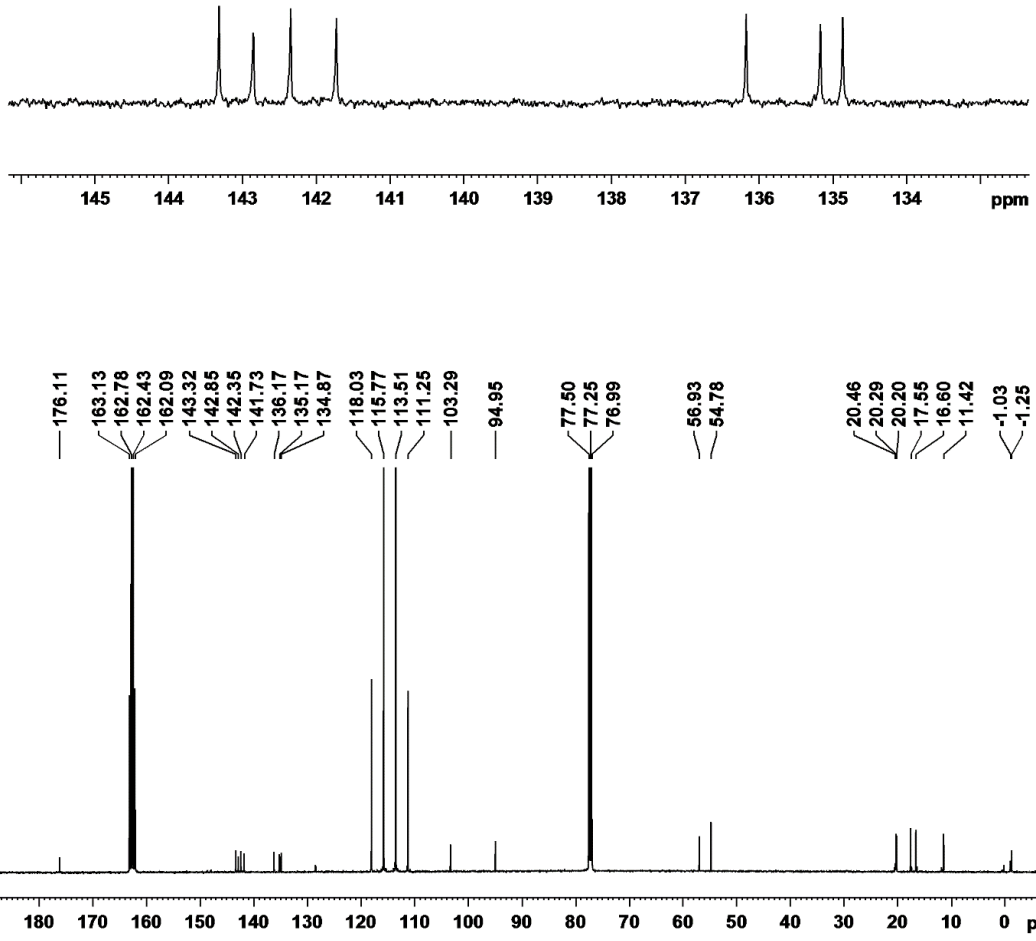

Figure A – 101: 125 MHz carbon-13 NMR spectrum of **117**H^+ in TFA-$CDCl_3$

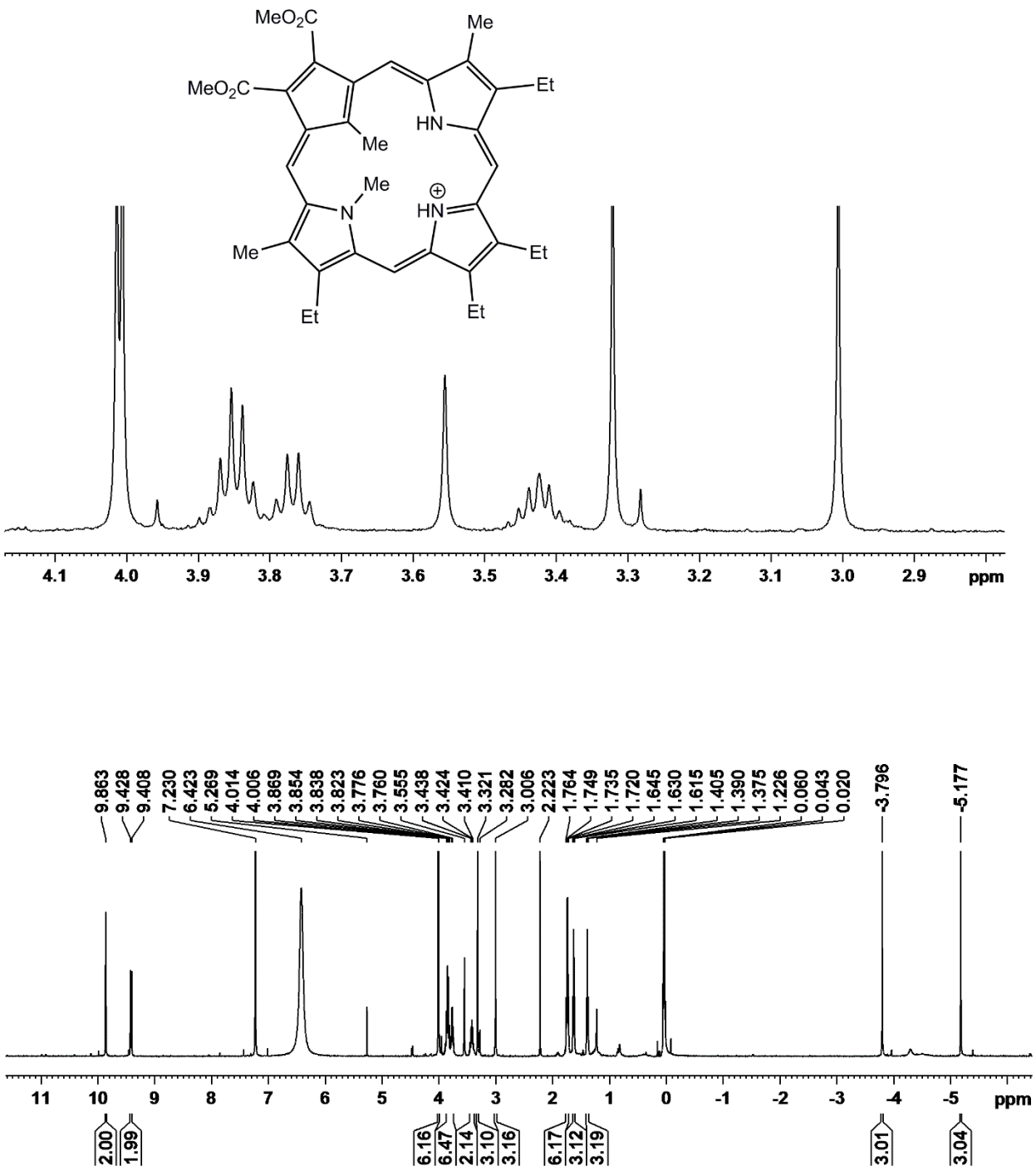

Figure A – 102: 500 MHz ^{1}H NMR Spectrum of **121**H^{+} in TFA-$CDCl_3$

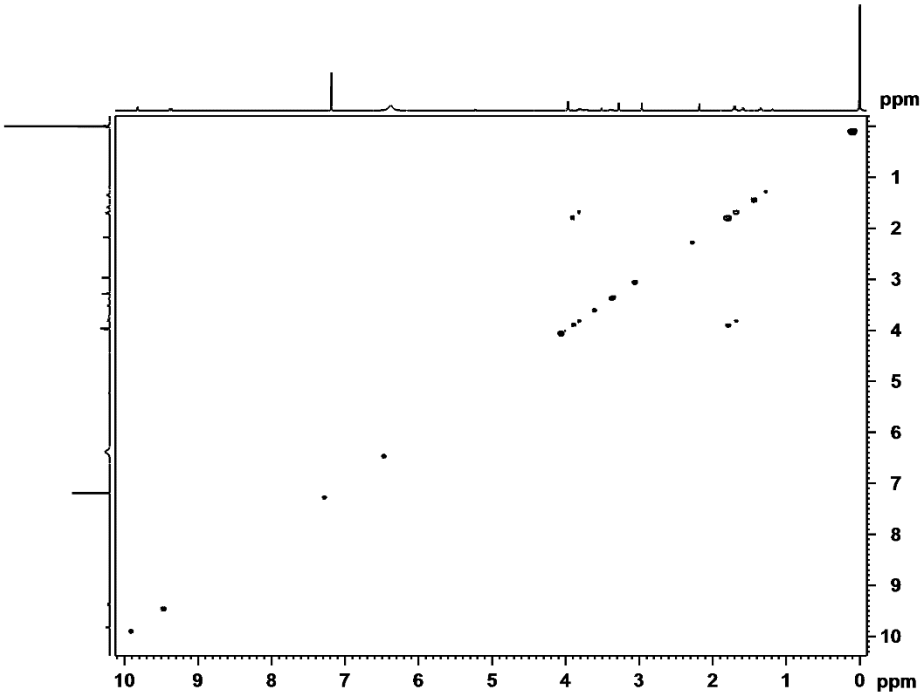

Figure A – 103: ^{1}H-^{1}H COSY NMR spectrum of **121**H^{+}in TFA-$CDCl_3$

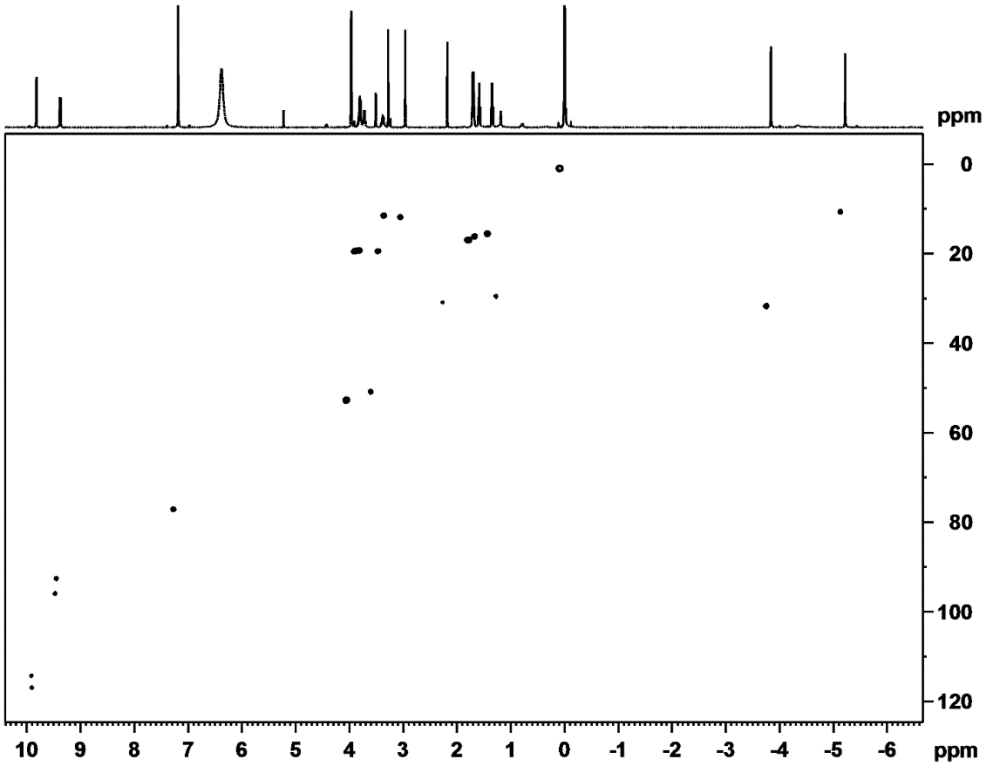

Figure A – 104: HSQC NMR spectrum of **121**H^{+} in TFA-$CDCl_3$

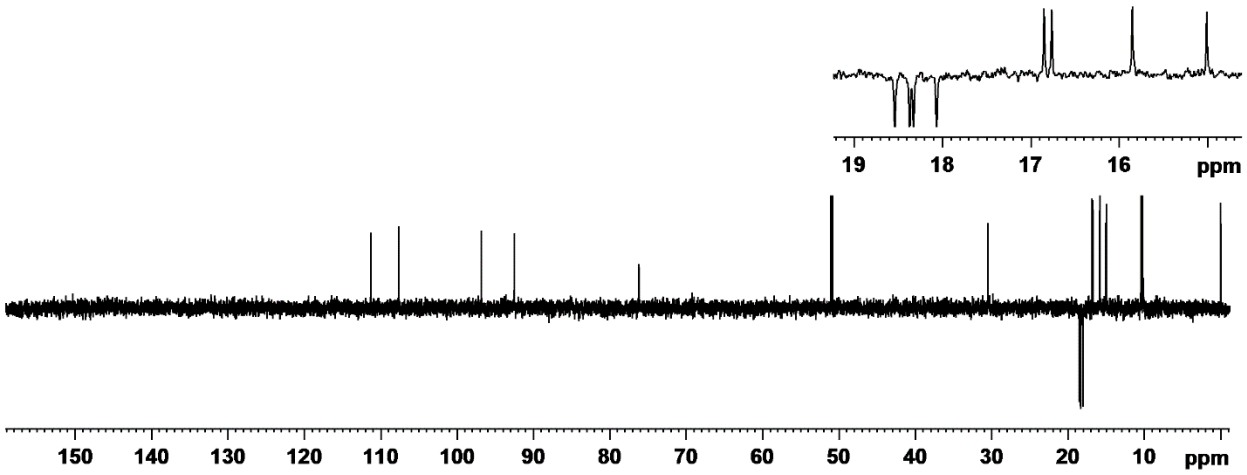

Figure A – 105: DEPT-135 NMR spectrum of **121**H^+ in TFA-$CDCl_3$

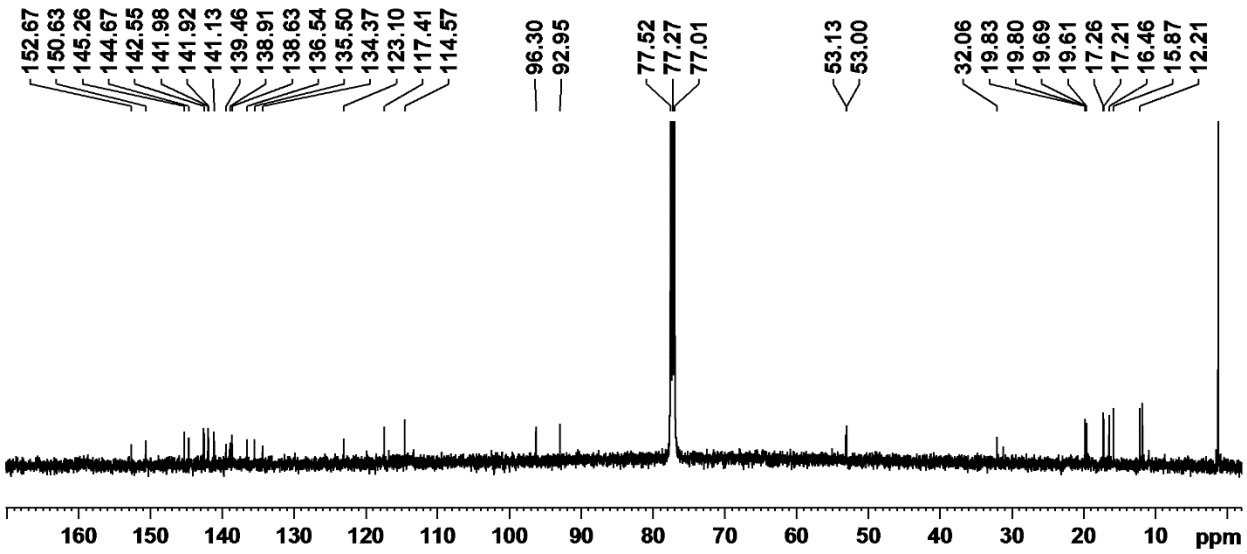

Figure A – 106: 125 MHz carbon-13 NMR spectrum of **121**H^+ in TFA-$CDCl_3$

APPENDIX B

SELECTED UV-VIS SPECTRA

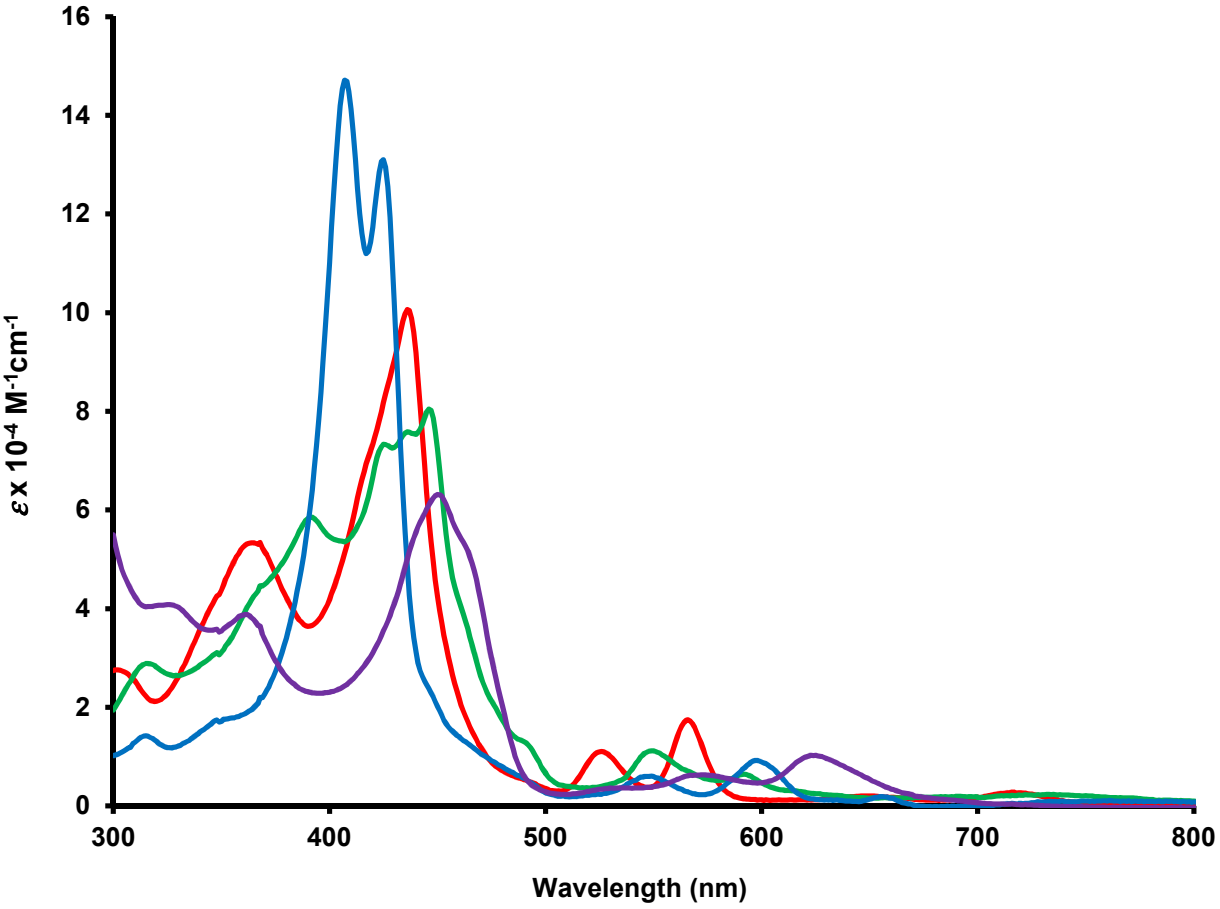

Figure B – 1: UV-Vis Spectra of **98** in dichloromethane (red line, free base), CH_2Cl_2 with 100 equiv TFA (green line, monocation), 50% TFA-CH_2Cl_2 (blue line, dication) and 5% DBU-CH_2Cl_2 (purple line, monoanion)

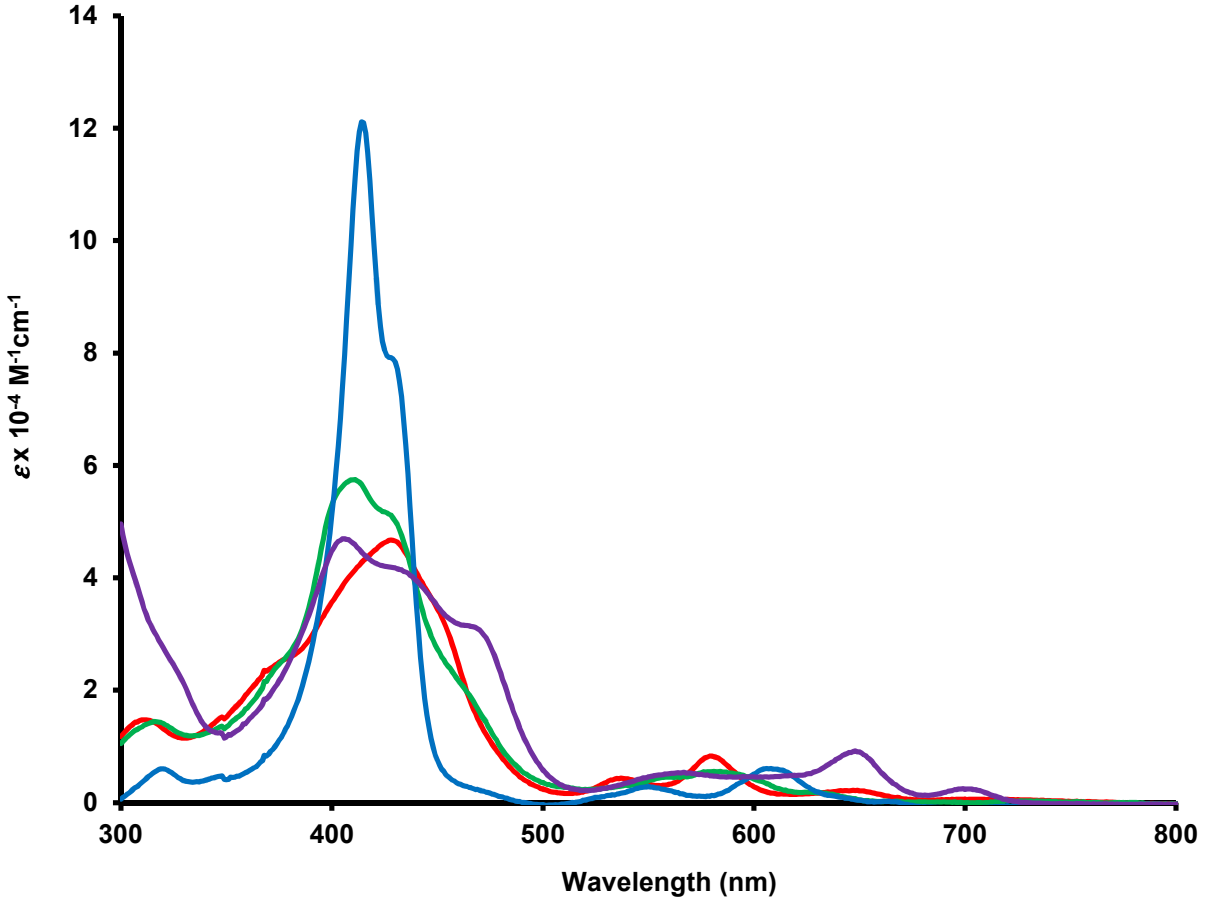

Figure B – 2: UV-vis spectra of **120** in dichloromethane (red line, free base), CH_2Cl_2 with 5 equiv TFA (green line, monocation), 25% TFA-CH_2Cl_2 (blue line, dication) and 5% DBU-CH_2Cl_2 (purple line, monoanion)

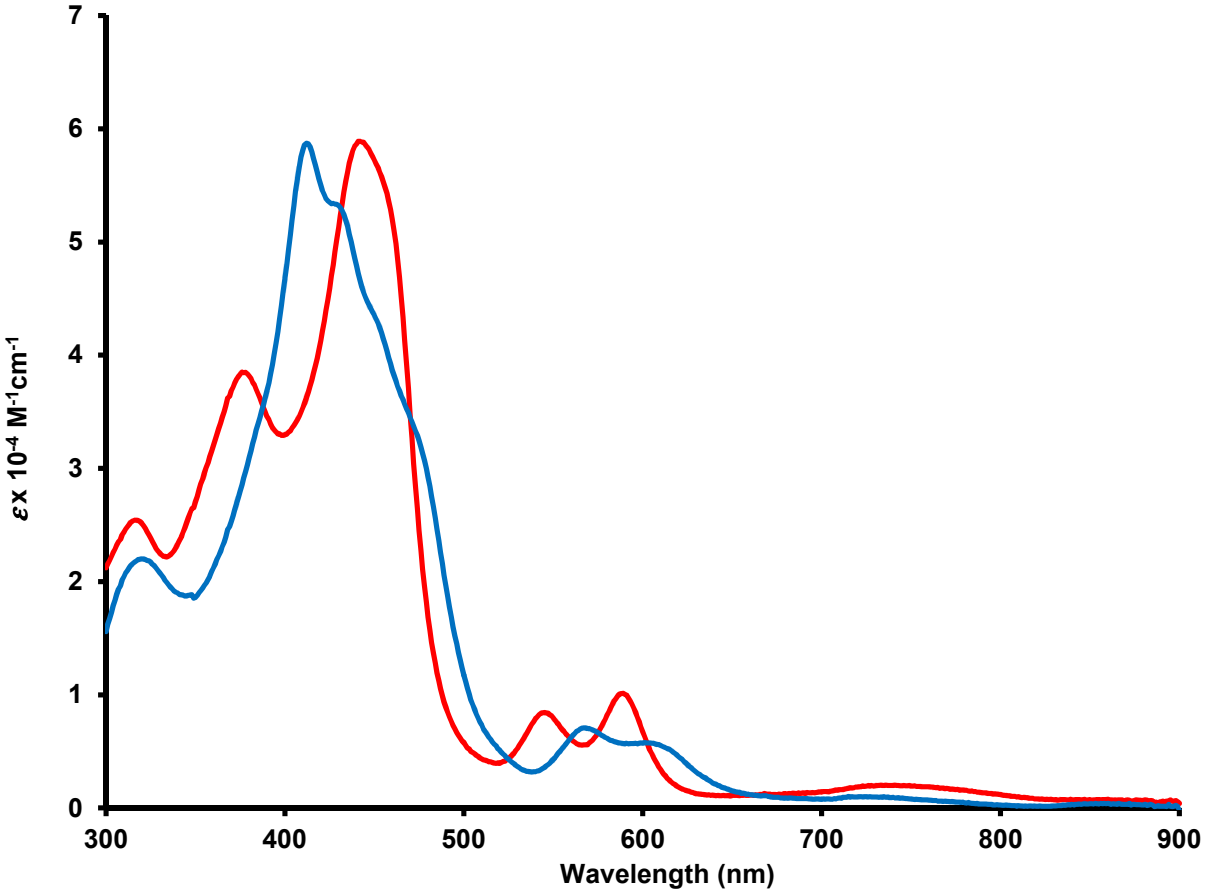

Figure B – 3: UV-vis spectra of **121** in 1% Et_3N-CH_2Cl_2 (red line, free base) and in CH_2Cl_2 with 50 equiv. TFA (blue line, monocation)

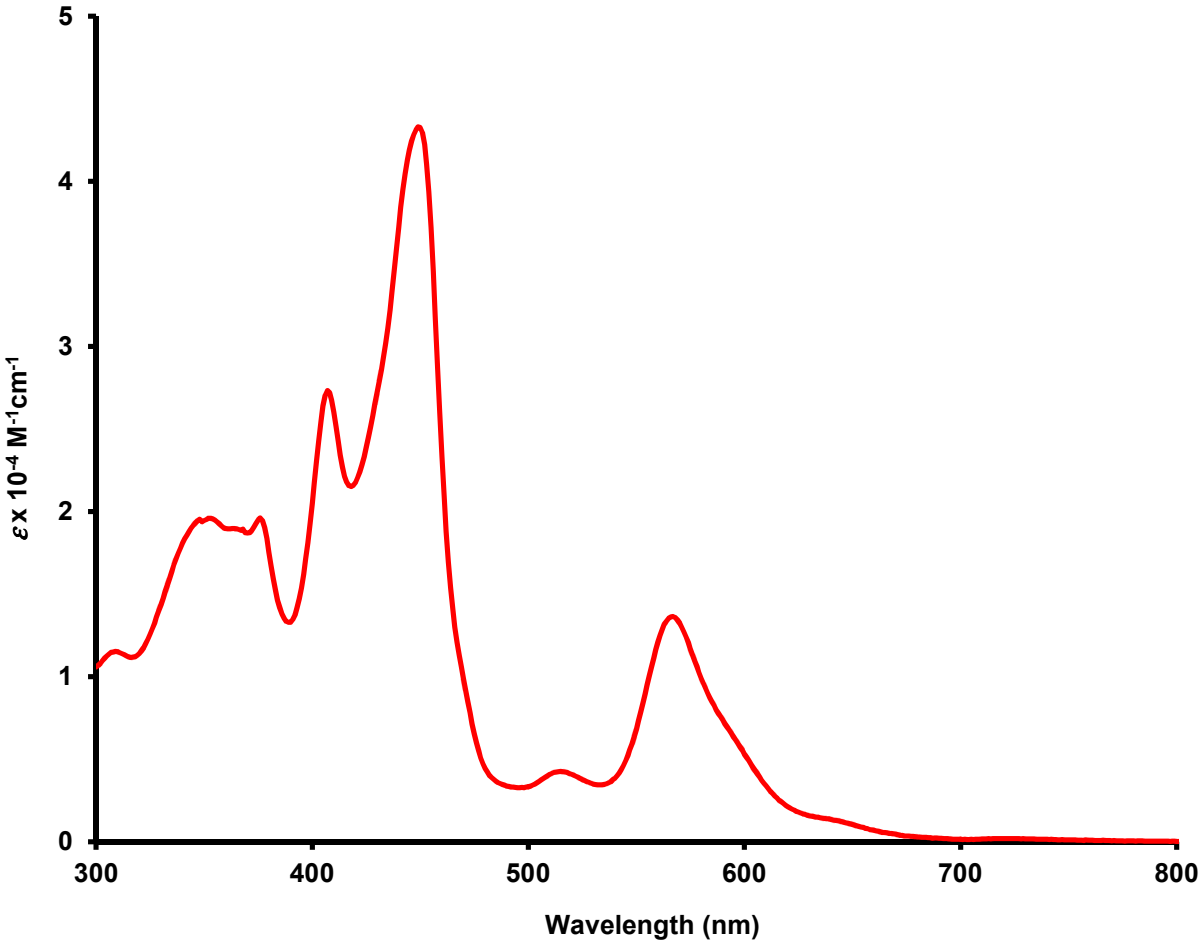

Figure B – 4: UV-vis spectrum of **118** in chloroform

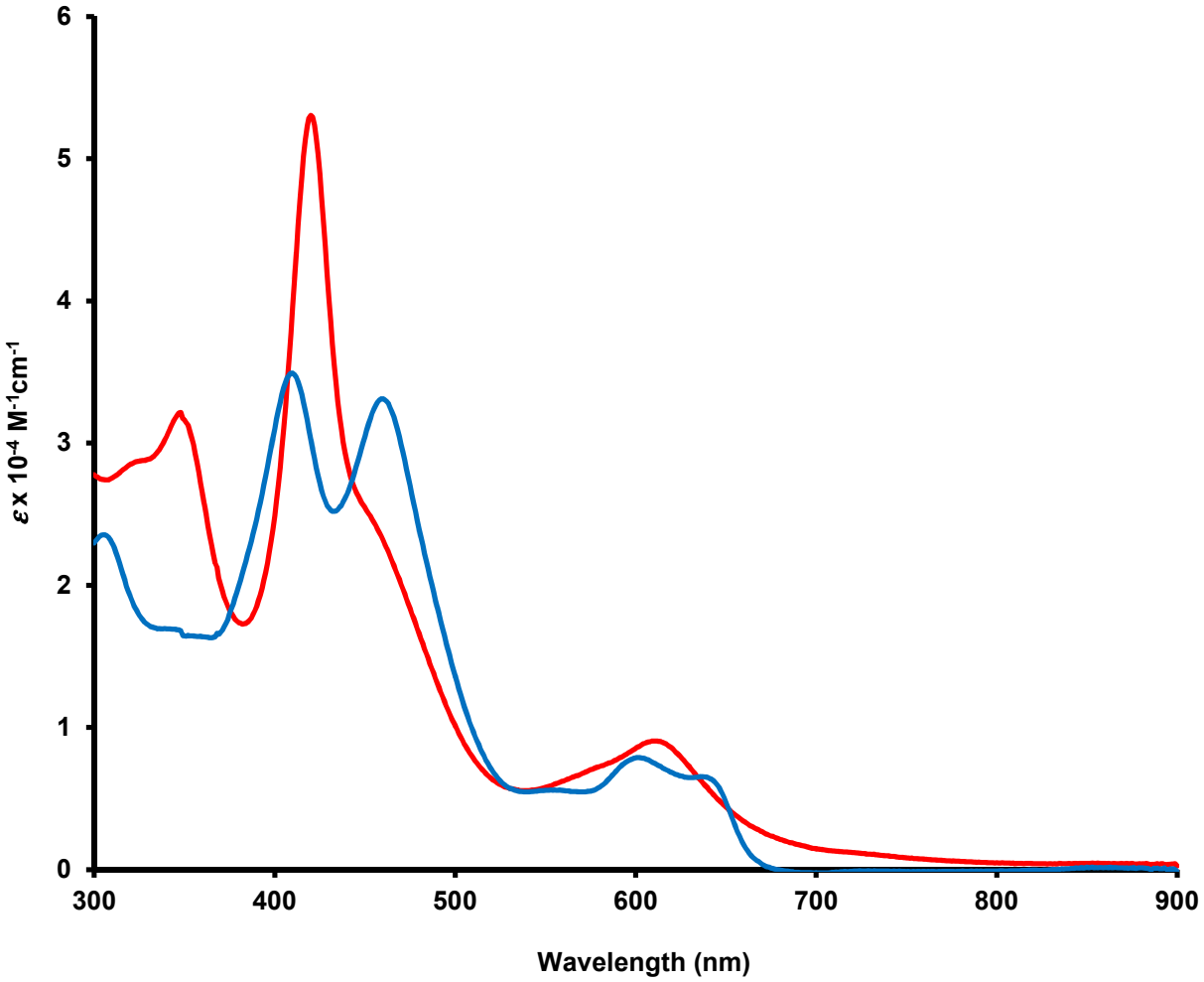

Figure B – 5: UV-vis spectra of **123** (red line) and **122** (blue line) in chloroform

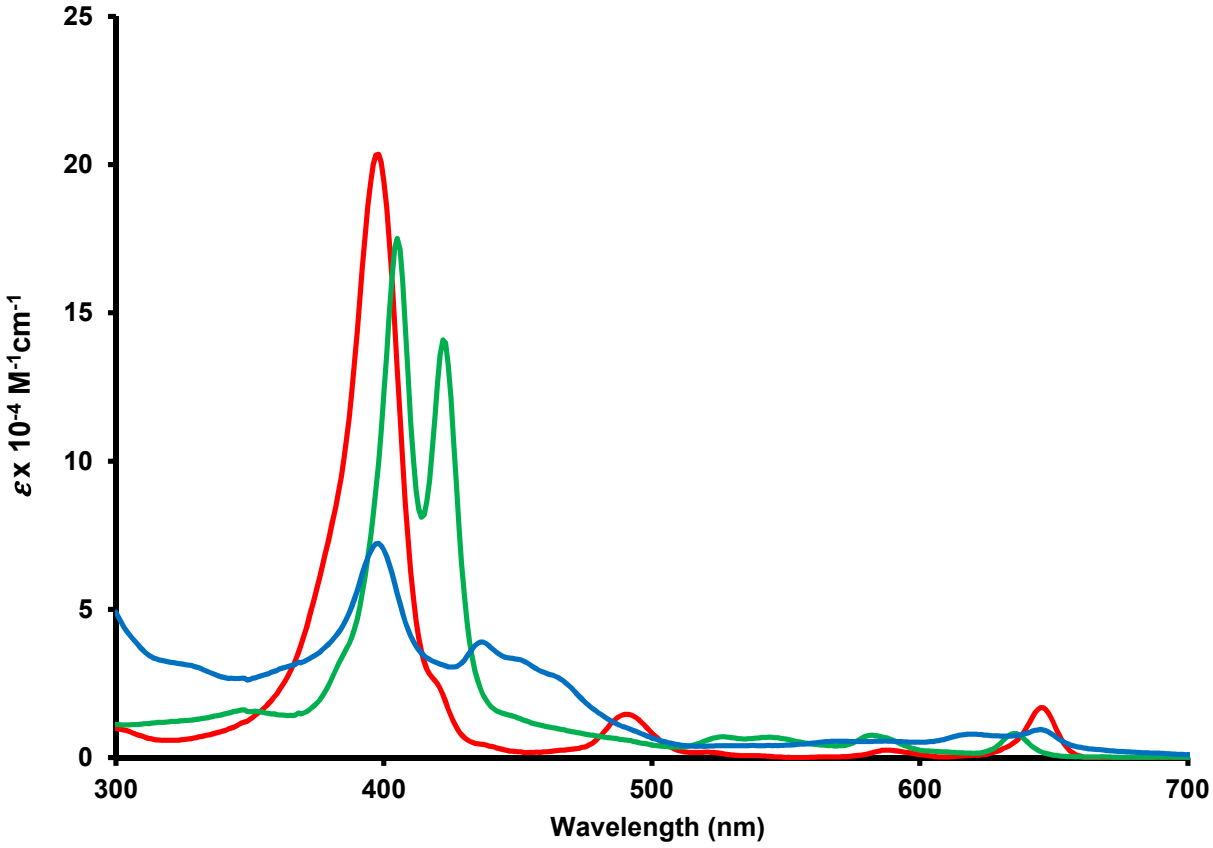

Figure B – 6: UV-vis spectra of **117** in dichloromethane (red line, free base), 5% TFA-dichloromethane (green line, monocation) and 5% DBU-dichloromethane (blue line)

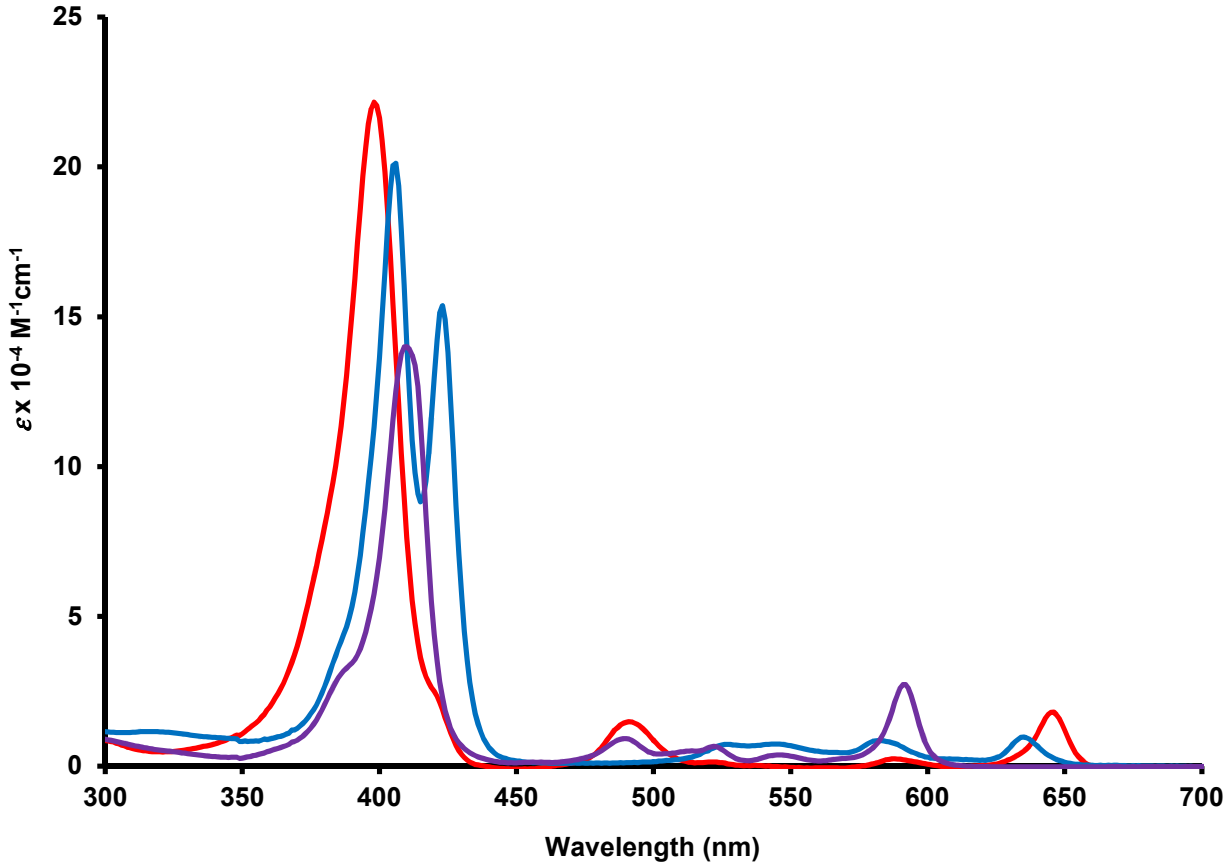

Figure B – 7: UV-vis spectra of carbachlorin **133** in dichloromethane (red line), carbachlorin monocation **133**H^+ in 5% TFA-dichloromethane and silver(III) chlorin **138** in dichloromethane (purple line)

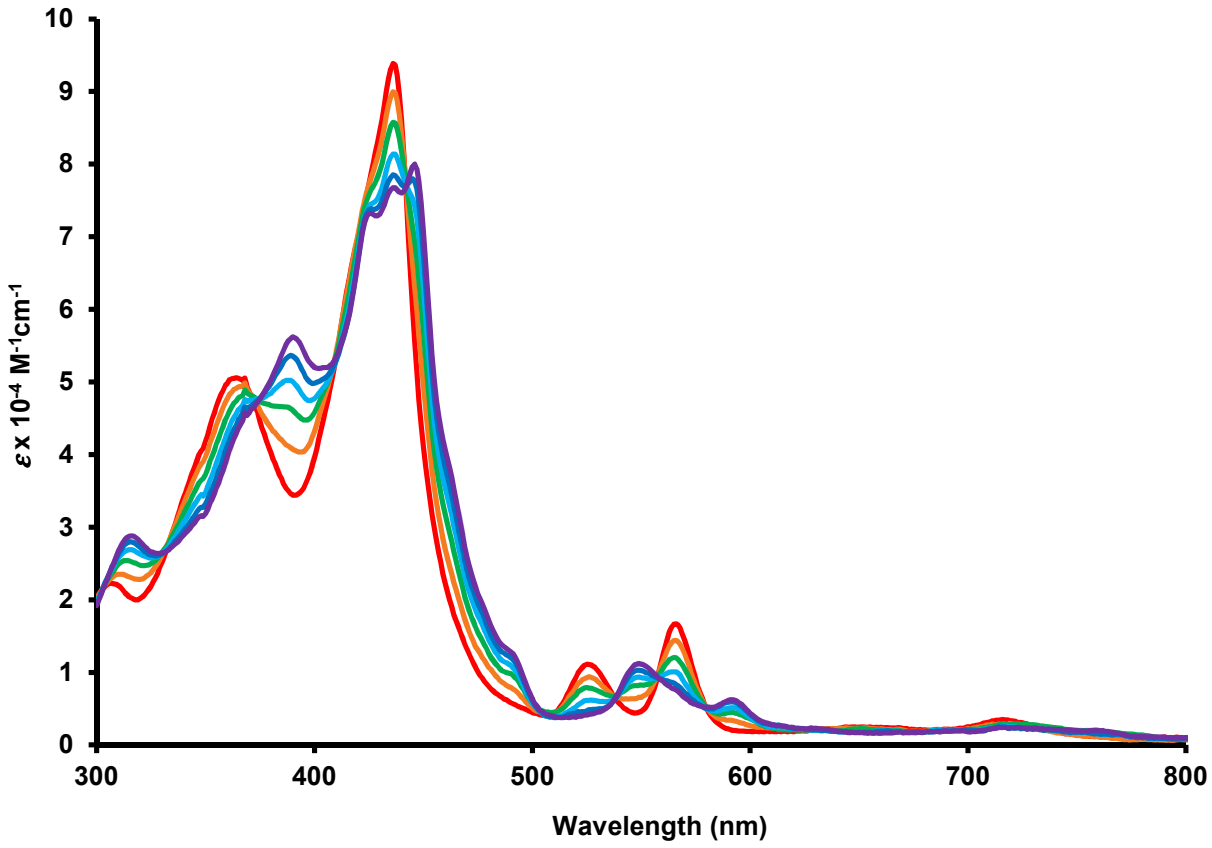

Figure B – 8: UV-vis spectra of **98** in dichloromethane with 0 equiv. TFA (red line), 2 equiv. TFA (orange line), 5 equiv. TFA (green line), 10 equiv. TFA (light blue line), 20 equiv. TFA (dark blue line) and 50 equiv. TFA (purple line)

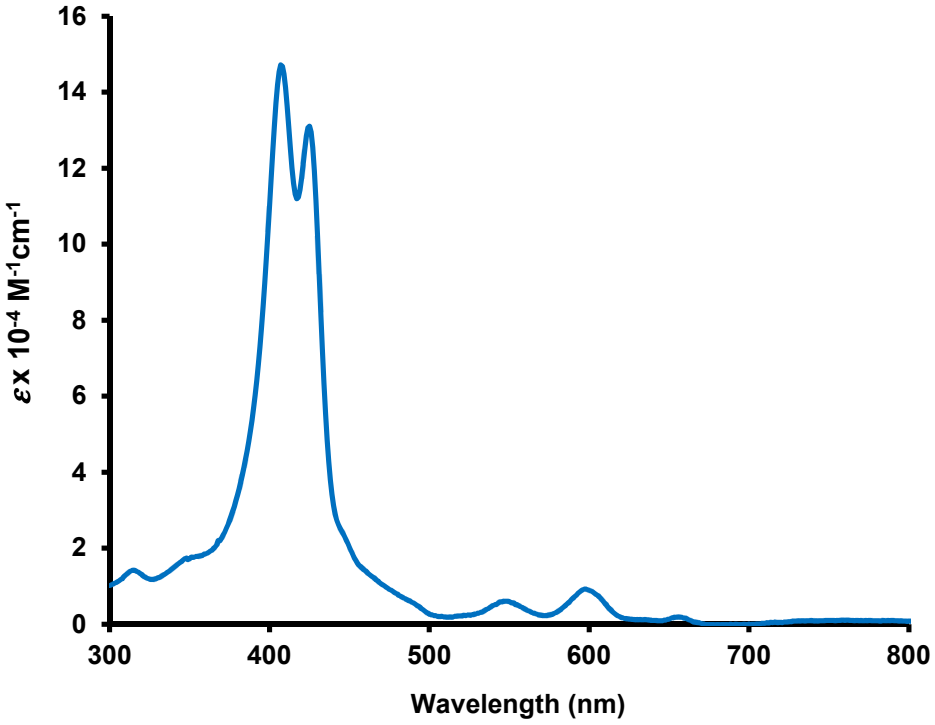

Figure B – 9: UV-vis spectrum of **98**H_2^{2+} in 50% TFA-CH_2Cl_2

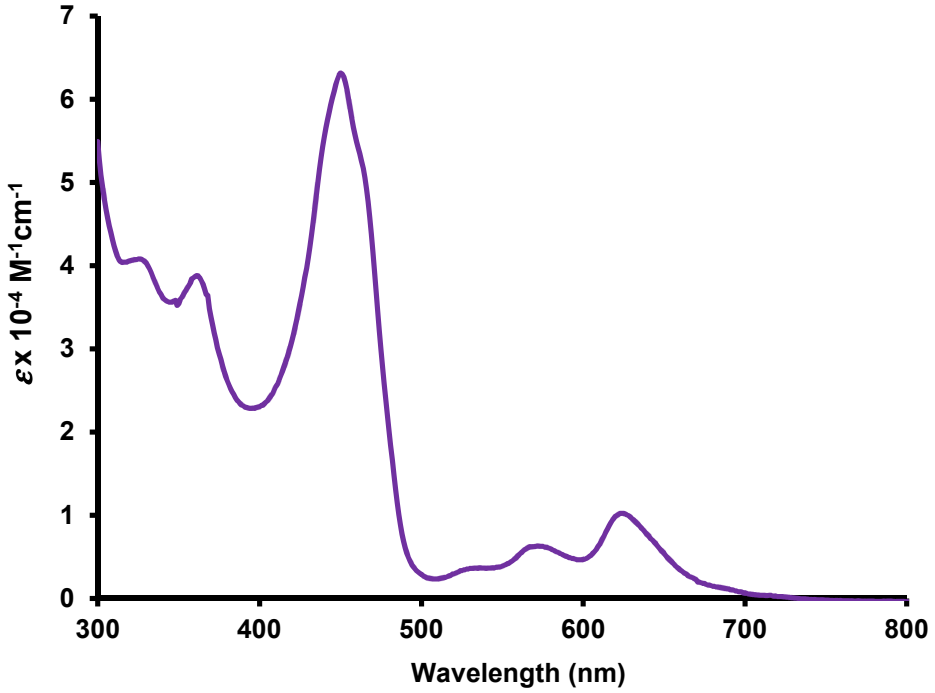

Figure B – 10: UV-vis spectrum of deprotonated carbaporphyrin **98** in 5% DBU

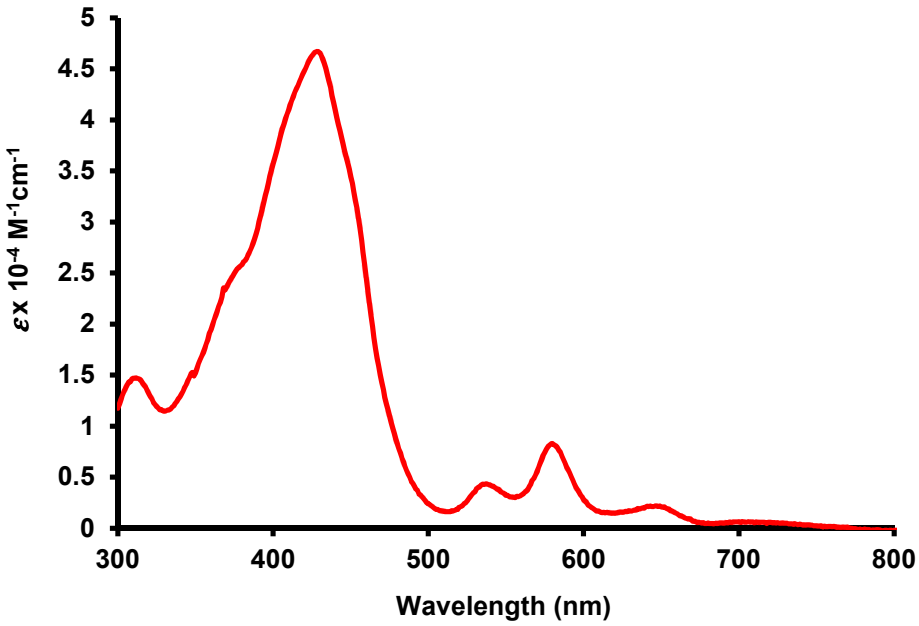

Figure B – 11: UV-vis spectrum of **120** in dichloromethane

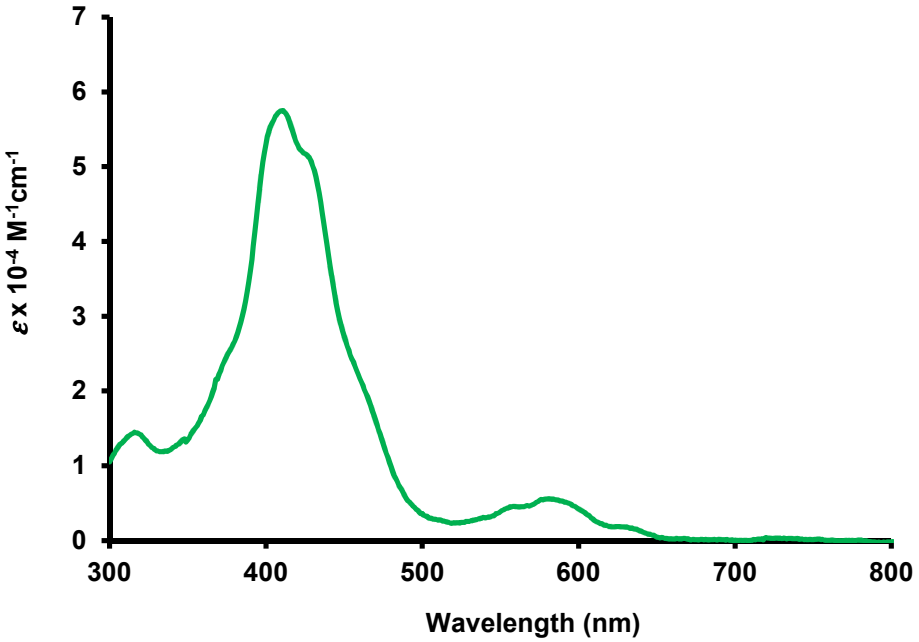

Figure B – 12: UV-vis spectrum of monoprotonated **120** in dichloromethane with 5 equiv TFA

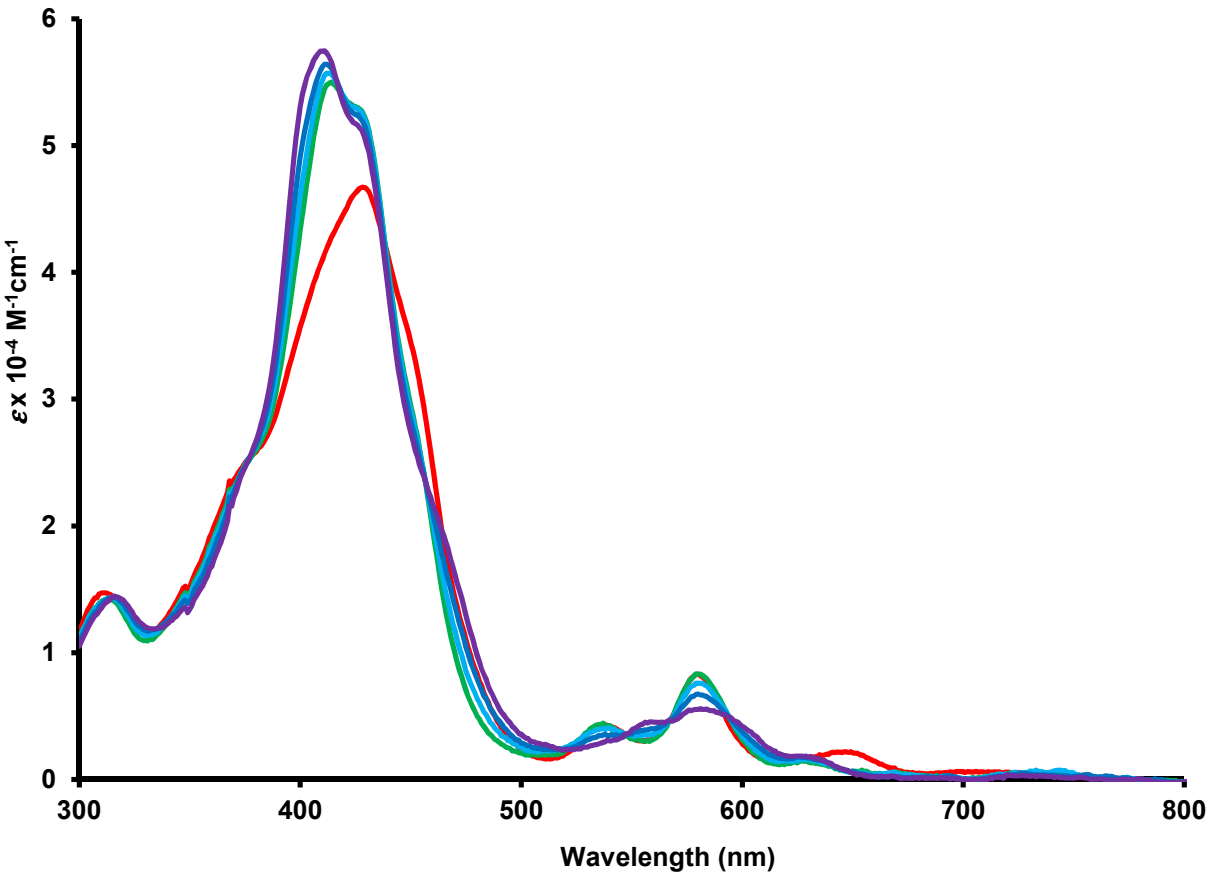

Figure B – 13: UV-vis spectra of **120** in dichloromethane with 0 equiv. TFA (red line), 0.5 equiv. TFA (green line), 1 equiv. TFA (light blue line), 2 equiv. TFA (dark blue line) and 5 equiv. TFA (purple line)

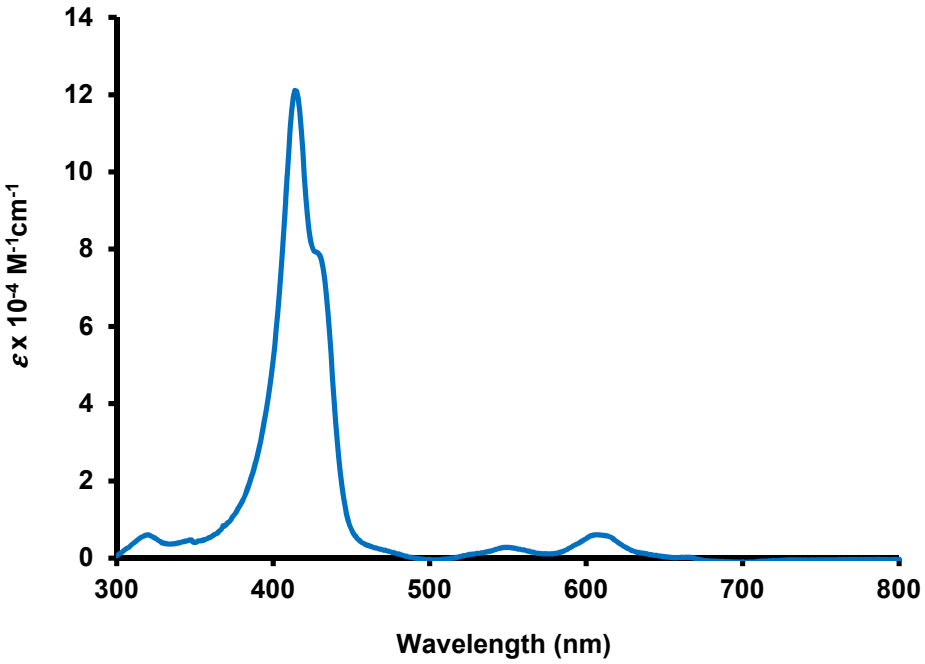

Figure B – 14: UV-vis spectrum of diprotonated **120** in 25% TFA-CH_2Cl_2

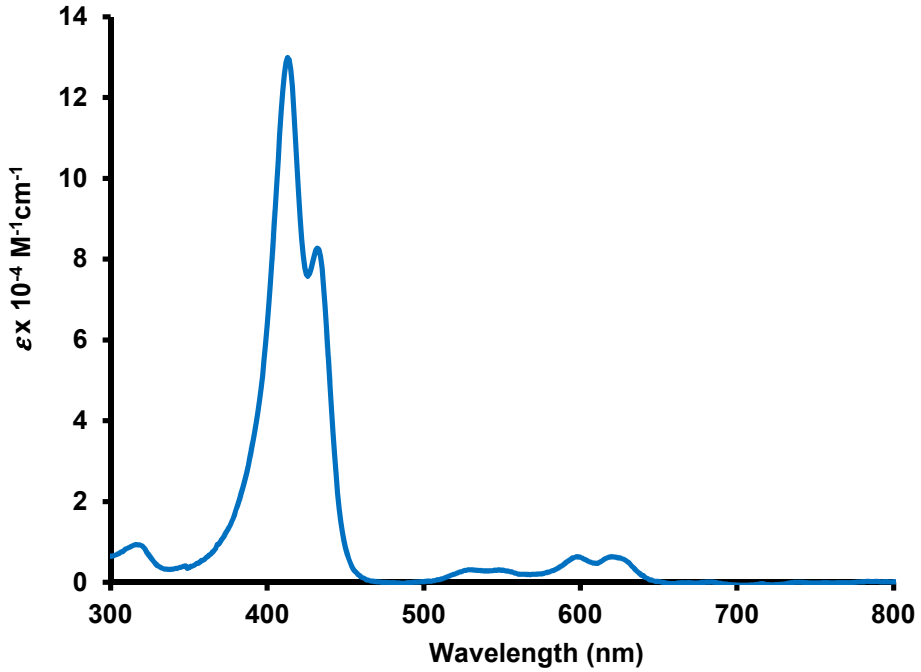

Figure B – 15: UV-vis spectrum of **120** in 50% TFA-CH_2Cl_2

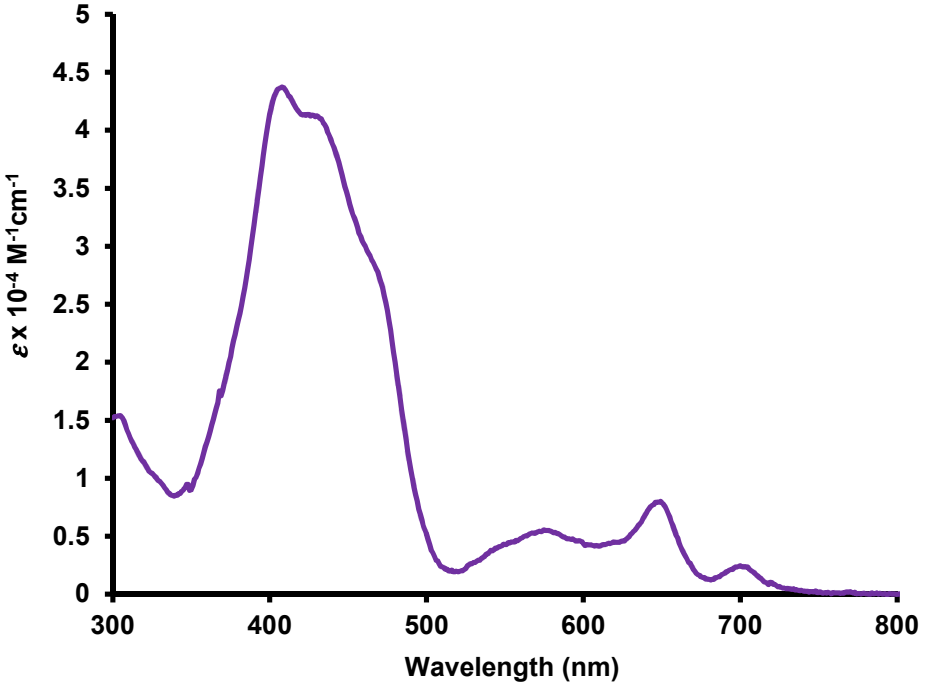

Figure B – 16: UV-vis spectrum of **120** in 1% Et_3N-dichloromethane showing partial deprotonation

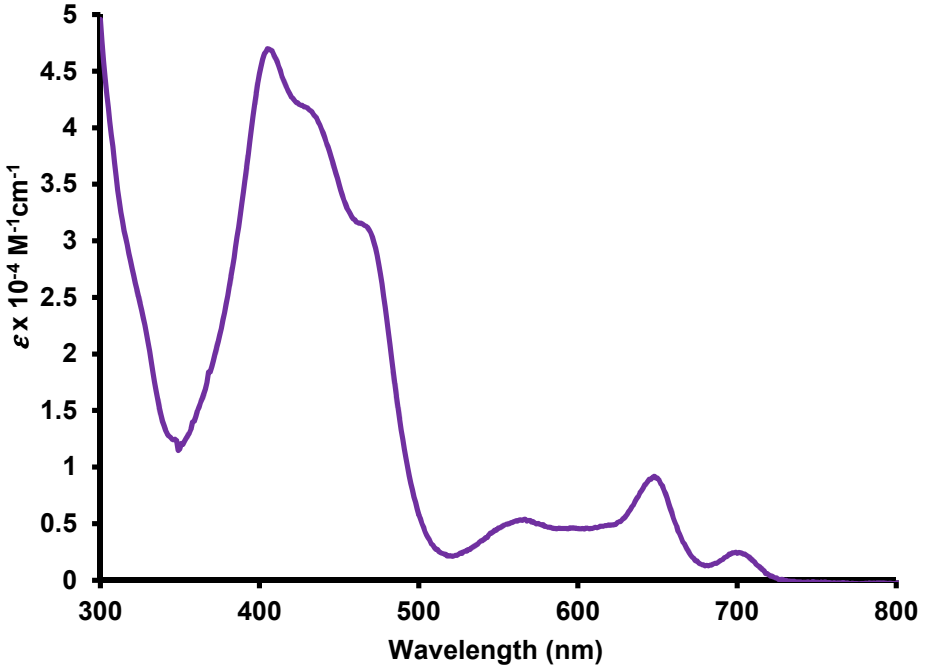

Figure B – 17: UV-vis spectrum of monodeprotonated **120** in 5% DBU-CH_2Cl_2

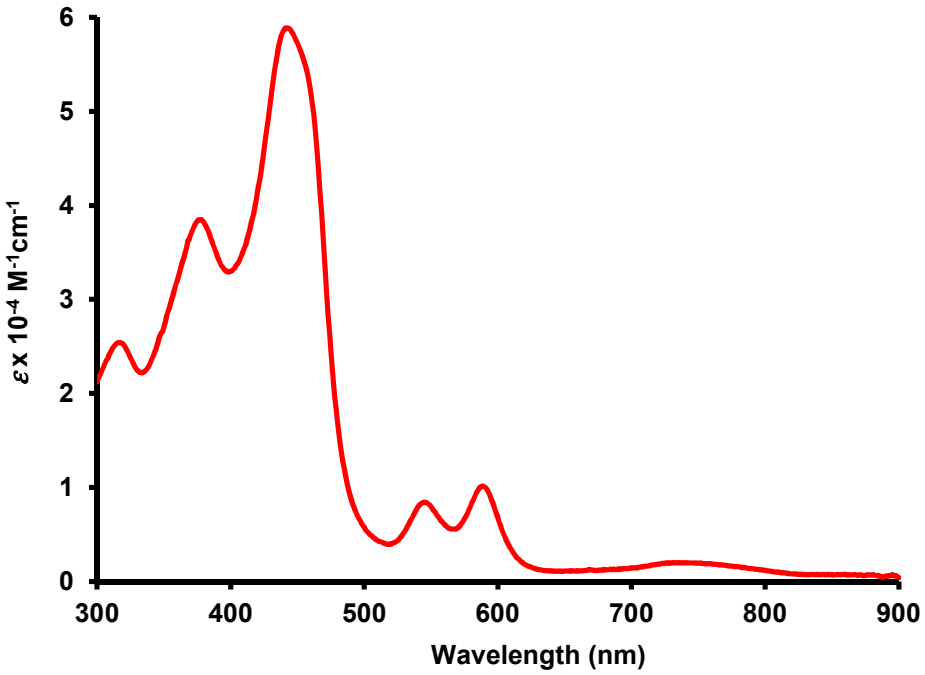

Figure B – 18: UV-vis spectrum of **121** in 1% Et_3N-CH_2Cl_2 (free base)

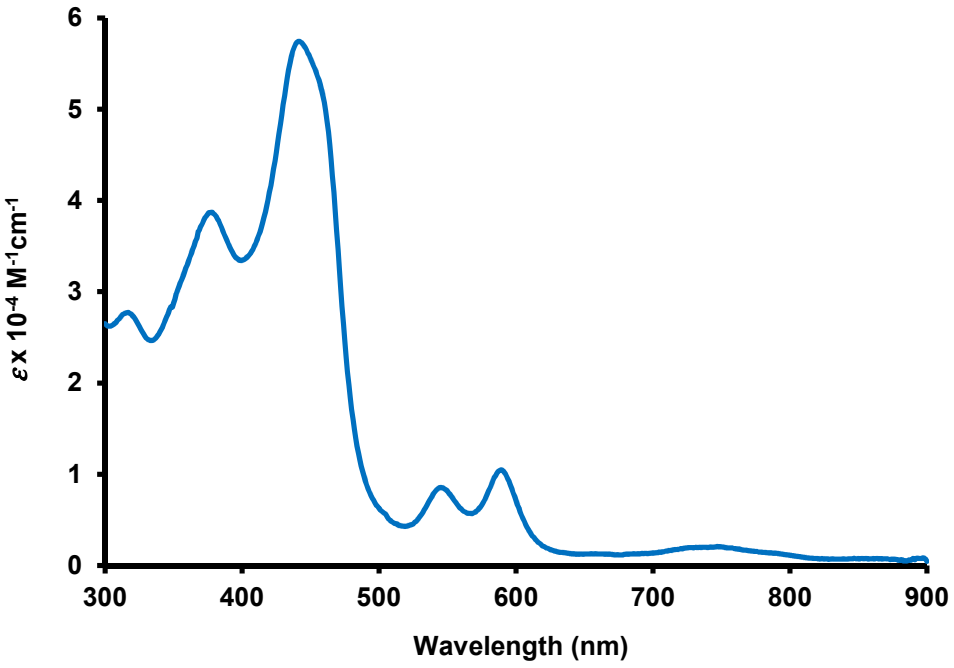

Figure B – 19: UV-vis spectrum of dimethylcarbaporphyrin **121** in 5% DBU-CH_2Cl_2

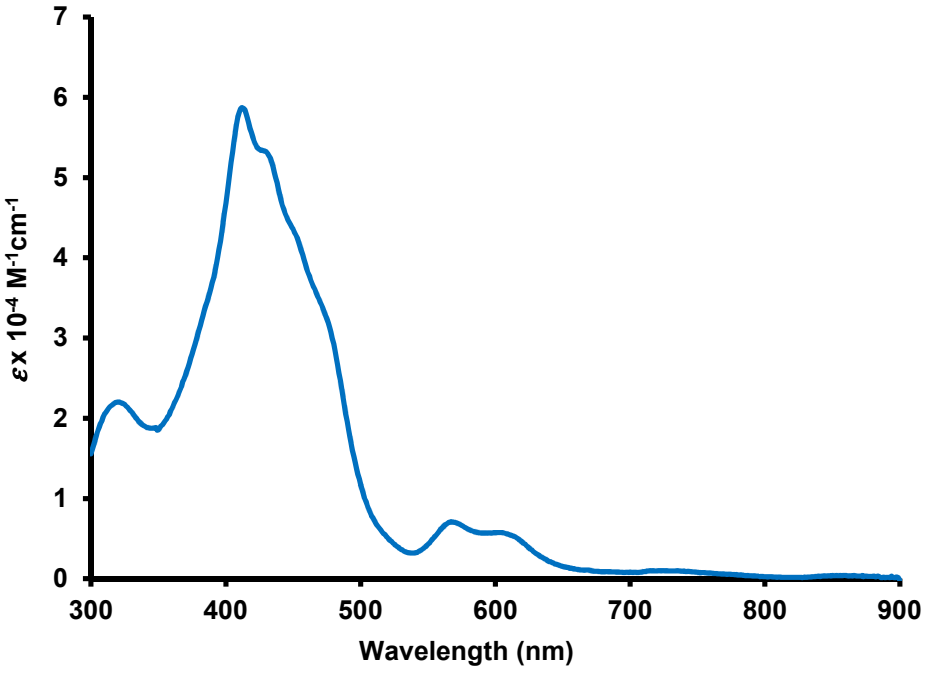

Figure B – 20: UV-vis spectrum of monoprotonated dimethylcarbaporphyrin **121** in in CH_2Cl_2 with 50 equiv. TFA

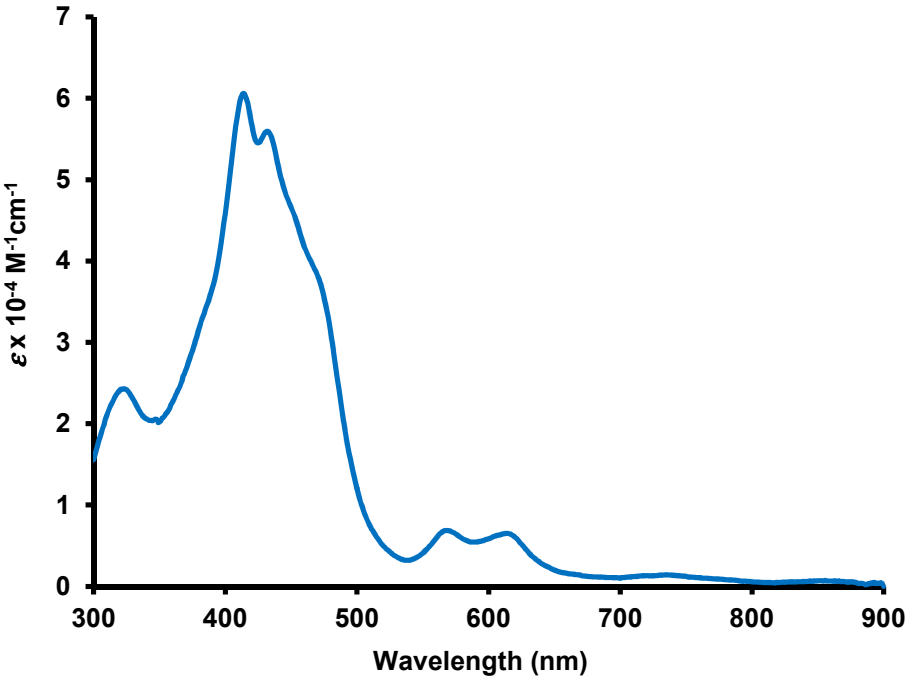

Figure B – 21: UV-vis spectrum of dimethylcarbaporphyrin **121** in 5% TFA-CH_2Cl_2

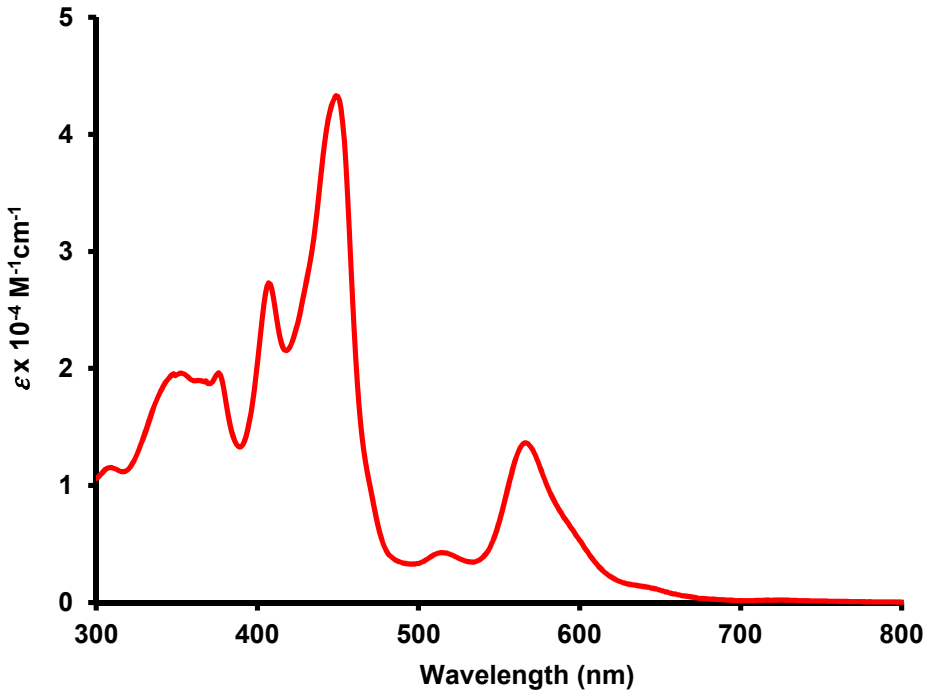

Figure B – 22: UV-vis spectrum of silver(III) carbaporphyrin **118** in chloroform

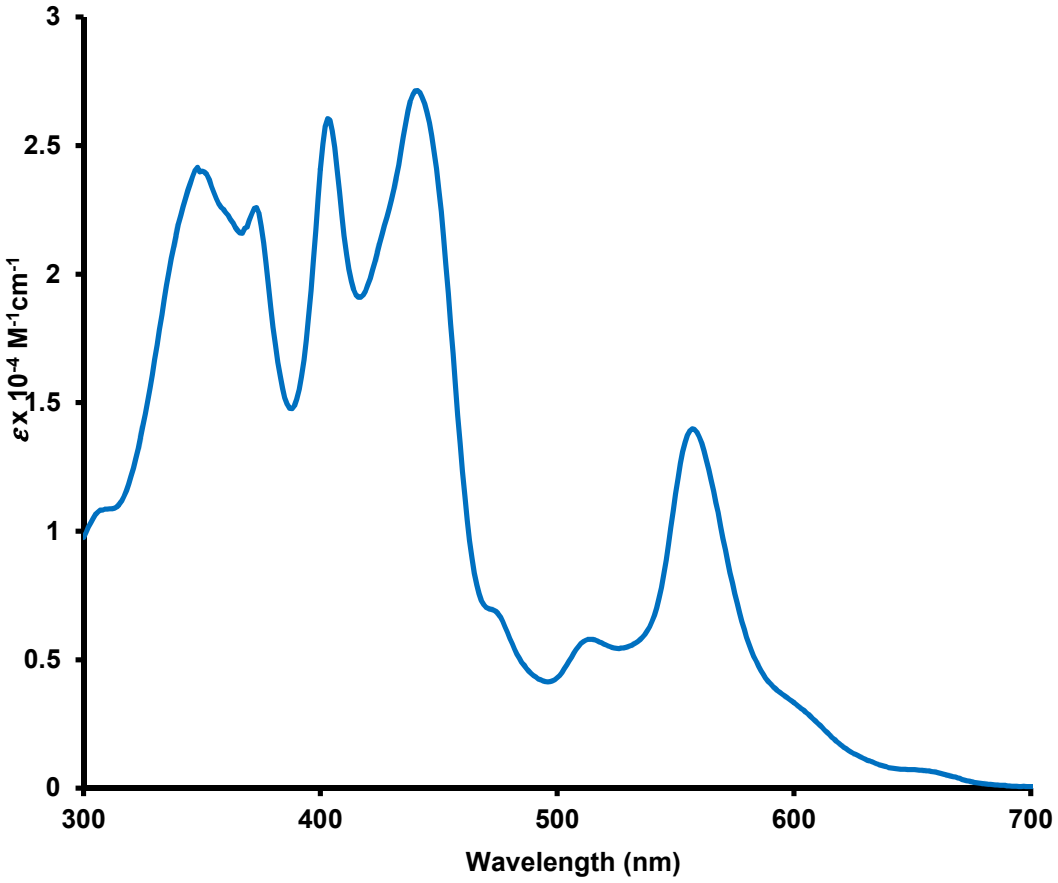

Figure B – 23: UV-vis spectrum of gold(III) carbaporphyrin **119** in chloroform

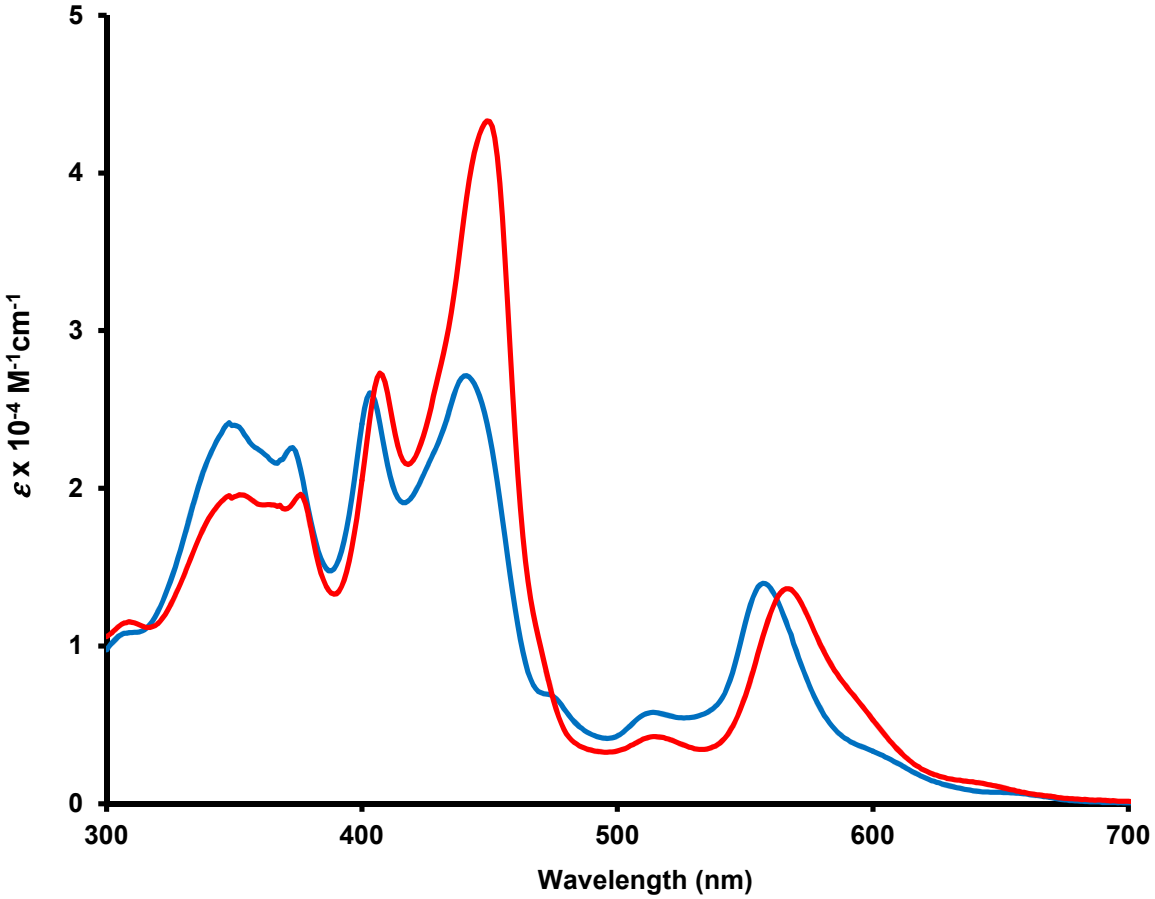

Figure B – 24: UV-Vis spectra on silver(III) carbaporphyrin (red line) and gold(III) carbaporphyrin (blue line) in chloroform

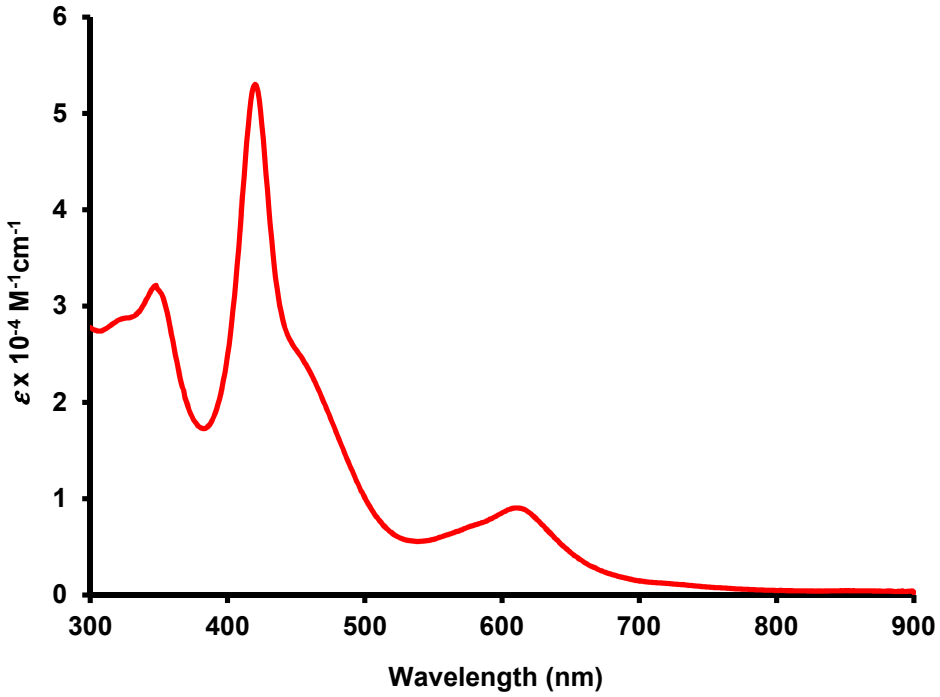

Figure B – 25: UV-vis spectrum of nickel(II) carbaporphyrin **123** in chloroform

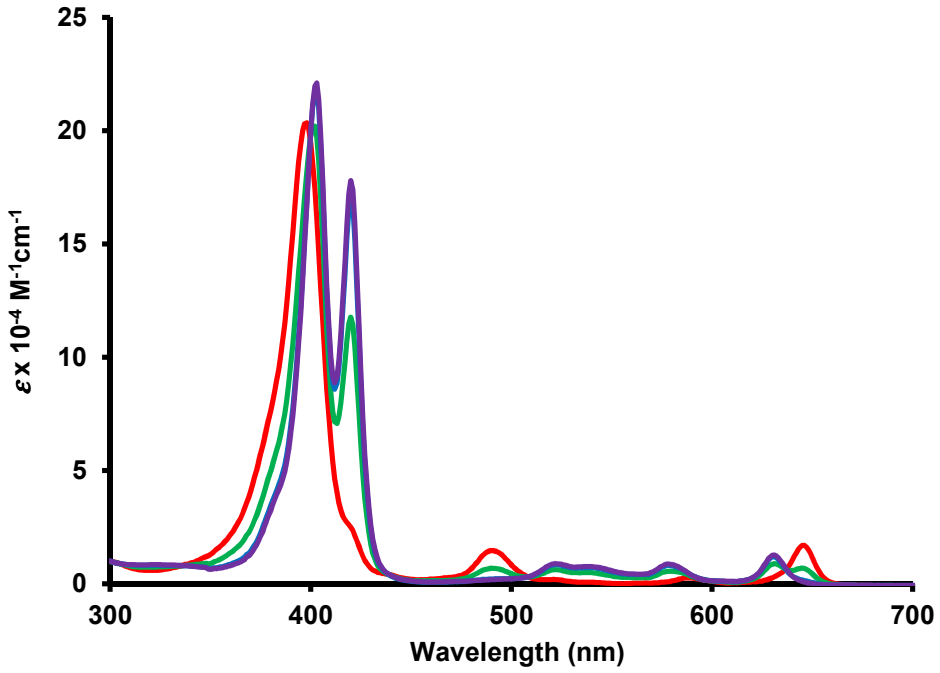

Figure B – 26: UV-vis spectra of carbachlorin by-product **117** in dichloromethane with 0 equiv. TFA (red line), 0.5 equiv. TFA (green line), 1 equiv. TFA (blue line), and 2 equiv. TFA (purple line)

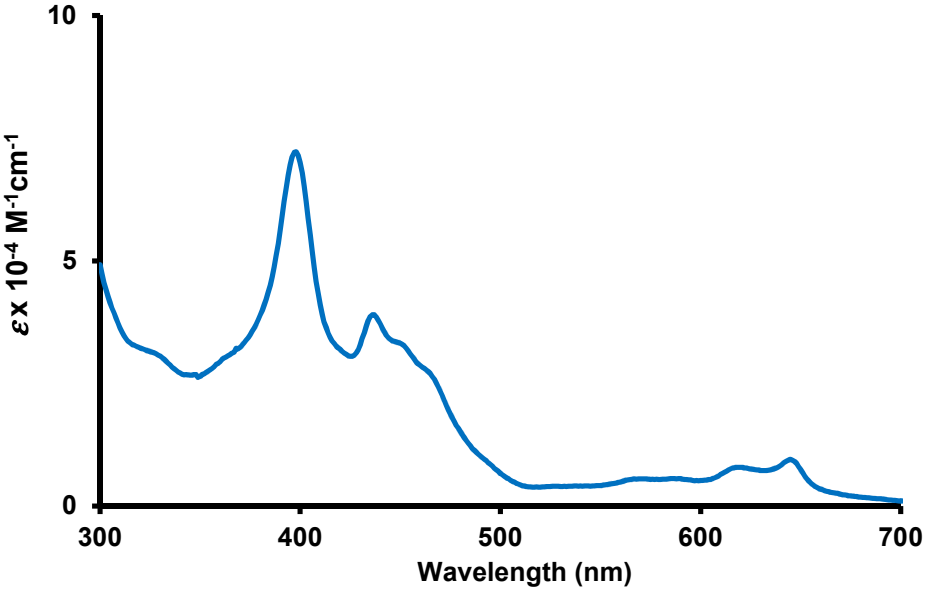

Figure B – 27: UV-vis spectrum of carbachlorin by-product **133** in 5% DBU-dichloromethane

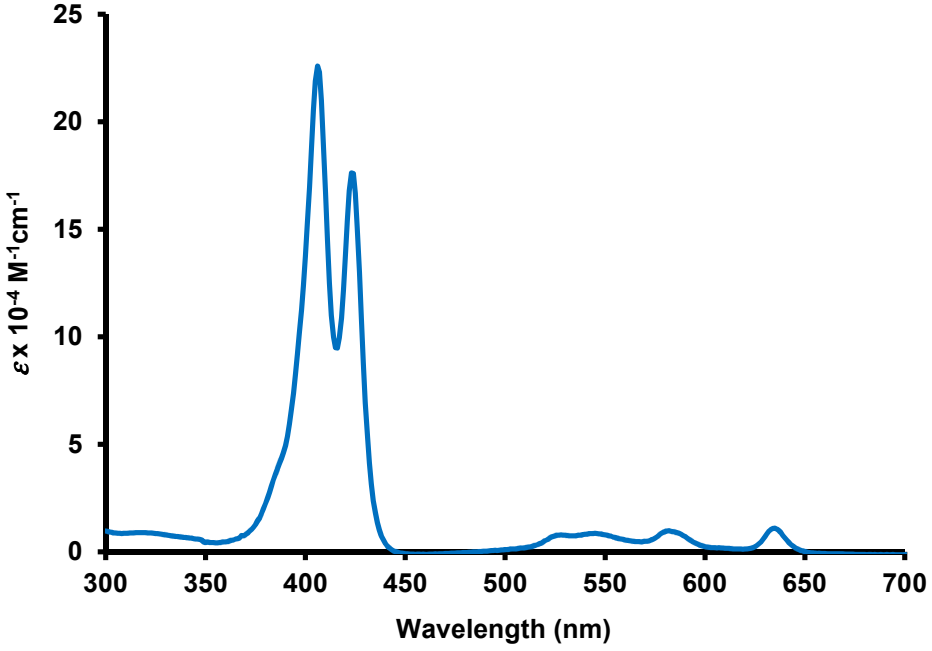

Figure B – 28: UV-vis spectrum of carbachlorin cation **133**H^+ in 1% TFA-dichloromethane

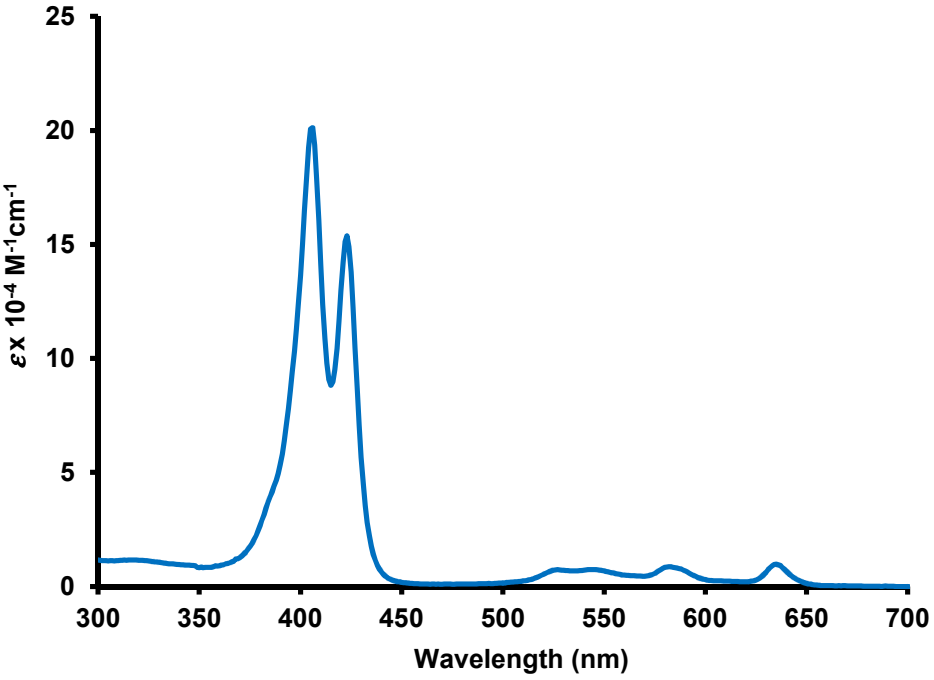

Figure B – 29: UV-vis spectrum of carbachlorin monocation **133**H^+ in 5% TFA-dichloromethane

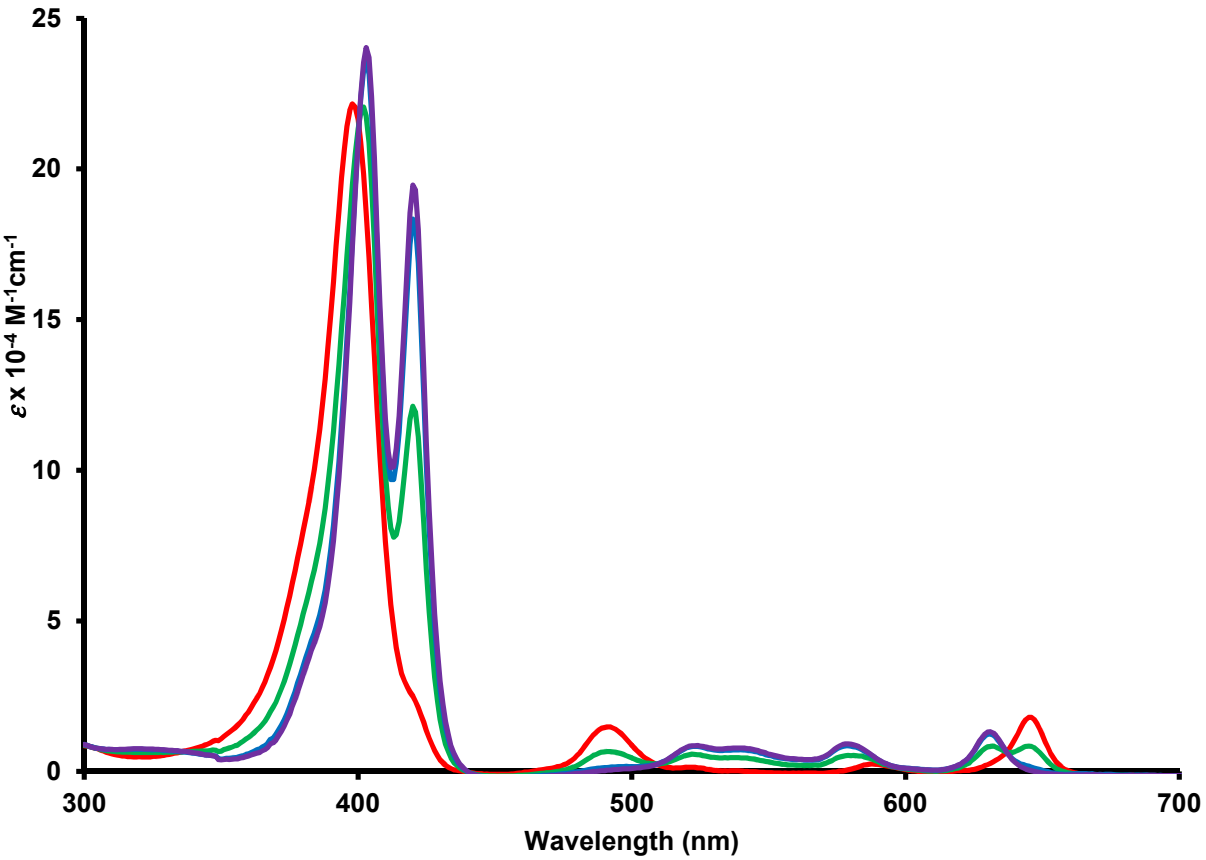

Figure B – 30: UV-vis spectra of carbachlorin **133** in dichloromethane with 0 equiv. TFA (red line), 0.5 equiv. TFA (green line), 1 equiv. TFA (blue line), and 2 equiv. TFA (purple line)